REV LTR

THE BOEING COMPANY

AIRPLANE DIVISION
P.O. BOX 707
RENTON, WASHINGTON 98055

D6-10741, PART I

TITLE: A METHOD OF OPTIMIZING CAMBER SURFACES FOR WING-BODY COMBINATIONS AT SUPERSONIC SPEEDS—THEORY AND APPLICATION

#74 Nasa

Prepared under NASA Contract

NAS2-2282

PREPARED BY F A Woodward 8/30/65

J. W. Larsen 8/30/65

SUPERVISED BY Richard E. Wallace 8-30-65

APPROVED BY Louis B. Gratzer 8-30-65
(DATE)

CONTENTS

1. SUMMARY

This report presents a numerical method for the analysis of wing-body combinations, and for the design of optimum wing camber surfaces in the presence of a body. The method is based on the linearized theory of supersonic flow. The wing and body are represented by a large number of singularities located in the plane of the wing, on the surface of the body, and along the body axis. The velocity components induced by these singularities at selected control points define a matrix of aerodynamic influence coefficients. The aerodynamic matrix is used to calculate the pressure distribution on the wing and body for given boundary conditions, or to determine the wing camber surface corresponding to a given aerodynamic loading. Also, the wing camber surface required to minimize the drag of the wing-body combination under given constraints of lift and pitching moment may be determined by additional operations on the aerodynamic matrix.

The method has been programmed for a digital computer. A special effort has been made to minimize the number of geometrical inputs required in the program by including a geometry definition section and a geometry paneling section as integral parts. A description of the program, including a flow chart and the input formats required for specific problems, is included in the report.

Application of the method to a wide variety of examples has shown good correlation with both theory and experiment. In particular, detailed pressure and force comparisons are made on a wind-tunnel model tested at Mach 1.8. The program also is used to predict the drag reduction that might be achieved by optimizing the wing camber surface on this model.

2. INTRODUCTION

Several methods are currently available (references 1 through 4) for calculating the camber surface of minimum drag for an isolated wing at a given lift coefficient in supersonic flow. However, none of these allows for the effect that a wing-mounted body may have in modifying the optimum wing camber surface. A new method, based on the linearized theory of supersonic flow is presented for calculating the optimum camber surface of a wing in the presence of a body. In this method, the boundary condition of tangential flow is satisfied simultaneously on both wing and body, eliminating any iteration procedures formerly required in solving problems of this type. The solution to this problem has important applications in the design of supersonic aircraft.

The primary objective of this study has been to develop a method of optimizing camber surfaces for a wing in the presence of a body. However, because of its formulation in terms of aerodynamic influence coefficients, the method is sufficiently general to solve a wide variety of equally important problems in supersonic flow. For example, it may be used to determine the pressures and forces acting on wing-body configurations of given shape or to design a wing having a given pressure distribution in the presence of a body. The effect of wing thickness in modifying surface pressures may also be included. In addition, the surface pressures and forces on isolated wings or bodies may be calculated. The bodies may have regular or irregular cross sections, camber, and incidence. In all of these problems, the accuracy of the results ultimately depends on the number of boundary points at which the flow equations are satisfied.

The aerodynamic methods described in this report are considered to be significant contributions to the linearized theory of supersonic flow. Although a similar approach has been presented recently by H. Carlson and W. Middleton of the NASA Langley Research Center (reference 5), their theory was restricted entirely to the analysis of isolated planar wings. In particular, the development of the nonplanar, constant-pressure solution to the linearized wave equation and its application to the analysis of supersonic wing-body interference problems are considered of additional significance.

This report (Part I) describes the details of the aerodynamic theory underlying the computer program, shows the agreement between the results and other theories, validates the method by comparison with experimental data, and presents a sample case of design optimization. It is also self-sufficient for guiding the reader in program usage. The second half of this report (Part II, reference 6) provides the details necessary for understanding the digital computer program. Subroutine descriptions, several sample problems, and a program listing provide the bulk of Part II.

The other report is Boeing Document D6-10740 (reference 7), Summary Description of Method of Optimizing Camber Surfaces for Wing-Body Combinations at Supersonic Speeds. It is a brief summary intended to introduce the scope of the work performed and put the results into context.

Much credit is due Dr. Tse Sun Chow, a mathematics research specialist at Boeing, for the integration and checking of the many functions used in the vortex singularity representation of the method. The aerodynamic work was accomplished by members of the Aerodynamics Research Unit, while the programming and checkout was accomplished by members of the Technical Support Section, all members of The Boeing Company Airplane Group.

3. LIST OF SYMBOLS

$a_{( )}$	Aerodynamic influence coefficient
a	Panel inclination
$[A]$	Matrix of aerodynamic influence coefficients
$A_{( )}$	Panel area
A	Aspect ratio
$b_{( )}$	Normalized panel edge slope
b	Wingspan
$[B]$	Matrix of velocity components
$c_{( )}$	Normal velocity component
c	Wing chord
C	Aerodynamic coefficient
D	Pressure drag
$D_{( )}$	Downwash function
F	Normal force
$F_{( )}$	Auxiliary function
J	Number of circumferential points on body
k	Line source strength
K	Number of line singularities in body
L	Lift
L	Body length
m	Panel edge slope
M	Mach number
M	Pitching moment
n	Unit normal vector
$n_{( )}$	Normal velocity component
N	Number of panels
p	Pressure
$p_{( )}$	Strengths of vortex singularities
$P_{( )}$	Pressure function
q	Dynamic pressure
r	Radial distance
r	Body radius
R	Fraction of panel chord defining control point location

S ( )	Sidewash function
S	Surface area
T	Strength of line singularities
u	Nondimensional perturbation velocity in x direction
U	Free-stream velocity
v	Nondimensional perturbation velocity in y direction
w	Nondimensional perturbation velocity in z direction
x, y, z	Transformed axis system
X, Y, Z	Definition axis system

Greek

α	Angle of attack
$\alpha_{(\ )}$	Panel inclination (see p. 42)
β	$\sqrt{M^2 - 1}$
γ	Ratio of specific heats for air (1.40)
Δ	Difference (e.g., Δp, $\Delta \theta$)
θ	Angular coordinate
θ	Panel inclination (see p. 42)
λ	Lagrange multiplier
Λ	Leading-edge slope
ν	Conormal vector
π	3.14159
ρ	Density of air
σ	Volterra's function
τ	Domain of dependence
φ	Velocity potential
ξ, η, ζ	Integration variables in Cartesian system
Ω	Arbitrary potential function

Subscripts

a	Axial component
A	Referred to body coordinate system
B	Body
c	Cross component
CP	Center of pressure
D	Referred to definition coordinate system

D	Doublet
D	Drag
F	Fin
i	Influenced panel number
j	Influencing panel number
k	Line singularity number
k	Corner point number
L	Lift
L	Lower surface
M	Moment
p	Pressure
r	Radial component
R	Reduced
R	Wing root
S	Source
T	Thickness (wing)
U	Upper surface
V	Vortex
W	Wing
x, y, z	Referred to Cartesian coordinates
x, y, z	Partial derivative
θ	Tangential component
∞	Free stream condition

Superscripts

'	Referred to primed system of coordinates
''	Referred to double primed system of coordinates
—	Fixed point or value

4. AERODYNAMIC THEORY

4.1 Description of Method

The method of aerodynamic influence coefficients is used to calculate the pressures, forces, and moments on arbitrary wing-body combinations at supersonic speeds, and to predict the optimum camber surface of the wing in the presence of the body. In this method, the wing and body are represented by a large number of singularities located in the plane of the wing, on the surface of the body, and along the body axis. It is assumed that the flow perturbations due to this system of singularities are sufficiently small that the equations governing the flow can be linearized without introducing significant errors into the analysis.

The three components of velocity induced by each elementary singularity are calculated at specified surface control points. In particular, the velocity component that is both normal to the body axis, and in a plane which is parallel to the body axis and perpendicular to the surface through each control point is required. The magnitude of this normal velocity component induced at control point i by the j^{th} singularity of unit strength is referred to as the aerodynamic influence coefficient a_{ij}. Thus the resultant normal velocity at point i is given by the sum of the products of the aerodynamic influence coefficients with their respective singularity strengths.

This resultant normal component of velocity is used to satisfy the surface slope boundary conditions at each control point, and the resulting system of linear equations is solved for the unknown singularity strengths. The matrix of the coefficients of this system of equations is known as the matrix of aerodynamic influence coefficients, or aerodynamic matrix, and plays an important part in the following analysis.

In actual practice, the singularity strengths required to satisfy the given boundary conditions are not solved in a single step. The boundary conditions corresponding to wing thickness, body thickness, and body camber and incidence are separated, and the strengths of the specific singularities used to satisfy them are determined independently. In the final stage of the calculation, these separate solutions are combined by linear superposition, and any residual interference effects are satisfied, together with the wing camber and incidence boundary conditions, by surface distributions of singularities on the wing and body.

In order to expedite the calculation of the aerodynamic influence coefficients, the wing and body are subdivided into a large number of small panels, as illustrated in figure 1. Each panel has one or more singularities associated with it, depending on the way the panel boundary conditions are specified. For example, the wing is represented by a maximum of 100 panels located in the wing reference plane. Two types of singularities are specified for each panel. First, a surface distribution of vorticity corresponding to a unit pressure difference across the panel is used to simulate the lifting effects of camber, twist, and incidence; and secondly, a surface distribution of sources is used to simulate the effect of wing thickness. It will be shown later how the boundary conditions on the surface of the wing can be completely satisfied by these two independent types of singularities.

The effects of body thickness, or camber and incidence are represented by a maximum of 50 line sources and doublets distributed along the body reference axis. In addition, the surface of the body is subdivided into a maximum of 100 panels, located in the region of influence of the wing-body intersection. These body panels simulate surface distributions of vorticity similar to those used on the wing, and are used to cancel the interference effects of the wing on the body in this region. The boundary conditions on the body, as on the wing, are specified so that they exactly match the number of singularities used to represent the flow.

The location, and geometric orientation of each elementary singularity is now defined. It remains to calculate the u, v, and w components of velocity induced at each of the specified control points due to a unit strength of the singularity under consideration. Formulae for these three perturbation velocity components are given in the text for each of the four independent types of singularities used in this report. In particular, the aerodynamic influence coefficients associated with each elementary singularity may be calculated from a combination

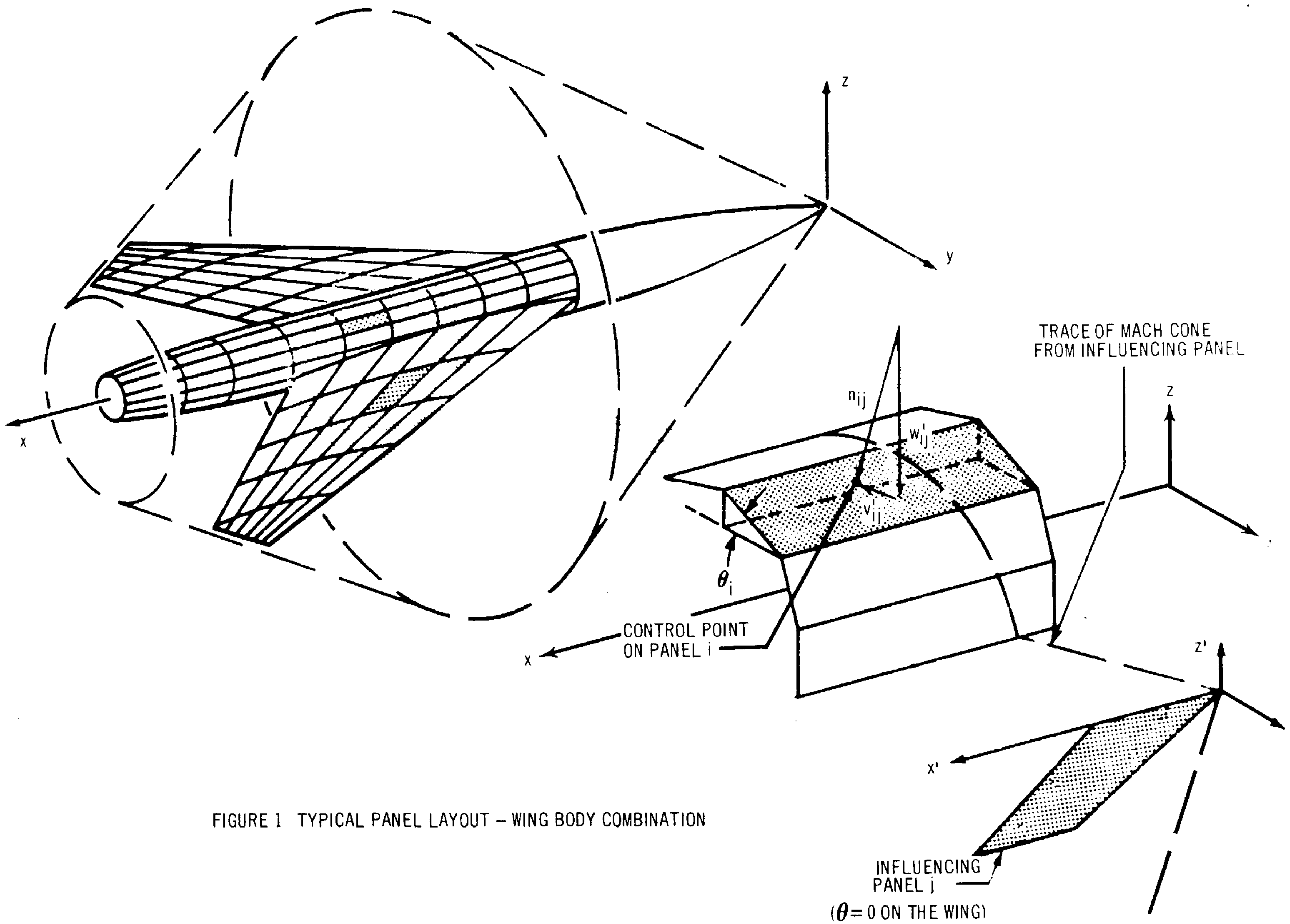

FIGURE 1 TYPICAL PANEL LAYOUT – WING BODY COMBINATION

of the v and w components of velocity, with due consideration being taken of the relative orientations of the panels involved.

Once the aerodynamic matrix has been formed and solved for the unknown singularity strengths, the surface pressures, forces, and moments acting on the wing-body combination can be calculated.

If the shape of the wing camber surface that will yield the minimum drag for the wing-body combination under specified conditions of lift and pitching moment is desired, a slightly different method is used to solve for the strengths of the singularities. In this case, an expression for the drag of the complete configuration is derived in terms of the unknown singularity strengths. The values of the singularity strengths which will give the smallest value of drag consistent with the constraints imposed by the lift and pitching moment are determined by application of the method of Lagrange multipliers to the system of equations so formed. These values may then be used to calculate the optimum shape of the camber surface, and the corresponding pressures, forces, and moments acting on the configuration.

4.2 Calculation of Velocity Components — Surface Singularities

Derivation of the generalized potential function. — The linearized differential equation for the velocity potential φ generated by a small perturbation of a steady supersonic flow is given below, where $\beta = \sqrt{M^2 - 1}$ and M is the free-stream Mach number.

$$\beta^2 \varphi_{xx} = \varphi_{yy} + \varphi_{zz} \tag{1}$$

Differential equations of identical form also govern the behavior of the three perturbation velocity components u, v, w in the flow. To extend the following analysis to include the calculation of these velocity components in addition to the potential, equation (1) will be rewritten in terms of an arbitrary variable Ω.

$$\beta^2 \Omega_{xx} = \Omega_{yy} + \Omega_{zz} \tag{2}$$

A general solution to equation (2) is given in reference 8, based on Volterra's solution of the two dimensional wave equation. This result is repeated below, and gives, in integral form, the value of Ω at any point P due to a small perturbation of the flow originating on a surface S.

$$\Omega(x, y, z) = -\frac{1}{2\pi}\frac{\partial}{\partial x}\iint_{\tau}\left(\frac{\partial \Omega}{\partial \nu} + \frac{\partial \Omega'}{\partial \nu'}\right)\sigma \, dS$$

$$+\frac{1}{2\pi}\frac{\partial}{\partial x}\iint_{\tau}(\Omega - \Omega')\frac{\partial \sigma}{\partial \nu}\, dS \tag{3}$$

The integrals are to be evaluated on the surface S throughout the "domain of dependence", τ, of point P(x, y, z). The unprimed variable Ω denotes the value of this variable on the same side of S as P, while the primed variable denotes its value on the opposite side of S as P. σ is the particular solution of equation (2) chosen by Volterra which vanishes, together with its derivative with respect to the conormal ν, everywhere on the surface of the Mach forecone from P. The function σ is given below:

$$\sigma = \cosh^{-1}\frac{x - \xi}{\beta\sqrt{(y - \eta)^2 + (z - \zeta)^2}} \tag{4}$$

It should be noted that σ is the indefinite integral of the fundamental solution of equation (2) representing a supersonic source in three dimensions.

The conormal to a surface S is defined to be a vector, the three components of which are related to the components of the normal vector n to the surface as follows:

$$\nu_1 = -\beta^2 n_1, \qquad \nu_2 = n_2, \qquad \nu_3 = n_3 \tag{5}$$

ν' is defined to be a vector having the opposite direction to ν on S.

In the following analysis, the surface S is chosen to lie in an inclined plane passing through the y axis. The equation of this plane is $\zeta = a\xi$. The sketch on the following page illustrates the conormal associated with this plane. Note that the conormal to the Mach wave originating from the leading edge of the surface S lies in the plane of that Mach wave.

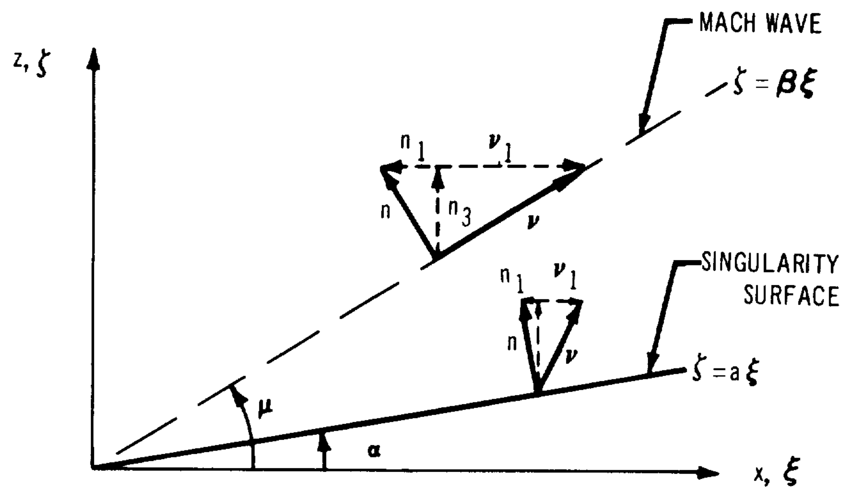

In this example

$$\frac{\partial \sigma}{\partial \nu} = \nu_1 \frac{\partial \sigma}{\partial \xi} + \nu_3 \frac{\partial \sigma}{\partial \zeta} = -\beta^2 n_1 \frac{\partial \sigma}{\partial \xi} + n_3 \frac{\partial \sigma}{\partial \zeta} \tag{6}$$

Now

$$n_1 = -\sin\alpha = -\frac{a}{\sqrt{1+a^2}}$$

$$n_3 = \cos\alpha = \frac{1}{\sqrt{1+a^2}}$$

Therefore

$$\frac{\partial \sigma}{\partial \nu} = \frac{\beta^2 a}{\sqrt{1+a^2}} \frac{\partial \sigma}{\partial \xi} + \frac{1}{\sqrt{1+a^2}} \frac{\partial \sigma}{\partial \zeta}$$

$$= \frac{-\beta^2 a + \dfrac{(x-\xi)(z-\zeta)}{(y-\eta)^2 + (z-\zeta)^2}}{\sqrt{1+a^2}\sqrt{(x-\xi)^2 - \beta^2(y-\eta)^2 - \beta^2(z-\zeta)^2}} \tag{7}$$

Note also that an elementary area dS in the plane may be written

$$dS = d\xi \; d\eta / \cos\alpha$$

$$= \sqrt{1 + a^2} \; d\xi \; d\eta \tag{8}$$

Consider now a semi-infinite triangular region in the plane $\zeta = a\xi$, such that the leading edge of the triangle has the projection $\eta = m\xi$ in the ξ, η plane, while the side edge lies in the ξ, ζ plane. The domain of dependence τ of the integrals in equation (3) is then the area on this oblique triangular region lying upstream of its intersection with the Mach forecone from P, OQR in figure 2. The equation of the curve QR is determined by substituting $\zeta = a\xi$ in the equation for the Mach forecone from P:

$$(x - \xi)^2 = \beta^2 (y - \eta)^2 + \beta^2 (z - a\xi)^2 \tag{9}$$

Thus, for a given η, the points S and T on an elementary strip of width $d\eta$ on the surface have the coordinates $S(\xi_1, \eta, a\xi_1)$ and $T(\xi_2, \eta, a\xi_2)$

where $\xi_1 = \eta/m$

and $$\xi_2 = \frac{x - \beta^2 a z}{1 - \beta^2 a^2}\left(1 - \sqrt{1 - \frac{1 - \beta^2 a^2}{(x - \beta^2 a z)^2}\left(x^2 - \beta^2 (y - \eta)^2 - \beta^2 z^2\right)}\right) \tag{10}$$

and the point Q has the coordinates $Q(\eta_3/m, \eta_3, a\eta_3/m)$

where $$\eta_3 = \frac{m\left(x - \beta^2 (my + az)\right)}{1 - \beta^2 (a^2 + m^2)}\left(1 - \sqrt{1 - \frac{\left(1 - \beta^2 (a^2 + m^2)\right)\left(x^2 - \beta^2 (y^2 + z^2)\right)}{\left(x - \beta^2 (my + az)\right)^2}}\right) \tag{11}$$

Equation (3) may now be written:

$$\Omega(x, y, z) = -\frac{\sqrt{1 + a^2}}{2\pi}\frac{\partial}{\partial x}\int_0^{\eta_3} d\eta \int_{\xi_1}^{\xi_2}\left(\frac{\partial\Omega}{\partial\nu} + \frac{\partial\Omega'}{\partial\nu'}\right)\cosh^{-1}\frac{x - \xi}{\beta\sqrt{(y - \eta)^2 - (z - a\xi)^2}}\, d\xi$$

$$+ \frac{1}{2\pi}\frac{\partial}{\partial x}\int_0^{\eta_3} d\eta \int_{\xi_1}^{\xi_2}(\Omega - \Omega')\frac{-\beta^2 a + \dfrac{(x - \xi)(z - a\xi)}{(y - \eta)^2 - (z - a\xi)^2}}{\sqrt{(x - \xi)^2 - \beta^2 (y - \eta)^2 - \beta^2 (z - a\xi)^2}}\, d\xi \tag{12}$$

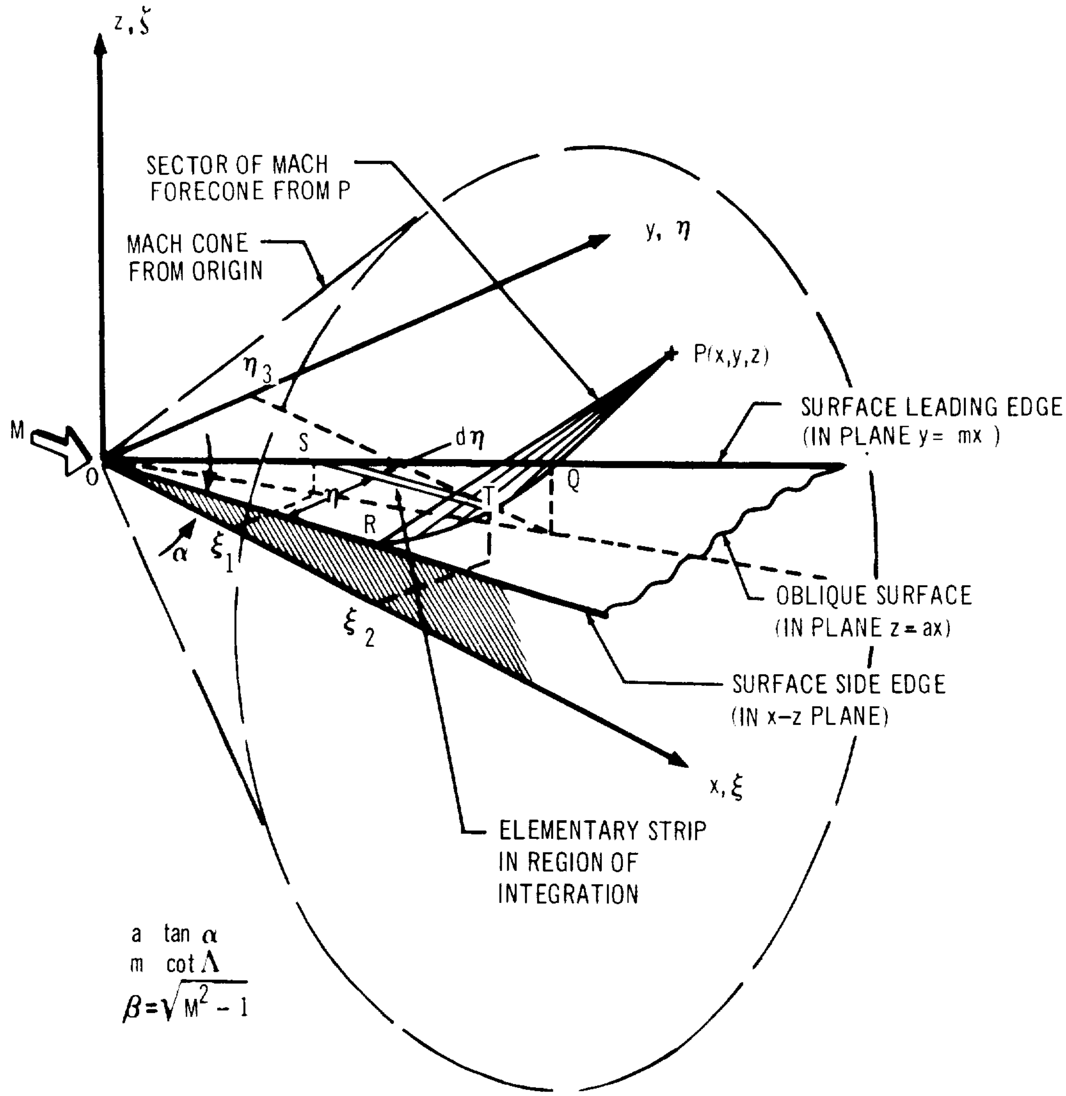

$$\xi_1 = \eta / m$$

$$\xi_2 = \frac{x - \beta^2 a z}{1 - \beta^2 a^2} \left[1 - \sqrt{1 - \frac{1 - \beta^2 a^2}{(x - \beta^2 a z)^2} \left(x^2 - \beta^2 (y - \eta)^2 - \beta^2 z^2\right)} \right]$$

$$\eta_3 = \frac{m(x - \beta^2 m y - \beta^2 a z)}{1 - \beta^2 (a^2 + m^2)} \left[1 - \sqrt{1 - \frac{\left[1 - \beta^2 (a^2 + m^2)\right]\left[x^2 - \beta^2 (y^2 + z^2)\right]}{(x - \beta^2 m y - \beta^2 a z)^2}} \right]$$

FIGURE 2 GEOMETRICAL ORIENTATION OF INCLINED SINGULARITY SURFACE

The integrals in equation (12) may now be evaluated, provided the expressions $(\Omega - \Omega')$ and $(\partial\Omega/\partial\nu + \partial\Omega'/\partial\nu')$ are prescribed on S. It is most convenient to set them equal to a constant, or zero. Two choices of Ω will now be described which will satisfy these conditions, and yield expressions for the potential function representing either a surface distribution of sources in the ξ, η plane, or a constant pressure jump across a lifting surface corresponding to a constant distribution of vorticity in the plane $\zeta = a\xi$.

Potential function for surface distribution of sources. —In equation (12), Ω is set equal to the perturbation velocity potential φ on the upper surface of S. The partial derivative $\partial\varphi/\partial\nu$ then represents the velocity component in the direction of the conormal to the upper surface of S. Similarly, $\partial\varphi'/\partial\nu'$ represents the velocity component of the lower surface potential function φ' in the direction of the conormal to the lower surface of S.

Now

$$\frac{\partial\varphi}{\partial\nu} = \frac{\beta^2 a}{\sqrt{1+a^2}}\frac{\partial\varphi}{\partial\xi} + \frac{1}{\sqrt{1+a^2}}\frac{\partial\varphi}{\partial\zeta}$$

$$= \frac{\beta^2 a}{\sqrt{1+a^2}}\,u + \frac{1}{\sqrt{1+a^2}}\,w \tag{13}$$

Similarly

$$\frac{\partial\varphi'}{\partial\nu'} = -\frac{\beta^2 a}{\sqrt{1+a^2}}\,u' - \frac{1}{\sqrt{1+a^2}}\,w' \tag{14}$$

The sketch on the following page illustrates the geometrical orientation of these velocity components.

It can be seen that if φ' has the same sign as φ, a discontinuity in the ν component of velocity will appear in the flow on the surface $\zeta = a\xi$ which in turn implies surface discontinuities in the u and w velocity components. In fact, if

$\varphi' = \varphi$, then $u' = -u$, $w' = -w$ on the surface.

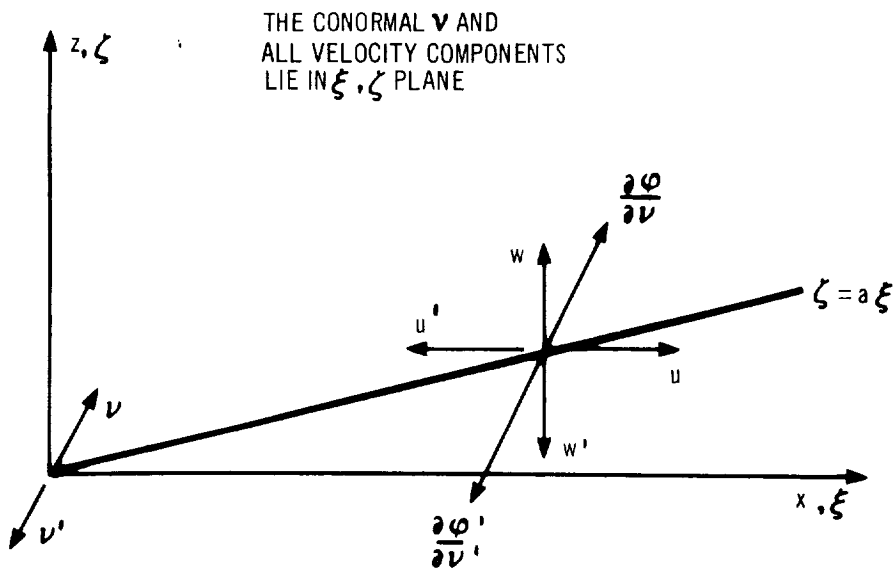

The second term in equation (12) then vanishes, and

$$\frac{\partial \varphi}{\partial \nu} + \frac{\partial \varphi'}{\partial \nu'} = \frac{2}{\sqrt{1 + a^2}} (\bar{w} + \beta^2 a \bar{u}) \tag{15}$$

where the bars denote the values of the velocity components on the surface .

If the quantity $(\bar{w} + \beta^2 a \bar{u})$ is constant, it can be taken outside the integral. If, in addition, the partial derivative of σ with respect to x is taken through the double integral, which is a legitimate operation in this case, equation (12) reduces to

$$\varphi(x, y, z) = - \frac{\bar{w} + \beta^2 a \bar{u}}{\pi} \int_0^{\eta_3} d\eta \int_{\xi_1}^{\xi_2} \frac{d\xi}{\sqrt{(x - \xi)^2 - \beta^2(y - \eta)^2 - \beta^2(z - a\xi)^2}} \tag{16}$$

For the special case a = 0, this expression reverts to the usual integral form for the potential due to a surface distribution of sources in the ξ, η plane. The integral will be evaluated in its most general form, however, as the resulting functions will be used later in the derivation of the potential due to a constant pressure difference across the surface S.

Applying the integration formulae appearing in Appendix A, and simplifying, the following result is obtained, for the case $\beta\sqrt{a^2 + m^2} < 1$ (subsonic leading edge):

$$\varphi(x, y, z) = \frac{\bar{w} + \beta^2 a \bar{u}}{\pi\sqrt{1 - \beta^2 a^2}} \int_0^{\eta_3} \cosh^{-1} \frac{(1 - \beta^2 a^2)\eta - m(x - \beta^2 az)}{\beta m\sqrt{(1 - \beta^2 a^2)(\eta - y)^2 + (z - ax)^2}} d\eta$$

$$= \frac{\bar{w} + \beta^2 a \bar{u}}{\pi} \left\{ \frac{z - ax}{1 - \beta^2 a^2} \tan^{-1} \frac{m(z - ax)\sqrt{x^2 - \beta^2(y^2 + z^2)}}{y[(y - mx) - \beta^2 a(ay - mz)] + (z - ax)^2} \right.$$

$$+ \frac{(1 - \beta^2 a^2) y - m(x - \beta^2 az)}{(1 - \beta^2 a^2)\sqrt{1 - \beta^2(a^2 + m^2)}} \cosh^{-1} \frac{x - \beta^2(my + az)}{\beta\sqrt{(y - mx)^2 + (z - ax)^2 - \beta^2(ay - mz)^2}}$$

$$\left. - \frac{y}{\sqrt{1 - \beta^2 a^2}} \cosh^{-1} \frac{x}{\beta\sqrt{y^2 + z^2}} \right\} \qquad (17)$$

If $\beta\sqrt{a^2 + m^2} \geqq 1$ (sonic or supersonic leading edge), the inverse hyperbolic cosine is replaced by the inverse cosine (see equation 40).

The perturbation velocity components may now be obtained by differentiation.

$$u = \frac{\partial\varphi}{\partial x} = \frac{-(\bar{w} + \beta^2 a \bar{u})}{\pi(1 - \beta^2 a^2)} \left\{ a \tan^{-1} \frac{m(z - ax)\sqrt{x^2 - \beta^2(y^2 + z^2)}}{y[(y - mx) - \beta^2 a(ay - mz)] + (z - ax)^2} \right.$$

$$\left. + \frac{m}{\sqrt{1 - \beta^2(a^2 + m^2)}} \cosh^{-1} \frac{x - \beta^2(my + az)}{\beta\sqrt{(y - mx)^2 + (z - ax)^2 - \beta^2(ay - mz)^2}} \right\}$$

$$v = \frac{\partial\varphi}{\partial y} = \frac{-(\bar{w} + \beta^2 a \bar{u})}{\pi} \left\{ \frac{1}{\sqrt{1 - \beta^2 a^2}} \cosh^{-1} \frac{x}{\beta\sqrt{y^2 + z^2}} \right. \qquad (18)$$

$$\left. - \frac{1}{\sqrt{1 - \beta^2(a^2 + m^2)}} \cosh^{-1} \frac{x - \beta^2(my + az)}{\beta\sqrt{(y - mx)^2 + (z - ax)^2 - \beta^2(ay - mz)^2}} \right\}$$

$$w = \frac{\partial\varphi}{\partial z} = \frac{(\bar{w} + \beta^2 a \bar{u})}{\pi(1 - \beta^2 a^2)} \left\{ \tan^{-1} \frac{m(z - ax)\sqrt{x^2 - \beta^2(y^2 + z^2)}}{y[(y - mx) - \beta^2 a(ay - mz)] + (z - ax)^2} \right.$$

$$\left. + \frac{\beta^2 a m}{\sqrt{1 - \beta^2(a^2 + m^2)}} \cosh^{-1} \frac{x - \beta^2(my + az)}{\beta\sqrt{(y - mx)^2 + (z - ax)^2 - \beta^2(ay - mz)^2}} \right\} \quad (18)$$

It should be noted that $\varphi = xu + yv + zw$. (19)

The results may be quickly verified by evaluating u and w on the surface $z = ax$.

Noting that

$$\tan^{-1} \frac{m(z - ax)\sqrt{x^2 - \beta^2(y^2 + z^2)}}{y[(y - mx) - \beta^2 a(ay - mz)] + (z - ax)^2} \quad (20)$$

$$= \pi \quad \text{for} \quad z = ax, \quad \text{and } 0 < y < mx$$

$$= 0 \quad \text{for} \quad z = ax, \quad \text{and } y < 0, \quad y > mx$$

Then, for $0 < y < mx$

$$\bar{u} = \frac{-(\bar{w} + \beta^2 a \bar{u})}{\pi(1 - \beta^2 a^2)} \left\{ a\pi + \frac{m}{\sqrt{1 - \beta^2(a^2 + m^2)}} \cosh^{-1} \frac{x(1 - \beta^2 a^2) - \beta^2 my}{\beta\sqrt{1 - \beta^2 a^2}\,|y - mx|} \right\}$$

$$\bar{w} = \frac{(\bar{w} + \beta^2 a \bar{u})}{\pi(1 - \beta^2 a^2)} \left\{ \pi + \frac{\beta^2 a m}{\sqrt{1 - \beta^2(a^2 + m^2)}} \cosh^{-1} \frac{x(1 - \beta^2 a^2) - \beta^2 my}{\beta\sqrt{1 - \beta^2 a^2}\,|y - mx|} \right\}$$

Therefore $\quad \bar{w} + \beta^2 a \bar{u} \equiv \dfrac{(\bar{w} + \beta^2 a \bar{u})}{(1 - \beta^2 a^2)\pi} (1 - \beta^2 a^2)\pi \quad (21)$

Thus the resulting flow satisfies the imposed boundary conditions on the semi-infinite triangular surface illustrated in figure 2. Off this surface, in the plane $z = ax$, the quantity $(\bar{w} + \beta^2 a \bar{u}) = 0$.

Two special cases of these results deserve attention, as they will be used later in the numerical analysis. In the first, for $a = 0$, the velocity components due to a surface distribution of sources in the x, y plane are simply obtained from equations (18):

$$u_1 = -\frac{\overline{w}}{\pi} m \left[\frac{1}{\sqrt{1 - \beta^2 m^2}} \cosh^{-1} \frac{x - \beta^2 my}{\beta\sqrt{(mx - y)^2 + (1 - \beta^2 m^2) z^2}} \right]$$

$$v_1 = \left(\frac{\overline{w}m}{\pi}\right) \left\{ \frac{1/m}{\sqrt{1 - \beta^2 m^2}} \cosh^{-1} \frac{x - \beta^2 my}{\beta\sqrt{(mx - y)^2 + (1 - \beta^2 m^2) z^2}} - \cosh^{-1} \frac{x}{\beta\sqrt{y^2 + z^2}} \right\}$$

$$w_1 = \left(\frac{\overline{w}m}{\pi}\right) \left[\frac{\tan^{-1}}{m} \frac{mz\sqrt{x^2 - \beta^2(y^2 + z^2)}}{y^2 + z^2 - mxy} \right] \tag{22}$$

In the second special case, the velocity components due to a line source along the x axis will be derived. The term $m\,\overline{w}/\pi$ is taken as a constant (for $m \rightarrow 0$) in the equations for the velocity components given by equation (22), and the limit of the resulting expressions evaluated as m approaches zero. The result is given below:

$$u_2 = -k \cosh^{-1} \frac{x}{\beta\sqrt{y^2 + z^2}}$$

$$v_2 = \frac{k\,y}{\sqrt{y^2 + z^2}} \sqrt{x^2 - \beta^2(y^2 + z^2)}$$

$$w_2 = \frac{k\,z}{\sqrt{y^2 + z^2}} \sqrt{x^2 - \beta^2(y^2 + z^2)} \tag{23}$$

where $k = \lim\limits_{m \to 0} \frac{m\,\overline{w}}{\pi} = \text{constant}.$

These velocity components will be used later to represent the flow surrounding a circular cone at zero incidence centered on the x axis. The potential function corresponding to this flow is:

$$\varphi_2 = k\left\{x \cosh^{-1} \frac{x}{\beta\sqrt{y^2 + z^2}} - \sqrt{x^2 - \beta^2(y^2 + z^2)}\right\} \tag{24}$$

Potential function for constant pressure surface. —In equation (12), Ω is set equal to the perturbation velocity u on the upper surface of S. The desired solution will have a constant discontinuity in u everywhere on S, that is $\Delta u = u - u' =$ constant. Before introducing this condition into equation (12), the derivative of u and u' with respect to the conormal is investigated. Following the same procedure used in deriving equation (6),

$$\frac{\partial u}{\partial \nu} = \frac{\beta^2 a}{\sqrt{1 + a^2}} \frac{\partial u}{\partial \xi} + \frac{1}{\sqrt{1 + a^2}} \frac{\partial u}{\partial \zeta}$$

$$\frac{\partial u'}{\partial \nu'} = \frac{-\beta^2 a}{\sqrt{1 + a^2}} \frac{\partial u'}{\partial \xi} - \frac{1}{\sqrt{1 + a^2}} \frac{\partial u'}{\partial \zeta} \tag{25}$$

Summing these expressions, the following result is obtained

$$\frac{\partial u}{\partial \nu} + \frac{\partial u'}{\partial \nu'} = \frac{1}{\sqrt{1 + a^2}} \left[\beta^2 a \frac{\partial}{\partial \xi} (u - u') + \frac{\partial}{\partial \zeta} (u - u')\right] = 0,$$

since (u - u') is constant on the surface S. Therefore the first term in equation (12) vanishes, and the equation reduces to:

$$u(x, y, z) = \frac{\Delta u}{2\pi} \frac{\partial}{\partial x} \int_0^{\eta_3} d\eta \int_{\xi_1}^{\xi_2} \frac{-\beta^2 a + \frac{(x - \xi)(z - a\xi)}{(y - \eta)^2 + (z - a\xi)^2}}{\sqrt{(x - \xi)^2 - \beta^2(y - \eta)^2 - \beta^2(z - a\xi)^2}} d\xi \tag{26}$$

Since $u = \partial\varphi/\partial x$, an expression for the potential function may be obtained by integrating equation (26) with respect to x. Since the potential is zero everywhere ahead of the envelope of Mach cones defined by the leading edge of the surface S, the constant of integration is zero, and the potential function, in integral form, becomes:

$$\varphi(x, y, z) = \frac{-1}{4\pi}\left(\frac{\Delta p}{q_\infty}\right)\int_0^{\eta_3} d\eta \int_{\xi_1}^{\xi_2} \frac{-\beta^2 a + \dfrac{(x-\xi)(z-a\xi)}{(y-\eta)^2+(z-a\xi)^2}}{\sqrt{(x-\xi)^2 - \beta^2(y-\eta)^2 - \beta^2(z-a\xi)^2}}\, d\xi \tag{27}$$

where Δu has been replaced by $-\Delta p/2q_\infty$. Δp is the pressure difference across the lifting surface S, and q_∞ is the dynamic pressure $\gamma\, p_\infty\, M^2/2$, where p_∞ is the static pressure in the undisturbed flow. Equation (27) thus gives the potential function corresponding to the oblique triangular region of constant lifting pressure illustrated in figure 2 .

Equation (27) breaks down naturally into two double integrals as follows:

$$\varphi(x, y, z) = \frac{\beta^2 a}{4\pi}\left(\frac{\Delta p}{q_\infty}\right)\int_0^{\eta_3} d\eta \int_{\xi_1}^{\xi_2} \frac{d\xi}{\sqrt{(x-\xi)^2 - \beta^2(y-\eta)^2 - \beta^2(z-a\xi)^2}}$$

$$- \frac{1}{4\pi}\left(\frac{\Delta p}{q_\infty}\right)\int_0^{\eta_3} d\eta \int_{\xi_1}^{\xi_2} \frac{(x-\xi)\,(z-a\xi)\, d\xi}{\left[(y-\eta)^2 + (z-a\xi)^2\right]\sqrt{(x-\xi)^2 - \beta^2(y-\eta)^2 - \beta^2(z-a\xi)^2}} \tag{28}$$

The integration with respect to ξ is carried out first, making use of the integration formulae in Appendix A. It should also be noted that the first integral is identical to that in equation (16) for the surface distribution of sources. After some simplification, the following result is obtained:

$$\varphi(x, y, z) = \frac{-\beta^2 a}{4\pi}\left(\frac{\Delta p}{q_\infty}\right)\int_0^{\eta_3} \frac{1}{\sqrt{1-\beta^2 a^2}} \cosh^{-1} \frac{(1-\beta^2 a^2)\,\eta - m(x-\beta^2 az)}{\beta m\sqrt{(1-\beta^2 a^2)(\eta-y)^2 + (z-ax)^2}}\, d\eta$$

$$- \frac{1}{4\pi a}\left(\frac{\Delta p}{q_\infty}\right)\int_0^{\eta_3} \left[\cosh^{-1} \frac{y - mx}{\beta\sqrt{(a\eta - mz)^2 + m^2(\eta-y)^2}}\right.$$

$$\left. - \frac{1}{\sqrt{1-\beta^2 a^2}} \cosh^{-1} \frac{(1-\beta^2 a^2)\,\eta - m(x-\beta^2 az)}{\beta m\sqrt{(1-\beta^2 a^2)\,(\eta-y)^2 + (z-ax)^2}}\right] d\eta$$

and combining terms

$$\varphi(x,y,z) = \frac{-1}{4\pi a}\left(\frac{\Delta p}{q_\infty}\right)\int_0^{\eta_3}\left[\cosh^{-1}\frac{y - mx}{\beta\sqrt{(a\eta - mz)^2 + m^2(\eta - y)^2}}\right.$$

$$\left. - \sqrt{1 - \beta^2 a^2}\cosh^{-1}\frac{(1 - \beta^2 a^2)\,\eta - m(x - \beta^2 az)}{\beta m\sqrt{(1 - \beta^2 a^2)(\eta - y)^2 + (z - ax)^2}}\right] d\eta \qquad (29)$$

By repeated application of the integration formulae in Appendix A, the integration with respect to η may be completed, after some lengthy computation, giving the final result:

$$\varphi(x,y,z) = \frac{-1}{4\pi}\left(\frac{\Delta p}{q_\infty}\right)\left\{x\tan^{-1}\frac{m(z - ax)\sqrt{x^2 - \beta^2(y^2 + z^2)}}{y\left[(y - mx) - \beta^2 a(ay - mz)\right] + (z - ax)^2}\right.$$

$$- \frac{y}{a^2 + m^2}\left[a\sqrt{1 - \beta^2(a^2 + m^2)}\cosh^{-1}\frac{x - \beta^2(my + az)}{\beta\sqrt{(mx - y)^2 + (ax - z)^2 - \beta^2(ay - mz)^2}}\right.$$

$$+ m\tan^{-1}\frac{(ay - mz)\sqrt{x^2 - \beta^2(y^2 + z^2)}}{x(my + az) - y^2 - z^2}$$

$$+ \frac{1}{a}\left(m^2\tanh^{-1}\frac{\sqrt{x^2 - \beta^2(y^2 + z^2)}}{x}\right.$$

$$\left.\left. - (a^2 + m^2)\sqrt{1 - \beta^2 a^2}\tanh^{-1}\frac{\sqrt{(1 - \beta^2 a^2)\left(x^2 - \beta^2(y^2 + z^2)\right)}}{x - \beta^2 az}\right)\right]$$

$$+ \frac{z}{a^2 + m^2}\left[m\sqrt{1 - \beta^2(a^2 + m^2)}\cosh^{-1}\frac{x - \beta^2(my + az)}{\beta\sqrt{(mx - y)^2 + (ax - z)^2 - \beta^2(ay - mz)^2}}\right.$$

$$- m\tanh^{-1}\frac{\sqrt{x^2 - \beta^2(y^2 + z^2)}}{x}$$

$$+ \frac{1}{a}\left(m^2\tan^{-1}\frac{(ay - mz)\sqrt{x^2 - \beta^2(y^2 + z^2)}}{x(my + az) - y^2 - z^2}\right.$$

$$\left.\left.\left. - (a^2 + m^2)\tan^{-1}\frac{m(z - ax)\sqrt{x^2 - \beta^2(y^2 + z^2)}}{y\left[(y - mx) - \beta^2 a(ay - mz)\right] + (z - ax)^2}\right)\right]\right\} \qquad (30)$$

This equation is valid only if $\beta\sqrt{a^2 + m^2} < 1$ (subsonic leading edge). If $\beta\sqrt{a^2 + m^2} \geq 1$ (sonic or supersonic edge) the inverse hyperbolic cosine is replaced by the inverse cosine (see equation 40).

The velocity components may now be obtained by differentiating equation (30), where

$$u = \frac{\partial\varphi}{\partial x}, \qquad v = \frac{\partial\varphi}{\partial y}, \qquad w = \frac{\partial\varphi}{\partial z}$$

The evaluation of these derivatives is rather lengthy; however, it can be proved that u, v, w are merely the coefficients of x, y, z respectively in the expression $\varphi(x, y, z)$, given by equation (30). Thus

$$\varphi(x, y, z) = xu + yv + zw \tag{31}$$

and u, v, w may be obtained from equation (30) by inspection (cf. equations 18 and 19).

The results may be verified by evaluating u on the surface z = ax. Substituting equation (20) into the first term of equation (30), then,

$$\bar{u} = \frac{-\Delta p}{4\, q_\infty} = -\frac{p - p'}{4\, q_\infty} \quad \text{for} \quad 0 < y < mx$$

$$= 0 \quad \text{for} \quad y < 0, \quad \text{or} \quad y > mx.$$

Thus the horizontal component of velocity on the upper surface exactly equals one quarter of the pressure difference between the lower and upper surfaces, divided by q_∞. Since the horizontal component of velocity on the lower surface $\bar{u}'$ is equal and opposite to $\bar{u}$, the pressure coefficient on the lower surface must also be equal and opposite to that on the upper. That is,

$$\begin{aligned} C_{P_{upper}} &= \frac{p}{q_\infty} = -2\bar{u} \\ C_{P_{lower}} &= \frac{p'}{q_\infty} = -2\bar{u}' = 2\bar{u} \end{aligned} \tag{32}$$

The velocity components will now be written out for the special case a = 0, in which the triangular region of constant pressure is located in the x, y plane. Two terms in each of the u and w velocity component formulae require special attention. The limits of these two terms as a goes to zero are written out below:

$$\lim_{a \to 0} \left\{ \frac{1}{a} \left[m^2 \tanh^{-1} \frac{\sqrt{x^2 - \beta^2(y^2 + z^2)}}{x} \right.\right.$$

$$\left.\left. - (a^2 + m^2)\sqrt{1 - \beta^2 a^2} \tanh^{-1} \frac{\sqrt{(1 - \beta^2 a^2)\left(x^2 - \beta^2(y^2 + z^2)\right)}}{x - \beta^2 az} \right] \right\}$$

$$= - \frac{m^2 z}{y^2 + z^2} \sqrt{x^2 - \beta^2(y^2 + z^2)} \tag{33}$$

$$\lim_{a \to 0} \left\{ \frac{1}{a} \left[m^2 \tan^{-1} \frac{(ay - mz)\sqrt{x^2 - \beta^2(y^2 + z^2)}}{x(my + az) - (y^2 + z^2)} \right.\right.$$

$$\left.\left. - (a^2 + m^2) \tan^{-1} \frac{m(z - ax)\sqrt{x^2 - \beta^2(y^2 + z^2)}}{y\left[(y - mx) - \beta^2 a(ay - mz)\right] + (z - ax)^2} \right] \right\}$$

$$= - \frac{m^2 y}{y^2 + z^2} \sqrt{x^2 - \beta^2(y^2 + z^2)} \tag{34}$$

The velocity components for this special case (a = o) may now be written:

$$u_3 = - \frac{\Delta p}{4\pi q_\infty} \tan^{-1} \frac{mz\sqrt{x^2 - \beta^2(y^2 + z^2)}}{y^2 + z^2 - mxy}$$

$$v_3 = \frac{\Delta p}{4\pi q_\infty} \left\{ \frac{1}{m} \tan^{-1} \frac{mz\sqrt{x^2 - \beta^2(y^2 + z^2)}}{y^2 + z^2 - mxy} - \frac{z}{y^2 + z^2} \sqrt{x^2 - \beta^2(y^2 + z^2)} \right\}$$

$$w_3 = - \frac{\Delta p}{4\pi q_\infty} \left\{ \frac{1}{m} \left[\sqrt{1 - \beta^2 m^2} \cosh^{-1} \frac{x - \beta^2 my}{\beta\sqrt{(mx - y)^2 + (1 - \beta^2 m^2) z}} \right.\right.$$

$$\left.\left. - \cosh^{-1} \frac{x}{\beta\sqrt{y^2 + z^2}} \right] - \frac{y}{y^2 + z^2} \sqrt{x^2 - \beta^2(y^2 + z^2)} \right\} \tag{35}$$

This expression for w_3, with $z = 0$, agrees with the downwash function presented by other investigators for a triangular plate with uniform loading. (See, for example, equation 32 of reference 8.)

Classification of the velocity functions. — It is apparent from the preceding analysis that certain functions appear repeatedly in the equations for the perturbation velocity components and potential functions, equations (18), (22), (23), (30), and (35). These functions are listed below:

$$F1 = \tan^{-1} \frac{m(z - ax)\sqrt{x^2 - \beta^2(y^2 + z^2)}}{y\left[(y - mx) - \beta^2 a(ay - mz)\right] + (z - ax)^2}$$

$$F2 = \frac{1}{\sqrt{1 - \beta^2(a^2 + m^2)}} \cosh^{-1} \frac{x - \beta^2(my + az)}{\beta\sqrt{(y - mx)^2 + (z - ax)^2 - \beta^2(ay - mz)^2}}$$

$$F3 = \tan^{-1} \frac{(ay - mz)\sqrt{x^2 - \beta^2(y^2 + z^2)}}{x(my + az) - (y^2 + z^2)}$$

$$F4 = \left(F3 - (1 + a^2/m^2)\ F1\right)(m/a)$$

$$F5 = \tanh^{-1} \frac{\sqrt{x^2 - \beta^2(y^2 + z^2)}}{x}$$

$$F6 = \sqrt{1 - \beta^2 a^2}\ \tanh^{-1} \frac{\sqrt{(1 - \beta^2 a^2)\left(x^2 - \beta^2(y^2 + z^2)\right)}}{x - \beta^2 az}$$

$$F7 = \left(F5 - (1 + a^2/m^2)\ F6\right)(m/a) \tag{36}$$

These functions may all be conveniently rewritten in terms of inverse cosines, or inverse hyperbolic cosines, as follows:

$$F1 = \frac{z - ax}{|z - ax|} \cos^{-1} \frac{y\left[(y - mx) - \beta^2 a(ay - mz)\right] + (z - ax)^2}{\sqrt{\left[(z - ax)^2 + (1 - \beta^2 a^2)y^2\right]\left[(y - mx)^2 + (z - ax)^2 - \beta^2(ay - mz)^2\right]}}$$

$$F2 = \frac{1}{\sqrt{1 - \beta^2(a^2 + m^2)}} \cosh^{-1} \frac{x - \beta^2(my + az)}{\beta\sqrt{(y - mx)^2 + (z - ax)^2 - \beta^2(ay - mz)^2}}$$

$$F3 = \frac{mz - ay}{|mz - ay|} \cos^{-1} \frac{-x(my + az) + (y^2 + z^2)}{\sqrt{(y^2 + z^2)\left[(y - mx)^2 + (z - ax)^2 - \beta^2(ay - mz)^2\right]}}$$

$$F4 = \left(F3 - (1 + a^2/m^2)\ F1\right)(m/a)$$

$$F5 = \cosh^{-1} \frac{x}{\beta\sqrt{y^2 + z^2}}$$

$$F6 = \sqrt{1 - \beta^2 a^2} \cosh^{-1} \frac{x - \beta^2 az}{\beta\sqrt{(z - ax)^2 + (1 - \beta^2 a^2)y^2}}$$

$$F7 = \left(F5 - (1 + a^2/m^2)\ F6\right)(m/a) \tag{37}$$

If $a = 0$, the limiting forms of F4 and F7 must be used. Referring to equations (33) and (34),

$$F4 = \frac{-m\ y}{y^2 + z^2} \sqrt{x^2 - \beta^2(y^2 + z^2)}$$

$$F7 = \frac{-m\ z}{y^2 + z^2} \sqrt{x^2 - \beta^2(y^2 + z^2)} \tag{38}$$

The behavior of the functions F1 and F3 will now be examined. In the plane of the singularity, $z = ax$, the function F1 jumps from the value of π, just above the plane, to $-\pi$ just below, for all points behind the leading edge. The function is continuous and zero everywhere in this plane ahead of the leading edge and outboard of the side edge. The function F3 similarly exhibits a discontinuity of 2π in the plane $z = (a/m)y$ for $0 < y < mx$, and is continuous and zero elsewhere in this plane. Both functions are asymmetric above and below their respective planes of discontinuity.

It should be recalled that the seven functions listed above were derived for a triangular surface having a subsonic leading edge, that is, the leading edge is swept back inside the Mach cone from the origin, and for which $\beta^2(a^2 + m^2) < 1$. In this case, it can easily be verified that all of the functions go to zero for $x \geq \beta\sqrt{y^2 + z^2}$, which includes all points on or outside of the Mach cone.

For the case in which the leading edge of the triangular surface touches, or extends outside the Mach cone from the origin (sonic or supersonic leading edge), all functions are unaltered for points inside the Mach cone from the origin, except F2, which becomes:

$$F2 = \frac{\sqrt{x^2 - \beta^2(y^2 + z^2)}}{x - \beta y} \qquad \text{for} \qquad \beta^2(a^2 + m^2) = 1 \tag{39}$$

and

$$F2 = \frac{1}{\sqrt{\beta^2(a^2 + m^2) - 1}} \cos^{-1} \frac{x - \beta^2(my + az)}{\beta\sqrt{(y - mx)^2 + (z - ax)^2 - \beta^2(ay - mz)^2}}$$

$$\text{for} \qquad \beta^2(a^2 + m^2) > 1 \tag{40}$$

The functions also go to zero for points on or outside the Mach cone from the origin, except in the region inside the envelope of Mach cones from the supersonic leading edge where the functions either go to zero, or take on constant values. The geometry is illustrated by the section at x = constant.

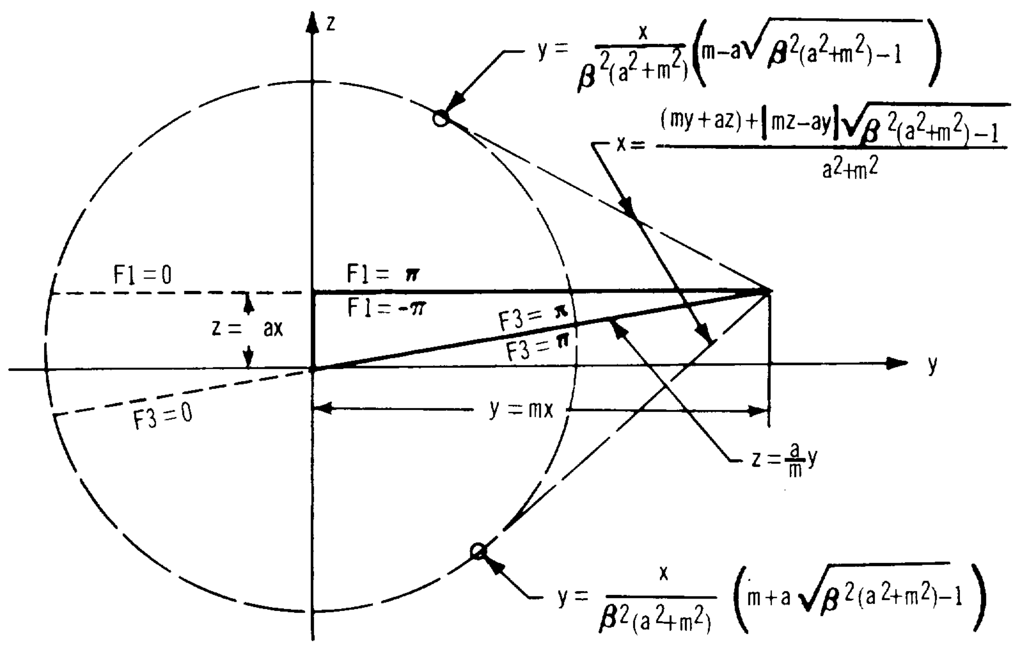

In this region, inside the envelope of Mach cones from the supersonic leading edge,

$$F1 = \pi \quad \text{for} \quad z \geq ax$$
$$\quad = -\pi \quad \text{for} \quad z < ax \tag{41}$$

$$F2 = \frac{\pi}{\sqrt{\beta^2(a^2 + m^2) - 1}} \tag{42}$$

In addition, F4 and F7 are unchanged, and F5 and F6 are zero. Thus an unsymmetric two-dimensional flow region is defined in which the velocity components are constant.

The perturbation velocity components may now be expressed very simply in terms of these new functions. For example

<u>Planar source distribution</u> $(a = 0)$

$$u_1 = -\frac{\bar{w}}{\pi} m \; F2$$

$$v_1 = \frac{\bar{w}}{\pi} (F2 - F5)$$

$$w_1 = \frac{\bar{w}}{\pi} F1 \tag{44}$$

<u>Line source located along x axis</u> $(a = 0, \quad m = 0)$

$$u_2 = -k \; F5$$

$$v_2 = k \; F4$$

$$w_2 = k \; F7 \tag{45}$$

<u>Oblique constant pressure lifting surface</u>

$$u_3 = -\frac{\Delta p}{4\pi q_\infty} F1$$

$$v_3 = \frac{\Delta p}{4\pi q_\infty} \frac{1}{a^2 + m^2} \left[a\left(1 - \beta^2 (a^2 + m^2)\right) F2 + m \, (F3 + F7) \right]$$

$$w_3 = \frac{-\Delta p}{4\pi q_\infty} \frac{m}{a^2 + m^2} \left[\left(1 - \beta^2 (a^2 + m^2)\right) F2 - F5 + F4 \right] \tag{46}$$

Visualization of velocity components. — The following figures depict the three components of velocity corresponding to oblique, constant-pressure lifting surfaces in supersonic flow. For the case $a = 0$ where the pressure discontinuity is located in the x-y plane (figures 3 to 5), the velocity components are given for triangular regions having subsonic, sonic, and supersonic leading edges. The dominant effect of the vortex-like flow around the side edge of the triangles is clearly visible, as is the narrow upwash field in the leading edge region of the subsonic leading-edge wing.

For the nonplanar case, $a = 0.2$, (figures 6 and 7), the velocity components are given only for subsonic and supersonic leading-edges. The flow disturbance is now seen to be centered about the plane $z = ax$, and is no longer symmetrical about the x-y plane. An additional discontinuity occurs in the v and w velocity components in the plane $z = (a/m)y$ (the plane through the x axis that just touches the leading edge), which corresponds to a sheet of vorticity being shed aft of the leading edge. It should also be noted that, for the supersonic leading-edge case, the sidewash and downwash are no longer equal and opposite above and below the plane of wing in the "two-dimensional region" forward of the Mach cone from the apex.

The velocity field in a plane perpendicular to the free-stream direction located one unit behind the apex of a subsonic leading edge, constant-pressure delta wing is presented in figure 8. The vortex sheet trailing from points along the leading edge can be seen to generate a circulatory type of flow on the suction side of the wing. This circulation above the wing may be comparable to the "ram's horn" vortex observed experimentally above the upper surface of highly swept delta wings.

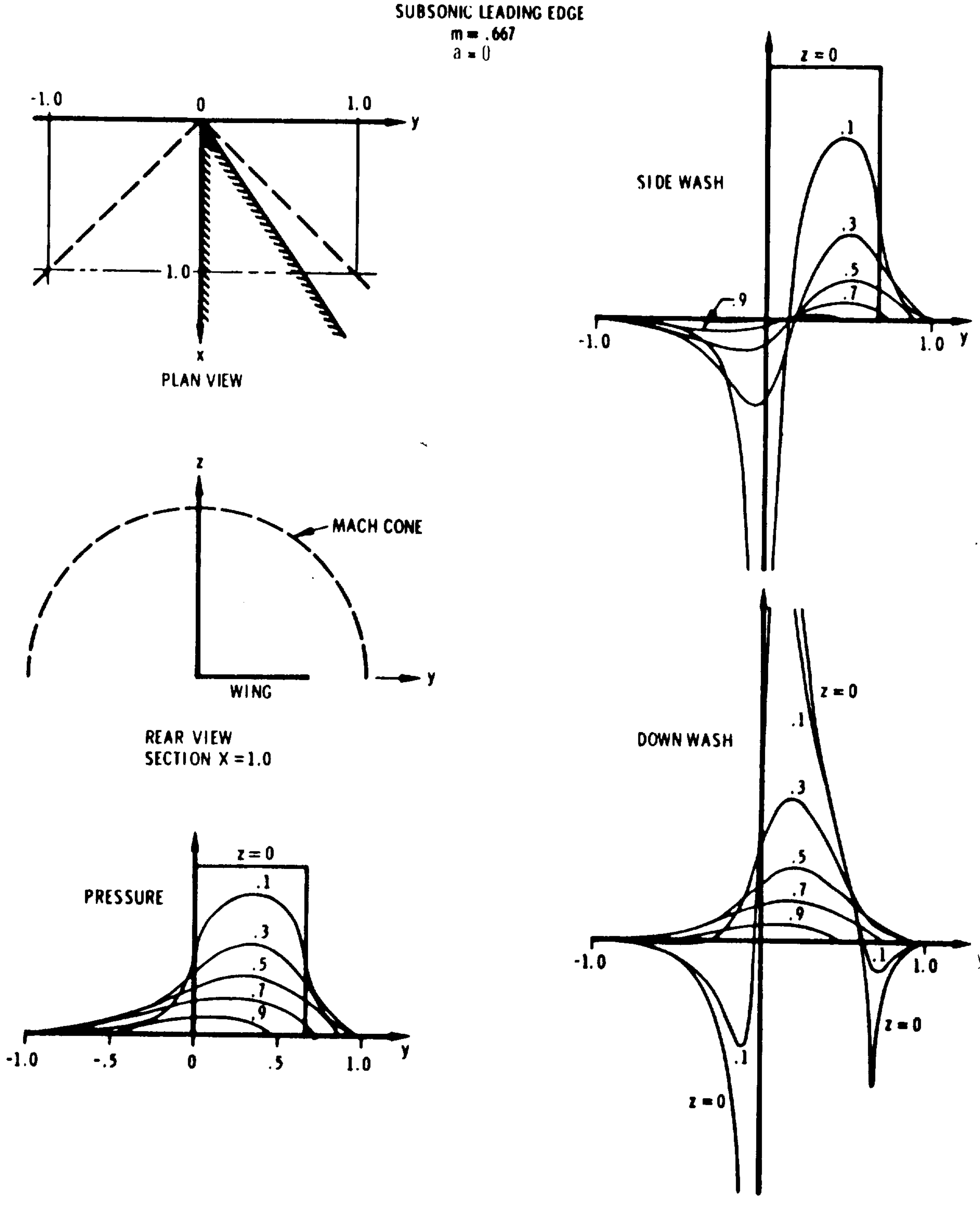

FIGURE 3 VELOCITY COMPONENTS – SUBSONIC LEADING EDGE

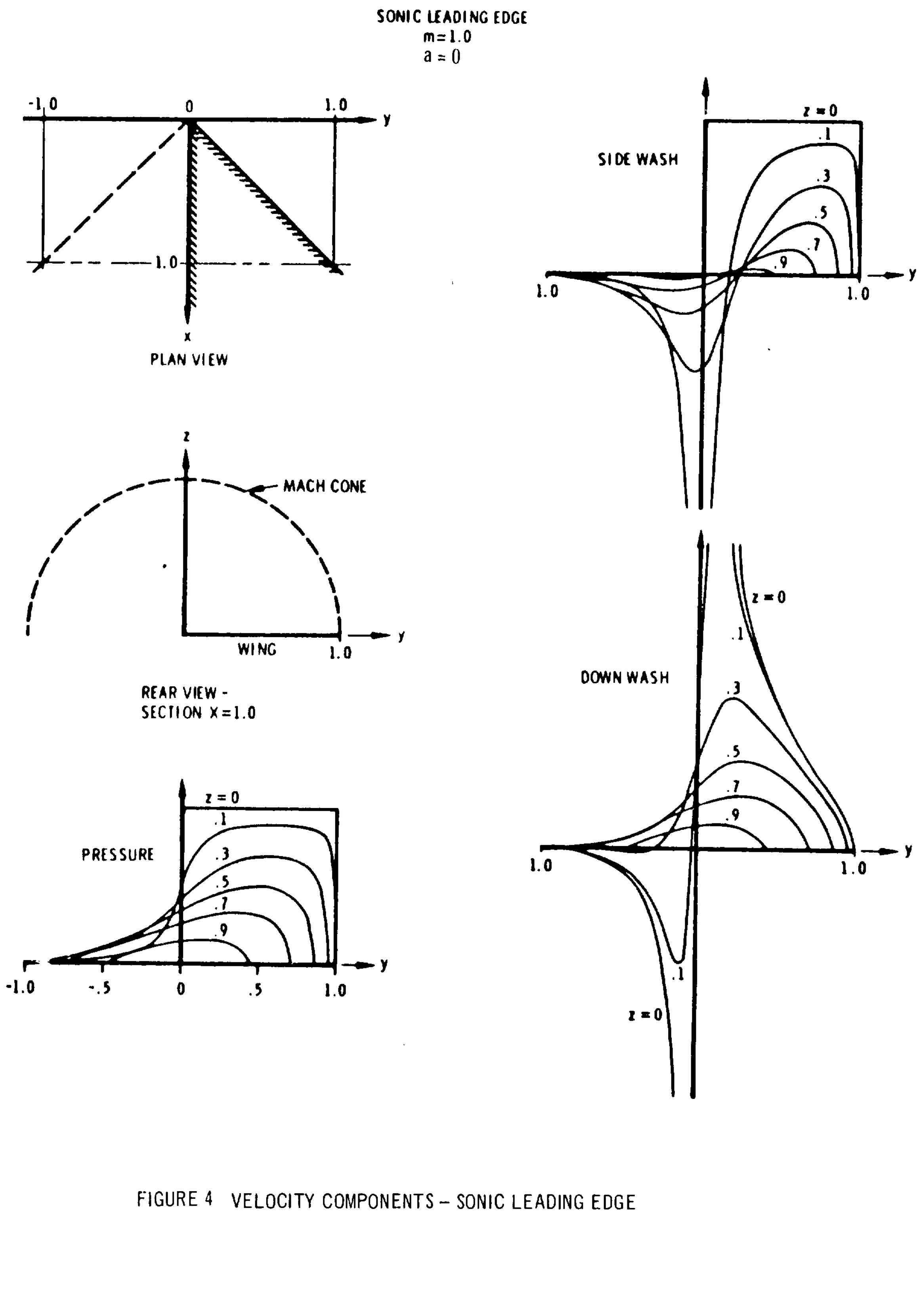

FIGURE 4 VELOCITY COMPONENTS – SONIC LEADING EDGE

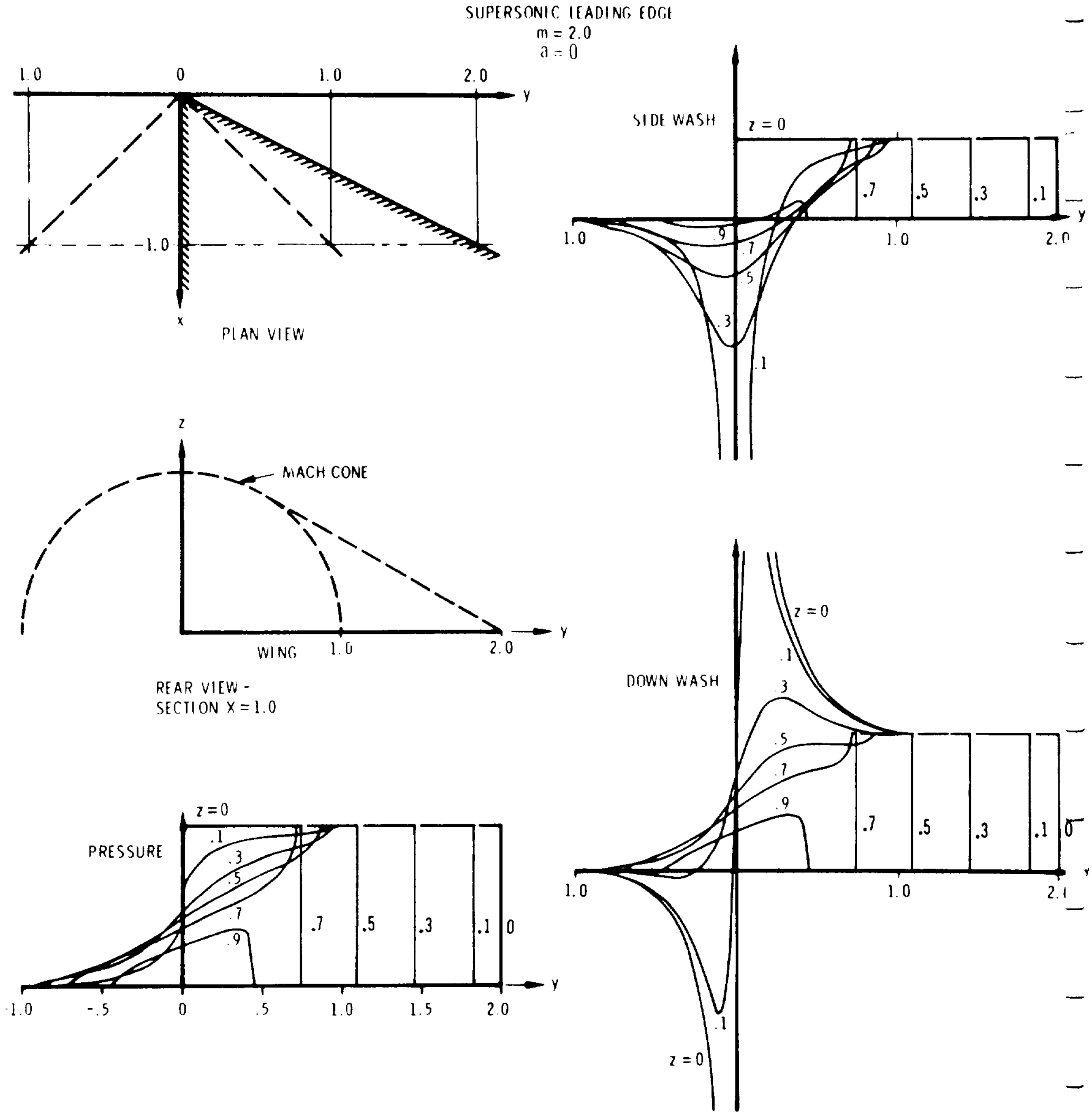

FIGURE 5 VELOCITY COMPONENTS– SUPERSONIC LEADING EDGE

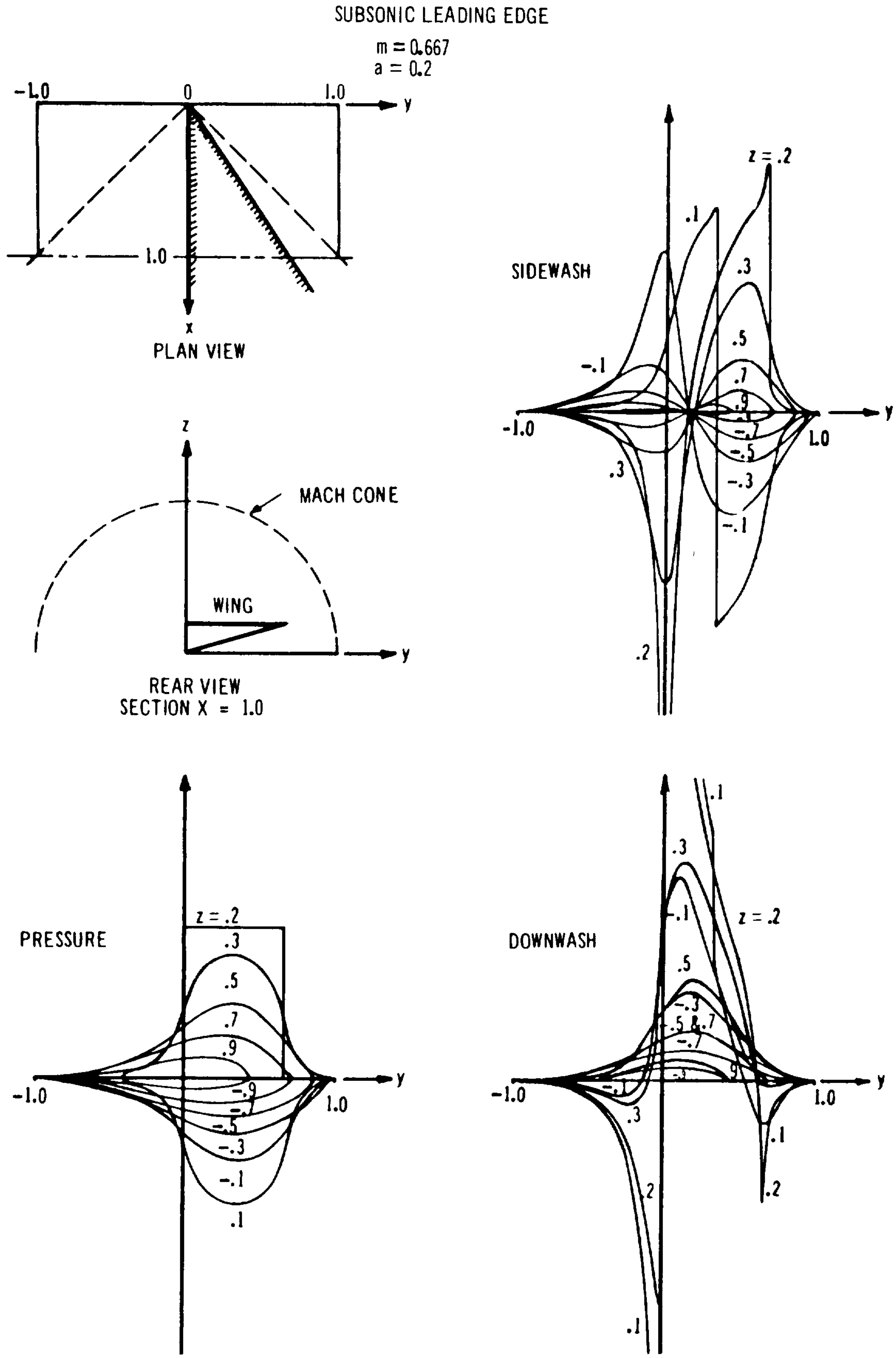

FIGURE 6 VELOCITY COMPONENTS FROM INCLINED SINGULARITY SURFACE – SUBSONIC LEADING EDGE

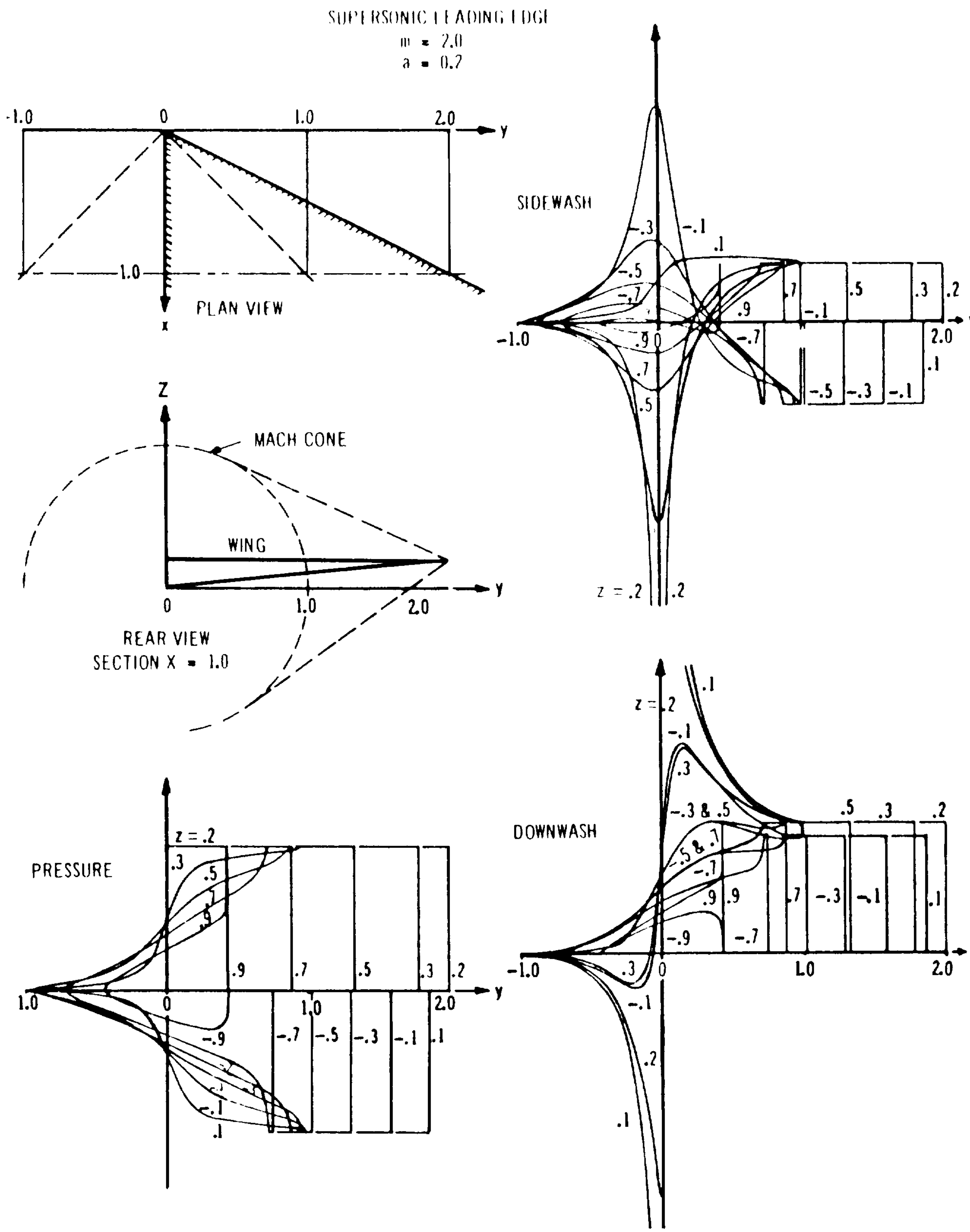

FIGURE 7 VELOCITY COMPONENTS FROM INCLINED SINGULARITY SURFACE – SUPERSONIC LEADING EDGE

CONSTANT PRESSURE DELTA WING

m = .667, a = −.2

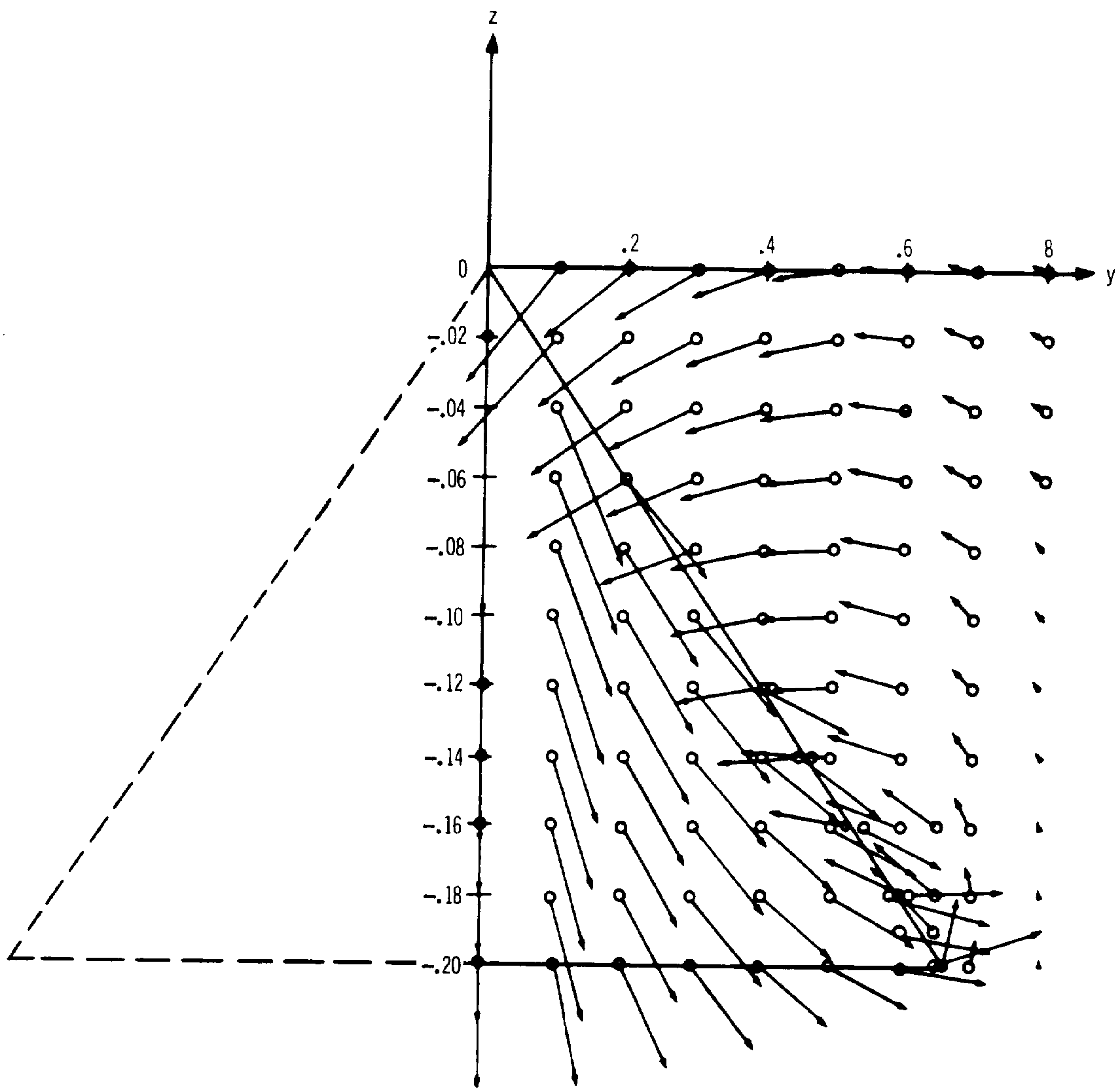

NOTE: VERTICAL SCALE ENLARGED FIVE TIMES

FIGURE 8 FLOW VISUALIZATION – CONSTANT PRESSURE DELTA WING

Derivation of potential equation. — Equation (1) may be rewritten in terms of the cylindrical coordinates x, r, and θ as follows:

$$\beta^2 \varphi_{xx} = \varphi_{rr} + \varphi_r/r + \varphi_{\theta\theta}/r^2 \tag{47}$$

To solve this equation, the perturbed flow will be resolved into two components: the axial component, defined by the axially symmetrical potential φ_a; and the cross component, defined by the potential φ_c. Place

$$\varphi = \varphi_a + \varphi_c \tag{48}$$

Then, for the axially symmetric flow,

$$\beta^2 \varphi_{a_{xx}} = \varphi_{a_{rr}} + \varphi_{a_r}/r \tag{49}$$

and for the cross flow,

$$\beta^2 \varphi_{c_{xx}} = \varphi_{c_{rr}} + \varphi_{c_r}/r + \varphi_{c_{\theta\theta}}/r^2 \tag{50}$$

The potential functions for the axially symmetric flow and the cross flow will be determined separately.

Potential function and velocity components for line sources. — The solution to equation (49) is well known, and is given in reference 9 as follows:

$$\varphi_a(x, r) = - \int_0^{\xi_1} \frac{f(\xi)\, d\xi}{\sqrt{(x - \xi)^2 - \beta^2 r^2}} \tag{51}$$

where $\xi_1 = x - \beta r$, is the intersection of the Mach fore cone from P(x, r) with the x axis.

For the case $f(\xi) = k_s$ = constant, equation (51) represents the potential due to a line source of constant strength distributed along the positive x axis. The solution of equation (51) for this case is given as:

$$\varphi_a = k_s \left(- x \cosh^{-1} \frac{x}{\beta r} + \sqrt{x^2 - \beta^2 r^2} \right) \tag{52}$$

It should be recalled that this same expression was derived earlier by taking the limit of the generalized potential function for a surface distribution of sources (equation 24).

The velocity components corresponding to the constant line source may be obtained by differentiating the potential function and are listed below:

$$u_a = \frac{\partial \varphi_a}{\partial x} = - k_S \cosh^{-1} \frac{x}{\beta r}$$

$$v_{r_a} = \frac{\partial \varphi_a}{\partial r} = \frac{k_S}{r} \sqrt{x^2 - \beta^2 r^2}$$

$$v_{\theta_a} = \frac{1}{r} \frac{\partial \varphi_a}{\partial \theta} = 0 \tag{53}$$

The velocity components in the Cartesian coordinate system are given by equation (23).

Potential function and velocity components for line doublets. — The solution to equation (50) is also given in reference 9 :

$$\varphi_c(x, r, \theta) = \frac{\cos \theta}{r} \int_0^{\xi_1} \frac{m(\xi)\ (x - \xi)\ d\xi}{\sqrt{(x - \xi)^2 - \beta^2 r^2}} \tag{54}$$

For the case $m(\xi) = k_D =$ constant, equation (54) represents the potential resulting from a line doublet of constant strength distributed along the positive x axis. The solution of equation (54) for this case yields:

$$\varphi_c = - k_D \frac{\beta^2 r \cos \theta}{2} \left(\cosh^{-1} \frac{x}{\beta r} - \frac{x}{\beta r} \sqrt{\frac{x^2}{\beta^2 r^2} - 1} \right) \tag{55}$$

The velocity components corresponding to this case may also be obtained by differentiation. The results are listed below:

$$u_c = \frac{\partial \varphi_c}{\partial x} = k_D \beta \cos \theta \sqrt{\frac{x^2}{\beta^2 r^2} - 1}$$

$$v_{r_c} = \frac{\partial \varphi_c}{\partial r} = - k_D \frac{\beta^2 \cos \theta}{2} \left(\cosh^{-1} \frac{x}{\beta r} + \frac{x}{\beta r} \sqrt{\frac{x^2}{\beta^2 r^2} - 1} \right)$$

$$v_{\theta_c} = \frac{1}{r} \frac{\partial \varphi_c}{\partial \theta} = - k_D \frac{\beta^2 \cos \theta}{2} \left(\cosh^{-1} \frac{x}{\beta r} - \frac{x}{\beta r} \sqrt{\frac{x^2}{\beta^2 r^2} - 1} \right) \tag{56}$$

4.4 Formation of the Aerodynamic Matrix

Geometrical considerations. —Some description of the geometry of the wing-body combination is deferred until section 5. In this section, only sufficient geometrical description will be given to continue the development of the aerodynamic theory.

Briefly, the wing and body geometry is specified with respect to an arbitrary coordinate system, or "defining axes" X, Y, Z, as illustrated in the following sketch. The defining axes may be inclined at an angle of attack α_D to the free stream.

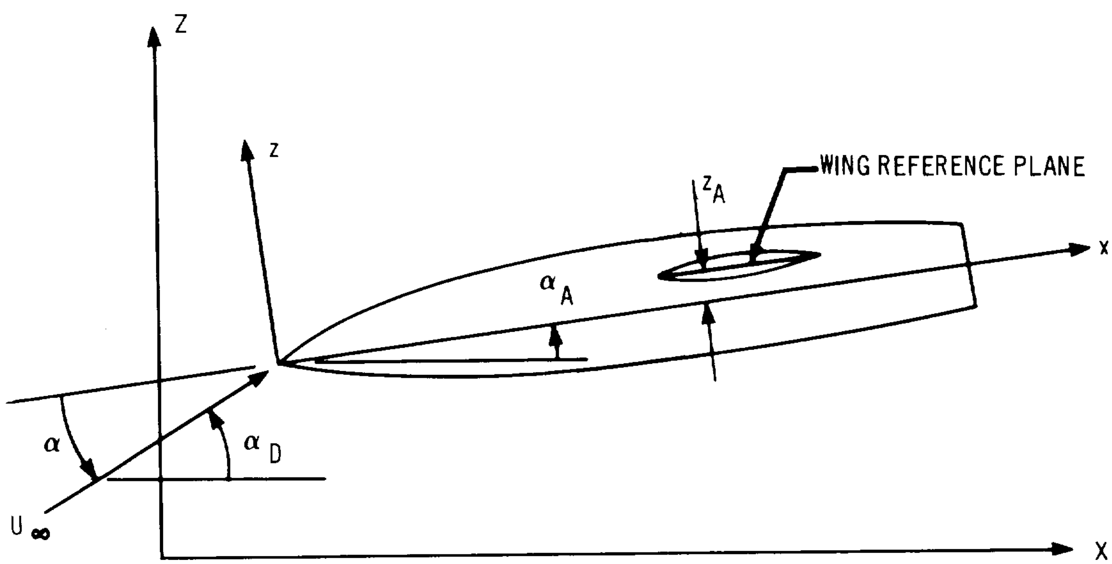

The body is restricted to have circular, or nearly circular, cross sections, but may have arbitrary camber and incidence. The wing may have any planform that can be approximated by straight-line segments, and can be mounted at any height above or below the body axis. The effect of dihedral is not included. The wing sections may have arbitrary camber, twist, incidence, and thickness distributions.

The "body axes" x, y, z are established by the geometry definition program so that the x axis passes through the centroids of the body cross sections at the nose and base, while the y axis remains parallel to the Y axis. The body coordinate system is therefore related to the defining axes by a simple transformation involving a translation of the body in the X-Z plane, followed by a rotation about the Y axis through the angle α_A. For many configurations, the wing and body can be specified most simply in terms of the body axes directly.

Referring to the sketch, it can be seen that in general the x-y plane will be inclined at an angle $\alpha = \alpha_D - \alpha_A$ with respect to the free stream. The component of the free-stream velocity parallel to the x axis is $U_\infty \cos \alpha$, and the component parallel to the z axis is $U_\infty \sin \alpha$. In the following analysis, it will be assumed that α is sufficiently small so that $\cos \alpha \approx 1$, and $\sin \alpha \approx \alpha$. Therefore, for all practical purposes the axial component of the free-stream velocity may be set equal to the free-stream velocity U_∞, while the cross component, which represents the additional effects of an angle of attack, is set equal to $U_\infty \alpha$. This approximation is consistent with the underlying assumptions of linear theory, and introduces considerable simplification into the analysis.

The transformed body is now approximated by an equivalent body of revolution about the x axis. Each section of the equivalent body has the same cross-sectional area as the original body, while the body camber is defined by the heights of the centroids of the original sections above the x axis. The transformed wing is defined to lie in a plane parallel to the x–y plane, located at an average height z_A above or below that plane. The line of intersection of this planar wing and the transformed body is calculated within the program.

Finally, the surfaces of the transformed wing and body are subdivided into a large number of rectilinear panels. The leading and trailing edges of these panels may be swept forward or back in an arbitrary way, but the side edges must be constrained to lie in planes parallel to the x axis. To meet this latter requirement, each panel may be further subdivided into two or three parts, to be described later. The panels are defined by the x, y, z coordinates of the four corner points. A typical panel arrangement on a wing-body combination is illustrated in figure 1 (page 11).

A primed system of coordinates is now introduced, originating at a specified corner point k of panel j. The x' axis is defined to be parallel to the x axis, while the y' axis is defined to lie in the plane of the panel as in figure 1. It can be seen that, in general, the x'-y' plane is inclined at an angle θ_j to the x-y plane. It should be noted that the panel may also be inclined to an angle $\alpha_j = dz'/dx'$ with respect to the x'-y' plane, as illustrated in the following sketch.

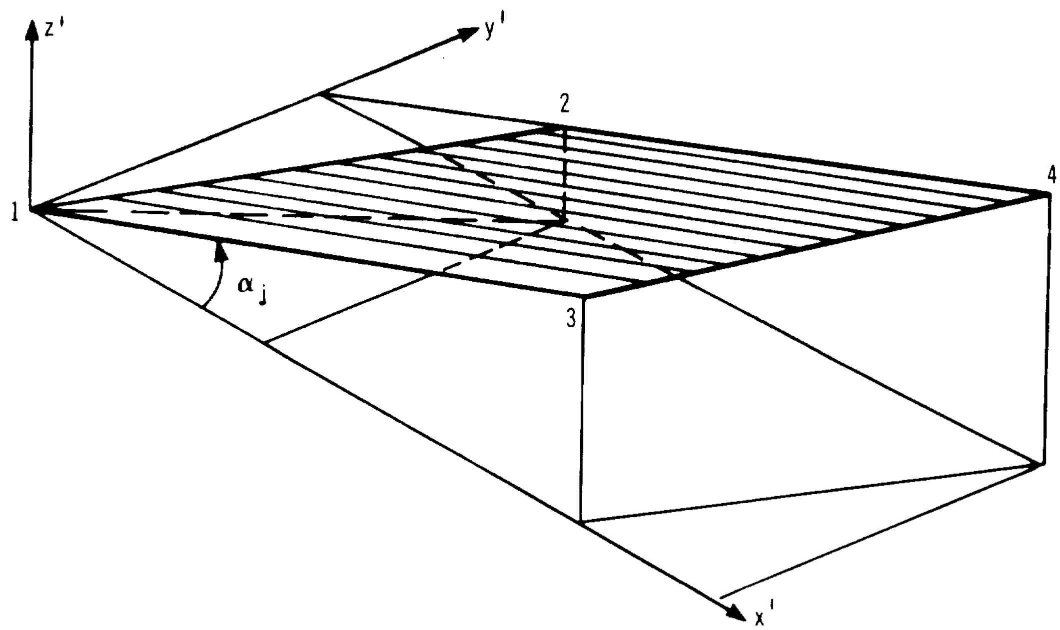

The panel corner point-numbering convention is shown on the sketch. The leading edge lies between points 1 and 2, and the trailing edge between points 3 and 4. The projection of the leading edge in the x'-y' plane has the slope m_{j1}, while the projection of the trailing edge in the x'-y' plane has the slope m_{j3}. Note that $m_{j1} = m_{j2}$ and $m_{j3} = m_{j4}$. The side edge between points 1 and 3 always lies in the x'-z' plane, and the side edge between points 2 and 4 always lies in a plane parallel to the x'-z' plane.

The coordinates of a point i (x_i, y_i, z_i) may be expressed in terms of the primed system of coordinates originating at corner k of panel j as follows:

$$x'_{ijk} = x_i - x_{jk}$$

$$y'_{ijk} = (y_i - y_{jk}) \cos \theta_j + (z_i - z_{jk}) \sin \theta_j$$

$$z'_{ijk} = (z_i - z_{jk}) \cos \theta_j - (y_i - y_{jk}) \sin \theta_j \tag{57}$$

where $\cos \theta_j = \dfrac{C_j}{\sqrt{B_j^2 + C_j^2}}$; $\sin \theta_j = \dfrac{B_j}{\sqrt{B_j^2 + C_j^2}}$

and

$$B_j = \begin{vmatrix} x_{j1} & z_{j1} & 1 \\ x_{j2} & z_{j2} & 1 \\ x_{j3} & z_{j3} & 1 \end{vmatrix} \quad ; \quad C_j = \begin{vmatrix} x_{j1} & y_{j1} & 1 \\ x_{j2} & y_{j2} & 1 \\ x_{j3} & y_{j3} & 1 \end{vmatrix}$$

In general, the point i will be located at the control point of panel i. Note that $\theta = 0$ for all wing panels is a linearizing assumption.

Superposition of the velocity components for the surface singularities. — Formulae for the three velocity components u, v, w are given in section 4.2 for the two types of surface singularities chosen: surface distributions of sources and surface distributions of vortices. The velocity components are derived for the elementary case in which the surface singularities are located on semi-infinite triangular regions, and are expressed in terms of the coordinate system originating at the apex of this triangular region.

The velocity components induced by a distribution of singularities over a finite panel may now be obtained by combining four such elementary solutions originating at each of the four corner points of the panel, using the method of superposition. The procedure is illustrated by the following sketch:

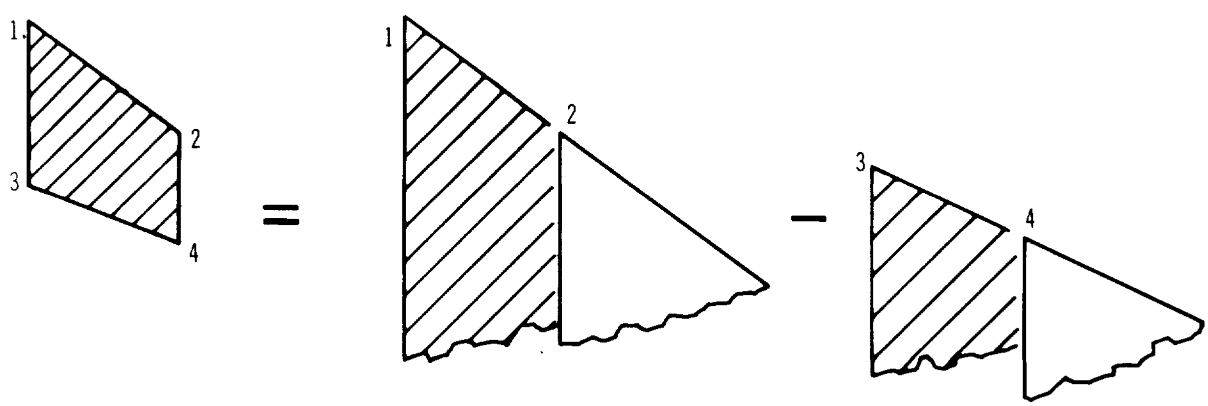

FINITE PANEL = (REGION 1 – REGION 2) – (REGION 3 – REGION 4)

The effect of a semi-infinite strip of singularities having the same width as the panel is obtained by subtracting the triangular region with origin at corner point 2 from that originating at corner point 1. Both regions must have the same leading-edge slope and constant singularity strengths. The singularity strength everywhere outside this strip is now zero. If the semi-infinite strip corresponding to the difference between the triangular regions originating at corner points 3 and 4 is now subtracted from the original strip, then it can be seen that the constant singularity strength will be limited to the area enclosed by the panel and will be zero elsewhere. It is not necessary for the second strip to have the same leading-edge slope as the first, but it must have equal strength.

In the method of aerodynamic influence coefficients, all the singularity distributions are defined to have unit strengths; consequently, the superposition of the velocity components corresponding to the elementary surface singularities may proceed directly. For example, the velocity components at the control point of panel i due to a distribution of singularities on panel j may be written as follows:

$$\begin{aligned} u'_{ij} &= q_{ij1} - q_{ij2} - q_{ij3} + q_{ij4} \\ v'_{ij} &= r_{ij1} - r_{ij2} - r_{ij3} + r_{ij4} \\ w'_{ij} &= c_{ij1} - c_{ij2} - c_{ij3} + c_{ij4} \end{aligned} \tag{58}$$

where

$$\begin{aligned} q_{ijk} &= P(a'_j,\ b'_{jk},\ \xi'_{ijk},\ y'_{ijk},\ z'_{ijk}) \\ r_{ijk} &= \beta\, S(a'_j,\ b'_{jk},\ \xi'_{ijk},\ y'_{ijk},\ z'_{ijk}) \\ c_{ijk} &= \beta\, D(a'_j,\ b'_{jk},\ \xi'_{ijk},\ y'_{ijk},\ z'_{ijk}) \end{aligned} \tag{59}$$

and

$$a'_j = \beta \tan \alpha_j = \beta\, \frac{(z_{j3} - z_{j1}) \cos \theta_j - (y_{j3} - y_{j1}) \sin \theta_j}{x_{j3} - x_{j1}} \tag{60}$$

$$\begin{aligned} b'_{jk} = \frac{1}{\beta\, m_{jk}} &= \frac{x_{j2} - x_{j1}}{\beta \left[(y_{j2} - y_{j1}) \cos \theta_j + (z_{j2} - z_{j1}) \sin \theta_j \right]},\ k = 1,\ 2 \\ &= \frac{x_{j4} - x_{j3}}{\beta \left[(y_{j4} - y_{j3}) \cos \theta_j + (z_{j4} - z_{j3}) \sin \theta_j \right]},\ k = 3,\ 4 \end{aligned} \tag{61}$$

Also, $\xi'_{ijk} = x'_{ijk}/\beta$ where x'_{ijk}, y'_{ijk}, and z'_{ijk} are defined by equation (57).

The functions P, S, and D in equation (59) are written out in full in Appendix B for both types of surface singularities.

Calculation of the aerodynamic influence coefficients for surface singularities. — The velocity component that is both normal to the body axis and in a plane which is parallel to the body axis and perpendicular to each panel surface through its control point, is required. The magnitude of this normal velocity component induced at control point i by the distribution of singularities of unit strength on panel j is defined to be the aerodynamic influence coefficient a_{ij}. An expression for the aerodynamic influence coefficients may be derived by an examination of the projections of the velocity components in a double-primed system of coordinates associated with panel i, as illustrated in the following sketch:

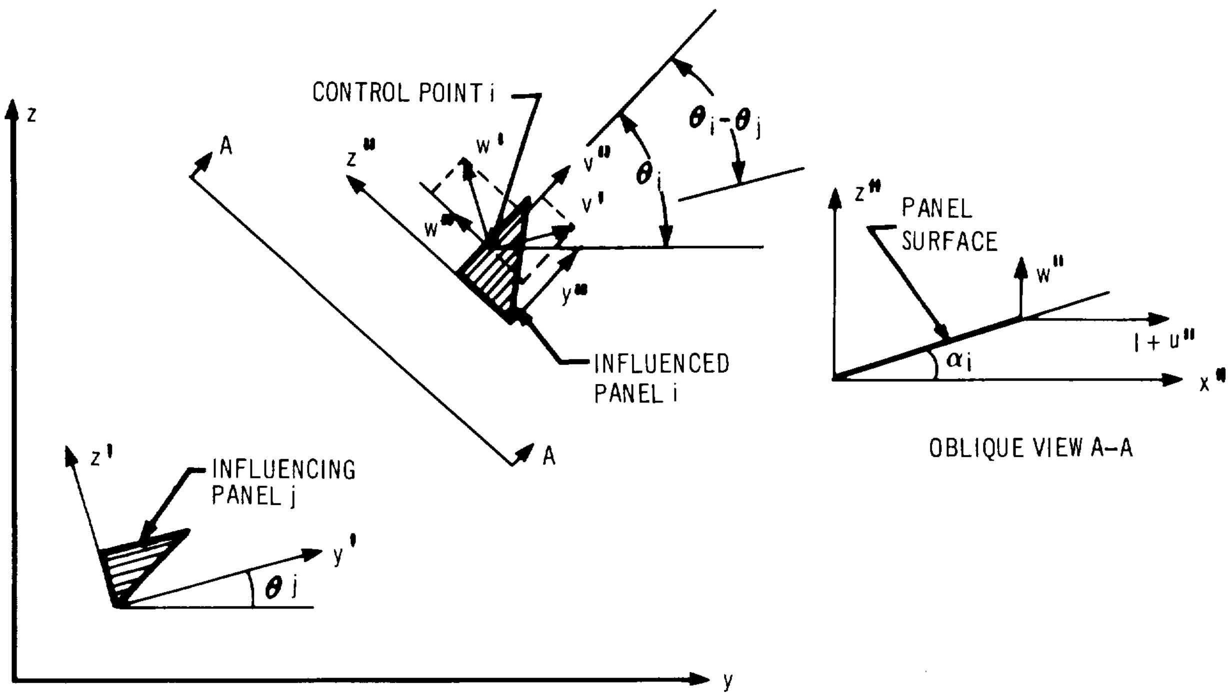

Then $$a_{ij} = w''_{ij} = w'_{ij} \cos(\theta_i - \theta_j) - v'_{ij} \sin(\theta_i - \theta_j) \tag{62}$$

The other two components of velocity may be written:

$$u''_{ij} = u'_{ij}$$

$$v''_{ij} = v'_{ij} \cos(\theta_i - \theta_j) + w'_{ij} \sin(\theta_i - \theta_j) \tag{63}$$

where u', v', and w' are given by equation (58).

Additional subscripts are used to classify the aerodynamic influence coefficients according to the location of the control point i on the wing or body, the location of the influencing panel j, and the type of singularity the panel contains. For example, the influence on wing panel i by a surface distribution of vorticity on body panel j is denoted by $a_{WBV_{ij}}$, and the influence on body panel i by a surface distribution of sources on wing panel j is denoted by $a_{BWS_{ij}}$.

Certain special cases will now be considered so that the formulation of the aerodynamic influence coefficients can be completed.

Multiple part panels: There are certain areas on the wing and body where the panels cannot be represented by a single planar region in which both side edges lie in planes parallel to, or coincident with, x'-z' plane. These areas may occur at wing tips, along wing-body intersections, and on the surfaces of opening or closing bodies. In these areas, the panels must be further subdivided into two or three parts, each part of which meets the side-edge requirement, as illustrated below. It should be noted that a triangular part is considered to have a side edge of zero length.

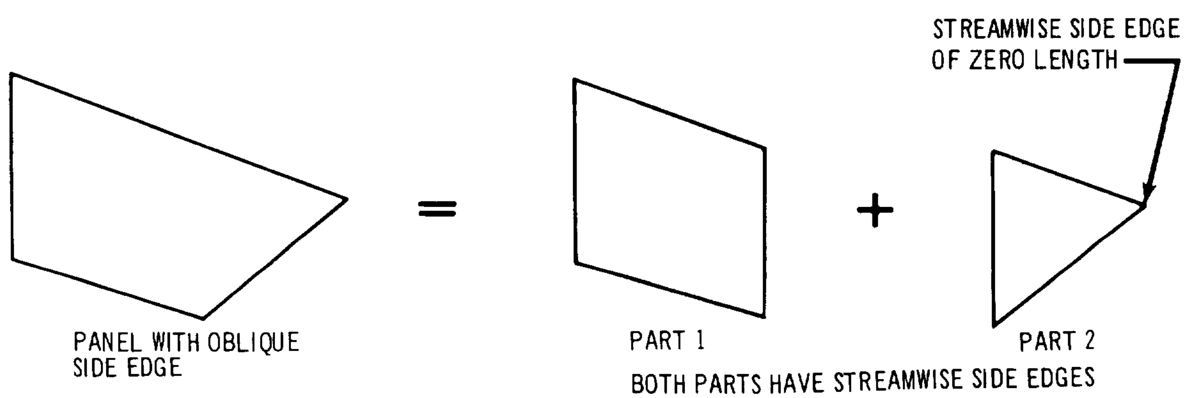

In case a multiple part panel is an influencing panel, the velocity components induced by each of the parts at a given control point are calculated separately, and the total contribution determined by adding these individual components together. The influence coefficient is then formed from these velocity components as before. If the influenced panel is a multiple part panel, the velocity components and influence coefficient are calculated at a single control point representing the combined areas.

Panels having negative slopes: The formulae for the velocity components have been presented only for the case in which the semi-infinite triangular region containing the singularities has a positive leading-edge slope ($m_{jk} \geq 0$). These formulae may be extended to the case in which the region has a negative leading-edge slope by applying a slight variation in the superposition procedure used to calculate the effect of a finite panel as sketched.

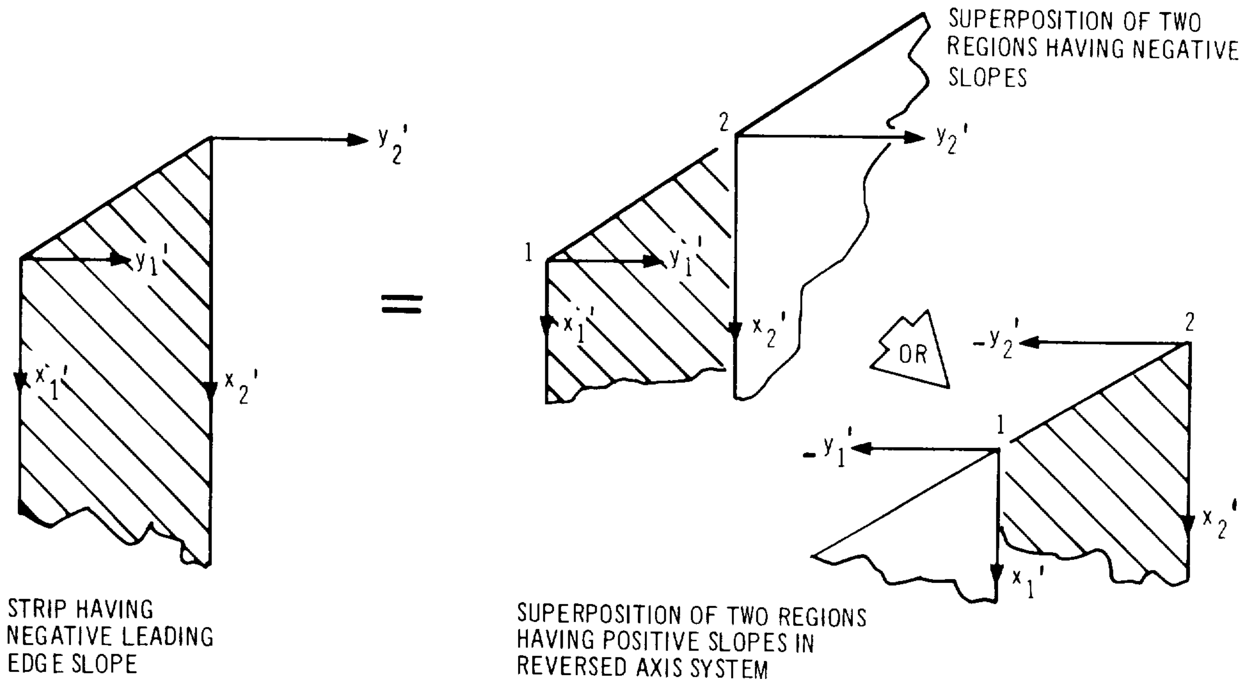

The influence of a semi-infinite strip of constant pressure at a given point i may be calculated by taking the difference of the influences of the two semi-infinite triangular regions of negative slope having vertices at corners 1 and 2, as before. However, this case is calculated in an equivalent manner by taking the difference between the influences of the two semi-infinite triangular regions having positive leading-edge slopes as shown in the right part of the sketch, where the order of subtraction and the direction of the y' axes from the corner points must be reversed. The velocity components are still given by the formulae of equation (58), with the following modifications to the terms q_{ijk}, r_{ijk}, and c_{ijk}:

$$
\begin{aligned}
q_{ijk} &= \pm P\,(a'_j, \pm b'_{jk}, \xi'_{ijk}, \pm y'_{ijk}, z'_{ijk}) \\
r_{ijk} &= \beta\, S\,(a'_j, \pm b'_{jk}, \xi'_{ijk}, \pm y'_{ijk}, z'_{ijk}) \\
c_{ijk} &= \pm \beta\, D\,(a'_j, \pm b'_{jk}, \xi'_{ijk}, \pm y'_{ijk}, z'_{ijk})
\end{aligned}
\tag{64}
$$

where $\qquad + \text{ is for } m_{jk} \geq 0$

and $\qquad - \text{ is for } m_{jk} < 0$

Panel symmetry effects: For configurations having panels located symmetrically on the right and left side of the x-z plane, it is possible to introduce considerable simplification into the computer program by calculating these symmetrical panels in pairs. The formulae for the velocity components in the double primed system of coordinates associated with panel i have been given by equations (62) and (63). If panel i has an image panel $\bar{i}$ associated with it, located on the opposite side of the x-z plane, the velocity components in the double primed system of this image panel may be written:

$$
\begin{aligned}
\overline{w}''_{ij} &= \overline{w}'_{ij} \cos(\theta_i + \theta_j) + \bar{v}'_{ij} \sin(\theta_i + \theta_j) \\
\bar{v}''_{ij} &= \overline{w}'_{ij} \sin(\theta_i + \theta_j) - \bar{v}'_{ij} \cos(\theta_i + \theta_j)
\end{aligned}
\tag{65}
$$

The sketch on the following page illustrates the geometrical relationship between the panel i and its image panel $\bar{i}$, and the location of the influencing panel. It can easily be seen that the velocity components for both cases can be expressed by the single pair of formulae as follows:

$$
\begin{aligned}
w''_{ij} &= w'_{ij} \cos(\theta_i \pm \theta_j) \pm \Big| \; v'_{ij} \sin(\theta_i \pm \theta_j) \\
v''_{ij} &= w'_{ij} \sin(\theta_i \pm \theta_j) \pm \Big| \; v'_{ij} \cos(\theta_i \pm \theta_j)
\end{aligned}
\tag{66}
$$

provided that the y'_{ijk} and z'_{ijk} coordinates used in equations (59) or (64) are replaced by

$$y'_{ijk} = (\pm y_i - y_{jk}) \cos \theta_j + (z_i - z_{jk}) \sin \theta_j$$

$$z'_{ijk} = (z_i - z_{jk}) \cos \theta_j - (\pm y_i - y_{jk}) \sin \theta_j \tag{67}$$

where the upper sign is used for i and j on the same side of the x-y plane and the lower sign is used for i and j on the opposite side of the x-y plane (image panel $\bar{i}$), in both of the above equations.

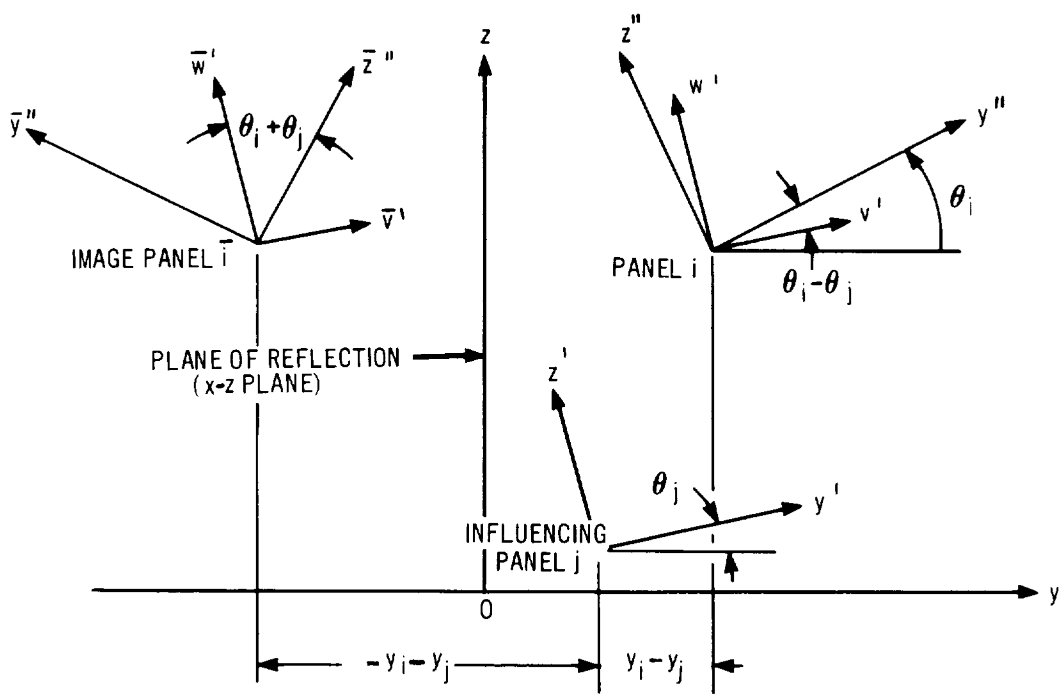

Calculation of the aerodynamic influence coefficients for line singularities. — The line singularities used to represent the effects of the body thickness, camber, and incidence are located along the positive x axis. The component of velocity induced by these singularities which is normal to the x axis and in a plane parallel to this axis and perpendicular to the surface at a control point is required. The magnitude of this velocity component induced at control point i by the k^{th} singularity of unit strength is defined to be the aerodynamic influence coefficient a_{ik}. The following sketch illustrates the geometry for a control point on the surface of the body and for a control point on an arbitrary panel.

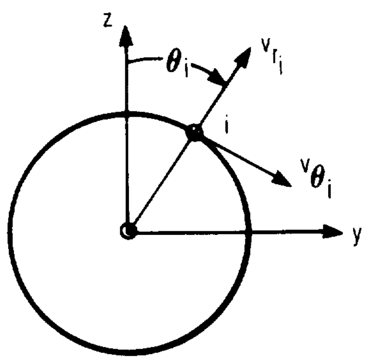

CONTROL POINT ON
BODY SURFACE

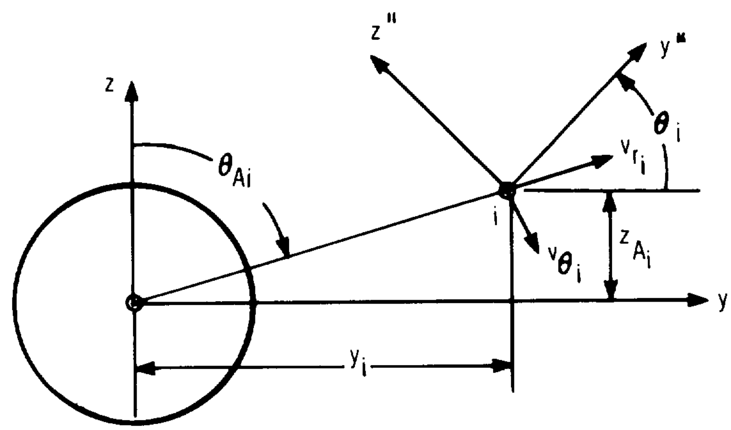

CONTROL POINT ON ARBITRARY (WING OR BODY) PANEL

On the surface of the body, θ_i is given by the angular position of point i, measured from the x-z plane. On wing (or body) panels θ_i is given by the inclination of the x''-y'' plane to the x-y plane as before.

On the surface of the body,

$$a_{ik} = v_{r_{ik}} \tag{68}$$

On the surface of a panel,

$$a_{ik} = v_{r_{ik}} \cos(\theta_i + \theta_A) - v_{\theta_{ik}} \sin(\theta_i + \theta_A) \tag{69}$$

where

$$\theta_{A_i} = \tan^{-1} \frac{y_i}{z_{A_i}}$$

$$v_{r_{ik}} = \beta \sqrt{\frac{(x_i - x_k)^2}{(\beta\, r_i)^2} - 1} \quad \text{for line sources, or}$$

$$= -\frac{\beta^2 \cos\theta_i}{2} \left(\cosh^{-1} \frac{x_i - x_k}{\beta\, r_i} + \frac{x_i - x_k}{\beta\, r_i} \sqrt{\frac{(x_i - x_k)^2}{(\beta\, r_i)^2} - 1} \right) \quad \text{for line doublets,}$$

$$v_{\theta_{ik}} = 0 \quad \text{for line sources, or} \tag{70}$$

$$= -\frac{\beta^2 \cos\theta_i}{2}\left(\cosh^{-1}\frac{x_i - x_k}{\beta\, r_i} - \frac{x_i - x_k}{\beta\, r_i}\sqrt{\frac{(x_i - x_k)^2}{(\beta\, r_i)^2} - 1}\right) \quad \text{for line doublets.}$$

and $\quad r_i = \sqrt{y_i^2 + z_i^2}$

x_k = x coordinate of the origin of the k^{th} line singularity.

The aerodynamic influence coefficients induced by the line singularities are also classified by the use of subscripts in a manner similar to that used for the surface singularities. For example, the influence on wing panel i by the k^{th} line source is denoted by $a_{WBS_{ik}}$, and the influence on body control point i by the k^{th} line doublet is denoted by $a_{BBD_{ik}}$.

<u>Resultant normal velocity at a control point</u>. — The resultant normal velocity at control point i may now be obtained by addition of the normal velocities due to the local cross flow to those induced by the various singularities. The local cross-flow velocity normal to the surface, nondimensionalized by the free-stream velocity U_∞, is $\alpha \cos\theta_i$. On the body, the local angle of attack is assumed to be the difference between the angle of attack, α, and the slope of the body camber line.

The resultant normal velocity on body panel i may be expressed as follows:

$$n_{B_i} = \left(\alpha - \frac{dz_c}{dx}\right)\cos\theta_i + n_{BBS_i} + n_{BBD_i} + n_{BBV_i} + n_{BWV_i} + n_{BWS_i} \tag{71}$$

where

$$n_{BBS_i} = \sum_{k=1}^{K} a_{BBS_{ik}} T_k \qquad \text{(due to body line sources)}$$

$$n_{BBD_i} = \sum_{k=1}^{K} a_{BBD_{ik}} T_{D_k} \qquad \text{(due to body line doublets)}$$

$$n_{BBV_i} = \sum_{j=1}^{N_B} a_{BBV_{ij}} p_{B_j} \qquad \text{(due to surface distribution of vorticity on body)}$$

$$n_{BWV_i} = \sum_{j=1}^{N_W} a_{BWV_{ij}}\, p_{W_j} \qquad \text{(due to surface distribution of vorticity on wing)}$$

$$n_{BWS_i} = \sum_{j=1}^{N_W} a_{BWS_{ij}}\, \alpha_{T_j} \qquad \text{(due to surface distribution of sources on wing)}$$

As indicated above, the normal velocities induced by the various singularities may be expressed as the sum of the products of the influence coefficients with their respective singularity strengths. The influence coefficients have been described previously, and the singularity strengths are defined below:

T_k = strength of body line source k

T_{D_k} = strength of body line doublet k

p_{B_j} = pressure difference across body panel j

p_{W_j} = pressure difference across wing panel j

$\alpha_{T_j} = \left(\dfrac{dz_T}{dx}\right)_j$ = thickness slope of wing panel j

For the summation limits above, there are $K \leq 50$ line sources and doublets, $N_B \leq 100$ body panels, and $N_W \leq 100$ wing panels. The number of singularities used may be chosen arbitrarily for each problem.

Likewise, the resultant normal velocity on wing panel i may be written:

$$n_{W_i} = \alpha + n_{WBS_i} + n_{WBD_i} + n_{WBV_i} + n_{WWV_i} + n_{WWS_i} \tag{72}$$

where

$$n_{WBS_i} = \sum_{k=1}^{K} a_{WBS_{ik}}\, T_k \qquad \text{(due to body line sources)}$$

$$n_{WBD_i} = \sum_{k=1}^{K} a_{WBD_{ik}}\, T_{D_i} \qquad \text{(due to body line doublets)}$$

$$n_{WBV_i} = \sum_{j=1}^{N_B} a_{WBV_{ij}}\, p_{B_j} \qquad \text{(due to surface distribution of vorticity on body)}$$

$$n_{WWV_i} = \sum_{j=1}^{N_W} a_{WWV_{ij}} \, p_{W_j} \qquad \text{(due to surface distribution of vorticity on wing)}$$

$$n_{WWS_i} = \sum_{j=1}^{N_W} a_{WWS_{ij}} \, \alpha_{T_j} \qquad \text{(due to surface distribution of sources on wing)}$$

Note that, by definition, $\theta_i = \theta_j = 0$ on all wing panels.

Boundary conditions. — The boundary conditions equate the local flow direction to the slope of the surface at the control points, where the local flow direction is defined as the ratio of the resultant normal velocity to the axial velocity. For example, the boundary condition at control point i on the wing may be expressed:

$$n_{W_i} = \left(\frac{dz}{dx}\right)_i \tag{73}$$

and on the body,

$$\frac{n_{B_i}}{1 + u_{B_i}} = \left(\frac{dr}{dx}\right)_i \tag{74}$$

The resultant normal velocities n_{B_i} and n_{W_i} are defined by equations (71) and (72), respectively. The resultant axial velocity, expressed as a fraction of the free-stream velocity, is assumed to be unity on the wing. On the body, however, it is customary to include the axial velocity perturbations due to the line sources and doublets. Correspondingly

$$u_{B_i} = u_{BBS_i} + u_{BBD_i} \tag{75}$$

All other axial velocity perturbations are assumed to be small and are neglected.

The boundary conditions may be used to determine the strengths of the various singularities representing the wing-body combination. In this report, the body geometry and wing thickness distribution and planform are always specified in advance. The wing camber and twist distribution either may be given, or will be determined by specifying the lifting pressure distribution or minimum drag condition. As a result, the boundary conditions are most easily satisfied by solving equations (73) and (74) in three steps.

In the first step, the boundary conditions on the wing are divided into two parts, one associated with the lifting effects, the other with the thickness effects. The surface slope of the wing may be expressed as follows:

$$\left(\frac{dz}{dx}\right)_i = \left(\frac{dz_c}{dx}\right)_i \pm \left(\frac{dz_T}{dx}\right)_i \tag{76}$$

where the upper sign refers to the upper surface, and the lower to the lower surface. Substituting equations (76) and (72) into equation (73)

$$\left(\frac{dz_c}{dx}\right)_i \pm \left(\frac{dz_T}{dx}\right)_i = \alpha + n_{WBS_i} + n_{WBD_i} + n_{WBV_i} + n_{WWV_i} + n_{WWS_i} \tag{77}$$

Now
$$n_{WWS_i} = \sum_{j=1}^{N_W} a_{WWS_{ij}} \left(\frac{dz_T}{dx}\right)_j = \pm \left(\frac{dz_T}{dx}\right)_i \tag{78}$$

since
$$a_{WWS_{ij}} = \pm 1 \quad \text{for } i = j$$
$$= 0 \quad \text{for } i \neq j$$

Thus, it can be seen that the given slope of the thickness distribution at control point i, $(dz_T/dx)_i$, is in fact the desired strength of the surface source distribution on wing panel i, and satisfies exactly the wing thickness boundary condition on both surfaces. Equation (77) may now be expressed in terms of the slope of the wing camber surface alone, as follows:

$$\left(\frac{dz_c}{dx}\right)_i = \alpha + n_{WBS_i} + n_{WBD_i} + n_{WBV_i} + n_{WWV_i} \tag{79}$$

The various normal velocity components are written out in terms of the aerodynamic influence coefficients following equation (72).

In the second step, the strengths of the line sources and doublets are determined that completely satisfy the given boundary conditions on the body, assuming no interference effects from the wing. For this step, equation (74) is written as follows:

$$\left(\frac{dr}{dx}\right)_i (1 + u_{BBS_i}) + \left(\frac{dr}{dx}\right)_i u_{BBD_i} = \left(\alpha - \frac{dz_c}{dx}\right) \cos \theta_i + n_{BBS_i} + n_{BBD_i}$$
$$+ n_{BBV_i} + n_{BWV_i} + n_{BWS_i} \tag{80}$$

This equation is now broken down into three parts so that the unknown singularity strengths, T_k and T_{D_k}, can be determined independently.

For the line sources,

$$\left(\frac{dr}{dx}\right)_i (1 + u_{BBS_i}) = n_{BBS_i} \tag{81}$$

For the line doublets,

$$\left(\frac{dr}{dx}\right)_i u_{BBD_i} = n_{BBD_i} + \left(\alpha - \frac{dz_c}{dx}\right) \cos \theta_i \tag{82}$$

The remainder of equation (80) then expresses the condition that the resultant normal velocity components on the body due to the wing must be canceled by the distribution of vorticity on the body panels, that is,

$$n_{BBV_i} = - (n_{BWV_i} + n_{BWS_i}) \tag{83}$$

The various normal velocity components appearing in equations (80), (81), (82), and (83) are written out in terms of the aerodynamic influence coefficients following equation (71). The third step is to solve equations (83) and (79) simultaneously to yield the pressure differences across the wing and body panels that satisfy the remaining boundary conditions on the wing, once the strengths of the line sources and doublets on the axis are determined from equations (81) and (82).

Determination of line sources and doublets. — The strengths of the body line sources may be determined from equation (81). Writing this equation out in terms of the aerodynamic influence coefficients:

$$\left(\frac{dr}{dx}\right)_i \left(1 + \sum_{k=1}^{K} u_{BBS_{ik}} T_k\right) = \sum_{k=1}^{K} a_{BBS_{ik}} T_k$$

or

$$\left(\frac{dr}{dx}\right)_i = \sum_{k=1}^{K} \left[a_{BBS_{ik}} - \left(\frac{dr}{dx}\right)_i u_{BBS_{ik}}\right] T_k \tag{84}$$

This equation is solved for the source strengths T_k either by inverting the matrix enclosed in the square brackets and multiplying the inverse by $(dr/dx)_i$, or by using the classical approach first proposed by von Karman and Moore (reference 10). To conserve storage on the digital computer, the latter method has been used in the computer program. The method is outlined below:

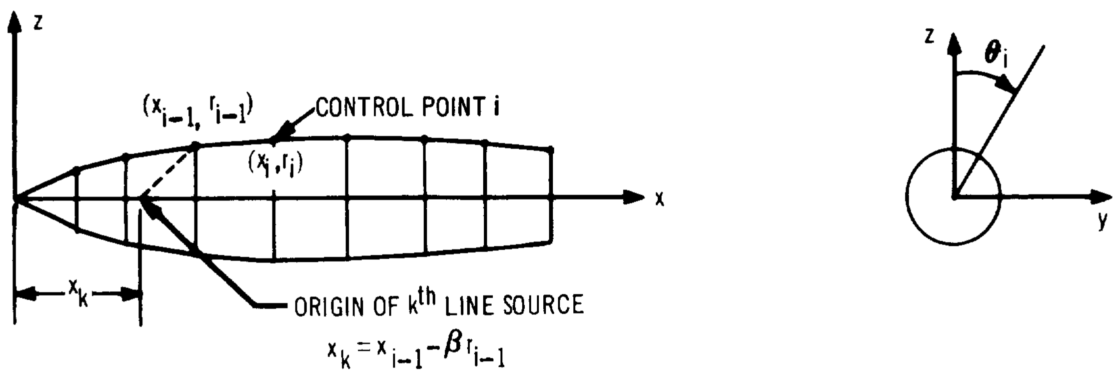

The body, considered to be made up of a series of truncated cones, is defined by the radius at K stations along its length. At station i, the slope is

$$\left(\frac{dr}{dx}\right)_i = \frac{r_i - r_{i-1}}{x_i - x_{i-1}} \tag{85}$$

For the first segment,

$$\left(\frac{dr}{dx}\right)_1 = \left[{}^{a}BBS_{11} - \left(\frac{dr}{dx}\right)_1 {}^{u}BBS_{11}\right] T_1$$

yielding
$$T_1 = \frac{\left(\frac{dr}{dx}\right)_1}{{}^{a}BBS_{11} - \left(\frac{dr}{dx}\right)_1 {}^{u}BBS_{11}}$$

For the second segment,

$$\left(\frac{dr}{dx}\right)_2 = \left[{}^{a}BBS_{21} - \left(\frac{dr}{dx}\right)_2 {}^{u}BBS_{21}\right] T_1 + \left[{}^{a}BBS_{22} - \left(\frac{dr}{dx}\right)_2 {}^{u}BBS_{22}\right] T_2$$

So $$T_2 = \frac{\left(\frac{dr}{dx}\right)_2 - \left[a_{BBS_{21}} - \left(\frac{dr}{dx}\right)_2 u_{BBS_{21}}\right] T_1}{a_{BBS_{22}} - \left(\frac{dr}{dx}\right)_2 u_{BBS_{22}}}$$

In general, for the i^{th} segment

$$T_i = \frac{\left(\frac{dr}{dx}\right)_i - \sum_{k=1}^{i-1} \left[a_{BBS_{ik}} - \left(\frac{dr}{dx}\right)_i u_{BBS_{ik}}\right] T_k}{a_{BBS_{ii}} - \left(\frac{dr}{dx}\right)_i u_{BBS_{ii}}} \tag{86}$$

In this analysis, it should be noted that the k^{th} line source has its origin at the distance $x_k = x_{k-1} - \beta\, r_{k-1}$ from the nose of the body.

The aerodynamic influence coefficient, $a_{BBS_{ik}}$, is given by equation (69).

The axial velocity component, $u_{BBS_{ik}}$, is given below:

$$u_{BBS_{ik}} = -\cosh^{-1} \frac{x_i - x_k}{\beta\, r_i} \tag{87}$$

The strengths of the body doublets may be determined from equation (82), since in terms of the aerodynamic influence coefficients,

$$\left(\frac{dr}{dx}\right)_i \sum_{k=1}^{K} u_{BBD_{ik}} T_{D_k} = \sum_{k=1}^{K} a_{BBD_{ik}} T_{D_k} + \left(\alpha - \frac{dz_c}{dx}\right)_i \cos\theta_i \tag{88}$$

Now both $u_{BBD_{ik}}$ and $a_{BBD_{ik}}$ contain $\cos\theta_i$ internally (see equations (56) and (69)); consequently, $\cos\theta_i$ is eliminated from equation (88)

by placing $$u'_{BBD_{ik}} = u_{BBD_{ik}}/\cos\theta_i$$

and $$a'_{BBD_{ik}} = a_{BBD_{ik}}/\cos\theta_i$$

The result may be written as follows:

$$\left(\alpha - \frac{dz_c}{dx}\right)_i = -\sum_{k=1}^{K} \left[a'_{BBD_{ik}} - \left(\frac{dr}{dx}\right)_i u'_{BBD_{ik}}\right] T_{D_k} \tag{89}$$

Again, this equation can be solved for T_{D_k} by inverting the matrix inside the square brackets and multiplying by the local angle of attack $(\alpha - dz_c/dx)_i$. However, it is solved in a similar fashion to the source equation (84).

Following the same procedure as before, the final result is obtained:

$$T_{D_i} = - \frac{\left(\alpha - \frac{dz_c}{dx} \right)_i + \sum_{k=1}^{i-1} \left[a'_{BBD_{ik}} - \left(\frac{dr}{dx} \right)_i u'_{BBD_{ik}} \right] T_{D_k}}{a'_{BBD_{ii}} - \left(\frac{dr}{dx} \right)_i u'_{BBD_{ii}}} \tag{90}$$

Note that $\left(\frac{dz_c}{dx} \right)_i = \frac{z_{c_i} - z_{c_{i-1}}}{x_i - x_{i-1}}$

The aerodynamic influence coefficient, $a_{BBD_{ik}}$, is given in equation (69) (doublet form). The axial velocity component, $u_{BBD_{ik}}$, is given below:

$$u_{BBD_{ik}} = \beta \cos \theta_i \sqrt{\frac{(x_i - x_k)^2}{\beta^2 r_i^2} - 1} \tag{91}$$

Calculation of lift distribution on the wing. —As stated earlier, equations (79) and (83) may now be solved for the magnitudes of the pressure differences across the wing and body panels required to satisfy the remaining boundary conditions. On the wing,

$$n_{WBV_i} + n_{WWV_i} = \left(\frac{dz_c}{dx} \right)_i - \alpha - n_{WBS_i} - n_{WBD_i} \tag{92}$$

where the last two terms represent the normal velocity on the wing due to the body line sources and doublets. To simplify the following analysis, these two terms are combined as follows:

$$n_{WB_i} = n_{WBS_i} + n_{WBD_i} = \sum_{k=1}^{K} a_{WBS_{ik}} T_k + \sum_{k=1}^{K} a_{WBD_{ik}} T_{D_k} \tag{93}$$

On the body,

$$n_{BBV_i} + n_{BWV_i} = - n_{BWS_i} = - \sum_{j=1}^{N_W} a_{BWS_{ij}} \alpha_{T_j} \tag{94}$$

The last term represents the normal velocity on the body resulting from the wing sources.

Equation (94) is the general expression for the normal velocity on the i^{th} body panel control point. There are $N_B \leq 100$ such equations. Similarly, equation

(92) is the general expression for the normal velocity at the i^{th} wing panel control point, resulting in another $N_W \leq 100$ equations. This combined system of $N_B + N_W$ equations is sufficient to determine the N_B values of p_{B_j}, and the N_W values of p_{W_j}. For example, the equations may be written out as follows:

$$\sum_{j=1}^{N_B} a_{BBV_{1j}} \cdot p_{B_j} + \sum_{j=1}^{N_W} a_{BWV_{1j}} \cdot p_{W_j} = - n_{BWS_1}$$

$$\sum_{j=1}^{N_B} a_{BBV_{2j}} \cdot p_{B_j} + \sum_{j=1}^{N_W} a_{BWV_{2j}} \cdot p_{W_j} = - n_{BWS_2}$$

$$\vdots \qquad\qquad\qquad\qquad \vdots$$

$$\sum_{j=1}^{N_B} a_{BBV_{N_Bj}} \cdot p_{B_j} + \sum_{j=1}^{N_W} a_{BWV_{N_Bj}} \cdot p_{W_j} = - n_{BWS_{N_B}}$$

$$\sum_{j=1}^{N_B} a_{WBV_{1j}} \cdot p_{B_j} + \sum_{j=1}^{N_W} a_{WWV_{1j}} \cdot p_{W_j} = \left(\frac{dz_c}{dx}\right)_1 - \alpha - n_{WB_1}$$

$$\sum_{j=1}^{N_B} a_{WBV_{2j}} \cdot p_{B_j} + \sum_{j=1}^{N_W} a_{WWV_{2j}} \cdot p_{W_j} = \left(\frac{dz_c}{dx}\right)_2 - \alpha - n_{WB_2}$$

$$\vdots \qquad\qquad\qquad\qquad \vdots$$

$$\sum_{j=1}^{N_B} a_{WBV_{N_Wj}} \cdot p_{B_j} + \sum_{j=1}^{N_W} a_{WWV_{N_Wj}} \cdot p_{W_j} = \left(\frac{dz_c}{dx}\right)_{N_W} - \alpha - n_{WB_{N_W}} \qquad (95)$$

This system of equations is more simply expressed in matrix form as shown on the next page.

$$
\left[\begin{array}{cccc|cccc}
a_{BBV_{11}} & a_{BBV_{12}} & \cdots & a_{BBV_{1N_B}} & a_{BWV_{11}} & a_{BWV_{12}} & \cdots & a_{BWV_{1N_W}} \\
a_{BBV_{21}} & a_{BBV_{22}} & & & & & & a_{BWV_{2N_W}} \\
\vdots & & & & & & & \vdots \\
a_{BBV_{N_B 1}} & & & & & & & \\
\hline
a_{WBV_{11}} & & & & a_{WWV_{11}} & & & \\
a_{WBV_{21}} & & & & & & & \\
\vdots & & & & & & & \\
a_{WBV_{N_W 1}} & & \cdots & & & & & a_{WWV_{N_W N_W}}
\end{array}\right]
\left\{\begin{array}{c}
p_{B_1} \\ p_{B_2} \\ \vdots \\ p_{B_{N_B}} \\ p_{W_1} \\ p_{W_2} \\ \vdots \\ p_{W_{N_W}}
\end{array}\right\}
=
\left\{\begin{array}{c}
-n_{BWS_1} \\ -n_{BWS_2} \\ \vdots \\ -n_{BWS_{N_B}} \\
\left(\frac{dz_c}{dx}\right)_1 - \alpha - n_{WB_1} \\
\left(\frac{dz_c}{dx}\right)_2 - \alpha - n_{WB_2} \\
\vdots \\
\left(\frac{dz_c}{dx}\right)_{N_W} - \alpha - n_{WB_{N_W}}
\end{array}\right\}
\tag{96}
$$

The matrix of aerodynamic influence coefficients is normally referred to as the aerodynamic matrix. This matrix can be conveniently partitioned into four parts, as indicated, one giving the influence of the body on the body $\left[A_{BB}\right]$, the next giving the influence of the body on the wing $\left[A_{WB}\right]$, the next giving the influence of the wing on the body $\left[A_{BW}\right]$, and the last giving the influence of the wing on the wing $\left[A_{WW}\right]$. In terms of these submatrices, equation (96) becomes

$$
\begin{bmatrix} \left[A_{BB}\right] & \left[A_{BW}\right] \\ \left[A_{WB}\right] & \left[A_{WW}\right] \end{bmatrix}
\left\{\begin{array}{c} p_B \\ p_W \end{array}\right\}
=
\left\{\begin{array}{c} -n_{BWS} \\ \frac{dz_c}{dx} - \alpha - n_{WB} \end{array}\right\}
\tag{97}
$$

This matrix equation may now be solved for $\left\{p_B\right\}$ and $\left\{p_W\right\}$ as though it were a system of two linear algebraic equations, as indicated below:

$$
\begin{aligned}
\left[A_{BB}\right]\left\{p_B\right\} + \left[A_{BW}\right]\left\{p_W\right\} &= -\left\{n_{BWS}\right\} \\
\left[A_{WB}\right]\left\{p_B\right\} + \left[A_{WW}\right]\left\{p_W\right\} &= \left\{\frac{dz_c}{dx} - \alpha - n_{WB}\right\}
\end{aligned}
\tag{98}
$$

The first equation gives:

$$\left\{ p_B \right\} = - \left[A_{BB} \right]^{-1} \left\{ \left\{ n_{BWS} \right\} + \left[A_{BW} \right] \left\{ p_W \right\} \right\} \tag{99}$$

Substituting this into the second equation,

$$\left[\left[A_{WW} \right] - \left[A_{WB} \left[A_{BB} \right]^{-1} \left[A_{BW} \right] \right] \right] \left\{ p_W \right\} = \left\{ \left[A_{WB} \right] \left[A_{BB} \right]^{-1} \left\{ n_{BWS} \right\} + \left\{ \frac{dz_c}{dx} - \alpha - n_{WB} \right\} \right\}$$

which yields the lift distribution on the wing, provided the slope of the camber surface and angle of attack are specified:

$$\left\{ p_W \right\} = \left[A_R \right]^{-1} \left\{ \left[A_{WB} \right] \left[A_{BB} \right]^{-1} \left\{ n_{BWS} \right\} + \left\{ \frac{dz_c}{dx} - \alpha - n_{WB} \right\} \right\} \tag{100}$$

where $\left[A_R \right] = \left[\left[A_{WW} \right] - \left[A_{WB} \right] \left[A_{BB} \right]^{-1} \left[A_{BW} \right] \right]$ (101)

is referred to as the "reduced" aerodynamic matrix.

The pressure difference across the body panels, $\left\{ p_B \right\}$, may now be determined from equation (99). This completes the determination of all the singularity strengths for a wing-body combination of given geometry.

4.5 Calculation of Pressures, Forces, and Moments

Pressure coefficients. — The pressure coefficients on the body resulting from line sources and doublets are calculated separately from those on the wing and body panels. The combined pressure coefficient on the body in the presence of the wing is the sum of these two calculations.

The pressure coefficients on the body resulting from line sources and doublets are calculated by the following formula:

$$C_{p_{B_i}} = \frac{p_{B_i} - p_\infty}{q_\infty} = - 2\, u_{B_i} + \beta^2\, u_{B_i}{}^2 - v_{r_{B_i}}{}^2 - v_{\theta_{B_i}}{}^2 \tag{102}$$

where

$$u_{B_i} = \sum_{k=1}^{K} u_{BBS_{ik}}\, T_k + \sum_{k=1}^{K} u_{BBD_{ik}}\, T_{D_k}$$

$$v_{r_{B_i}} = \sum_{k=1}^{K} v_{r_{BBS_{ik}}}\, T_k + \sum_{k=1}^{K} v_{r_{BBD_{ik}}}\, T_{D_k}$$

$$v_{\theta_{B_i}} = \sum_{k=1}^{K} v_{\theta_{BBS_{ik}}} T_k + \sum_{k=1}^{K} v_{\theta_{BBD_{ik}}} T_{D_k}$$

and
$$u_{BBS_{ik}} = -\cosh^{-1} \frac{x_i - x_k}{\beta r_i}$$

$$u_{BBD_{ik}} = \beta \cos \theta_i \sqrt{\frac{(x_i - x_k)^2}{\beta^2 r_i^2} - 1}$$

The remaining coefficients are defined by equation (70).

The pressure coefficients on the body panels resulting from surface distributions of singularities on the body and wing are given by:

$$C_{p_{B_i}} = -2 u_{B_i} + \beta^2 u_{B_i}^2 - v_{B_i}^2 - w_{B_i}^2 \tag{103}$$

where
$$u_{B_i} = u_{BBV_i} + u_{BWV_i} + u_{BWS_i}$$

$$u_{BBV_i} = \sum_{j=1}^{N_B} u_{BBV_{ij}} p_{B_j}$$

$$u_{BWV_i} = \sum_{j=1}^{N_W} u_{BWV_{ij}} p_{W_j}$$

$$u_{BWS_i} = \sum_{j=1}^{N_W} u_{BWS_{ij}} \alpha_{T_j}$$

and
$$v_{B_i} = v_{BBV_i} + v_{BWV_i} + v_{BWS_i}$$

$$v_{BBV_i} = \sum_{j=1}^{N_B} (v_{BBV_{ij}} \cos \theta_j - w_{BBV_{ij}} \sin \theta_j) p_{B_j}$$

$$v_{BWV_i} = \sum_{j=1}^{N_W} (v_{BWV_{ij}} \cos \theta_j - w_{BWV_{ij}} \sin \theta_j) p_{W_j}$$

$$v_{BWS_i} = \sum_{j=1}^{N_W} (v_{BWS_{ij}} \cos \theta_j - w_{BWS_{ij}} \sin \theta_j) \alpha_{T_j}$$

and
$$w_{B_i} = w_{BBV_i} + w_{BWV_i} + w_{BWS_i}$$

$$w_{BBV_i} = \sum_{j=1}^{N_B} (w_{BBV_{ij}} \cos \theta_j + v_{BBV_{ij}} \sin \theta_j) \, p_{B_j}$$

$$w_{BWV_i} = \sum_{j=1}^{N_W} (w_{BWV_{ij}} \cos \theta_j + v_{BWV_{ij}} \sin \theta_j) \, p_{W_j}$$

$$w_{BWS_i} = \sum_{j=1}^{N_W} (w_{BWS_{ij}} \cos \theta_j + v_{BWS_{ij}} \sin \theta_j) \, \alpha_{T_j}$$

The various velocity coefficients are given by equation (58), selected according to the type of singularity under consideration.

Finally, the pressure coefficients on the wing panels are calculated in a single step by the use of the following formula:

$$C_{p_{W_i}} = -2 u_{W_i} + \beta^2 u_{W_i}^{\;2} - v_{W_i}^{\;2} - w_{W_i}^{\;2} \qquad (104)$$

where $u_{W_i} = u_{WBS_i} + u_{WBD_i} + u_{WBV_i} + u_{WWV_i} + u_{WWS_i}$

$$u_{WBS_i} = \sum_{k=1}^{K} u_{WBS_{ik}} \, T_k$$

$$u_{WBD_i} = \sum_{k=1}^{K} u_{WBD_{ik}} \, T_{D_k}$$

$$u_{WBV_i} = \sum_{j=1}^{N_B} u_{WBV_{ij}} \, p_{B_j}$$

$$u_{WWV_i} = \sum_{j=1}^{N_W} u_{WWV_{ij}} \, p_{W_j}$$

$$u_{WWS_i} = \sum_{j=1}^{N_W} u_{WWS_{ij}} \, \alpha_{T_j};$$

and $v_{W_i} = v_{WBS_i} + v_{WBD_i} + v_{WBV_i} + v_{WWV_i} + v_{WWS_i}$

$$v_{WBS_i} = \sum_{k=1}^{K} (v_{r_{s_{ik}}} \sin \theta_{A_i} + v_{\theta_{s_{ik}}} \cos \theta_{A_i}) \, T_k$$

$$v_{WBD_i} = \sum_{k=1}^{K} (v_{r_{D_{ik}}} \sin \theta_{A_i} + v_{\theta_{D_{ik}}} \cos \theta_{A_i}) T_{D_k}$$

$$v_{WBV_i} = \sum_{j=1}^{N_B} (v_{WBV_{ij}} \cos \theta_j - w_{WBV_{ij}} \sin \theta_j) p_{B_j}$$

$$v_{WWV_i} = \sum_{j=1}^{N_W} (v_{WWV_{ij}} \cos \theta_j - w_{WWV_{ij}} \sin \theta_j) p_{W_j}$$

$$v_{WWS_i} = \sum_{j=1}^{N_W} (v_{WWS_{ij}} \cos \theta_j - w_{WWS_{ij}} \sin \theta_j) \alpha_{T_j} ;$$

and
$$w_{W_i} = w_{WBS_i} + w_{WBD_i} + w_{WBV_i} + w_{WWV_i} + w_{WWS_i}$$

$$w_{WBS_i} = \sum_{k=1}^{K} (v_{r_{s_{ik}}} \cos \theta_{A_i} - v_{\theta_{s_{ik}}} \sin \theta_{A_i}) T_k$$

$$w_{WBD_i} = \sum_{k=1}^{K} (v_{r_{D_{ik}}} \cos \theta_{A_i} - v_{\theta_{D_{ik}}} \sin \theta_{A_i}) T_{D_k}$$

$$w_{WBV_i} = \sum_{j=1}^{N_B} (w_{WBV_{ij}} \cos \theta_j + v_{WBV_{ij}} \sin \theta_j) p_{B_j}$$

$$w_{WWV_i} = \sum_{j=1}^{N_W} (w_{WWV_{ij}} \cos \theta_j + v_{WWV_{ij}} \sin \theta_j) p_{W_j}$$

$$w_{WWS_i} = \sum_{j=1}^{N_W} (w_{WWS_{ij}} \cos \theta_j + v_{WWS_{ij}} \sin \theta_j) \alpha_{T_j} .$$

The computer program is designed so that the user has the option of calculating the pressure coefficients either by the "nonlinear" formulae, equations (102) through (104), or by the usual linear formula:

$$C_{p_i} = - 2 u_i \tag{105}$$

which consists merely of the first term of the preceding pressure coefficient equations.

Forces and moments on the isolated body. — The lift, drag, and pitching moment of the body due to the line sources and doublets alone are calculated neglecting any interference effects from the wing. Such interference terms are added later. The body is considered to be approximated by K truncated cones. The forces and moments on a body segment having an angular width $\Delta\theta_j$, and located between x_i and x_{i-1}, will first be determined.

The lift of this segment is

$$\left(\frac{\Delta L}{q}\right)_{ij} = \left[C_{p_{B_j}} (x_i - x_{i-1}) (r_i + r_{i-1}) \cos \theta_j\right] \Delta\theta_j/2 \tag{106}$$

The pressure drag is given by

$$\left(\frac{\Delta D}{q}\right)_{ij} = C_{p_{B_j}} (r_i^2 - r_{i-1}^2) \, \Delta\theta_j/2 \tag{107}$$

The notation is the same as that illustrated in the sketch preceding equation (85), and $C_{p_{B_j}}$ is given by equation (102) at J points around the circumference.

The total lift, pressure drag, and pitching moment may now be obtained by summing the segment contributions. For example

$$C_{L_B} = \frac{L_B}{q\, S_W} = \frac{1}{S_W} \sum_{j=1}^{J} \sum_{i=1}^{K} \left(\frac{\Delta L}{q}\right)_{ij}$$

$$C_{D_B} = \frac{D_B}{q\, S_W} = \frac{1}{S_W} \sum_{j=1}^{J} \sum_{i=1}^{K} \left(\frac{\Delta D}{q}\right)_{ij}$$

$$C_{M_B} = \frac{M_B}{q\, S_W\, \bar{c}} = \frac{1}{S_W\, \bar{c}} \sum_{j=1}^{J} \sum_{i=1}^{K} \left\{ \left(\frac{\Delta D}{q}\right)_{ij} (r_i \cos \theta_j - \bar{z}) - \left(\frac{\Delta L}{q}\right)_{ij} \left[\frac{x_i + x_{i-1}}{2} - \bar{x}\right] \right\} \tag{108}$$

where the moments are computed about the point $(\bar{x}, \bar{z})$, $\bar{c}$ is a reference chord, and S_W is the reference wing area. The forces and moments are computed for the half-body only.

Forces and moments on the wing. — The forces and moments acting on the wing are determined by calculation of the forces and moments acting on the upper surface of the wing and adding them to those acting on the lower surface. The pressure coefficient on a wing panel is given by equation (104). The normal force on the surface of a panel is the product of the dynamic pressure, the pressure coefficient and the panel area

$$F_i = q \, C_{p_i} \, A_i \tag{109}$$

Resolution of this force into components normal and parallel to the free-stream direction yields

$$\begin{aligned} L_i &= - F_i \\ D_i &= F_i \left[\left(\frac{dz}{dx} \right)_i - \alpha \right] \end{aligned} \tag{110}$$

where $\left(\frac{dz}{dx} \right)_i = \left(\frac{dz_c}{dx} \right)_i \pm \left(\frac{dz_T}{dx} \right)_i$

is the slope of the panel with respect to the x-y plane. The upper sign refers to the upper surface, the lower to the lower surface.

The pitching moment with respect to a point $(\bar{x}, 0, \bar{z})$ is:

$$M_i = - L_i (x_i - \bar{x}) + D_i (z_i - \bar{z}) \tag{111}$$

The sum of the forces and moments on the upper and lower surfaces, divided by the product of the dynamic pressure and the reference wing area, results in the lift, drag, and pitching moment coefficients for the wing:

$$\begin{aligned} C_{L_W} &= \frac{1}{q \, S_W} \sum_{i=1}^{N_W} (L_{U_i} + L_{L_i}) \\ C_{D_W} &= \frac{1}{q \, S_W} \sum_{i=1}^{N_W} (D_{U_i} + D_{L_i}) \\ C_{M_W} &= \frac{1}{q \, S_W \, \bar{c}} \sum_{i=1}^{N_W} (M_{U_i} + M_{L_i}) \end{aligned} \tag{112}$$

where the subscripts U and L refer to the upper and lower surfaces.

Interference forces and moments on body panels. — The forces and moments on the body panels are similarly calculated. The normal force on the panel surface is given by equation (109). The interference lift and drag may now be calculated, making due allowance for the inclination of the panel,

$$L_i = -F_i \cos \theta_i$$

$$D_i = F_i \left[\left(\frac{dz'}{dx} \right)_i - \alpha \cos \theta_i \right] \qquad (113)$$

where dz'/dx is the slope of the panel with respect to the primed system of coordinates having its origin in the foremost panel corner, as illustrated in figure 1 (page 11). As before, the pitching moment is given by equation (111).

The lift, drag, and pitching moment coefficients are given by equation (112), omitting the terms with subscript L.

Forces and moments on wing-body combination. — The resultant lift, drag, and pitching moment coefficients may now be obtained by adding the isolated body coefficients, equation (108), to the wing coefficients and the body interference coefficients, both from equation (112). This completes the determination of the forces and moments on the wing-body combination at a given angle of attack.

4.6 Applications to Specific Problems

The method of aerodynamic influence coefficients can be applied to a wide variety of aerodynamic problems involving supersonic flows about wing-body combinations. The generality of the method is primarily due to the matrix formulation of the problem, which introduces considerable simplification into the algebraic manipulations involved. For example, either the direct problem of determining the pressures, forces, and moments on configurations of given geometry, or the inverse problem of determining the geometry which will result in certain desired aerodynamic properties can be solved with equal ease. In particular, the wing camber and twist required to minimize the drag of a wing-body combination under given constraints of lift, or lift and pitching moment, may be determined by additional straightforward operations on the aerodynamic matrix. The various applications will be outlined in the following sections.

Direct problems. — The determination of the aerodynamic pressures, forces, and moments acting on a wing-body combination of given geometry has been outlined in section 4.5. Briefly, the problem is solved in three steps, beginning with the analysis of the isolated body, followed by the analysis of the wing in the presence of the body, and completed by calculation of the interference effects of the wing on the body. This technique is fundamental to the solution of both direct and inverse problems, once the geometry of the configuration has been defined. The specific direct problems that can be treated with this method are outlined below. Examples giving results for selected cases are presented in section 4.7.

Body alone: Given a body having circular, or nearly circular cross sections, and having arbitrary camber and angle of attack, determine the pressures, forces, and moments.

Wing alone: Given a wing planform that can be approximated by a series of straight line segments, and having arbitrary angle of attack, camber, twist, and thickness distributions; determine the pressures, forces, and moments. This problem can be solved at a number of angles of attack to give the theoretical lift and moment curves and the drag polar.

Special cases include the calculation of plane wings at incidence, non-lifting thick wings, and the effect of control surface deflections.

Wing-body combinations: All cases described above may be calculated for the combined wing and body, taking into account all the interference effects of one on the other. In particular, the effects of symmetrical body contouring may be included in the analysis.

Inverse problems. — Inverse problems fall into two categories. The first category includes the determination of the wing camber and twist distribution required to support a given lift distribution. In the second category, the wing camber and twist are found that will satisfy the condition of minimum drag under given constraints of lift and pitching moment. These two categories are described in detail below.

Given lift distribution: The slope of the camber surface that will support a given lift distribution, p_W, may be determined by inverting equation (100) thus:

$$\left\{\frac{dz_c}{dx}\right\} = \alpha + \left\{n_{WB}\right\} + \left[A_R\right]\left\{p_W\right\} - \left[A_{WB}\right]\left[A_{BB}\right]^{-1}\left\{n_{WBS}\right\} \qquad (114)$$

where $\left\{n_{WB}\right\}$ is the normal velocity distribution induced on the wing by the body line sources and doublets, $\left[A_R\right]$ is the reduced aerodynamic matrix, given by equation (101), and $\left[A_{WB}\right]\left[A_{BB}\right]^{-1}\left\{n_{WBS}\right\}$ is the normal velocity component induced on the wing by the cancellation of the normal velocity components induced by the wing-thickness distribution on the body.

A special case results when the lift distribution on the wing is constant. In this case, however, if additional pressures are introduced by the wing and body thickness distributions, or body camber and angle of attack effects, then the pressure distributions on the upper and lower surfaces of the wing will not be constant.

Minimum drag for given lift and pitching moment: The wing camber and twist required to minimize the drag of a wing-body combination under given constraints of lift and pitching moment may be determined by applying the calculus of variations to the drag equation. The problem is formulated by defining a function F in terms of the N_W variables p_{Wi} and the two auxiliary variables, or Lagrange multipliers, λ_1 and λ_2. The function F is chosen so it will be equal to the drag when the wing lift and pitching moment are equal to their constrained values $\overline{L}$ and $\overline{M}$, respectively. One such function is

$$F = D + \lambda_1 (L - \overline{L}) + \lambda_2 (M - \overline{M}) \qquad (115)$$

where
$$L = - \sum_{i=1}^{N_W} A_i \, p_{W_i}$$
$$D = \sum_{i=1}^{N_W} L_i \left(\frac{dz_c}{dx}\right)_i = - \sum_{i=1}^{N_W} A_i \left(\frac{dz_c}{dx}\right)_i p_{W_i}$$
$$M = - \sum_{i=1}^{N_W} L_i \, (x_i - \bar{x}) = \sum_{i=1}^{N_W} A_i \, (x_i - \bar{x}) \, p_{W_i}$$

and A_i is the area of panel i

p_{W_i} is the pressure difference across panel i

$\left(\frac{dz_c}{dx}\right)_i$ is the surface slope of panel i

x_i is the coordinate of the centroid of panel i

$\bar{x}$ is the x coordinate of the moment center

It is assumed that the moment center lies on the center line of the configuration and in the wing reference plane.

The $N_W + 2$ conditions for minimum drag may now be written

$$\frac{\partial F}{\partial p_{W_i}} = \frac{\partial D}{\partial p_{W_i}} + \lambda_1 \frac{\partial L}{\partial p_{W_i}} + \lambda_2 \frac{\partial M}{\partial p_{W_i}} = 0, \qquad i = 1, \cdots N_W$$

$$\frac{\partial F}{\partial \lambda_1} = L - \bar{L} = 0$$

$$\frac{\partial F}{\partial \lambda_2} = M - \bar{M} = 0 \tag{116}$$

To evaluate these partial derivatives it is necessary to express the camber surface slopes $(dz_c/dx)_i$ in terms of the pressure differences across the wing panels p_{W_i}. The boundary conditions on the wing require that the slope of the camber surface be equal to the resultant normal velocity component at each point. Therefore

$$\left(\frac{dz_c}{dx}\right)_i = n_{WB_i} + n_{WBV_i} + n_{WWV_i} \tag{117}$$

where n_{WB_i}, the normal velocity on the wing due to the body line sources and doublets, is given by equation (93) for a specified body shape. Expressions for n_{WBV_i} and n_{WWV_i} are given following equation (72) and are repeated below for convenience. The normal velocity on the wing due to the distributions of vorticity on the wing panels is given directly in terms of p_{W_i} as follows

$$n_{WWV_i} = \sum_{j=1}^{N_W} a_{WWV_{ij}} \, p_{W_j} \tag{118}$$

However, the normal velocity on the wing due to the distributions of vorticity on the body panels is given in terms of the pressure difference across the body panels, p_{B_i},

$$n_{WBV_i} = \sum_{j=1}^{N_B} a_{WBV_{ij}} \, p_{B_j} \tag{119}$$

Thus an expression is required relating p_{B_i} to p_{W_i}. Equation (99) gives the desired result in matrix notation,

$$\left\{p_B\right\} = - \left[A_{BB}\right]^{-1} \left\{n_{BWS}\right\} - \left[A_{BB}\right]^{-1} \left[A_{BW}\right]\left\{p_W\right\} \tag{120}$$

where $\left\{n_{BWS}\right\}$ is an array giving the normal velocity components on the body panels due to the wing thickness distribution. For wings without thickness, this term will not appear in the above equation.

Finally, substituting equations (118) and (119) into equation (117), and simplifying, gives the desired result:

$$\left(\frac{dz_c}{dx}\right)_i = n_{WB_i} - \sum_{j=1}^{N_B} b_{ij} \, n_{BWS_j} + \sum_{j=1}^{N_W} a_{R_{ij}} \, p_{W_j} \tag{121}$$

where b_{ij} is an element of the matrix:

$$\left[B_{ij}\right] = \sum_{k=1}^{N_W} \left[A_{WB_{ik}}\right] \left[A_{BB_{kj}}\right]^{-1}$$

and $a_{R_{ij}}$ is an element of the reduced aerodynamic matrix given by equation (101):

$$\left[A_{R_{ij}}\right] = \left[\left[A_{WW}\right] - \left[A_{WB}\right] \left[A_{BB}\right]^{-1} \left[A_{BW}\right]\right]$$

In the above expressions, $\left[A_{WB}\right]$ is the matrix of the influence coefficients $a_{WBV_{ij}}$, $\left[A_{BB}\right]$ is the matrix of the influence coefficients $a_{BBV_{ij}}$, and so on, as described following equation (96).

The partial derivatives indicated in equation (116) may now be evaluated. The expression for the drag becomes:

$$D = \sum_{i=1}^{N_W} D_i = - \sum_{i=1}^{N_W} A_i \, p_{W_i} \left(n_{WB_i} - \sum_{j=1}^{N_B} b_{ij} \, n_{BWS_j} + \sum_{j=1}^{N_W} a_{R_{ij}} \, p_{W_j} \right) \tag{122}$$

Therefore,

$$\frac{\partial D}{\partial p_{W_i}} = - \left[A_i \left(n_{WB_i} - \sum_{j=1}^{N_B} b_{ij} \, n_{BWS_j} + \sum_{j=1}^{N_W} a_{R_{ij}} \, p_{W_j} \right) + \sum_{j=1}^{N_W} A_j \, a_{R_{ji}} \, p_{W_j} \right]$$

$$= - A_i \left(n_{WB_i} - \sum_{j=1}^{N_B} b_{ij} \, n_{BWS_j} \right) - \sum_{j=1}^{N_W} \left(A_i \, a_{R_{ij}} + A_j \, a_{R_{ji}} \right) p_{W_j} \tag{123}$$

also,

$$\frac{\partial L}{\partial p_{W_i}} = - A_i$$

$$\frac{\partial M}{\partial p_{W_i}} = A_i \, (x_i - \bar{x}) \tag{124}$$

Similarly,

$$\frac{\partial F}{\partial \lambda_1} = - \sum_{j=1}^{N_W} A_i \, p_{W_i} - \bar{L}$$

$$\frac{\partial F}{\partial \lambda_2} = \sum_{j=1}^{N_W} A_i \, p_{W_i} \, (x_i - \bar{x}) - \bar{M} \tag{125}$$

Substituting these partial derivatives into equation (116) gives a system of $N_W + 2$ linear equations. This system of equation may be written in matrix form, as follows, where N_W has been replaced by N for simplicity.

$$
\begin{bmatrix}
-(A_1 a_{R_{11}} + A_1 a_{R_{11}}) & -(A_1 a_{R_{12}} + A_2 a_{R_{21}}) & \cdots & -A_1 & (x_1 - \bar{x})\, A_1 \\
-(A_2 a_{R_{21}} + A_1 a_{R_{12}}) & -(A_2 a_{R_{22}} + A_2 a_{R_{22}}) & \cdots & -A_2 & (x_2 - \bar{x})\, A_2 \\
-(A_3 a_{R_{31}} + A_1 a_{R_{13}}) & & & & \vdots \\
\vdots & & & & \\
-(A_N a_{R_{N1}} + A_1 a_{R_{1N}}) & \cdots & & -A_N & (x_N - \bar{x})\, A_N \\
-A_1 & -A_2 & \cdots & 0 & 0 \\
(x_1 - \bar{x})\, A_1 & (x_2 - \bar{x})\, A_2 & & 0 & 0
\end{bmatrix}
\begin{Bmatrix}
p_{W_1} \\ p_{W_2} \\ \vdots \\ p_{W_N} \\ \lambda_1 \\ \lambda_2
\end{Bmatrix}
=
\begin{Bmatrix}
A_1 \left(n_{WB_1} - \sum_{j=1}^{N} b_{1_j}\, n_{BWS_j}\right) \\
A_2 \left(n_{WB_2} - \sum_{j=1}^{N} b_{2_j}\, n_{BWS_j}\right) \\
\vdots \\
A_N \left(n_{WB_N} - \sum_{j=1}^{N} b_{N_j}\, n_{BWS_j}\right) \\
\bar{L} \\
\bar{M}
\end{Bmatrix}
\tag{126}
$$

The wing pressure distribution for minimum drag may be found by inverting the matrix and postmultiplying it by the array on the right-hand side of the equation. If the lift only is to be constrained, the row and column of the matrix corresponding to λ_2 is omitted before the inversion. Finally, the optimum camber shape may be calculated by equation (114).

The method of Lagrange multipliers outlined above may be extended to include many other cases of interest. Examples of cases that have been determined by this method, but not reported here, are:

1) Optimization of the wing camber surface while keeping the total lift, or total lift and pitching moment, of the wing plus body constrained to given values.

2) Optimization of the wing twist for a given camber and lift (or lift and pitching moment) on the wing.

3) Optimization of any consecutively numbered group of panels on the wing, while constraining the camber and twist of the remaining panels, and the wing lift, or lift and pitching moment. This case may be useful for determining optimum flap settings at given cruise conditions.

4) Calculation of the incidence at which a given cambered wing will achieve a given lift coefficient.

4.7 Theoretical Comparisons

In this section results of the method of aerodynamic influence coefficients are compared with linear theory calculations published by other investigators. Theoretical solutions for isolated wings, bodies, and wing-body combinations are compared. The form of the pressure distributions, and the prediction of the lift and drag of the examples studied are emphasized. In particular, the reasons underlying the choice of the various control points used in the calculations are discussed.

Pressure distributions on flat plate wings. —Pressure distributions have been calculated for delta, double delta, arrow, and constant-chord wings over a range of supersonic Mach numbers and compared with linearized theory results published by other investigators.

It was found that location of the panel control points had a dominant effect on the form of the wing pressure distributions obtained. Figure 9 shows the calculated chordwise pressure distributions (corresponding to two control-point locations) on an inclined, planar, constant-chord wing with sonic leading edges. The upper plot shows the result obtained when the control point is located at the panel centroids. A strong oscillatory tendency in the chordwise pressure distribution is observed that does not agree with the exact linear theory solution, except towards the trailing edge of the wing. The plot on the lower right shows the result obtained for control points located at 95 percent of the streamwise chord through the panel centroid. The chordwise pressure distributions are now smooth, and they follow the linear theory solution closely, except very near the leading edge and in the region of the strong discontinuity introduced by the wing-tip Mach wave.

The effect of the control point location on the pressures calculated for three panels on the inboard row of this wing is shown in the sketch on the lower left of the illustration. Here the pressures converge smoothly towards the correct linear theory value as the control point is moved towards the trailing edge of the panel. This is true for panels having sonic or supersonic trailing edges. For panels having subsonic trailing edges, however, the normal velocity at the trailing edge is infinite, and the panel pressure becomes indeterminate. To avoid this difficulty, and to maintain a good approximation to the exact linear theory pressure coefficients, the control points have been arbitrarily located

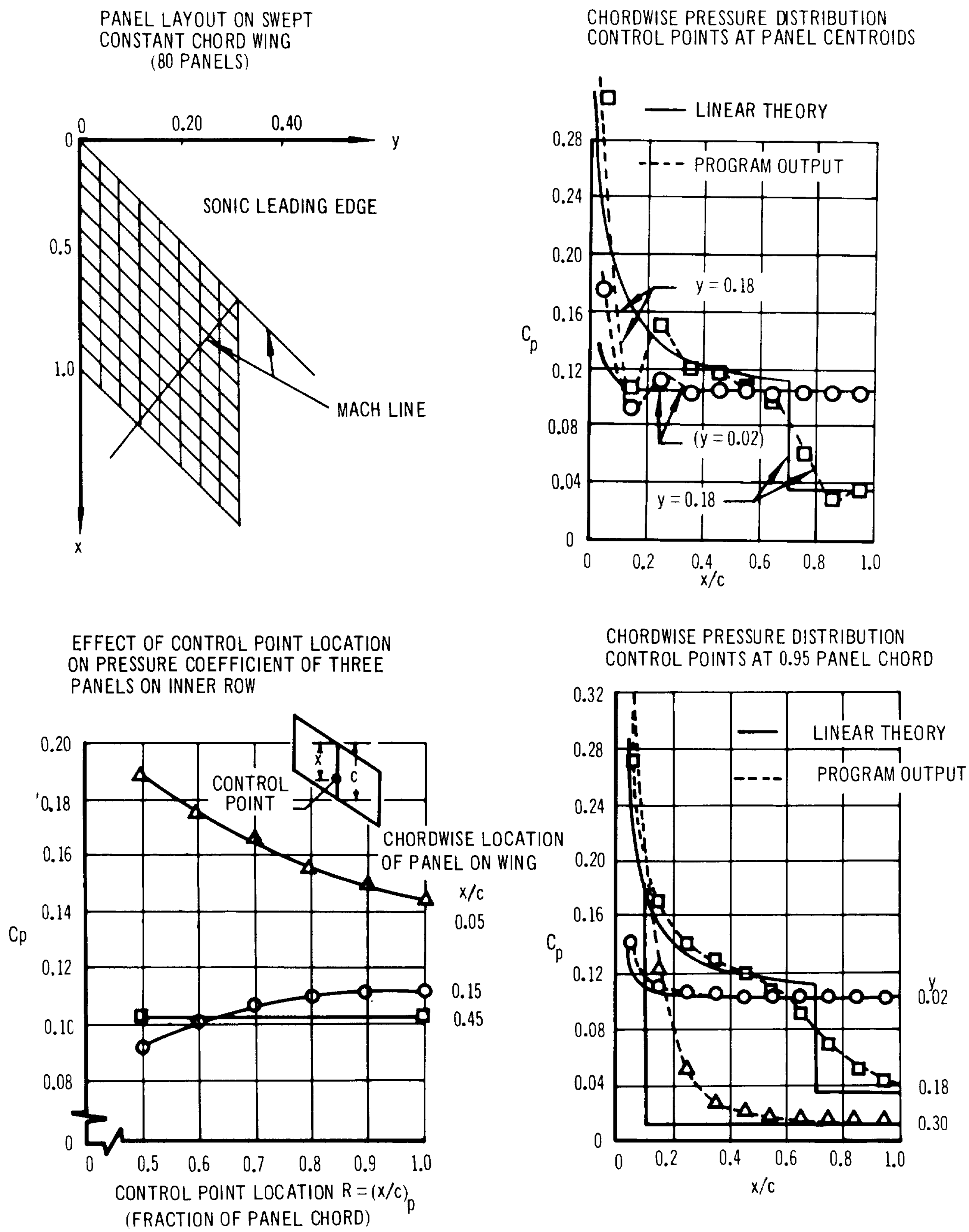

FIGURE 9 EFFECT OF CONTROL POINT LOCATION

at 95 percent of the streamwise chord through the panel centroid. This choice of control-point location has given an adequate representation of the pressure distribution for all cambered or uncambered lifting wings so far investigated.

Examples illustrating the results obtained for isolated wings are presented on the following pages. In all these examples, the wing has been subdivided into 100 panels, spaced evenly in 10-percent increments in both chordwise and spanwise directions.

Figure 10 shows the pressure distribution calculated for flat-plate delta wing at incidence, compared to an exact linearized theory solution. The wing planform corresponds to that of Example II of reference 11, and has a subsonic leading edge with tan Λ / β = 1.2. The present theory agrees reasonably well with the exact result, except in the region of the wing tip, or near the leading edge. The overall lift coefficient of the wing is 3.58, compared to the exact value of 3.55. The wing center of pressure is correctly located at a point two thirds of the root chord from the apex.

Figure 11 shows the pressure distribution calculated for a flat-plate arrow wing at incidence. These results are compared with both the exact linear theory solution and to another influence coefficient method recently published by Carlson and Middleton (reference 5). The wing has a subsonic leading edge and supersonic trailing edge at Mach 2.0. This particular wing planform has been studied extensively at the NASA Langley Research Center and as a result, both theoretical and experimental data are available for comparison. The present method agrees reasonably well with both the exact linear theory result and the cited numerical method.

The final example, showing the pressure distribution of a flat-plate, double-delta wing, is shown in figure 12. This was chosen to illustrate the application of the method to more general planforms. The exact linear theory analysis of this planform, based on a superposition procedure, was presented in reference 12. This particular planform was also analyzed by Middleton and Carlson in reference 2. The illustration shows the spanwise pressure distributions at two stations on the wing, which were obtained by interpolating chordwise pressure distribution plots. The pressure distribution shows the same magnitude and trends as the exact solution, but does not reproduce the pressure discontinuities predicted by the method of superposition.

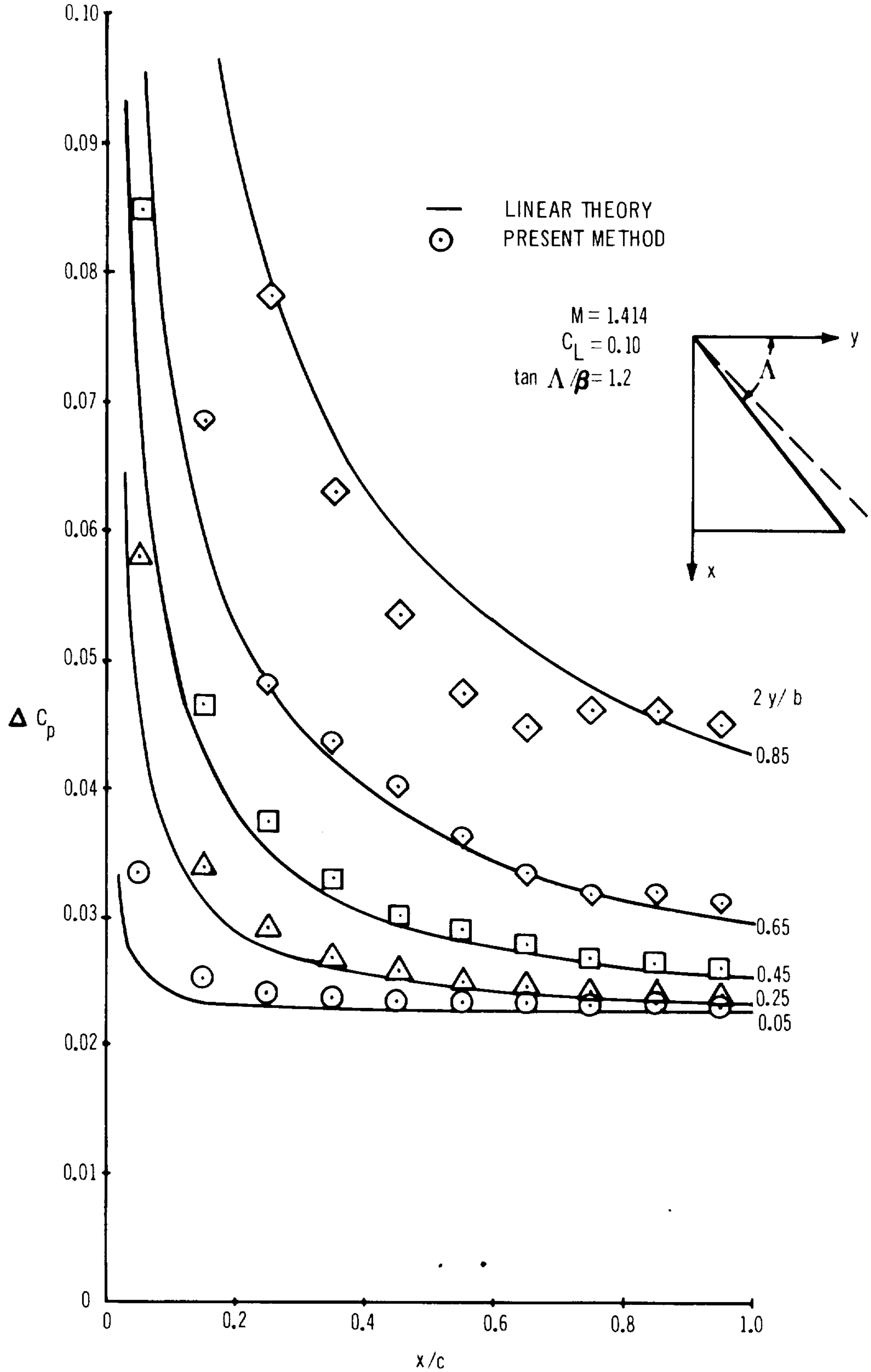

FIGURE 10 PRESSURE DISTRIBUTION – FLAT PLATE DELTA WING

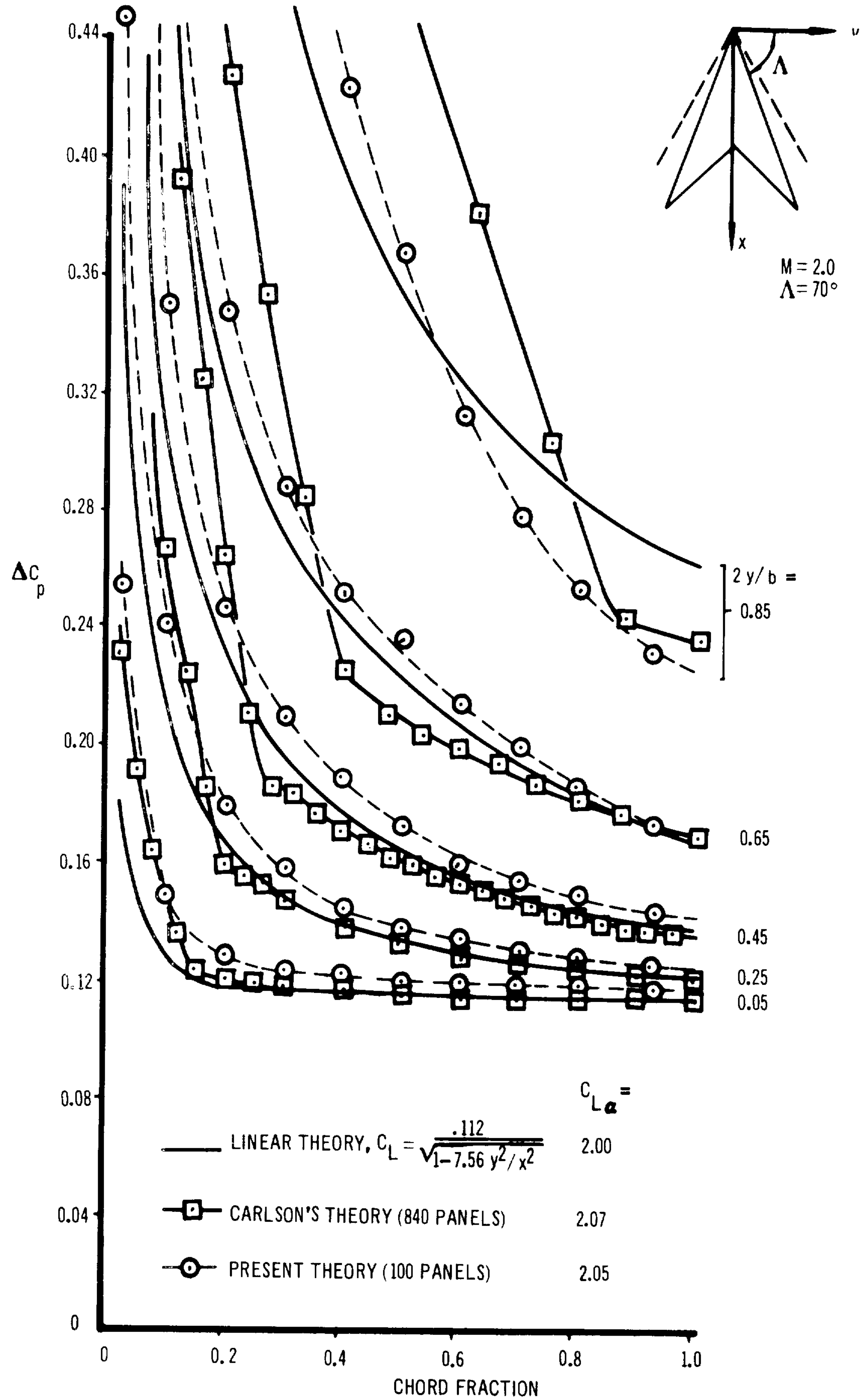

FIGURE 11 PRESSURE DISTRIBUTION – FLAT PLATE ARROW WING

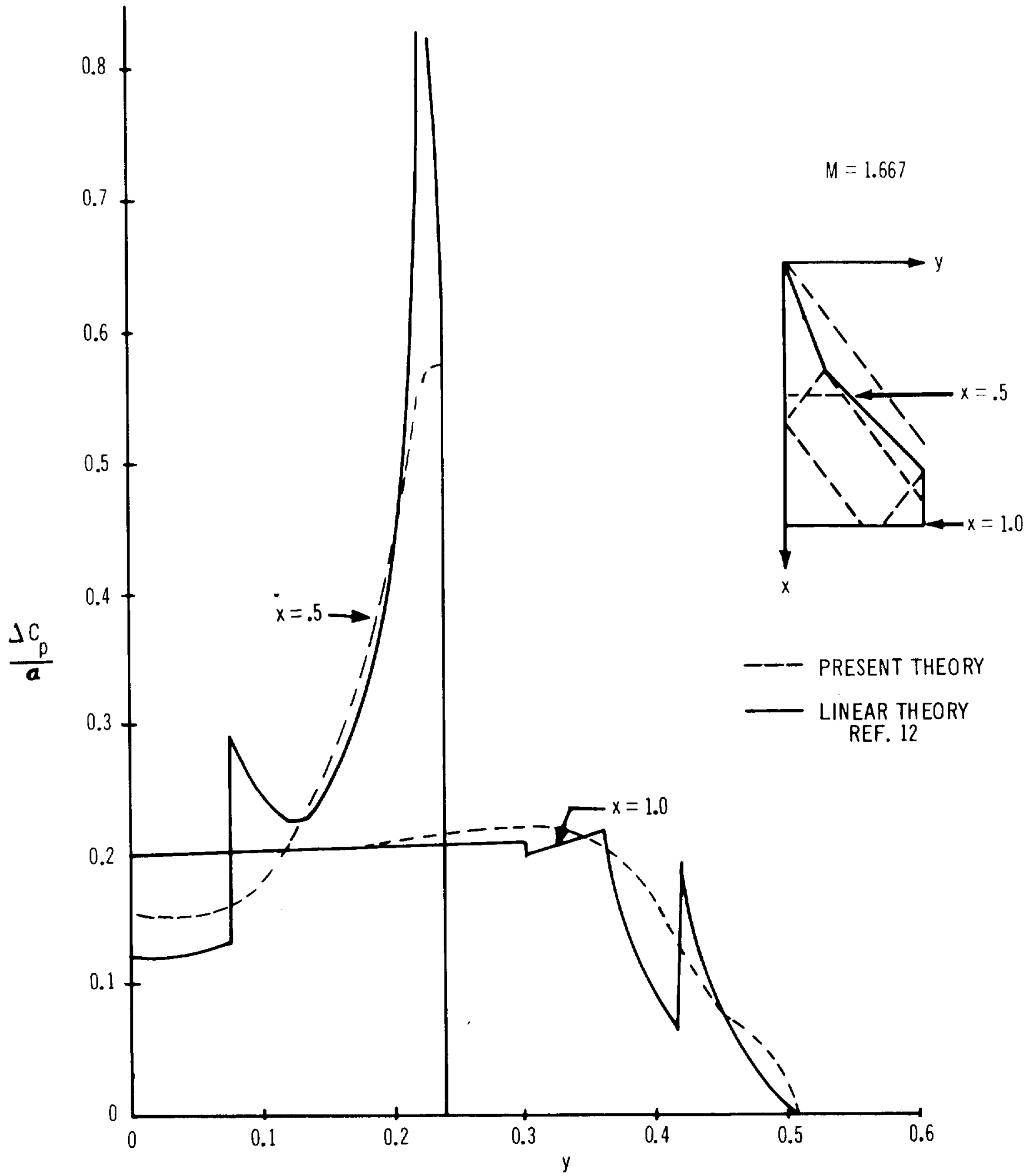

FIGURE 12 PRESSURE DISTRIBUTION – FLAT PLATE DOUBLE DELTA WING

The lift and center of pressure at two Mach numbers were estimated with reasonable precision, however, and are presented for comparison in the following table:

METHOD	M = 1.414		M = 1.667	
	C_L	X_{CP}	C_L	X_{CP}
Superposition Analysis (12)	0.0514	0.682	0.0461	—
Present Method	0.0516	0.691	0.0448	0.697
Carlson and Middleton (2)	0.0507	0.687	0.0449	0.686

Pressure distribution due to wing thickness.—Wing-thickness effects are simulated by constant distributions of sources on the panels. The behavior of these singularities is sufficiently different from the constant distributions of vorticity used to represent the lifting surfaces that a new control point must be defined for calculating the velocity components and pressures resulting from thickness. Best results were obtained when the thickness control points were located at the centroids of the panels.

The source singularities approximate the wing by a series of flat, wedge-like surfaces bounded by ridge lines along the panel edges. The slope of these surfaces corresponds to the actual surface slope only at the panel centroids; along the panel edges, the surface slope is discontinuous.

This method of representing the wing thickness appears to be adequate, provided no panel edges have the same slope, or nearly the same slope, as the Mach line. If this occurs, the solution diverges and an undesirable oscillation in the chordwise pressure coefficient generally appears in the calculation in the region of the sonic panel edge. An example of this effect is shown by the unsmoothed distributions ($\alpha = 0°$) in figure 27 (page 157) for a subsonic leading-edge arrow wing. The oscillation is insignificant inboard, but grows to an unacceptable magnitude as the tip section is approached. Fortunately, it is usually possible to fair a smooth curve through the end points of the pressure oscillation, a curve that will give a better approximation to the true chordwise pressure distribution in these cases. It should be noted that this pressure oscillation can be minimized by adding a singularity of higher-order to the present source representation. This additional singularity introduces a linear variation of the source distribution in the x direction, and would make it possible to eliminate the discontinuities in the surface slopes along the panel edges inside the wing planform.

Pressure distribution on cambered wings. — The pressure distribution on cambered wings is calculated in the same manner as the pressure distribution for flat wings at incidence. The slope of the camber surface must, however, be calculated at the panel control points. A sample calculation showing the chordwise pressure distributions on a cambered arrow wing with thickness at three angles of attack is presented in figure 28, on page 158.

The inverse problem of calculating the camber surface corresponding to a given pressure distribution is numerically simpler than the preceding problem and generally yields excellent results. An example giving the camber surface of a delta wing planform corresponding to a linearly varying chordwise pressure distribution is shown in figure 13. The camber surface is seen to agree very closely to that predicted by the method of reference 11.

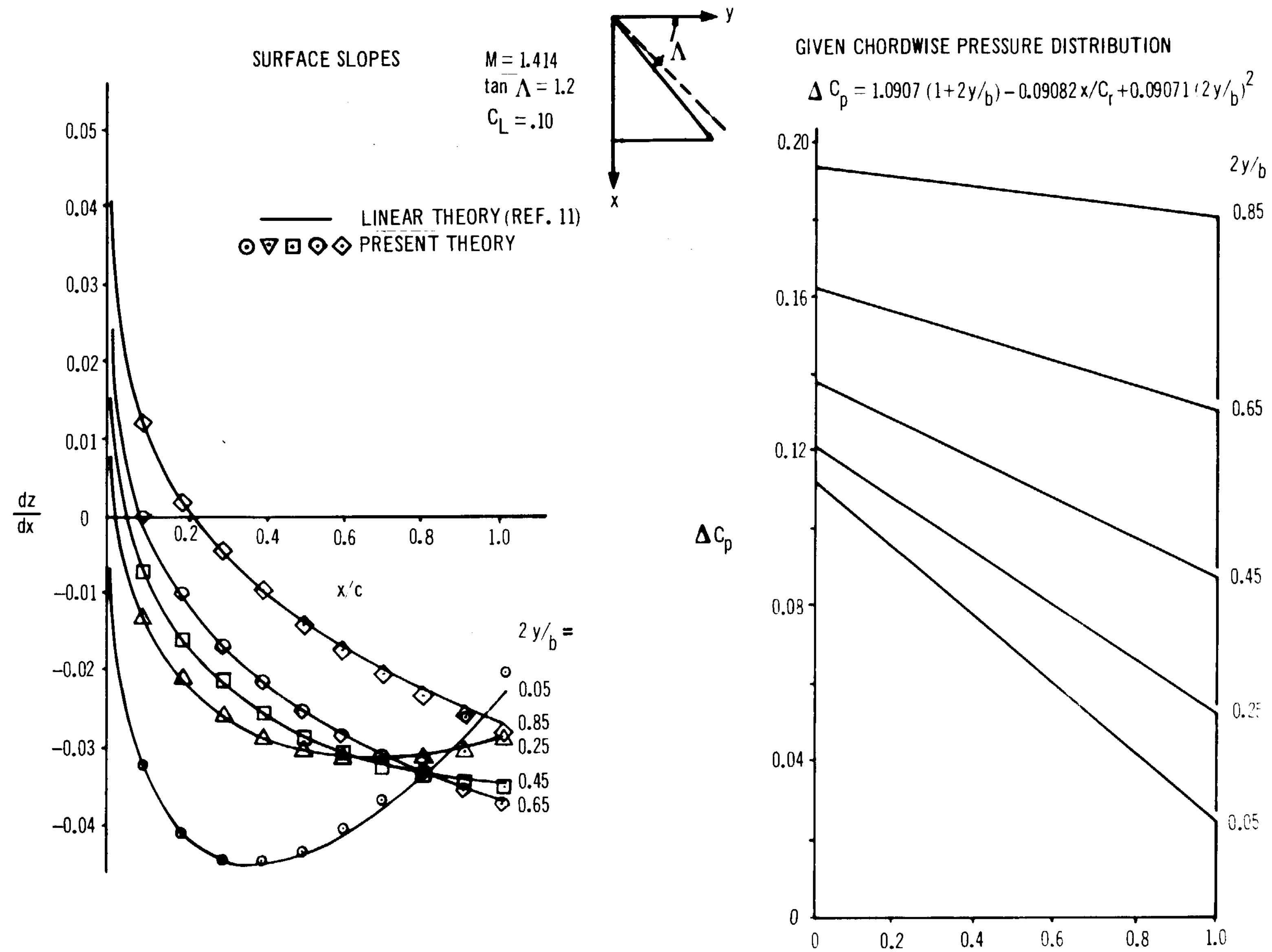

FIGURE 13 CAMBER SURFACE SLOPES FOR GIVEN PRESSURE DISTRIBUTION

Drag of cambered wings. — The pressure drag of a cambered surface is given by the double integral of the product of the surface pressure and slope, evaluated over the wing area:

$$D = -q \int_{-b/2}^{b/2} \int_{LE}^{TE} C_p \left(\frac{dz}{dx}\right) dx\, dy \tag{127}$$

In equation (110), this integral is replaced by a summation over the wing panels, as follows.

$$D = -q \sum_{i=1}^{N_W} C_{p_i} \left(\frac{dz}{dx}\right)_i A_i \tag{128}$$

where the slope of each panel is defined at its control point. This formula is adequate to calculate the drag of uncambered wings because the pressure on each panel is assumed to be constant, and the surface slope is constant between control points. For cambered wings, on the other hand, the surface slope of the wing varies continuously between control points, and may even approach infinity near the leading edge, as illustrated in figure 13. As a result, equation (128) will not in general yield a good approximation to the drag unless the term $(dz/dx)_i$ is replaced by the average slope of panel i.

As illustrated in figure 14, the slope of a cambered wing is approximated by a series of straight lines through the control points. The slope at any point on a given panel is estimated by a linear interpolation formula. If the panel lies along the leading edge, the slope is estimated by a linear extrapolation of the slope of the first two panels. The formulae are given below:

For leading-edge panels,

$$\left(\overline{\frac{dz}{dx}}\right)_1 = \left(\frac{dz}{dx}\right)_1 + \frac{\overline{R} - R}{1 + R\left(\frac{c_2}{c_1} - 1\right)} \left[\left(\frac{dz}{dx}\right)_2 - \left(\frac{dz}{dx}\right)_1\right] \tag{129}$$

For the remaining panels,

$$\left(\overline{\frac{dz}{dx}}\right)_i = \left(\frac{dz}{dx}\right)_i + \frac{\overline{R} - R}{1 + R\left(\frac{c_i}{c_{i-1}} - 1\right)} \cdot \frac{c_i}{c_{i-1}} \cdot \left[\left(\frac{dz}{dx}\right)_i - \left(\frac{dz}{dx}\right)_{i-1}\right] \tag{130}$$

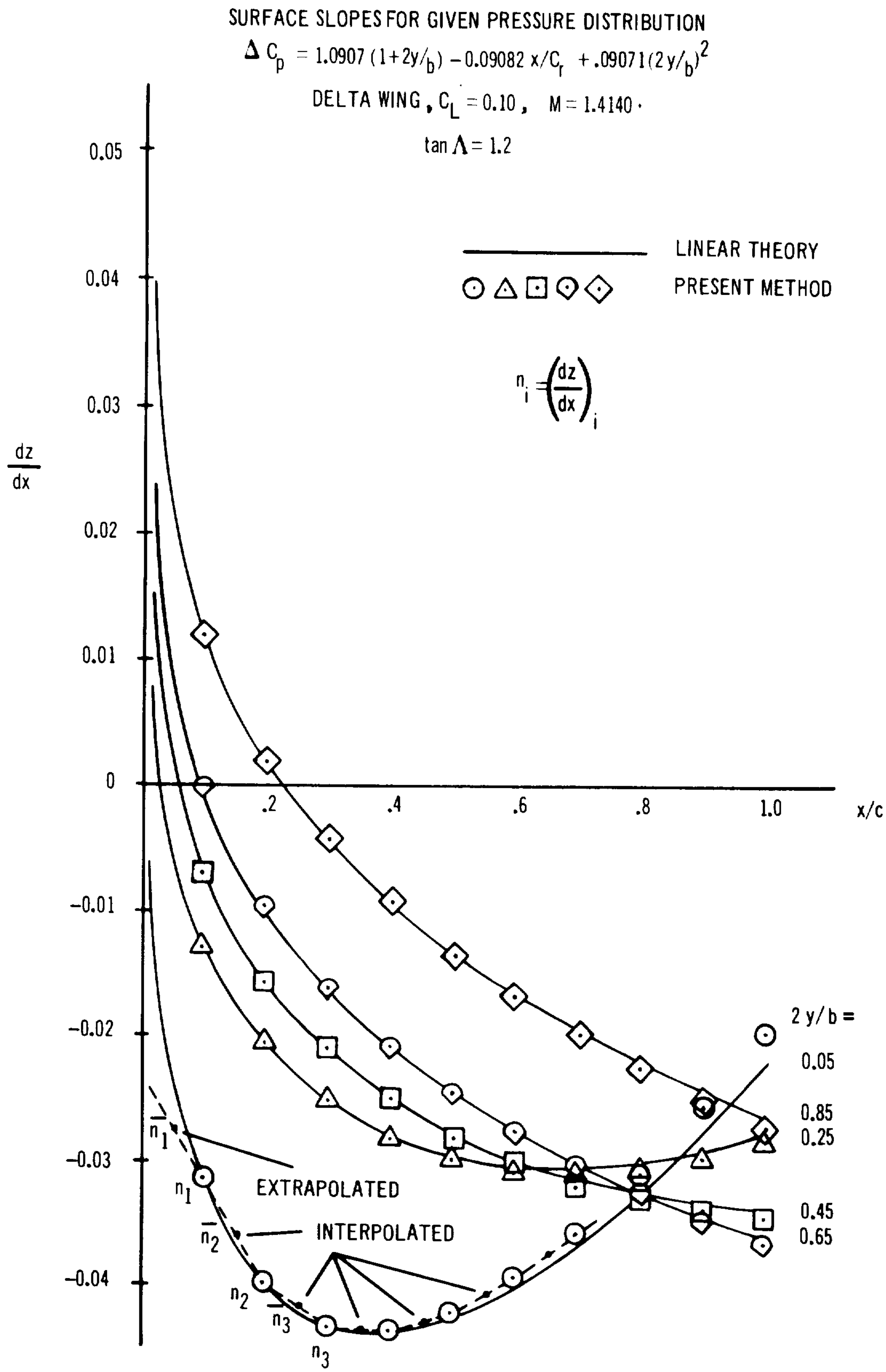

FIGURE 14 DETERMINATION OF SURFACE SLOPES FOR DRAG CALCULATION

where R is panel chord fraction defining the location of the panel control point

$\bar{R}$ is the panel chord fraction defining the average slope

c_i is the panel chord

c_{i-1} is the chord of the preceding panel

In equation (129) the subscripts 1 and 2 refer to the first and second panels along the leading edge in any given row.

The value of $\bar{R}$ has been chosen by making a comparison between the drag given by the program for a constant pressure delta wing, and the exact linear theory solution for this wing, which is:

$$C_D = \frac{\beta C_L^2}{4}\left[1 - \frac{2}{\pi}\left(b \cosh^{-1} b - \cos^{-1}\frac{1}{b} - \sqrt{b^2 - 1}\cosh^{-1}\frac{b^2 + 1}{2b}\right)\right] \quad \text{for } b = \frac{\tan\Lambda}{\beta} > 1.0$$

$$= \frac{\beta C_L^2}{4} \quad \text{for } b \le 1.0 \qquad (131)$$

The results are presented in figure 15. It can be seen that the drag given by the program varies linearly with $\bar{R}$, and increases as the point used for defining the slope moves towards the trailing edge of the panels. For subsonic leading-edge delta wings, agreement occurs for $0.675 < \bar{R} < 0.825$, depending on the wing aspect ratio. It should be emphasized that the drag given by the program deviates very little from the exact value over the entire range of R for wings having sonic leading edges, but that the deviation increases as the sweep-back increases. Wings having supersonic leading edges showed results almost independent of the choice of $\bar{R}$.

Additional correlations of this kind are required to confirm the validity of this method for calculating the drag of cambered wings. On the basis of the present limited study, however, it was decided to use the value of $\bar{R} = 0.75$ in the program for computing the effective panel slope used in the drag calculations. This choice of $\bar{R}$ gives values of $C_D/\beta C_L^2$ which differ by less than 2 percent for wings having the lowest aspect ratios studied, and less than 1 percent for the sonic leading-edge planform.

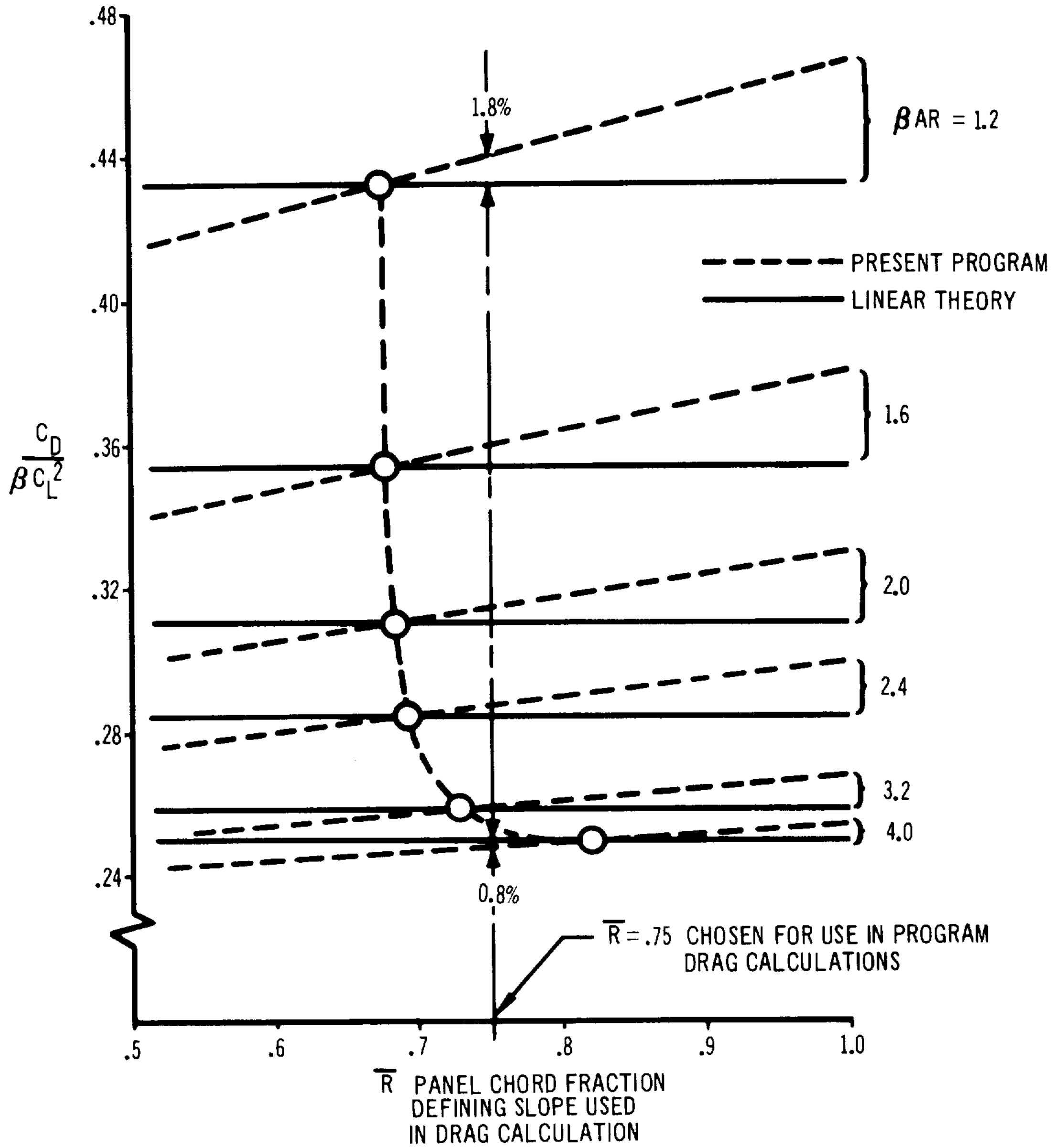

FIGURE 15 EFFECT OF SURFACE SLOPE INTERPOLATION ON DRAG OF CONSTANT PRESSURE DELTA WING

Wing camber for minimum drag. — Plots showing the minimum drag of a family of isolated delta and clipped-tip arrow wings are presented in figures 16 and 17 for comparison with data presented in reference 3 . The present theory calculates the surface shape for minimum drag by first calculating the optimum pressure distribution by inverting the matrix of equation (126), and then substituting this result into equation (114) to obtain the corresponding panel slopes. Both the aerodynamic matrix and the panel slopes are calculated for control points located at 95 percent of the local panel chords, to avoid undesirable oscillations in the results. The slope interpolation formulae developed in the previous section are then applied to calculate the drag of the resulting cambered wing. The interpolated panel slope corresponding to $\overline{R} = 0.75$ was used in the drag calculations shown in the figures.

Figure 16 shows the results obtained for a family of delta wings. The minimum drag calculated by the present program is somewhat higher than that estimated by the methods of reference 3 for wings having subsonic leading edges. On the other hand, the results do agree reasonably well with the predictions of the aerodynamic influence coefficient method of reference 1 . The drag predicted for the flat-plate wing without leading-edge suction agrees closely in all three methods, however.

Figure 17 shows similar results for a family of clipped-tip arrow wings. As indicated on the figure, excellent agreement is obtained between this result and the minimum drags estimated by the methods of both references 1 and 3.

It is apparent from an examination of these results that further correlations between the present theory and other known minimum drag solutions will be very desirable in order to obtain confidence in the range of application of the method. In the meantime it is sufficient to say that the method gives good agreement with other accepted procedures for determining the wing camber surface for minimum drag.

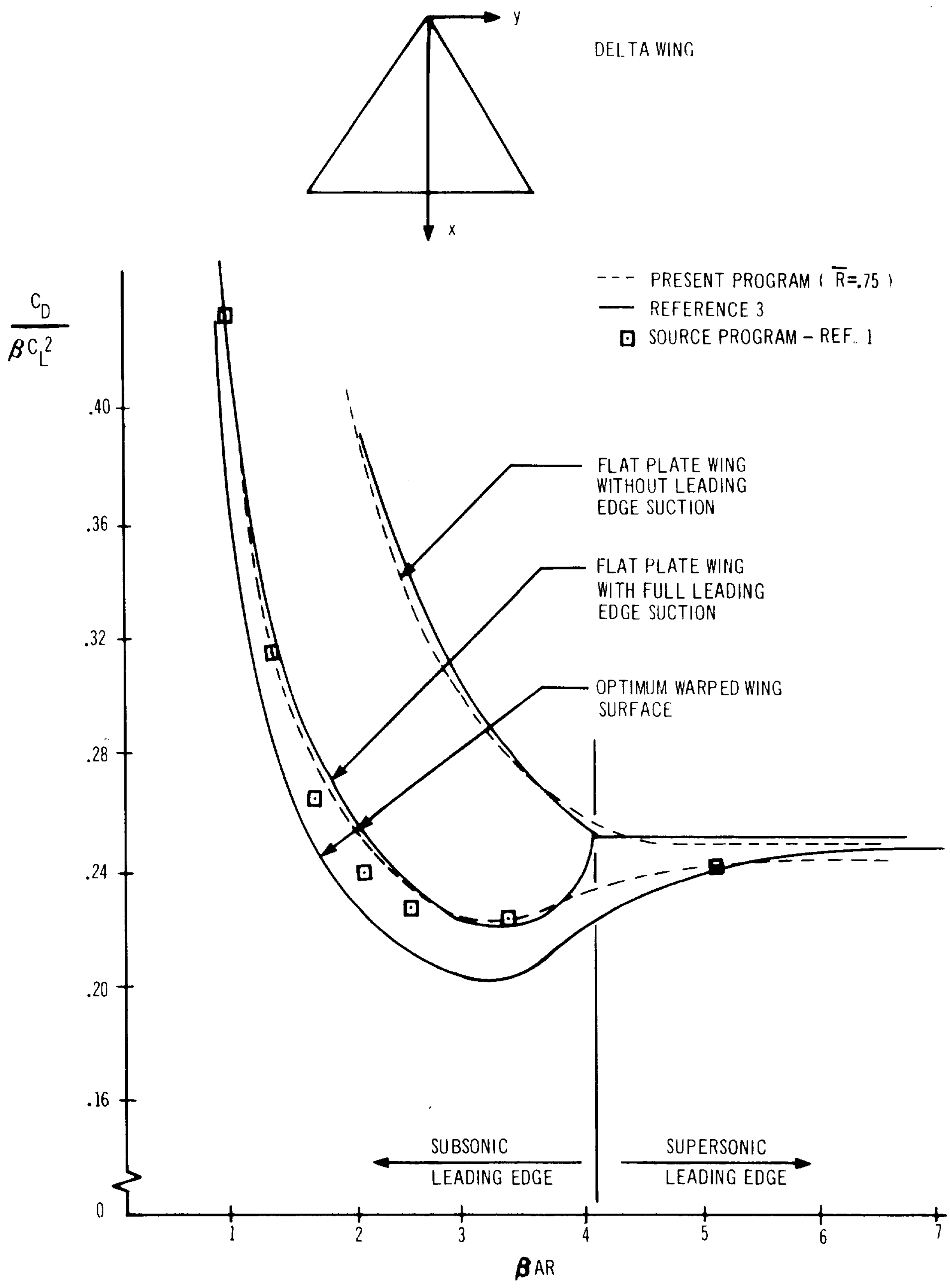

FIGURE 16 MINIMUM DRAG OF DELTA WINGS

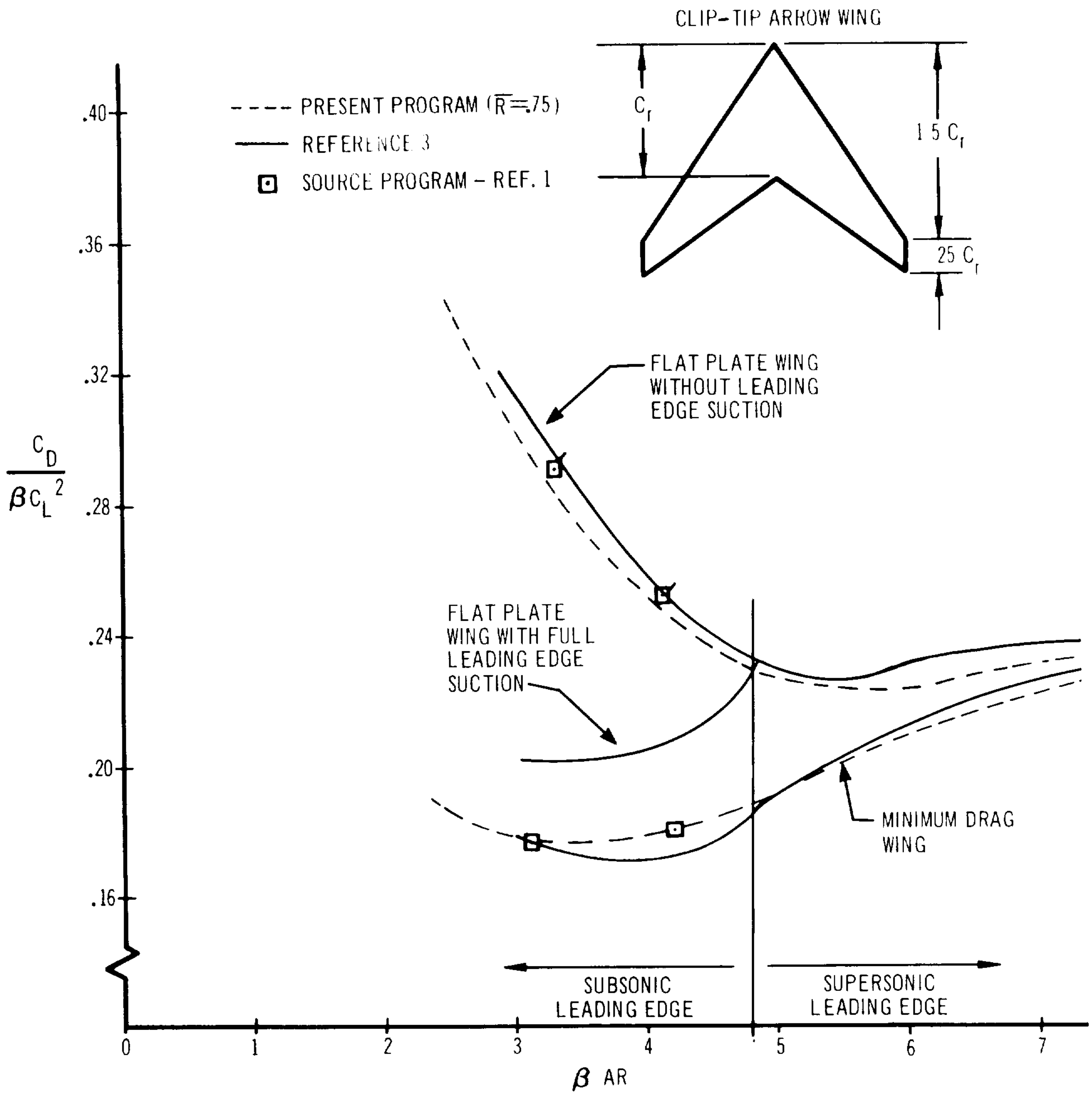

FIGURE 17 MINIMUM DRAG OF CLIPPED TIP ARROW WINGS

Pressure distribution on a cone. — The circumferential pressure distribution at Mach 2.0 for a 10-degree circular cone at an incidence of 0.10 radian is presented in figure 18. The pressure distributions are identical at all sections along the length of the cone. The results obtained with both the linear and nonlinear pressure coefficient formulae are illustrated. On the basis of the nonlinear formula (equation 102) the program predicts a lift coefficient only half the exact theoretical value of 0.185 given by the cone tables. The lift coefficient of the cone is predicted much more accurately if the linear pressure coefficient formula (equation 105) is used in the program.

At zero incidence, the linear formula again gives a closer approximation to the exact value. The cone tables give the value for $C_p = 0.104$, while the linear formula gave $C_p = 0.114$, and the nonlinear formula $C_p = 0.087$.

For bodies of revolution of arbitrary shape, it has been found that, in general, the nonlinear pressure coefficient formula gives the best approximation to the experimental results at zero incidence. Lift effects, on the other hand, are best estimated by the linear formula. An example comparing the theoretical and experimental pressure distributions on a parabolic body of revolution is shown in figure 25 (page 153).

Pressure distribution on wing-fin combination. — The pressure distributions calculated for a rectangular wing in the presence of an inclined rectangular fin are presented in figure 19, and compared with the linear theory solution given by Snow in reference 13.

The theoretical solution for the case in which the wing has an incidence α, and zero fin incidence, is given below:

On the wing

$$C_p = 2\alpha\left[\frac{B}{\gamma} + \frac{2}{\pi}\tan^{-1}\frac{R^{\pi/\gamma}\sin\pi B/\gamma}{1 - R^{\pi/\gamma}\cos\pi B/\gamma}\right] \tag{132}$$

On the fin

$$C_p = 2\alpha\left[\frac{B}{\gamma} + \frac{2}{\pi}\tan^{-1}\frac{R^{\pi/\gamma}\sin\pi B/\gamma}{1 + R^{\pi/\gamma}\cos\pi B/\gamma}\right] \tag{133}$$

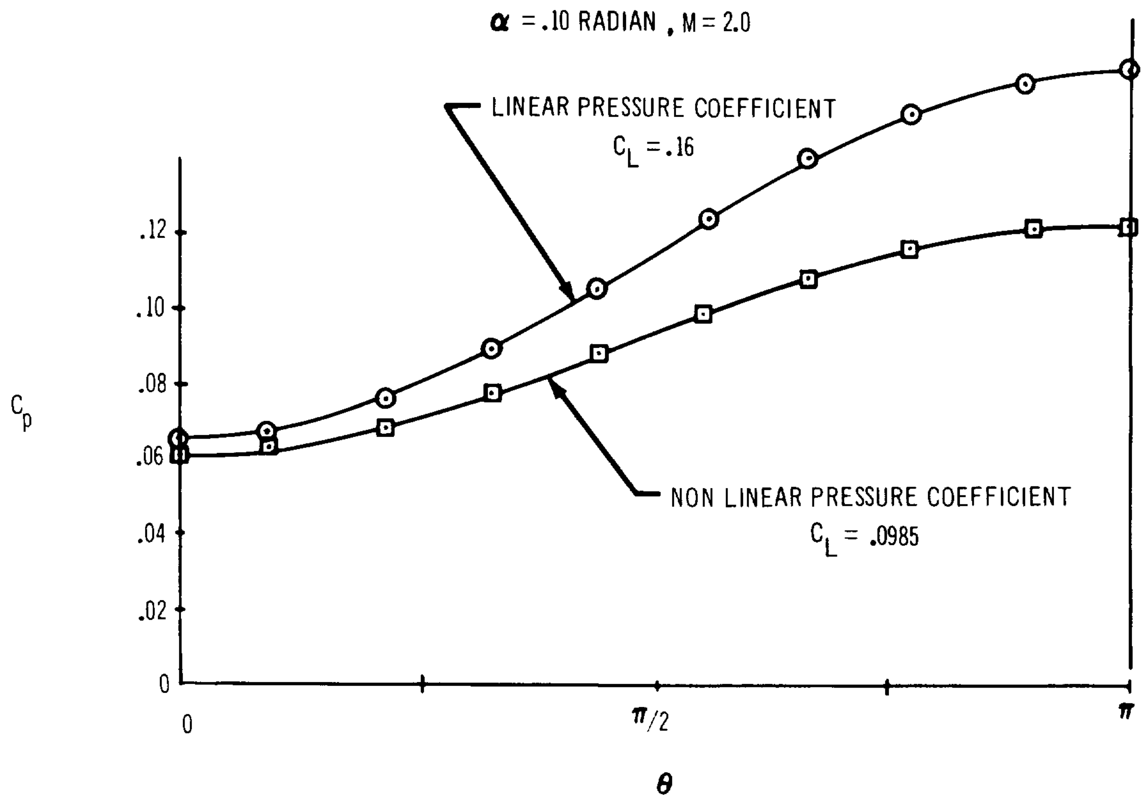

FIGURE 18 PRESSURE DISTRIBUTION ON 10° CONE AT INCIDENCE

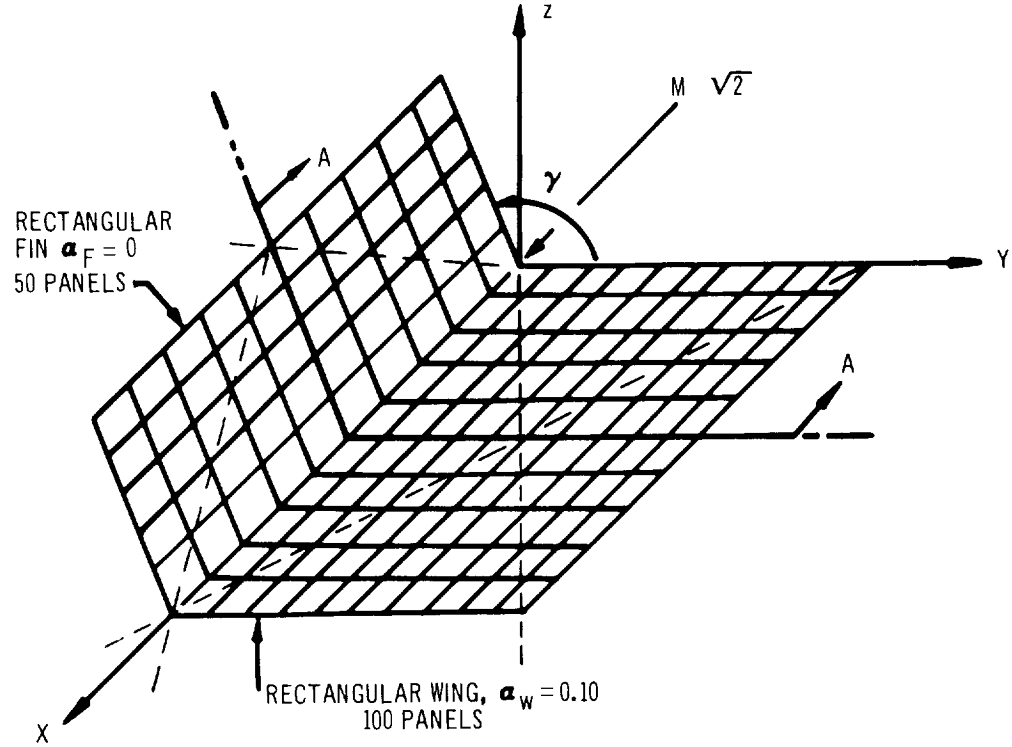

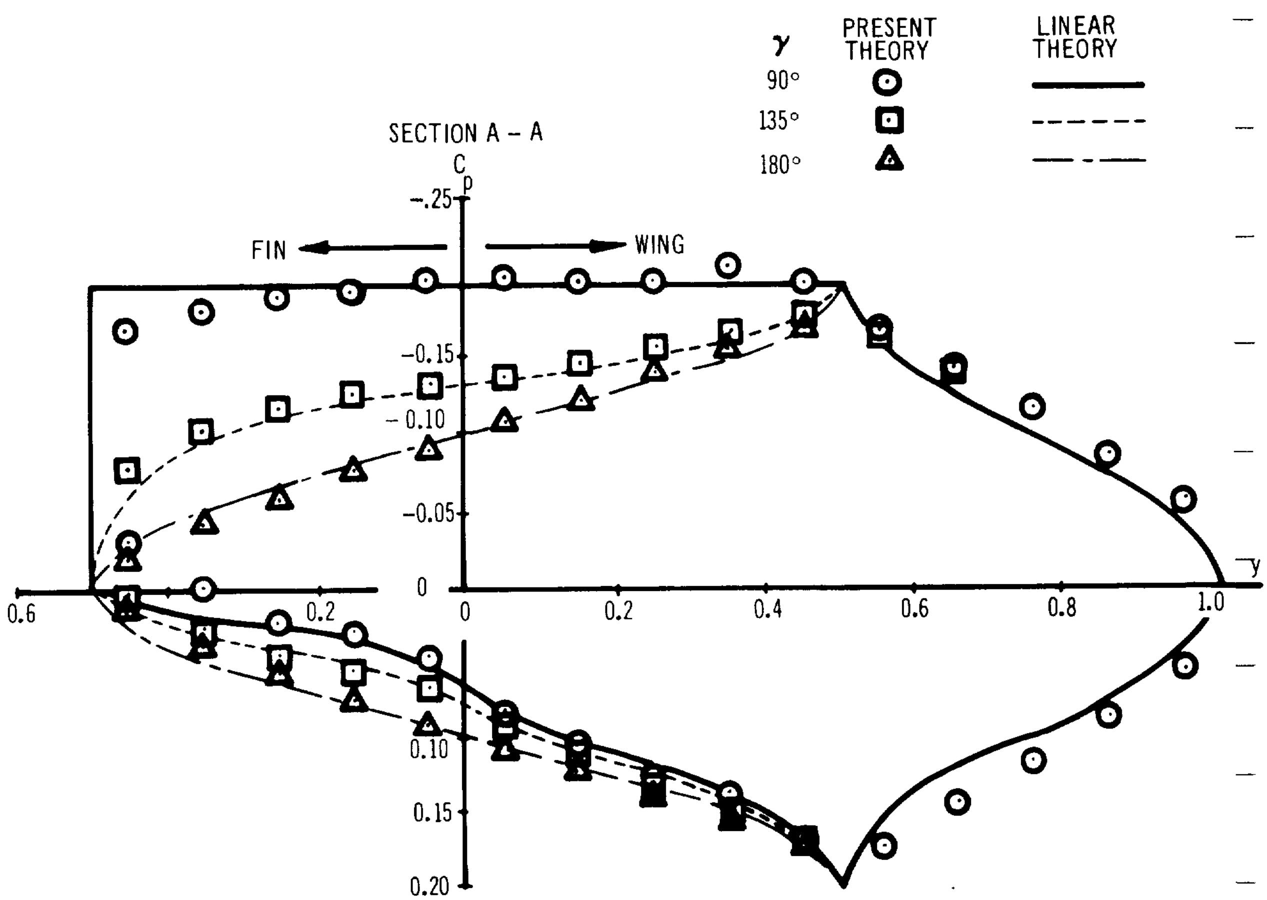

FIGURE 19 PRESSURE DISTRIBUTION ON WING-FIN COMBINATION

where $B = \cos^{-1}\left(\frac{\tan \Lambda}{\beta}\right)$

$$R = \left(1 - \sqrt{1 - r^2}\right)/r$$

and $r = \beta \sqrt{y^2 + z^2}/x$.

In the figure, the spanwise pressure distributions at the midchord are compared for three fin inclinations. The agreement is excellent.

The program, in its present form, will no longer admit cases involving wing-fin combinations as shown. This is the result of specializing the geometry definition and paneling sections of the program, which restricts its application to configurations composed of wings and circular bodies only.

Pressure Distributions on Wing-Body Combinations.—Figure 20 shows the pressure distributions calculated for a rectangular wing-rectangular body combination analyzed byLu Ting in reference 14. The calculated pressure coefficients oscillate above and below the theoretical results published by Lu Ting, particularly in the area of the wing-body intersection. The reason for this oscillatory behavior is not known at present, although an instability inherent in the numerical analysis is suspected. It is interesting to note that similar instabilities did not occur for the polygonal bodies used to approximate bodies of revolution in the other examples presented in this report.

Wing and body pressure distributions calculated at Mach 1.48 for a configuration composed of an unswept rectangular wing centrally mounted on a circular body are presented in figures 30 through 33 (pages 161 through 164). The presure distributions calculated by Nielsen (reference 15) are presented in terms of an incremental pressure coefficient P, obtained by taking the difference between the local pressure coefficients for the lifting case and the non-lifting case ($\alpha_W = \alpha_B = 0$). In this way, the effects of the nose shape on pressure distributions are eliminated. It should be remarked that the present theory calculates the surface pressure distributions including the effect of the nose shape; consequently, the results presented are the difference between two calculations. The incremental pressure coefficients calculated on the wing and body agree favorably with Nielsen's theoretical results, both for wing only at incidence and for the case in which both wing and body are at incidence.

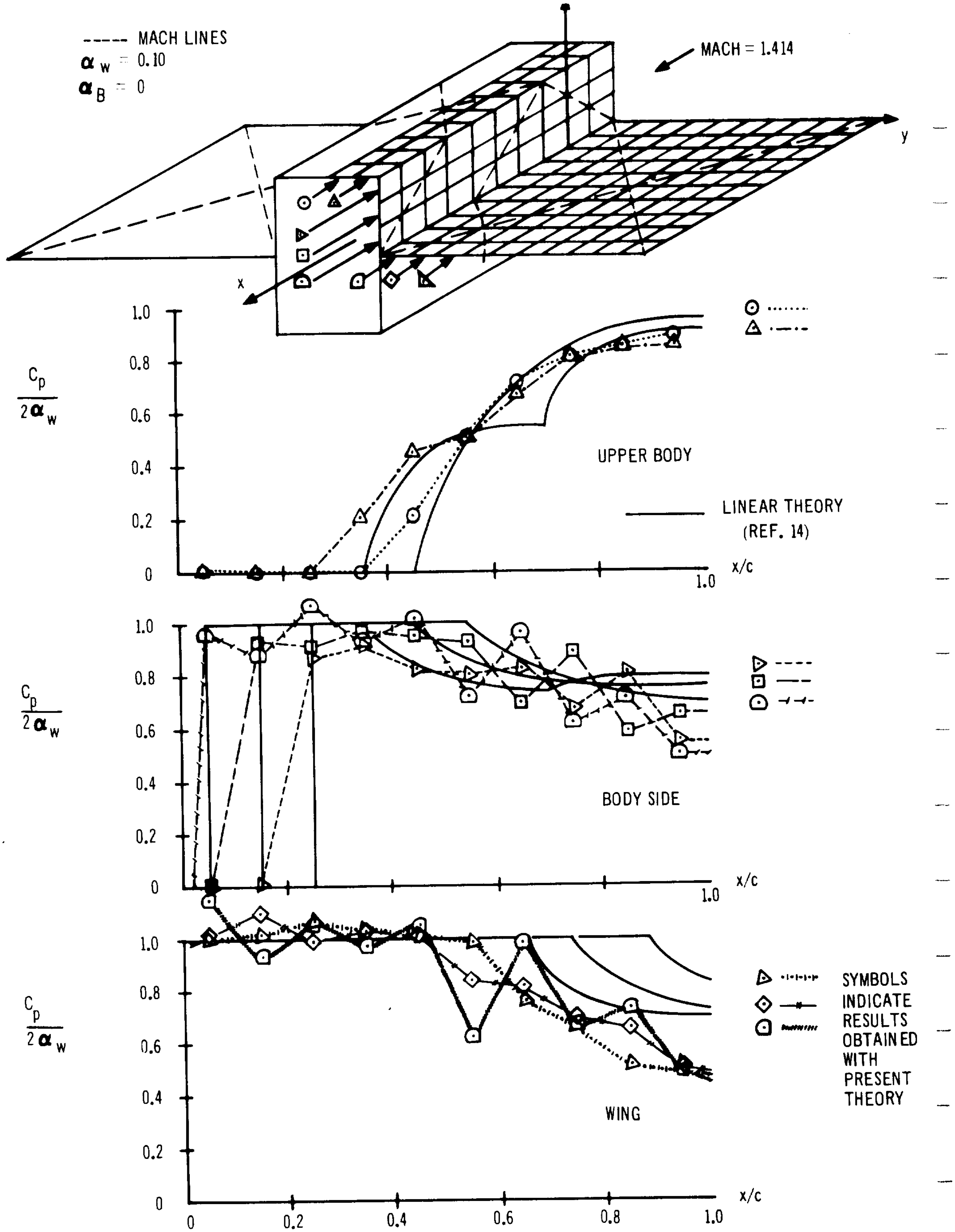

FIGURE 20 PRESSURE DISTRIBUTION OF RECTANGULAR WING – RECTANGULAR BODY COMBINATION

5. COMPUTER PROGRAM

5.1 Description

The digital computer program described in this section has been developed to solve the problem of optimization of wing camber surfaces for wing-body combinations at supersonic speeds. Direct and other indirect aerodynamic problems can also be solved.

The program is coded in FORTRAN IV and MAP languages for the IBM 7090/7094 (32K) digital computer under the Systems Monitor, IBSYS Version 12. It is compatible with the NASA-Ames direct-coupled IBM 7040/7094 computer system. Because the program exceeds the capacity of a single core load, the Loader Overlay feature is used which allows the complete program to be subdivided into smaller segments, or links. The links are processed in a specified order to solve a particular problem.

The Overlay feature requires one of the system units to be used as the input-output tape on which the links are written. This unit is specified on the $ORIGIN control card according to the procedure outlined in Part II. In addition to the input and output tapes, the program uses seven tape units for scratch purposes. The choice of tape units to be used will depend on the particular computer installation, and tapes must be changed as required. A special purpose subroutine, OPCAMI, initializes all the tape units and assigns a logical number to each. To make any tape changes, it will be sufficient to change only the logical designations in this subroutine (see Part II).

The complete program consists of four sections: Geometry Definition, Geometry Transformation, Geometry Paneling, and Aerodynamics, as outlined by the flow chart (figure 21). The first two sections provide a suitable geometric description of the configuration and the third section subdivides the configuration into panels. The Aerodynamics section performs all aerodynamic calculations and solves the problem under consideration.

Program execution is controlled by the subroutine OPCAM, a control program located in link 0 under the program Overlay structure. Those control cards within the data deck that determine which program sections are used to process the case, are read by the subroutine OPCAM and lower-level subroutines in each of the following four program sections:

1. GEOMD in link 5 (Geometry Definition section)
2. TFLAT in link 11 (Geometry Transformation section)
3. PANEL in link 12 (Geometry Paneling section)
4. AERO in link 20 (Aerodynamics section)

Multiple cases, each involving a different wing-body configuration, can be run. When a nonsystems error condition occurs during processing within a section of the program, an error message appears, execution of the present case is terminated, a partial data printout is given, and the following case is processed.

Execution time averages 7 to 8 minutes for a typical (100 panels) body-alone or wing-alone case and 18 to 20 minutes for a wing-body combination of 200 panels. The computer time and number of printout lines for a single configuration can be estimated from the following equations based on experience on an IBM 7094/M2.

Time (minutes) $= 2.2 + 0.3G + (3.8 \cdot 10^{-4} \cdot P^2) \cdot A + 0.6C,$

where G indicates type of paneling:

- = 0., no paneling
- = 1., wing paneling only
- = 2., wing and body paneling

P is number of panels (if no paneling is required, use P = 10)

A indicates aerodynamic calculations:

- = 0., no aerodynamic calculations
- = 1., aerodynamic calculations requested

C is number of aerodynamic cases. Each of the following are considered a case:

Wing optimization case

Direct aerodynamic case

Indirect aerodynamic case

Each angle of a polar series

Output (lines) $= 100 + \{500 + (10 \cdot P^{1/2}) \cdot V \cdot C\} \cdot T$

where V indicates velocity component printout:

= 1., no velocity component printout

= 2., velocity components requested

T indicates type of case:

= 1., wing-alone case

= 2., body-alone case

= 3., wing-body case

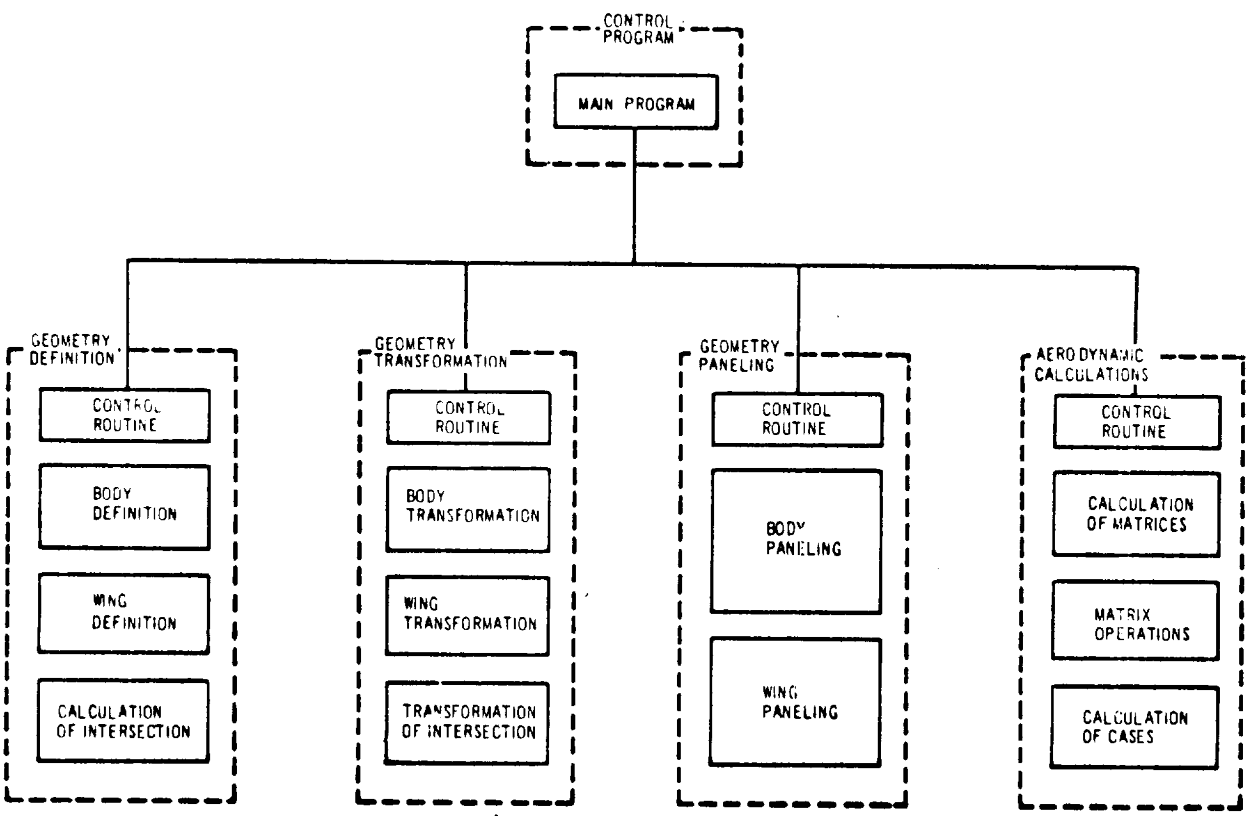

FIGURE 21 PROGRAM FLOW CHART

5.2 Program Usage

The program solves a problem in three steps. In the first step the configuration geometry is defined and transformed to a more convenient representation from input information. A wing alone, body alone, or wing-body combination can be defined. In the second step the configuration is paneled and required geometric data are calculated. Figure 22 illustrates the definition and paneling sequence. The third and final step performs the aerodynamic calculations for each case requested. Discussion of the body alone, wing alone and wing-body problems follows.

Body alone. — For the body-alone case, no paneling is required. The entire body is represented as an equivalent body of circular cross section by a series of equally spaced line sources and doublets. The user may define a cambered body with arbitrary cross section and have the program determine the equivalent body of revolution, or an equivalent body may be input with its camber specified separately.

The user specifies the body by a number of X-stations at which an array of radii (ρ) and angles (θ) are given. A maximum of 50 body stations may be specified. The program assumes that all bodies are symmetrical about the vertical plane; therefore, only data for half-bodies are specified, that is, 0 degrees $\leq \theta \leq 180$ degrees where the top meridian line corresponds to $\theta =$ 0 degrees and the bottom meridian line corresponds to $\theta = 180$ degrees. Alternate techniques for specifying body stations are presented in the discussion of card input format, section 5.3.

An axis, referred to as the body definition axis, is established parallel to the computer reference X-axis. The body definition axis location is established by specifying a Y,Z coordinate pair through which the axis must pass. Points, from which the ρ - θ arrays generate body sections at each station, are specified relative to the body definition axis at each defining station. After the ρ - θ array has been computed, the program constructs longitudinal meridian lines through sets of radii end points. The resulting computer definition will look similar to the following sketch:

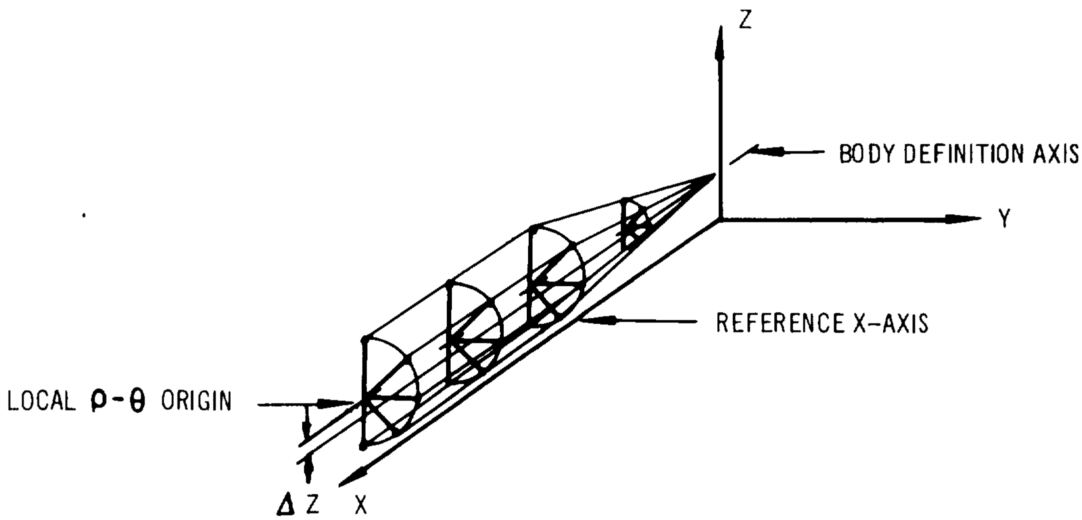

The locations of the cross-section centroids of the aft body station and the forward body station are then determined by the program. Centroid locations are determined from the station cross-section geometry. The section area and centroid depend on the type of interpolation chosen to define the fairing between the given points. If linear interpolation is requested, a polygonal area will be formed. If biquadratic interpolation is requested, a somewhat different area will result as shown below.

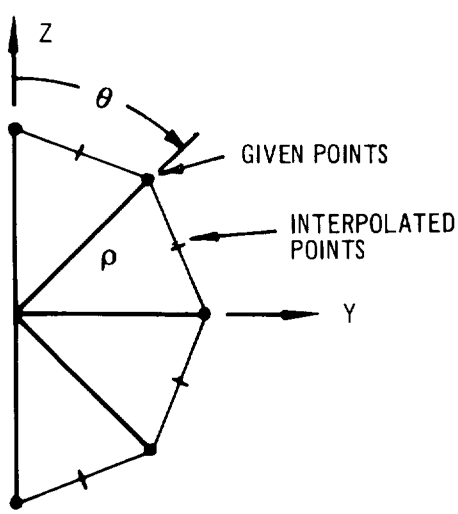

BODY STATION AREA FOR LINEAR INTERPOLATION

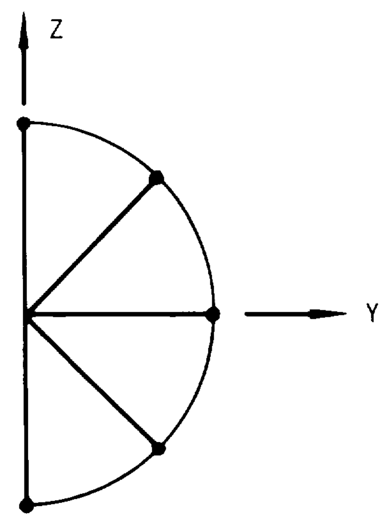

BODY STATION AREA FOR BIQUADRATIC INTERPOLATION

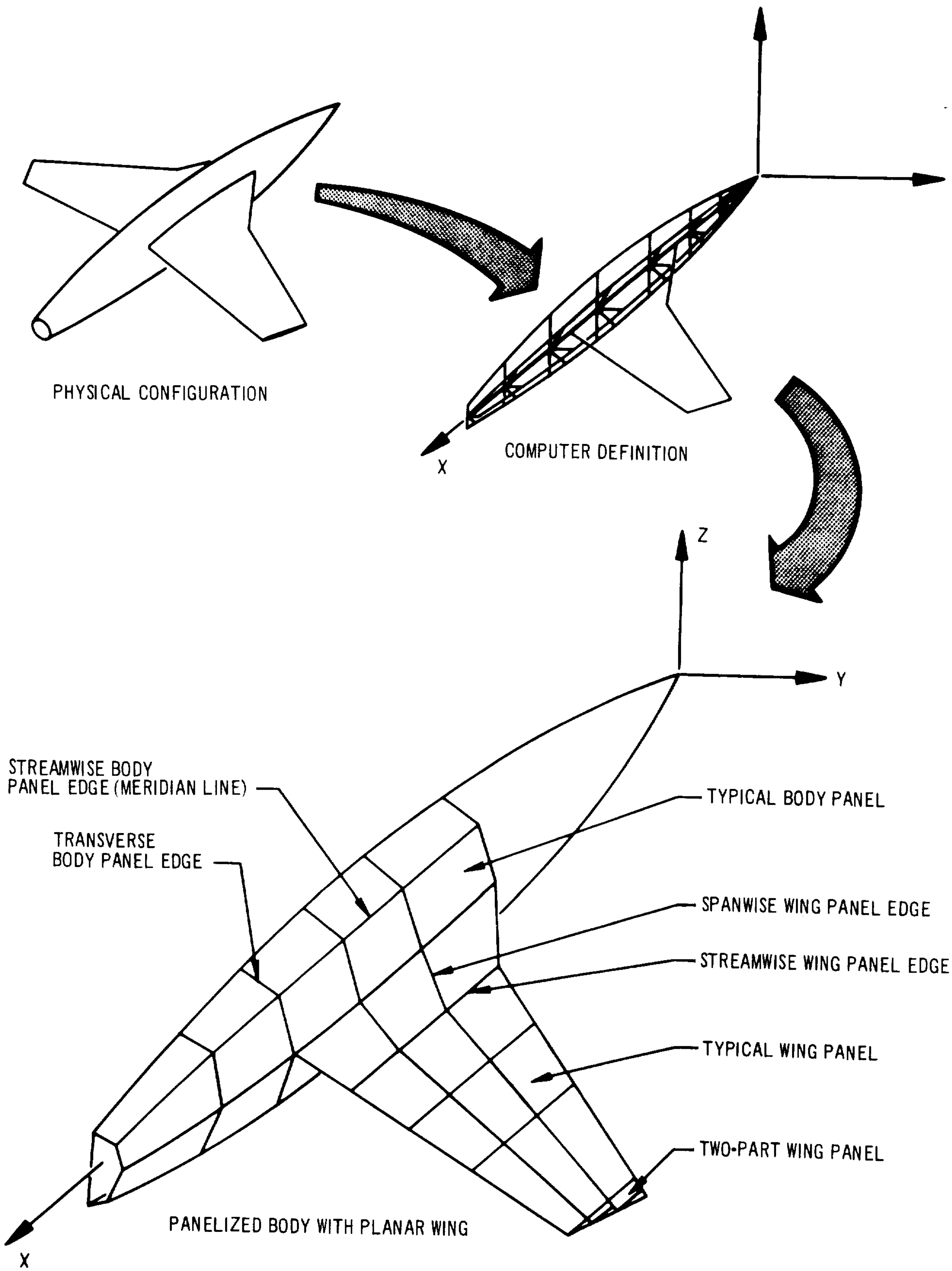

FIGURE 22-DEFINITION AND PANELING SEQUENCE

If a body of revolution is being defined (constant ρ at each station), a symmetrical θ-array should be specified or the centroid location will be incorrect. The sketch below shows how a nonsymmetrical θ-array can cause an error in the centroid location.

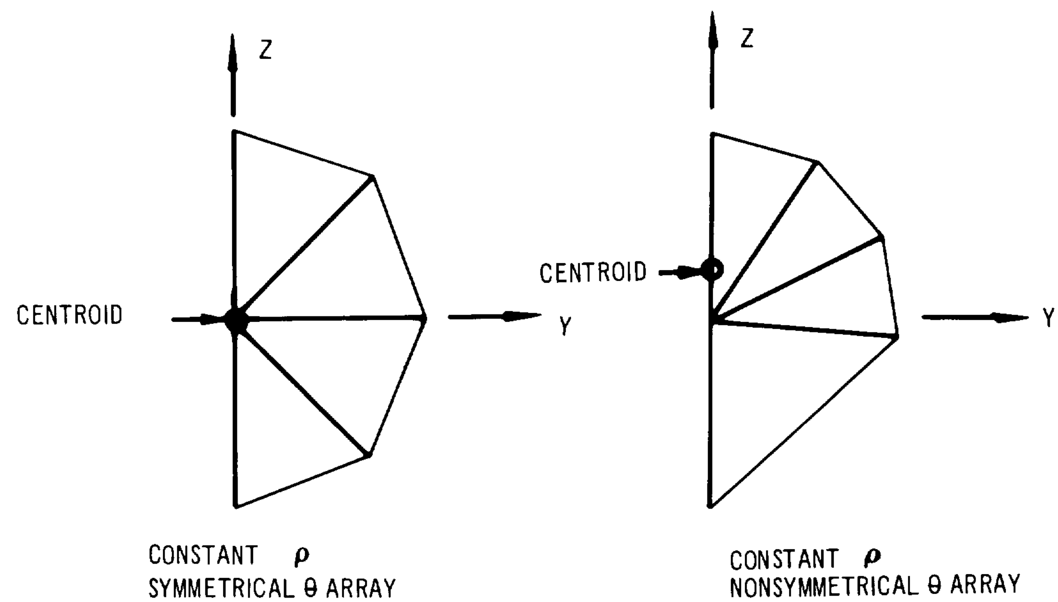

After the fore and aft section centroids have been determined a new body axis, the x-axis, is constructed through these centroids. All remaining calculations are performed relative to the new body axis system. An equivalent body of revolution about the x-axis is determined. The number of stations along the new body axis at which line source boundary conditions are located is specified. Because these stations are evenly spaced along the body length, the specification of the number of sources effectively establishes their location. The body is cut at each source control station by transverse planes. Centroid locations relative to the body axis are determined from the body sections resulting from these transverse cuts.

The average of the radii connecting the x-axis with meridian lines at each source control station is used as the radius of the equivalent body with circular cross sections. These radii are used by the aerodynamic section to determine the body source strengths.

The aerodynamic section now determines the axial and circumferential velocities and pressure coefficients at source control stations. Total C_L, C_D, and C_M are determined for the specified Mach number and angle of attack. The program input for a parabolic body having a fineness ratio of eleven is presented on page 134 and 135 in section 5.4.

Wing alone. — It is first necessary to define the wing planform by specifying the coordinates of all corner points and break points. Control chords, except perhaps the wing tip control chord, are defined streamwise through each corner point and break point. A minimum of two control chords must be specified. A pointed wing tip is considered as a control chord of zero length. The wing planform is defined by projecting the actual wing into the X,Y plane as shown below.

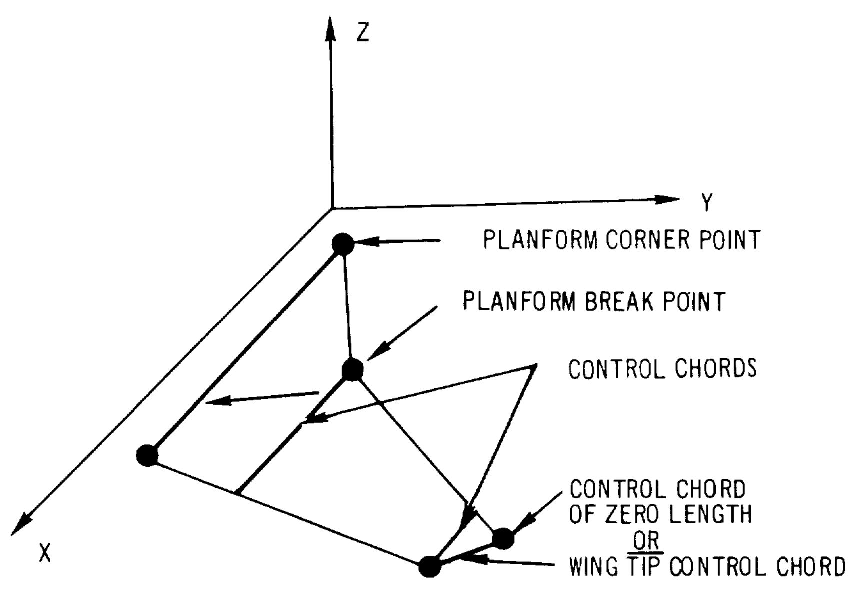

The program paneling section is used to panel the wing. A maximum of 100 wing panels may be specified. Spanwise panel edges are specified by a single set of constant percent chord lines. Streamwise panel edges are specified by a series of wing buttock line locations. Wing tips can be paneled in two different ways as shown below:

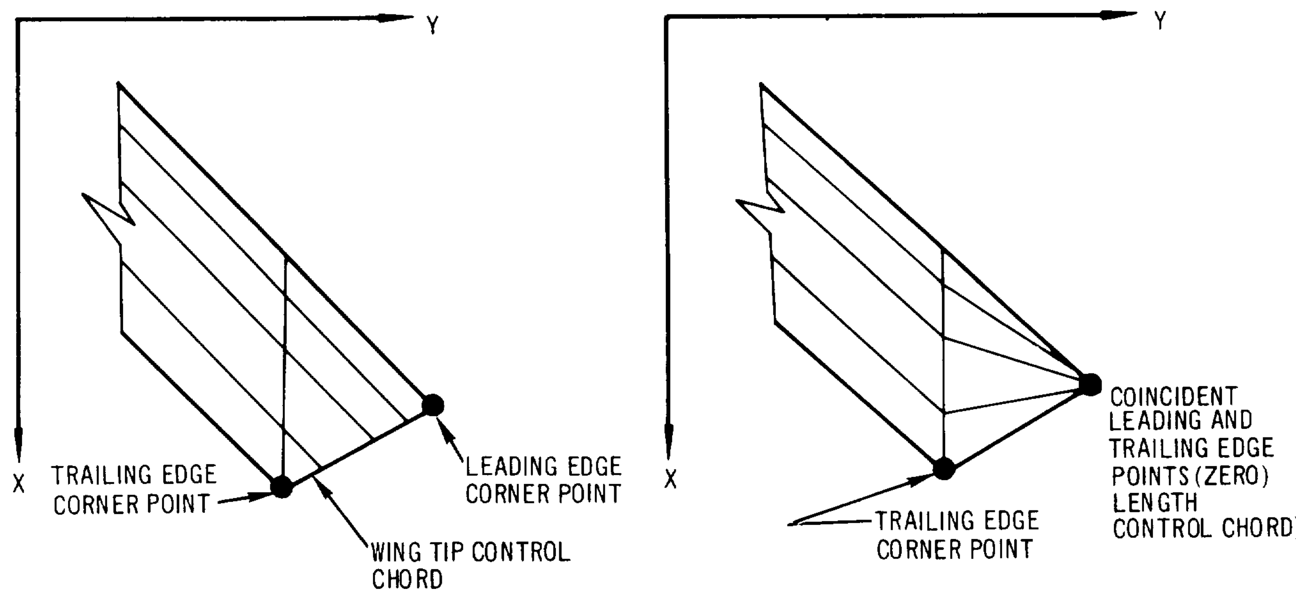

Tip paneling is in part controlled by the technique of defining the wing. If a planform corner point on the trailing edge is joined to a corner point on the leading edge by a wing-tip control chord of finite length, the spanwise panel edges will form quadralateral tip panels. If the planform leading and trailing edge tip points are specified as coincident, the tip will have triangular panels.

Wing thickness is specified by tables of upper and lower airfoil ordinates. Camber and twist can be either included in these ordinates or input as slopes in the aerodynamic section. The airfoils, one for each streamwise column of panels, must be oriented streamwise at spanwise locations corresponding to the Y-centroid of each column. A nondimensional airfoil ordinate array can be specified, because the program scales every array to fit the chord length at the specified span location. Further, for wings having no twist and the same airfoil from root to tip, only one ordinate table is needed. The program will scale and correctly locate the airfoils across the span.

Program inputs for an arrow wing having camber, twist, and thickness are shown in section 5.4 (page 137). The aerodynamic section calculates pressure and force coefficient data for the specified wing geometry at Mach 2.05 for an angle of attack series (θ = 0, -2, 2, 6 degrees). In addition, the wing camber shape, pressure coefficients, and force coefficients for a wing with identical planform and thickness distribution are determined for two cases. One has a constant ΔC_p distribution and the other is a minimum drag wing. Both are constrained to a total $C_L = 0.1$.

Wing-body combination. — The wing-body case, the most complex both geometrically and aerodynamically, requires full utilization of the program. The wing and body are defined as in the previous discussions on wing alone and body alone. However, because the effect of the wing on the body is desired, it is necessary to panel the body in the region aft of the wing leading-edge intersection. The effect of the wing on the body is determined by the influence coefficient method. Body pressures caused by body thickness and camber are still determined by the source-doublet method. A maximum of 100 body panels and 100 wing panels may be specified.

The program panels the defined body. If it is desired that the equivalent body of circular cross section be paneled, the body defined must be the equivalent body. Note that in a body alone case, the radii and station centroid locations determined by the geometry section are passed directly to the aerodynamic section for calculating the source and doublet strengths. This procedure bypasses the paneling section. Therefore, the paneling section operates on the body definition.

The geometry section defines the body in the same manner as the body-alone case. The meridian lines constructed in the definition section form the streamwise body panel edges. Therefore, it is necessary to know the desired body paneling when the body definition is being established, because the θ-array determines the radial location of meridian lines. The transverse body panel edges are specified in the paneling section. Wing paneling is handled the same as in the wing alone case except that the inboard wing panel edges formed by the wing-body intersection are determined by the program. The wing definition should extend into the body. This ensures that a wing-body intersection will be found by the program. Only the exposed wing planform is paneled.

The procedure of establishing a body axis system through the forward and aft body-station centroids is the same as the body-alone case. In addition, the wing is oriented parallel to the x-y plane. The wing height, z_A, is computed by the program as the average of the leading and trailing edge heights above the x-y plane.

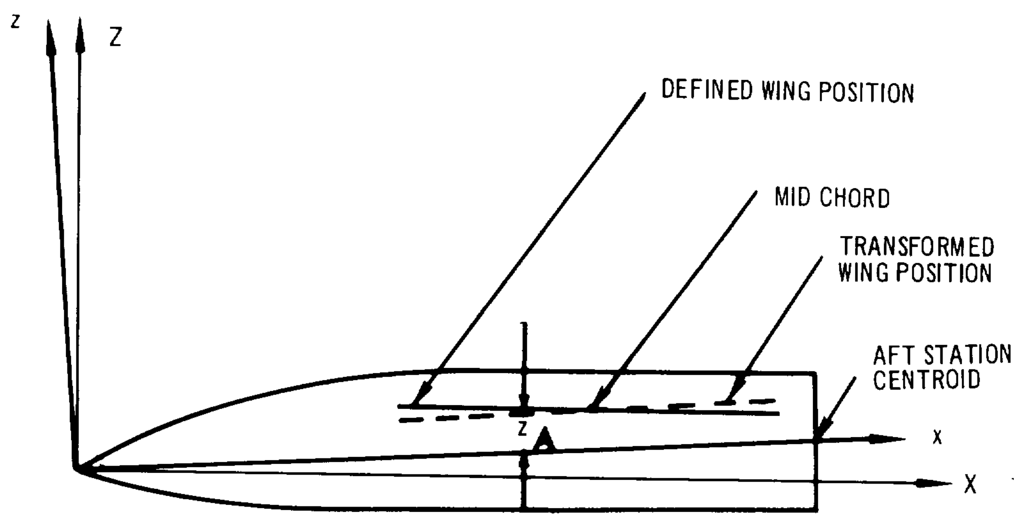

This transformed wing-body combination in the body axis system is the configuration that is paneled. All panel corner points, centroids, and control points are determined relative to the body axis system. Any wing incidence desired relative to the x-axis may be given by specifying an airfoil ordinate table with the correct incidence or may be input as slopes in the aerodynamic section. The airfoil ordinate tables affect neither wing nor body paneling.

The wing intersection must not cross a body definition meridian line. This can be prevented either by choosing a θ-array that straddles the wing intersection region or by specifying a θ that directly corresponds to the wing-body intersection in the body axis system.

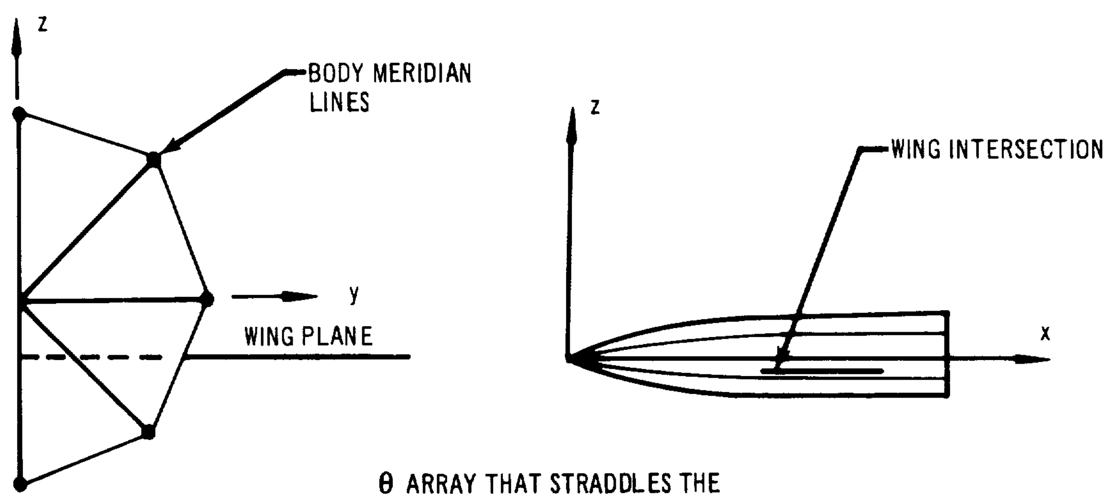

θ ARRAY THAT STRADDLES THE WING INTERSECTION REGION

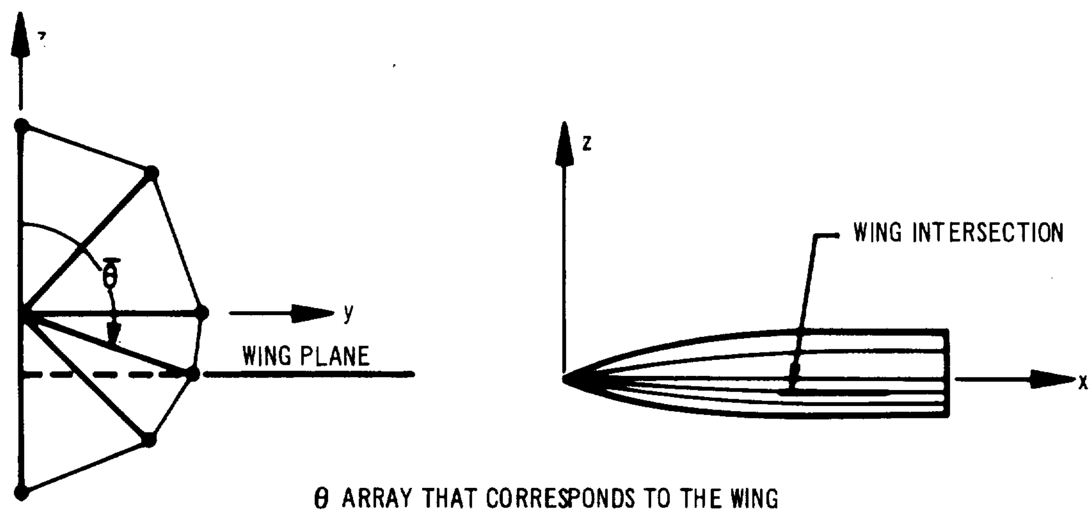

θ ARRAY THAT CORRESPONDS TO THE WING INTERSECTION ALONG A BODY MERIDIAN LINE

If the body is defined with the wing intersection between meridian lines, the paneling section will construct an additional longitudinal panel edge running aft from the wing trailing edge as shown in the following sketch. This completes the additional body panel strip formed by the wing intersection. The number of panels located around the body will be the same at all stations, and the additional panels created by this procedure must be included within the maximum of 100 body panels.

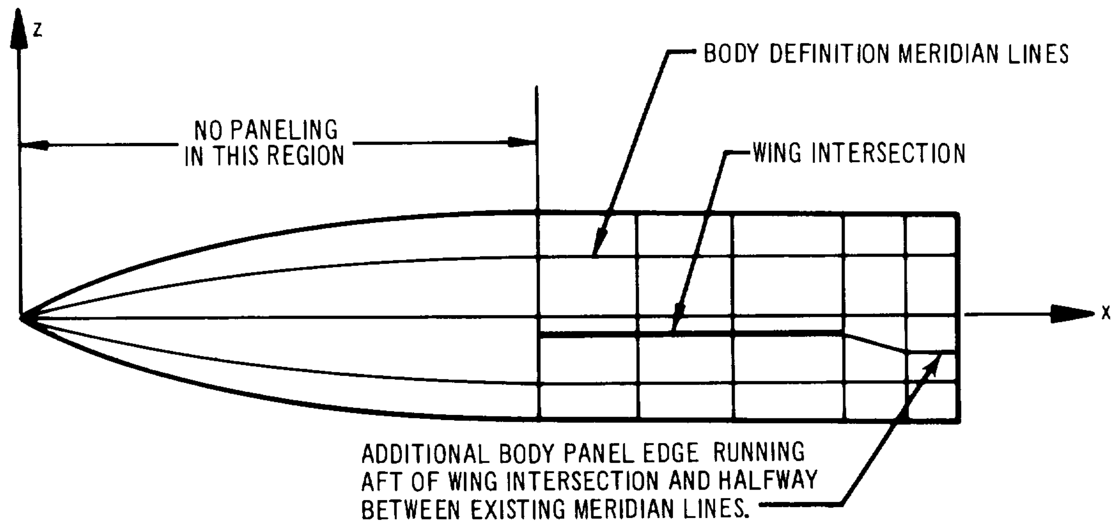

Body pressures due to thickness are determined from a set of equivalent body radii. For bodies with unusual camber or cross-section geometry, it is often more practical to define and panel the uncambered equivalent body of revolution. A two-pass technique can be used to facilitate determination of the equivalent body.

With the two-pass procedure only the definition and paneling sections are used for the first run. The actual body is defined as described in the section on bodies alone. All aerodynamic cards are omitted. The set of equivalent radii (one radius for each source control station) used to determine the body source strengths are calculated. This array of equivalent radii may then be used to define the new equivalent body for the second computer run, which then includes all desired aerodynamic data. This equivalent body can also be cambered by specifying the desired displacement of the source control station centroids from the x-axis. The body camber table which is in the aerodynamic input card set is used to specify such a body camber.

Transverse body panel edges in the wing intersection region must coincide with the spanwise wing panel edges, but do not have to be as numerous as the spanwise edges. The body panel edges in this region are specified by a table of integers that identify those spanwise wing panel edges, which continue around the body to form transverse body panel edges. The spanwise wing panel edges are numbered consecutively from leading edge to trailing edge, as sketched below. The integers corresponding to those edges that continue around the body appear in sequence in the table. The table must always start with the integer 1 and terminate with the wing trailing-edge number.

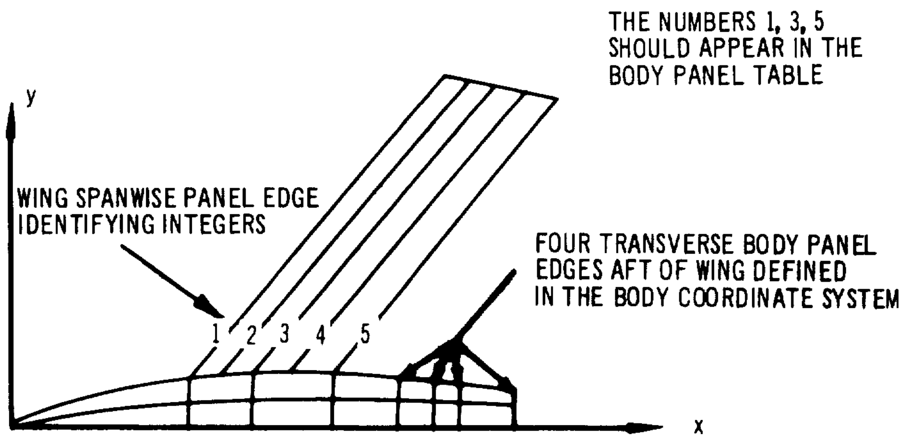

Transverse body panel edges aft of the wing trailing edge are defined in the body coordinate system.

Paneling the body is more complex than paneling a wing planform, since many multipart panels may occur. Two-part panels also can occur on some wing tips and along the inboard strip of wing panels if the wing intersects the body in a region of closure as shown below.

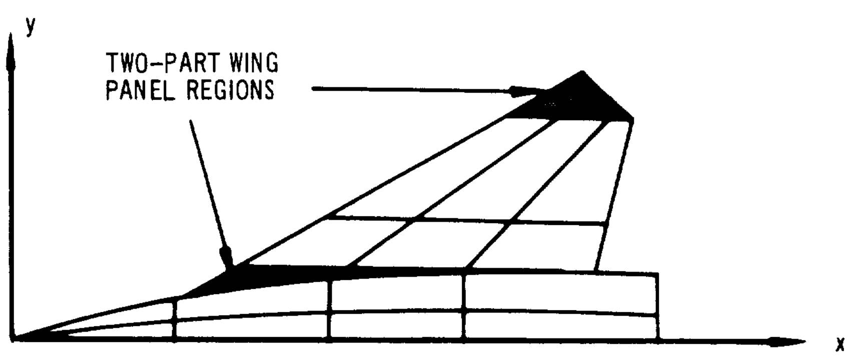

Body panels occurring in regions of closure are three-part panels. All wing and body panels must be quadrilateral with two streamwise edges. When paneling situations occur that do not satisfy these conditions, a multipart panel whose individual parts satisfy the conditions is constructed. A typical body panel and its parts are shown here:

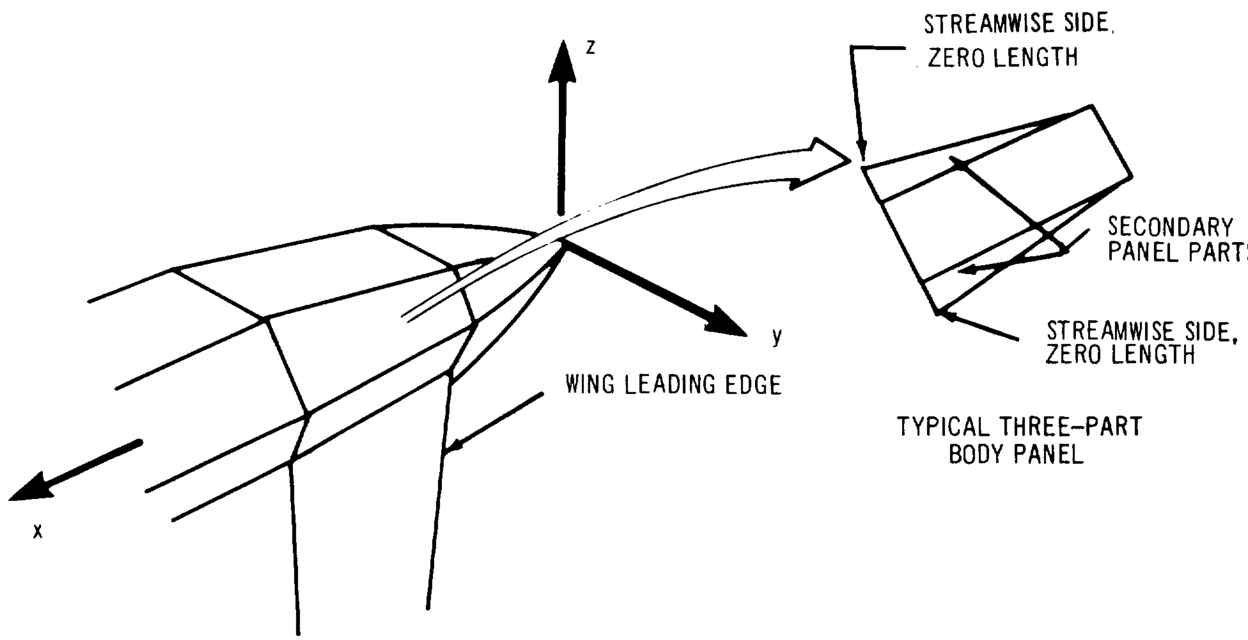

Most supersonic bodies do not have regions of rapid closure (hypersonic blunt bodies are not adaptable to the linearized analysis techniques of this program); therefore, the secondary body panel parts are usually very small. If these secondary areas are nearly zero, the matrix of influence coefficients can become singular, preventing matrix inversion. A tolerance control on the leading-edge slope of these secondary panel parts can be used to avoid this matrix problem. This tolerance is specified in the paneling section. The same matrix problem can result from secondary wing panel parts. A control tolerance on these wing panel parts also is specified in the paneling section. Program input illustrating the use of these tolerance controls (cards 5P and 9P) is contained in section 5.4 (pages 146 and 147).

5.3 Program Card Input Format

Aerodynamic cases that can be solved for the various configuration problems are the following:

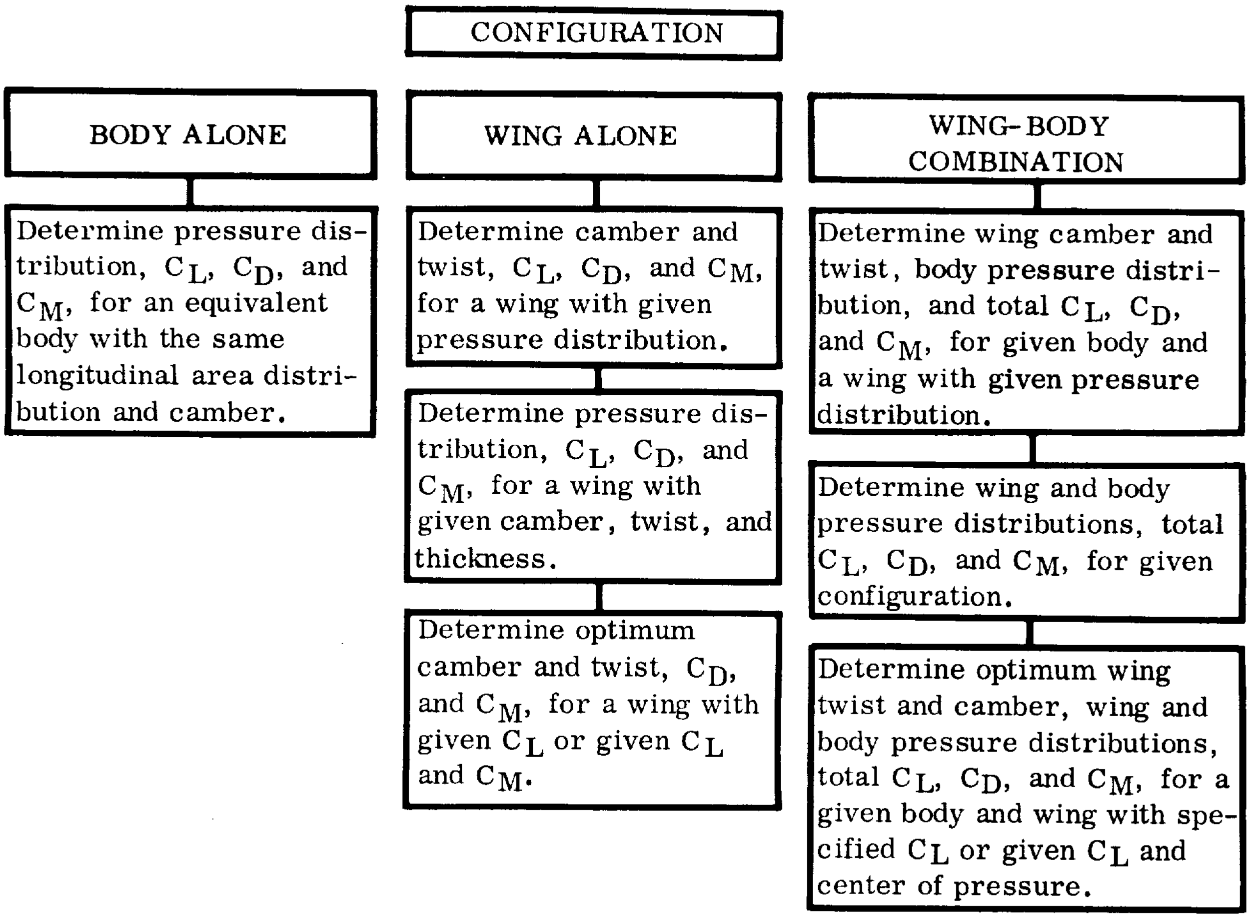

The corresponding input card sets needed to define and analyze a configuration are outlined by figure 23. A completed input data deck will resemble the illustration of figure 24. Multiple aerodynamic cases on a given geometry for a given Mach number may be requested in the aerodynamic set. If the Mach number of configuration are changed, the geometry must be redefined.

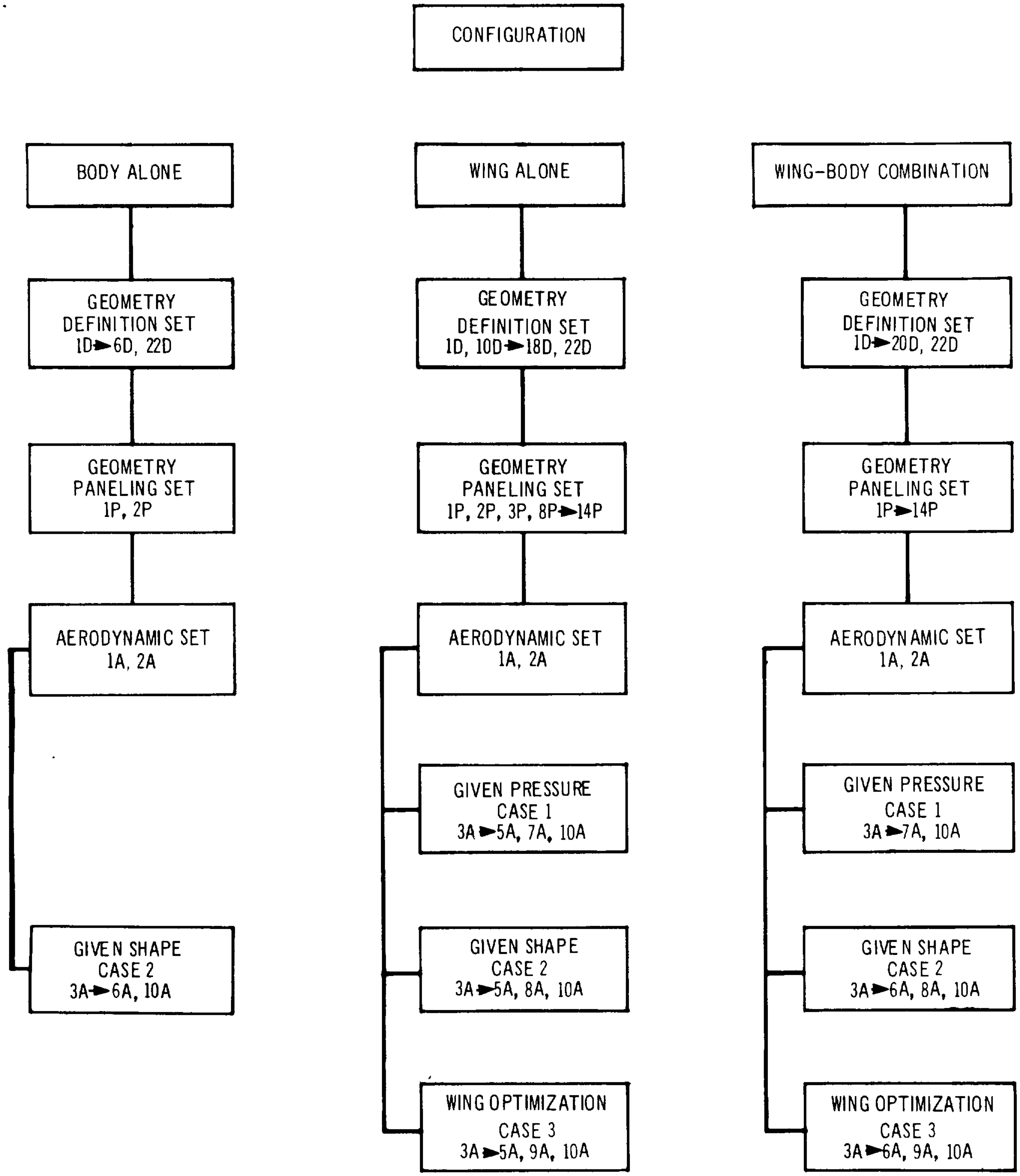

FIGURE 23 OUTLINE OF INPUT CARDS NEEDED TO DESCRIBE AND ANALYZE A CONFIGURATION

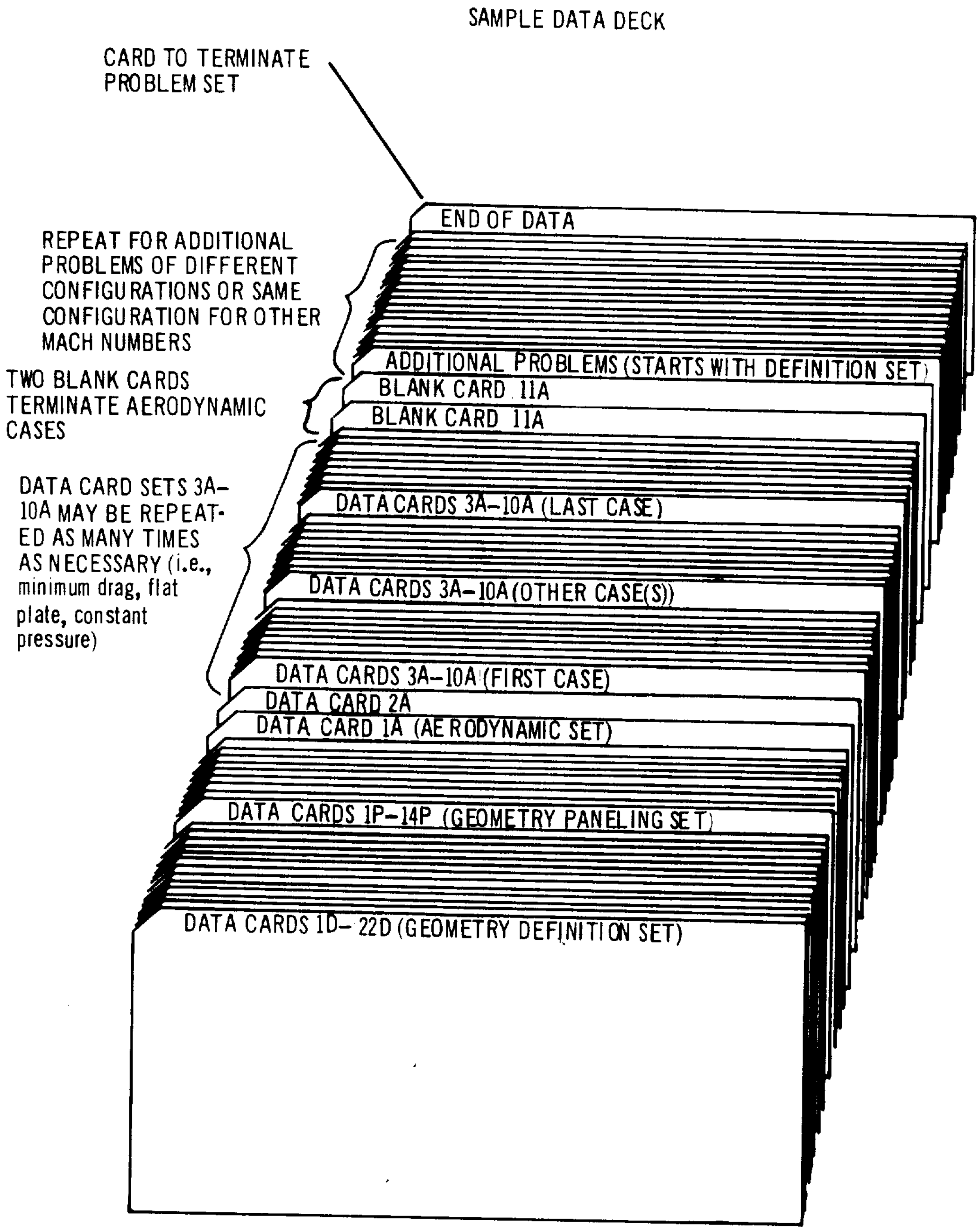

FIGURE 24 EXAMPLE DATA DECK

GEOMETRY DEFINITION CARD SET

All geometry definition data, except title cards and literal statements, are punched in six-field, ten-digit format. A decimal point is required in each data field.

For a body-alone problem definition, cards 10D through 19D are omitted.

For a wing-alone problem definition, cards 2D through 6D, 19D, and 20D are omitted.

	Column	Code	Explanation
Card 1D	1-6	DEFINE	Columns 1-6 contain the word DEFINE.
Card 2D	1-4	BODY	Columns 1-4 contain the word BODY. Card 2D is used only when a body or wing-body combination is defined.
Card 3D	1-72	TITLE	Any desired title.
Card 4D	1-10	BNS	Number of defining body stations. 2. ≤ BNS ≤ 50..
	11-20	BTHETA	Number of points on each defining body station, i.e., the number of ρ, θ or Y, Z pairs per station. 2. ≤ BTHETA ≤ 16..
	21-30	AXIS(1)	Y-coordinate of body definition axis (cf. page 99).
	31-40	AXIS(2)	Z-coordinate of body definition axis (cf. page 99).
	41-50	CHDB	Dimensional tolerance to be used in generating additional body meridian line points between given stations. If CHDB ≤ 0. or if BNS < 4., no additional points will be generated. If 0. < CHDB < 0.001, then a value of 0.001 will be used (see page 202 of Part II).

	Column	Code	Explanation
Card(s) 5D (3 maximum)	1-10 ⋮ 51-60	θ_1 ⋮ θ_6 etc.	Array of angles (θ), in degrees at each defining station. There must be exactly BTHETA angles ≤ 16, six per card.
Card(s) 6D* (50 maximum)	1-10	STA	X-coordinate of body station.
	11-20	YZ(1)	Δ Y-increment added to body definition axis to establish a local origin from which all ρ, θ for this station are measured.
	21-30	YZ(2)	Δ Z-increment added to body definition axis to establish a local origin from which all ρ, θ for this station are measured (see page 99).
	31-40	SCODE	= 0. this cross section is identical to previous section.

Note — if options 1, 4, 5, or 6 are designated, the added information card(s) 7D, 8D, or 9D must be inserted behind that station card 6D and before the next station card 6D.

= 1. this cross section is specified by BTHETA values of ρ (on cards 7D). The θ-array of card(s) 5D will be used.

= 2. this cross section is a circle. (Radius given in columns 41-50.)

= 3. this cross section is an ellipse. (Horizontal semi-axis is given in columns 41-50, the vertical in columns 51-60.)

= 4. this cross section is circular (radius given in columns 41-50) with an angle array (on card(s) 8D) different from the θ-array on card(s) 5D. This option allows local deviations in the meridian lines.

= 5. this cross section is specified by a set of ρ (on card(s) 7D) and by a nonstandard set of θ (on card(s) 8D).

*One card is needed for each defining station.

	Column	Code	Explanation
			= 6. this cross section is given by a set of Y, Z pairs (on cards 9D).
	41-50	RAD(1)	Radius of section if SCODE = 2. or 4.. Horizontal semi-axis if SCODE = 3.. Not used otherwise.
	51-60	RAD(2)	Vertical semi-axis, if SCODE = 3.. Not used otherwise.
Card(s) 7D (3 maximum per station)	1-10 ⋮ 51-60 etc.	ρ_1 ⋮ ρ_6	A set of body radii ρ if SCODE = 1. or 5.. There must be BTHETA $\leq$ 16 values of ρ.
Card(s) 8D (3 maximum per station)	1-10 ⋮ 51-60 etc.	θ_1 ⋮ θ_6	A set of θ if SCODE = 4. or 5.. There must be BTHETA $\leq$ 16 values of θ.
Card 9D (6 maximum per station)	1-10	Y_1	Array of Y, Z coordinate pairs if SCODE = 6..
	11-20	Z_1	
	21-30	Y_2	
	31-40	Z_2	
	41-50	Y_3	
	51-60 etc.	Z_3	
Card 10D	1-4	WING	Columns 1-4 contain the word WING. This card is used whenever a wing is defined. For the case of a body alone, omit cards 10D through 19D. After reading a WING card, the program expects wing definition data.
Card 11D	1-72	TITLE	Any desired title.
Card 12D	1-10	PNLE	Number of corner or break points defining the planform leading edge (see page 102).

	Column	Code	Explanation
	11-20	PNTE	Number of corner or break points defining the planform trailing edge.
	21-30	AFN	Number of planform control chords. AFN ≥ 2., including the wing-tip control chord.
	31-40	PLN	Number of constant percent chord lines used to form spanwise panel edges. Wing leading and trailing edges are counted in this number.
	41-50	WUL	= 1.
	51-60	CHD	Must be left blank.
Card 13D	1-10	PCODE	= 1.
	11-20	ACODE	= 1.
	21-30	EPS	Must be left blank.
Card(s) 14D	1-10	X_1	Array of points defining the planform leading edge, arranged in order from inboard to outboard. There must be PNLE point pairs; three coordinates per card.
	11-20	Y_1	
	21-30	X_2	
	31-40	Y_2	For wing-body combinations, X_1 and Y_1 must lie inside the body so that an intersection can be calculated.
	41-50	X_3	
	51-60	Y_3	
	etc.		
Card(s) 15D	1-10	X_1	Array of points defining the planform trailing edge, arranged in order from inboard to outboard. There must be PNTE point pairs; three coordinates per card.
	11-20	Y_1	
	21-30	X_2	
	31-40	Y_2	For wing-body combinations, X_1 and Y_1 must lie inside the body so that an intersection can be calculated.
	41-50	X_3	

Column	Code	Explanation
51-60	Y_3	
	etc.	

<u>Cards 16D</u> Cards 16D and 17D always occur in pairs (unless AFNU = 0. on card 16D) to define the wing control chord. There must be AFN $\geq$2. pairs of 16D and 17D cards.

Column	Code	Explanation
1-10	AFK	Code to indicate how the control chord is oriented on the planform. See sketches below.

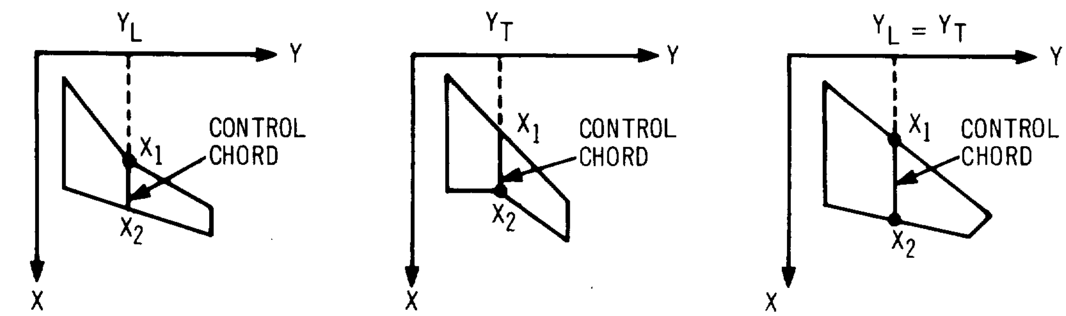

AFK = 1. LEADING EDGE POINT DEFINES CONTROL CHORD

AFK = 2. TRAILING EDGE POINT DEFINES CONTROL CHORD

AFK = 3. CONTROL CHORD DEFINED BY BOTH LEADING AND TRAILING EDGE POINTS

INTERNAL WING CONTROL CHORD DEFINITION, $\beta \equiv 0$

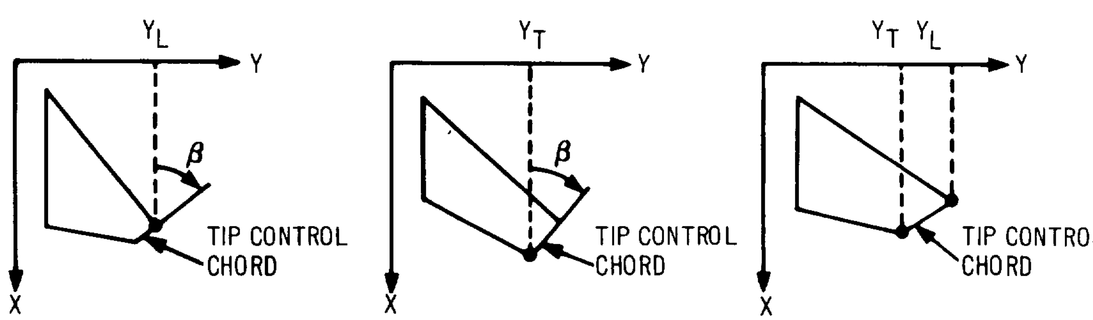

AFK = 1. AFK = 2. AFK = 3.

WING TIP CONTROL CHORD DEFINITION, $\beta \leq 0$

	Column	Code	Explanation
			Two of the three quantities Y_L, Y_T, or β must be given. AFK indicates the appropriate pair.
	11-20	BETA	The angle β, zero for all wing control chords, except the wing tip (positive as shown above). BETA is ignored if AFK = 3..
	21-30	Y_L	Y-coordinate of the leading edge. Y_L is ignored if AFK = 2..
	31-40	Y_T	Y-coordinate of the trailing edge. Y_T is ignored if AFK = 1..
	41-50	AFNU	= 2. the height and true chord length are specified on the following card 17D.
			= 0. the previous 17D card values are used. Card 17D should not follow if AFNU = 0..
Card(s) 17D	1-10	X_O	= 0.
	11-20	Z_O	Z-coordinate at the leading edge of control chord.
	21-30	X_C	The control chord true length. If $Z_O = Z_C = 0$, X_C may be given an arbitrary length, which is then scaled by the program to make X_C equal to the true chord length.
	31-40	Z_C	Z-coordinate of control chord at the trailing edge.
Card(s) 18D	1-10 ⋮ 51-60 etc.	P_1 ⋮ P_6	Array of constant percent chord values corresponding to the panel spanwise edges. The leading-edge value P_1 = 0.. There are PLN values required with the last value (for the trailing edge) = 100.

	Column	Code	Explanation
Card 19D	1-3	WBX	Columns 1-3 contain the letters WBX. This card indicates that a wing-body intersection is desired. For wing only or body alone cases, this card is omitted.
Card 20D	1-10		= 1. linear interpolation used on body station perimeters to compute additional points between meridian lines in the wing intersection region. See upper sketch on page 106, which illustrates linear interpolation for the wing intersection. = 2. biquadratic interpolation used on body station perimeters to compute additional points between meridian lines in the wing intersection region.
	11-20		Dimensional intersection tolerance. Specifies the accuracy desired in locating wing-body intersection points. A value of 0.001 is suggested.
Card 21D	1-5	TDUMP	Columns 1-5 contain the letters TDUMP. This card is included if a dump of geometry definition and geometry transformation tapes is desired. See Appendix C of Part II for a detailed description of these tapes.
Card 22D	1-6	DEFEND	Columns 1-6 contain the word DEFEND. This card ends the definition set and must not be omitted.

GEOMETRY PANELING CARD SET

All paneling data, except title cards and literal statements, are punched in six-field, ten-digit format. A decimal point is required in each data field.

For body-alone case, cards 3P-14P are omitted.

For wing-alone case, cards 4P-7P are omitted.

	Column	Code	Explanation
Card 1P	1-5	PANEL	Columns 1-5 contain the word PANEL. This is the first card in the paneling link and must always follow the DEFEND card.
Card 2P	1-10		The number of source control stations at which the radius for an equivalent body of circular cross section and the actual body station centroid height are computed. A maximum of 50 stations may be requested. The radius at each control station is used to determine the source strength necessary to simulate the body thickness. In wing-alone problem card 2P is blank.
	11-20		Dimensional tolerance applied to the additional points generated between meridian lines on the perimeter of body defining stations. This controls the area and centroid location calculations. A value of 0.001 is suggested.
	21-30		This field contains an interpolation code. The program first determines an equivalent radius, R, at each body defining section, X, and then establishes an R vs. X array. Interpolation for additional radii at other stations is performed on this array. The same technique is used to determine centroid locations.

	Column	Code	Explanation
			= 1. linear interpolation for equivalent radii and centroid locations of the source control stations that are between body defining stations.
			= 2. biquadratic interpolation for equivalent radii and centroid locations at the source control stations that are between body defining stations.
	31-40		= 1. linear interpolation between meridian line points on the body definition sections.
			= 2. if biquadratic interpolation is desired.
	41-50		A dimensional tolerance value, E, such that if any equivalent radius length or centroid height, (z centroid), is less than E, its value will be set equal to zero. A value of 0.001 is suggested.
Card 3P	1-10	XPER	Fraction of local streamwise panel chord at which panel control point is located. 0. < XPER < 1..
			NOTE: XPER = .95 for all cases discussed in this report.
	11-20	YPER	Fraction of local panel width at which panel control point is located. 0. < YPER < 1..
			NOTE: YPER = 0. is a code used to locate the panel control point on the chord through the panel centroid. YPER = 0., for all cases discussed in this report.
Card 4P	1-10	BODY PANEL	Columns 1-10 contain the words BODY PANEL.

	Column	Code	Explanation
Card 5P	1-10	PLNB*	Number of transverse body panel edges aft of wing trailing edge-body intersection ≤ 21. See upper sketch on page 108. If PLNB = 0., omit card 6P.
	11-20	PLNW*	Number of transverse body panel edges within the wing body intersection region ≤ 16.
	21-30	TOLB	Slope tolerance on body secondary panel part leading edges. Panel parts with slopes $\leq \left\lvert \frac{\Delta Y}{\Delta X} \right\rvert$ = TOLB (in the local) panel coordinate system) are eliminated. TOLB = 0.02 is suggested.
Card(s) 6P	1-10 ⋮ 51-60 etc.	$XCEPTB_1$ ⋮ $XCEPTB_6$	x-values of transverse body panel edges aft of the wing trailing edge - body intersection. There are PLNB values. Omit this card(s) if PLNB = 0.
Card(s) 7P	1-10 ⋮ 51-60 etc.	$CODEBW_1$ ⋮ $CODEBW_6$	Each field contains an integer identifying those spanwise wing panel edges which continue around the body to form transverse body panel edges at the body intersection. The table must always start with the integer 1 and terminate with the wing trailing-edge number. See upper sketch on page 108. There are PLNW values.
Card 8P	1-10	WING PANEL	Columns 1-10 contain the words WING PANEL.
Card 9P	1-10	PLANE	Number of buttock lines which locate the streamwise wing panel edges specified by cards 10P and 11P. Wing-alone problem: PLANE is the number of buttock lines locating the streamwise panel edges including both the wing tip and centerline.

*(PLNB + PLNW) ≤ 21

Column	Code	Explanation
		Wing-body problem: PLANE is the number of buttock lines locating the streamwise panel edges, but does not include the inboard edge located by the program at the wing-body intersection. PLANE $\geq$ 2.. See sketches below.

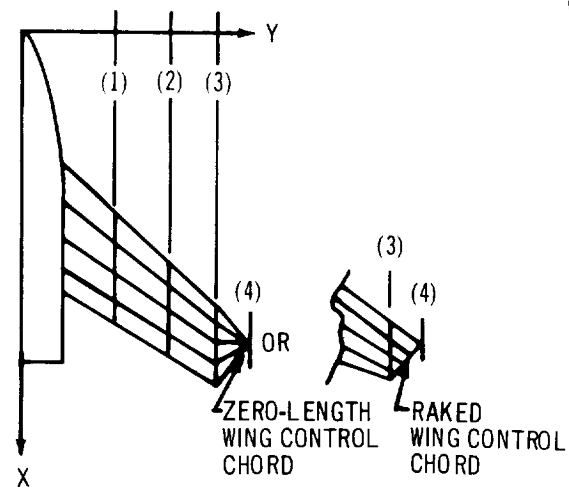

PLANE = 4.

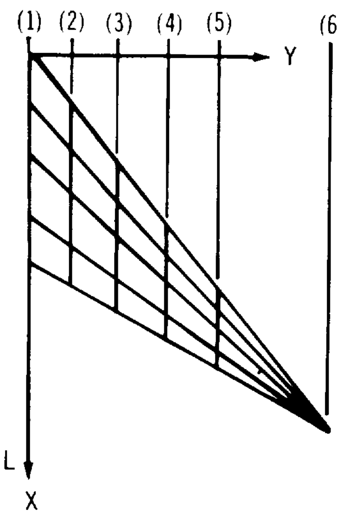

PLANE = 6.

11-20	OPTF	= 1. upper and lower airfoil ordinates are read in (cards 12P and 13P) at each wing buttock line passing through the panel centroids. If the wing is untwisted and has the same airfoil section from root to tip, only one airfoil table is necessary. The program will scale this table to fit the appropriate chord.
		= 0. no tables are read in and the wing is a flat plate at zero incidence.
21-30	SNUM	Number of given airfoil ordinate tables.
		= 0., OPTF = 0.

	Column	Code	Explanation
			= 1., same airfoil section from wing root to tip.
			= (PLANE - 1), wing alone case airfoils specified.
			= PLANE, wing-body case airfoils specified.
	31-40	TOLW	Slope tolerance on wing secondary panel part leading edges. Panel parts with slopes $\leq \left\| \frac{\Delta Y}{\Delta X} \right\| =$ TOLW are eliminated. TOLW = 0.01 is suggested.
Card(s) 10P	1-10 ⋮ 51-60 etc.	$YCEPT_1$ ⋮ $YCEPT_6$	Wing buttock line values at which streamwise panel edges are specified. There are (PLANE -1) values. The tip edge is specified on card 11P. NOTE: This card controls the outboard panel edge and in no way influences the spanwise edges which are established by the geometry definition (see page 103). The outboard panel edge is usually made coincident with the definition wing tip, but it may be used to truncate the defined wing tip and the spanwise panel edges anywhere between the two outboard wing buttock lines specified by card 9P. If truncation is specified, the wing span and area are reduced.
Card 11P	1-10	CPNT	Code indicating how the most outboard panel edge or wing tip is specified.
			= 0. X and Y coordinates of the wing tip leading and trailing edge are given. Use VALUE(1) through (4).

Column	Code	Explanation
		= 1. X and Y coordinates of the leading edge and the slope ($\Delta X/\Delta Y$) of the wing tip are given. Use VALUE(1), (2) and (5).
		= 2. X and Y coordinates of the trailing edge and the slope ($\Delta X/\Delta Y$) of the wing tip are given. Use VALUE(3), (4) and (5).
11-20	VALUE(1)	X-coordinate of wing tip leading edge if CPNT = 0. or 1..
21-30	VALUE(2)	Y-coordinate of wing tip leading edge if CPNT = 0. or 1..
31-40	VALUE(3)	X-coordinate of wing tip trailing edge if CPNT = 0. or 2..
41-50	VALUE(4)	Y-coordinate of wing tip trailing edge if CPNT = 0. or 2..
51-60	VALUE(5)	wing tip slope, $\frac{\Delta X}{\Delta Y}$, if CPNT = 1. or 2..

Cards 12P and 13P give the SNUM sets of airfoil coordinates. These card sets (12P and 13P) are always used in pairs to define each airfoil at a given panel centroid buttock line. The card sets are omitted if OPTF = 0..

Cards 12P

	Column	Code	Explanation
First Card	1-10	XNUM(1)	Number of points (X, Z coordinate pairs) in upper surface airfoil ordinate table. 4. $\leq$ XNUM(1) $\leq$ 25..
Second Cards	1-10	$XFOIL_1$	Upper surface airfoil ordinate table. Local X and Z coordinates are given from leading edge to trailing edge. If the wing has no twist, an unscaled set of ordinates may be given and the program will scale the airfoil to the local chord.
	11-20	$ZFOIL_1$	
	⋮	⋮	
	41-50	$XFOIL_3$	
	51-60	$ZFOIL_3$	
	etc.		

	Column	Code	Explanation
Cards 13P			
First Card	1-10	XNUM(2)	Number of points (x, z coordinate pairs) in lower surface airfoil ordinate table. 4. ≤ XNUM(2) ≤ 25..
Second Cards	1-10	$XFOIL_1$	Lower surface airfoil ordinate table.
	11-20	$ZFOIL_1$	
	⋮	⋮	
	41-50	$XFOIL_3$	
	51-60	$ZFOIL_3$	
	etc.		
Card 14P	1-6	PANEND	Columns 1-6 contain the word PANEND. This card ends the paneling set and must be used whenever any paneling is performed. It is not needed for a body-alone problem.

AERODYNAMIC CARD SET

All aerodynamic data, except title cards and literal statements, are punched in seven-field, ten-digit format. A decimal point is required in each data field. Data cards 1A and 2A are input only once for a given configuration and Mach number. The remaining aerodynamic data cards may be repeated as necessary to solve the selected aerodynamic cases.

	Column	Code	Explanation
Card 1A	1-11	AERODYNAMIC	Columns 1-11 contain the word AERODYNAMIC.
Card 2A	1-10	XMACH	Mach number.
	11-20	SYM	= 0. the aerodynamic problem solved is unsymmetric about the vertical X-Z plane (image panels not included, see page 49). = 1. the aerodynamic problem solved is symmetric about the vertical X-Z plane (image panels included, see page 49).
Card 3A	1-72	TITLE	Any desired title.
Card 4A	1-10	CASE	= 1. calculates wing twist and camber for a given ΔC_p distribution on wing where $\Delta C_p = C_{p\ lower} - C_{p\ upper}$ = 2. calculates pressure distribution over the configuration. Wing and body camber can be changed within this option. = 3. optimizes wing twist and camber for minimum drag. NOTE: For body-alone problems, only case = 2. option is available.

	Column	Code	Explanation
	11-20	CPCALC	= 0. C_p calculations use linear equation; $C_p = -2u$.
			= 1. C_p calculations use nonlinear equation; $C_p = -2u + \beta u^2 - v^2 - w^2$.
	21-30	POLAR	= 0. drag polar not requested.
			= 1. drag polar requested. A series of incremental angles of attack is specified on cards 10A.
	31-40	THICK	= 0. wing thickness pressures are not calculated.
			= 1. wing thickness pressures are calculated.
	41-50	VOUT	= 0. the velocity components are not printed.
			= 1. the velocity components are printed.
Card 5A	1-10	RFAREA	Half-wing reference area. If this field is left blank, the program sums the wing panel areas to obtain the reference area which is the half wing exposed area. For the body-alone problem, a value must be input, or a unit area is used.
	11-20	XP	x-coordinate about which the pitching moments are computed.
	21-30	ZP	z-coordinate about which the pitching moments are computed.

Card(s) 6A

For configurations that include a body, two options are available for specifying body camber. The first word on the first card is the key to the type of input the program expects. Omit this card set for wing-alone problems.

Column	Code	Explanation
		Option A
1-5	GIVEN	Columns 1-5 contain the word GIVEN. The program takes the body camber to be that calculated in the geometry definition section. No additional cards are necessary for this option.
7-80	Any additional identifying symbols	
		Option B
1-80	Any identifying symbols	The first card contains any arbitrary identifying symbols (other than GIVEN or CONSTANT as the first word) to describe the body camber and the program expects additional cards immediately following to specify the body camber.
1-10 ⋮ 61-70 etc.	z_1 ⋮ z_7	z-values or cross-section centroid heights for Option B giving the body camber at the x-locations of the source control stations (see Card 2P). To determine the exact source control stations, it is necessary to have previously run the configuration through the geometry sections of this program.

Card(s) 7A — Calculates wing twist and camber for a given wing ΔC_p distribution (CASE = 1., field 1 of card 4A). Two options are available for specifying the ΔC_p distribution. These options are selected by the first word on the first card of this set. Omit this set for body-alone problems or CASE = 2. or 3..

Column	Code	Explanation
		Option A
1-8	CONSTANT	Columns 1-8 contain the word CONSTANT. This option restricts the wing to have a constant ΔC_p distribution. This constant value is specified on the following card.
9-80	Any additional identifying symbols	
1-10	ΔC_p	ΔC_p for Option A.

Column	Code	Explanation
		Option B
1-80	Any identifying symbols	The first card contains any appropriate identifying symbols (other than GIVEN or CONSTANT as the first word) to select Option B. ΔC_p for each panel is specified on the following card set.
1-10 ⋮ 61-70 etc.	ΔC_{p_1} ⋮ ΔC_{p_7}	ΔC_p's for Option B. This array must be ordered starting with the inboard panel at the leading edge and running aft to the trailing edge, then proceeding outboard to the tip in the same manner.

Card(s) 8A Calculates the pressure distribution over the configuration (CASE = 2., field 1 of card 4A). Three options are available for specifying the camber shape of the wing. The options are selected by the first word on the first card of this set. Omit this set for body-alone problems or CASE = 1. or 3..

Column	Code	Explanation
		Option A
1-8	CONSTANT	Columns 1-8 contain the word CONSTANT. This option restricts the wing
9-80	Any additional identifying symbols	camber shape to have a constant slope for each wing panel. This constant value is specified on the following card.
1-10	$\Delta z/\Delta x$	$\Delta z/\Delta x$ for Option A.
		Option B
1-5	GIVEN	The wing camber shape is specified by the input geometry. The panel slopes
7-80	Any additional identifying symbols	are read internally from a tape generated in the paneling section of the program. In this case, no additional cards are necessary.
		Option C
1-80	Any identifying symbols	Any appropriate identifying symbols (other than GIVEN or CONSTANT as the first word) on the first card of this set are used to select this option. The wing camber shape is specified by a slope for each panel. Additional cards must be input which contain the slope values.

Column	Code	Explanation
1-10 ⋮ 61-70	$\Delta z_1/\Delta x_1$ ⋮ $\Delta z_7/\Delta x_7$ etc.	Wing panel slopes for Option C. The array must be ordered starting with the inboard panel at the leading edge and running aft to the trailing edge, then proceeding outboard to the tip in the same manner.

Card 9A

Optimizes wing twist and camber for minimum drag (CASE = 3., field 1 of card 4A). Two options are available. The first option optimizes the wing for a given wing lift constraint and the second option optimizes the wing for both the wing lift and center of pressure constraints. Only one data card is required. Omit this card for a body-alone problem or CASE = 1. or 2..

1-10	CONSNT	= 0. the wing is optimized for minimum drag with a wing lift constraint. = 1. the wing is optimized for minimum drag with both wing lift and x-coordinate of the center of pressure constraints.
11-20	CLBAR	Wing lift coefficient constraint.
21-30	XCPBAR	The x-coordinate of the wing center of pressure constraint. If the center of pressure is not constrained, omit this field.

Card(s) 10A

When the drag polar option is selected (POLAR = 1., field 3 of card 4A), the values of incremental angles of attack added to the immediately preceding case of the defined configuration are given here. These values in degrees are specified in columns 1-10, one value per card for as many cards as necessary. The angle of attack series will be terminated by a blank card. Omit these cards if the polar option is not selected (POLAR = 0.).

NOTE: Additional aerodynamic cases may be requested by returning to card 3A or the aerodynamic cases for this configuration and Mach number may be terminated by proceeding to cards 11A (see figure 24 page 112).

	Column	Code	Explanation
Cards 11A	Two blank cards must be placed behind the last data card of each problem, to terminate the selected aerodynamic cases for a given configuration and Mach number. Additional problems (new configurations or Mach numbers) may be stacked consecutively each starting with card 1D.		
Terminal Card	Finally, a data card with the words END OF DATA punched in columns 1-11 will terminate the run.		

5.4 Sample Input Formats

Program card input formats for three types of geometric configurations with successive aerodynamic cases are presented on the following pages:

Body alone; pages 134-135

Wing alone; pages 137-143

Wing-body combination; pages 145-149

Body alone. — A parabolic body of revolution with a fineness ratio of 11 is defined by 21 body stations. Ten equally spaced meridian lines are constructed. Because each body station is circular, only one radius per station is given and code 2. (on cards 6D, column 31) is used. On card 2P, 50 equally-spaced source control stations are requested. Although no body paneling is required, two panel cards (1P and 2P) are necessary to define the number of source stations and the method by which the equivalent body radii at the source stations are interpolated.

The two aerodynamic cases specified for the parabolic body are for CASE = 2. (card 4A), that is, calculations of pressure distribution over the given configuration. Both linear and nonlinear C_p calculations are requested for two angles of attack (α = 0 degrees, is given automatically, $\Delta \alpha$ = 5 degrees is specified). Body camber is zero as given by the geometry description.

SEVEN FIELD, TEN DIGIT CRD FORMAT

1–10	11–20	21–30	31–40	41–50	51–60	61–70	71	72–80 IDENT
DEFINE								1D
BODY								2D
PARABOLIC BODY		L/D = 11.						3D
21.	10.	0.	0.	.001				4D
0.	20.	40.	60.	80.	100.			5D
120.	140.	160.	180.					5D
0.	0.	0.	2.	0.				6D
.05	0.	0.	2.	.00826				6D
.10	0.	0.	2.	.01569				6D
.15	0.	0.	2.	.02230				6D
.20	0.	0.	2.	.02808				6D
.25	0.	0.	2.	.03304				6D
.30	0.	0.	2.	.03717				6D
.35	0.	0.	2.	.04047				6D
.40	0.	0.	2.	.04295				6D
.45	0.	0.	2.	.04460				6D
.50	0.	0.	2.	.04543				6D
.55	0.	0.	2.	.04460				6D
.60	0.	0.	2.	.04295				6D
.65	0.	0.	2.	.04047				6D
.70	0.	0.	2.	.03717				6D
.75	0.	0.	2.	.03304				6D
.80	0.	0.	2.	.02808				6D
.85	0.	0.	2.	.02230				6D
.90	0.	0.	2.	.01569				6D
.95	0.	0.	2.	.08260				6D
1.	0.	0.	2.	0.				6D

TITLE PARABOLIC BODY ALONE NAME DATE PAGE 1 OF 2

AD 3775 R1 6-8200

SEVEN FIELD, TEN DIGIT CRD FORMAT

1–10	11–20	21–30	31–40	41–50	51–60	61–70	71	72	IDENT 80
DEFEND									22D
PANEL									1P
50.	.001	2.	2.						2P
AERODYNAMIC									1A
1.92	1.								2A
PARABOLIC	BODY ONLY	LINEAR	CP						3A
2.	0.	1.	0.	1.					4A
0.	1.	0.							5A
GIVEN BODY CAMBER									6A
5.									10A
									BLANK
PARABOLIC BODY ONLY NON-LINEAR CP									3A
2.	1.	1.	0.	1.					4A
0.	1.	0.							5A
GIVEN BODY CAMBER									6A
5.									10A
									BLANK
									11A
									11A
END OF DATA									

TITLE PARABOLIC BODY ALONE NAME DATE PAGE 2 OF 2

AD 2778 R1 8-9200

Wing alone. — The input for a cambered and twisted arrow wing with thickness is shown on the following pages. The wing planform is defined by four points, two on the leading edge and two on the trailing edge (cards 14D, and 15D). Two points are coincident at the tip. Two control chords are given on cards 16D through 17D. The eleven constant-percent chord lines that form spanwise panel edges are specified on cards 18D. Wing buttock lines forming the ten streamwise panel edges are specified on cards 10P and 11P. A total of 100 wing panels are formed as shown in figure 26 (page 156). The remaining cards in the paneling set are airfoil ordinate tables, one table for each of the ten streamwise columns of panels. Each table specifies the thickness, camber, and twist by giving upper and lower airfoil ordinates along wing buttock lines through the spanwise centroid of each streamwise column of panels. Examples of three aerodynamic cases are given for this configuration. The first example illustrates the input card set for CASE = 1. (card 4A), calculation of wing twist and camber for constant pressure distribution, $C_L = .1$. An additional angle of attack of 5.73 degrees (0.1 radian) is also specified. The second example shows the input card set for CASE = 2., calculation of pressure distribution over a given configuration. Pressure distributions are determined at $\alpha = 0$ degrees, -2 degrees, 2 degrees, 6 degrees. The last example shows the input card set for CASE = 3., wing optimization. A constraint of $C_L = .1$ is specified; pressures and wing shape are determined for $\alpha = 0$ degrees and 5.73 degrees (0.1 radian). All the above aerodynamic cases specify linear C_p calculations.

SEVEN FIELD, TEN DIGIT CRD FORMAT

1 — 10	11 — 20	21 — 30	31 — 40	41 — 50	51 — 60	61	69	70	71	72	DENT — 80
DEFINE											1D
WING											10D
CARLSON WING	2.										11D
2.	2.	2.	11.	1.	0.						12D
1.	1.	0.									13D
0.	0.	30.	10.919								14D
19.5	0.	30.	10.919								15D
3.	0.	0.	0.	2.							16D
0.	0.	1.	0.								17D
3.	0.	10.919	10.919	2.							16D
0.	0.	0.	0.								17D
0.	5.	15.	25.	35.	45.						18D
55.	65.	75.	85.	100.							18D
DEFEND											22D
PANEL											1P
0.	0.	0.	0.	0.							2P
.95	0.										3P
WING PANEL											8P
11.	1.	10.									9P
0.	.546	1.638	2.73	3.822	4.914						10P
6.005	7.097	8.189	9.281								10P
0.	30.	10.919	30.	10.919							11P
13.											12P
0.	.814	.4753	.817	.9506	.814						12P
1.9013	.80	3.8025	.75	5.7038	.655						12P
7.605	.532	9.5063	.388	11.4075	.212						12P
13.3088	0.	15.21	-.222	17.1113	-.485						12P

TITLE CAMBERED ARROW WING NAME DATE PAGE 1 OF 7

AD 3779 R1 6-9200

SEVEN FIELD, TEN DIGIT CRD FORMAT

1–10	11–20	21–30	31–40	41–50	51–60	61–69	70	71	72	DENT 80
19.013	-.762									12P
13.										13P
0.	.814	.4753	.764	.9506	.706					13P
1.9013	.602	3.8025	.382	5.7038	.175					13P
7.605	-.0015	9.5063	-.183	11.4075	-.338					19P
13.3088	-.475	15.21	-.593	17.1113	-.668					13P
19.013	-.762									13P
13.										12P
0.	.367	.4388	.4047	.8775	.4329					12P
1.755	.463	3.51	.465	5.265	.4298					12P
7.02	.3562	8.775	.2539	10.53	.125					12P
12.285	-.0019	14.04	-.175	15.795	-.355					12P
17.55	-.5512									12P
13.										13P
0.	.376	.4388	.3574	.8775	.3319					13P
1.755	.273	3.51	.127	5.265	-.012					13P
7.02	-.15	8.775	-.2731	10.53	-.381					13P
12.285	-.461	14.04	-.513	15.795	-.5454					13P
17.55	-.5512									13P
13.										12P
0.	.132	.39	.1617	.78	.1938					12P
1.56	.2333	3.12	.2652	4.68	.2513					12P
6.24	.1668	7.8	.2244	9.36	.0829					12P
10.92	-.0211	12.48	-.1476	14.04	-.2899					12P
15.6	-.444									12P
13.										13P
0.	.132	.39	.1167	.78	.1038					13P

TITLE CAMBERED ARROW WING NAME DATE PAGE 2 OF 7

AD 3779 R1 8-8200

SEVEN FIELD, TEN DIGIT CRD FORMAT

1–10	11–20	21–30	31–40	41–50	51–60	61	69/70	71	72	DENT 80
1.56	.0643	3.12	-.0348	4.68	-.1317					13P
6.24	-.2245	7.8	-.3012	9.36	-.3661					13P
10.92	-.4141	12.48	-.4476	14.04	-.4589					13P
15.6	-.4476	14.04								13P
13.										12P
0.	.0408	.341	.0731	.6825	.1006					12P
1.365	.1431	2.73	.1863	4.095	.1984					12P
5.46	.1869	6.825	.152	8.19	.0925					12P
9.55	.0160	10.92	-.081	12.285	-.1935					12P
13.96	-.324									12P
13.										13P
0.	.0408	.341	.0341	.6825	.0226					13P
1.365	-.0039	2.73	-.076	4.095	-.146					13P
5.46	-.2061	6.825	-.2868	8.19	-.3285					13P
9.55	-.3525	10.92	-.343	12.285	-.3565					13P
13.65	-.324									13P
13.										12P
0.	.0544	.2925	.081	.585	.1055					12P
1.17	.1483	2.34	.2013	3.51	.2255					12P
4.68	.2235	5.85	.2107	7.02	.1683					12P
8.19	.1227	9.36	.053	10.53	-.0397					12P
11.7	-.144									12P
13.										13P
0.	.0544	.2925	.047	.585	.038					13P
1.17	.0213	2.34	-.0237	3.51	-.0695					13P
4.68	-.1035	5.85	-.1403	7.02	-.158					13P
8.19	-.1723	9.36	-.173	10.53	-.1667					13P

TITLE CAMBERED ARROW WING NAME DATE PAGE 3 OF 7

AD 3775 R1 6-9200

SEVEN FIELD, TEN DIGIT CRD FORMAT

1–10	11–20	21–30	31–40	41–50	51–60	61–70	71	72	IDENT 80
11.7	-.144								13P
13.									12P
0.	.0672	.2438	.0908	.4875	.112				12P
.975	.1485	1.95	.2031	2.925	.231				12P
3.9	.2365	4.875	.2265	5.85	.2005				12P
6.825	.159	7.8	.1031	8.775	.0333				12P
9.75	-.0512								12P
13.									13P
0.	.0672	.2438	.0628	.4875	.056				13P
.975	.043	1.95	.0161	2.925	-.015				13P
3.9	-.0445	4.875	-.066	5.85	-.0805				13P
6.825	-.087	7.8	-.0839	8.775	-.0717				13P
9.75	-.0512								13P
13.									12P
0.	.0784	.195	.099	.39	.1235				12P
.78	.1513	1.56	.1998	2.34	.2276				12P
3.12	.2373	3.9	.237	4.68	.2229				12P
5.46	.1876	6.24	.151	7.02	.1049				12P
7.8	.0432								12P
13.									13P
0.	.0784	.195	.077	.39	.068				13P
.78	.0663	1.56	.0498	2.34	.0316				13P
3.12	.0123	3.9	0.	4.68	-.0021				13P
5.46	-.0084	6.24	.001	7.02	.014				13P
7.8	.0432								13P
13.									12P
0.	.0912	.1463	.1093	.2925	.1242				12P

TITLE CAMBERED ARROW WING NAME DATE PAGE 4 OF 7

AD 3779 R1

SEVEN FIELD, TEN DIGIT CRD FORMAT

1 10	11 20	21 30	31 40	41 50	51 60	61	69-70	71	72	IDENT 80
.585	.1515	1.17	.192	1.755	.2175					12P
2.34	.2328	2.925	.236	3.51	.228					12P
4.095	.2103	4.68	.1856	5.265	.1515					12P
5.85	.1088									12P
13.										13P
0.	.0912	.1463	.0923	.2925	.0902					13P
.585	.0885	1.17	.08	1.755	.0705					13P
4.095	.0648	4.68	.060	5.265	.060					13P
4.095	.0633	4.68	.0736	5.265	.0885					13P
5.85	.1088									13P
13.										12P
0.	.104	.0975	.1199	.195	.1278					12P
.39	.149	.78	.1791	1.17	.2026					12P
1.56	.216	1.95	.2217	2.34	.2208					12P
2.73	.2138	3.12	.2007	3.51	.181					12P
3.9	.1568									12P
13.										13P
0.	.104	.0975	.1089	.195	.1058					13P
.39	.107	.78	.1041	1.17	.1046					13P
1.56	.104	1.95	.1047	2.34	.1088					13P
2.73	.1158	3.12	.1257	3.51	.139					13P
3.9	.1568									13P
13.										12P
0.	.115	.0488	.1218	.0975	.1271					12P
.195	.1385	.39	.1561	.585	.1709					12P
.78	.1832	.975	.1903	1.17	.1936					12P
1.365	.1949	1.56	.1929	1.755	.1873					12P

TITLE CAMBERED ARROW WING NAME DATE PAGE 5 OF 7

AD 3779 (8) 6-0230

SEVEN FIELD, TEN DIGIT CRD FORMAT

1–10	11–20	21–30	31–40	41–50	51–60	61–70	71	72	DENT 80
1.9	.1792								12P
13.									13P
0.	.115	.0488	.1172	.0975	.1161				13P
.195	.1175	.39	.1191	.585	.1219				13P
.78	.1272	.975	.1303	1.17	.1376				13P
1.365	.1459	1.56	.1559	1.755	.1663				13P
1.9	.1792								13P
PANEND									14P
AERODYNAMIC									1A
2.05	1.								2A
CARLSON WING	2.	CONSTANT CL							3A
1.	0.	1.	1.	1.					4A
0.	0.	0.							5A
CONSTANT-CL									7A
.1									7A
5.72957795									10A
									BLANK
CARLSON WING	2								3A
2.	0.	1.	1.	1.					4A
0.	0.	0.							5A
GIVEN CAMBER	= 0.								8A
-2.									10A
4.									10A
4.									10A
									BLANK
CARLSON ARROW	WING 2			MIN DRAG					3A
3.	0.	1.	1.	1.					4A

TITLE CAMBERED ARROW WING NAME DATE PAGE 6 OF 7

AD 3775 R1 6 8200

SEVEN FIELD, TEN DIGIT CRD FORMAT

1 10	11 20	21 30	31 40	41 50	51 60	61 69	70	71	72	DENT 80
0.	0.	0.								5A
0.	.1									9A
5.72957795										10A
										BLANK
										11A
										11A
END OF DATA										

TITLE CAMBERED ARROW WING | NAME | DATE | PAGE 7 OF 7

AD 2778 R1 | 6-9200

Wing-body combination. — The card input format for a Boeing wing-body configuration is shown on the following pages. The configuration has a constant-chord swept wing, mounted below the axis of a cambered body of circular cross section. Section 6.4 describes the configuration and paneling scheme.

Along the X-axis, 24 body stations are specified. No body camber is specified in the definition card set. Eight meridian lines are requested. The θ array is specified so that a meridian line ($\bar{\theta}$ = 102.19 degrees) coincides with the wing plane. The wing planform is defined by four points and four control chords. Cards 16D and 17D contain the four chords which locate the wing 0.25 inch below the X-Y plane. Eleven equally spaced constant percent chord lines are specified on the wing. Card 3P locates the panel control points at 0.95 of the local streamwise panel chords through the panel centroids. Four transverse body panel edges aft of the wing trailing edge are located at body stations 25, 27, 29.5, and 32.415. There are no body panels aft of station 32.415.

The wing is divided into 100 panels. Wing buttock lines defining streamwise panel edges outboard of the wing-body intersection are specified on cards 10P The nonstreamwise wing tip edge is specified on card 11P. Only one airfoil ordinate table is given since the wing has no twist or change in camber.

Two aerodynamic cases are specified. The first case shows the input card set required to calculate the nonlinear pressure coefficients over the wing and body at α = 0, 2, 3, 4, and 5 degrees. Body camber is specified on cards 6A at each of 50 source control stations. The x-locations of the source control stations are determined by first running the geometry definition and paneling sections of the program. (To do this, the PANEND card is immediately followed by the END OF DATA card, and all aerodynamic cards are omitted.) All force and moment coefficients are based on the half-wing area of 89.375 in.^{2}, as specified on card 5A.

The second case considered shows the input card set required to optimize the wing for minimum drag at a wing C_L of 0.1 degrees and Mach 1.8. Body camber is again specified. The END OF DATA card terminates the input. Discussion of results obtained for the Boeing wing-body configuration from a similar set of input cards is contained in section 6.4.

SEVEN FIELD, TEN DIGIT CRD FORMAT

1–10	11–20	21–30	31–40	41–50	51–60	61–70	71	72	IDENT 80
DEFINE									1D
BODY									2D
TR-805/EQUIVALENT/BODY									3D
24.	8.								4D
0.	25.	50.	75.	102.19	130.				5D
155.	180.								5D
0.	0.	0.	2.	0.					6D
1.5	0.	0.	2.	.270					6D
3.	0.	0.	2.	.4464					6D
4.5	0.	0.	2.	.5943					6D
6.	0.	0.	2.	.7234					6D
7.5	0.	0.	2.	.837					6D
9.	0.	0.	2.	.9364					6D
10.5	0.	0.	2.	1.0223					6D
12.	0.	0.	2.	1.0936					6D
13.5	0.	0.	2.	1.1479					6D
15.	0.	0.	2.	1.184					6D
15.1	0.	0.	0.						6D
17.5	0.	0.	0.						6D
20.	0.	0.	0.						6D
22.5	0.	0.	0.						6D
25.	0.	0.	0.						6D
27.5	0.	0.	0.						6D
29.9	0.	0.	0.						6D
31.	0.	0.	2.	1.174					6D
32.	0.	0.	2.	1.154					6D
33.	0.	0.	2.	1.124					6D

TITLE BOEING WING-BODY MODEL NAME DATE PAGE 1 OF 5

SEVEN FIELD, TEN DIGIT CRD FORMAT

1–10	11–20	21–30	31–40	41–50	51–60	61–69	70	71	72	DENT 80
34.	0.	0.	2.	1.084						6D
35.	0.	0.	2.	1.034						6D
36.	0.	0.	2.	1.						6D
WING										10D
TR-805 WING	(TWP = -.25)									11D
2.	2.	4.	11.	1.	0.					12D
1.	1.	.001								13D
10.67	0.	40.27	10.774							14D
19.88	0.	43.518	8.603							15D
3.	0.	0.	0.	2.						16D
0.	-.25	9.21	-.25							17D
1.	0.	5.								16D
1.	70.	10.774	0.	2.						16D
0.	-.25	3.15	-.25							17D
3.	0.	10.774	8.603	2.						16D
0.	-.25	3.9068	-.25							17D
0.	10.	20.	30.	40.	50.					18D
60.	70.	80.	90.	100.						18D
WBX										19D
2.	.0001									20D
DEFEND										22D
PANEL										1P
50.	0.	1.	1.	.001						2P
.95	0.									3P
BODY PANEL										4P
4.	11.	.02								5P
25.	27.	29.5	32.415							6P

TITLE BOEING WING-BODY MODEL NAME DATE PAGE 2 OF 5

AD 3775 R1 6-8200

SEVEN FIELD, TEN DIGIT CRD FORMAT

1 10	11 20	21 30	31 40	41 50	51 60	61 69 70	71	72	IDENT 80
1.	2.	3.	4.	5.	6.				7P
7.	8.	9.	10.	11.					7P
WING PANEL									8P
10.	1.	1.	.05						9P
1.7	2.62	3.54	4.46	5.38	6.3				10P
7.22	8.14	8.603							10P
0.	40.27	10.774	43.518	8.603					11P
15.									12P
0.	0.	.025	.0108	.05	.01556				12P
.1	.02155	.15	.02548	.2	.02832				12P
.3	.03215	.4	.0342	.5	.03385				12P
.6	.03112	.7	.02599	.8	.01915				12P
.9	.01084	.95	.00616	1.	0.				12P
15.									13P
0.	0.	.025	-.00257	.05	-.00325				13P
.1	-.00428	.15	-.0051	.2	-.00581				13P
.3	-.00701	.4	-.00735	.5	-.0065				13P
.6	-.00469	.7	-.00239	.8	-.00068				13P
.9	0.	.95	0.	1.	0.				13P
PANEND									14P
AERODYNAMIC									1A
1.8	1.								2A
TR-805 GIVEN	SHAPE								3A
2.	1.	1.	1.	1.					4A
89.375	0.	0.							5A
TR-805 BODY	CAMBER								6A
-.2	-.17	-.152	-.136	-.123	-.111	-.10			6A

TITLE BOEING WING-BODY MODEL NAME DATE PAGE 3 OF 5

AD 3779 R1 6-9200

SEVEN FIELD, TEN DIGIT CRD FORMAT

1 10	11 20	21 30	31 40	41 50	51 60	61	69 70	71	72	DENT 80
-.089	-.078	-.0675	-.058	-.048	-.040	-.032				6A
-.025	-.019	-.013	-.008	-.004	-.001	0.				6A
0.	0.	0.	0.	0.	0.	0.				6A
0.	0.	0.	0.	0.	0.	0.				6A
0.	0.	0.	0.	0.	0.	0.				6A
0.	0.	0.	0.	0.	0.	0.				6A
0.										6A
GIVEN WING CAMBER										8A
2.										10A
1.										10A
1.										10A
1.										10A
										BLANK
TR-805 MIN DRAG CL BAR = .1										3A
3.	0.	0.	1.	1.						4A
89.375	0.	0.								5A
TR-805 BODY CAMBER										6A
-.2	-.17	-.152	-.136	-.123	-.111	-.10				6A
-.089	-.078	-.0675	-.058	-.048	-.040	-.032				6A
-.025	-.019	-.013	-.008	-.004	-.001	0.				6A
0.	0.	0.	0.	0.	0.	0.				6A
0.	0.	0.	0.	0.	0.	0.				6A
0.	0.	0.	0.	0.	0.	0.				6A
0.	0.	0.	0.	0.	0.	0.				6A
0.										6A
0.	.1									9A
										11A

TITLE BOEING WING-BODY MODEL NAME DATE PAGE 4 OF 5

AD 3779 R1 6-8200

SEVEN FIELD, TEN DIGIT CRD FORMAT

1 10	11 20	21 30	31 40	41 50	51 60	61 69	70	71	72	DENT 80
										11A
END OF DATA										

TITLE BOEING WING–BODY MODEL | NAME | DATE | PAGE 5 OF 5

AD 3779 R1 6-0200

6. EXPERIMENTAL VERIFICATION

Four comparisons of experimental data with computed data are presented and discussed. The first comparison, given in section 6.1 is for a parabolic body. Section 6.2 discusses two arrow wings, one with camber and thickness and one with thickness only. Pressure distributions at three angles of attack are compared for each wing. Finally, two constant-chord, wing-body configurations are considered in sections 6.3 and 6.4. One configuration has an unswept wing, while the second has wing leading edges swept behind the Mach cone. Body and wing pressure distributions for both configurations are compared.

6.1 Body Alone

Wind-tunnel pressure data for a body of revolution with a parabolic profile are published in reference 16. The fineness ratio of the body is 11. The pressure coefficients measured on the body at Mach 1.93 for zero incidence are presented in the lower half of figure 25, and compared with pressure coefficients calculated by the nonlinear formulae given by equation (102). The longitudinal pressure distribution for zero angle of attack agrees very closely with the wind-tunnel data.

The circumferential pressure distributions predicted by the method using the nonlinear pressure coefficient formula for the lifting case (α = 5 degrees) do not follow the experimental data closely. However, they exhibit similar trends and show comparable C_p levels. The shape of the circumferential pressure curve at x/L = .13 predicted by the linear C_p formula shows the better trend, although the level is too high. A hybrid theory, similar to that suggested by Van Dyke in reference 17 can be used to improve the agreement on the body ahead of the maximum diameter. The hybrid theory proposes the use of the nonlinear pressure coefficient formula given by equation (102) to estimate the pressure due to body thickness, and the linear pressure coefficient formula given by equation (105) to estimate the additional pressure due to camber and incidence. The effect of the hybrid theory is to shift the linear pressure curve toward the nonlinear curve along the C_P axis. Use of this technique on the body behind the maximum diameter does not result in an improvement of pressure curve shapes or levels in this example.

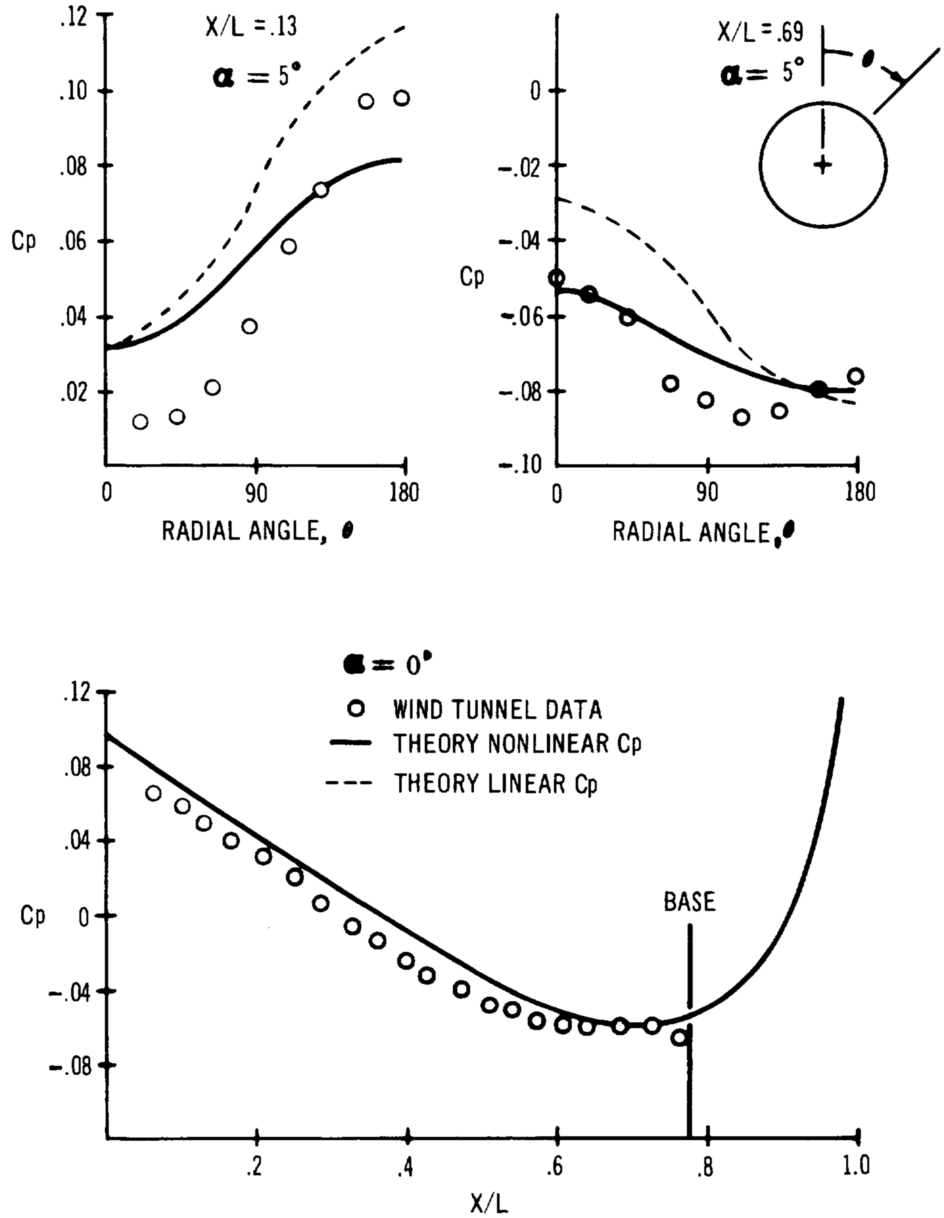

FIGURE 25 COMPARISON OF THEORETICAL AND EXPERIMENTAL PRESSURE DISTRIBUTIONS ON A PARABOLIC BODY OF REVOLUTION AT M = 1.93. FINENESS RATIO = 11.

6.2 Wing Alone

Two arrow wings of identical planform were analyzed. A complete tabulation of the experimental data for both wings is presented in reference 18. Both wings have a 3-percent biconvex symmetrical thickness distribution. Wing 1 has no camber or twist. Wing 2 is cambered and twisted to give theoretical minimum drag at a design C_L of 0.08 for a given leading edge pressure constraint. Comparison of experimental and theoretical data is made at Mach 2.05 and presented at five spanwise stations for three angles of attack. Figure 26 shows the planform and the 100-panel layout for both wings. The paneling was chosen so that the spanwise locations of the calculated pressures corresponded to the pressure taps on the test wings.

The unsmoothed theoretical pressure coefficient data shown in figure 27 for α = 0 degrees are a direct point-to-point pilot of the program output for Wing 1. A distinct oscillation in the calculated C_p is apparent near the tip. Since this wing has no camber, the pressure coefficients at α = 0 degrees are due to airfoil thickness alone. The use of source singularities to represent wing thickness results in chordwise pressure oscillations in regions where spanwise panel edges have the same slope, or nearly the same slope, as the Mach line. The oscillations are amplified in the tip region of planforms having pointed tips and subsonic leading edges. A good representation of the chordwise pressure distribution can be provided by fairing through the end points of the oscillation. This type of fairing has been applied to all the arrow wing chordwise pressure plots and is presented as the smoothed theoretical data.

Agreement between the smoothed theoretical data and experimental data is good, except near the tip, for both wings at low and moderate angles of attack. At higher angles of attack the experimental pressure distributions show a distinct change in pattern and no longer agree with linear theory predictions. This is probably associated with an overexpansion of the flow on the upper surface, followed by the formation of a shock wave and vortex.

Satisfactory prediction of lift curves and drag polar shapes is illustrated by the Wing 2 comparison shown below:

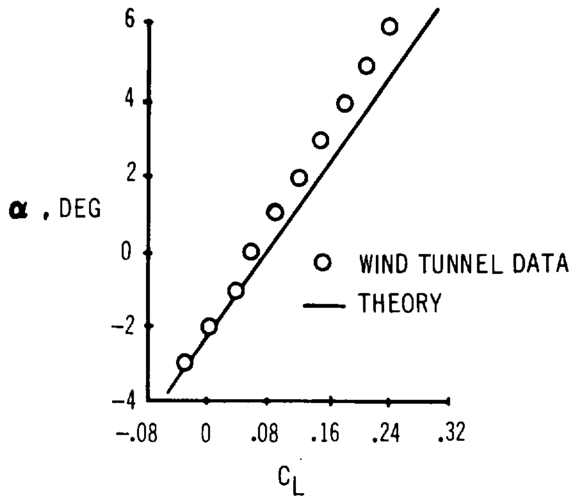

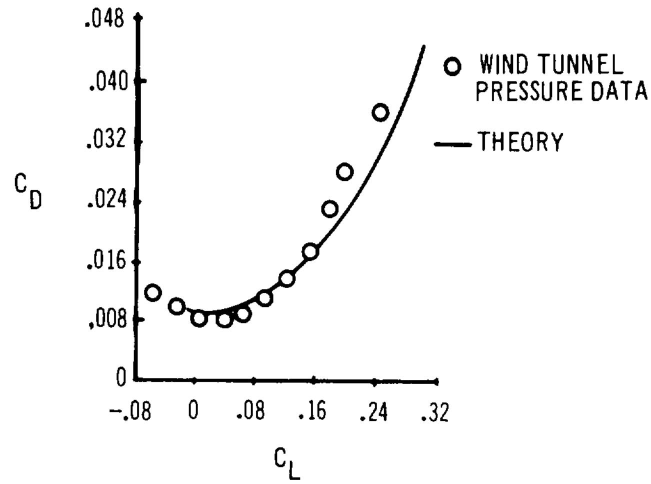

The pressure distributions predicted by the program also agree well with the linear theory calculations presented in reference 18.

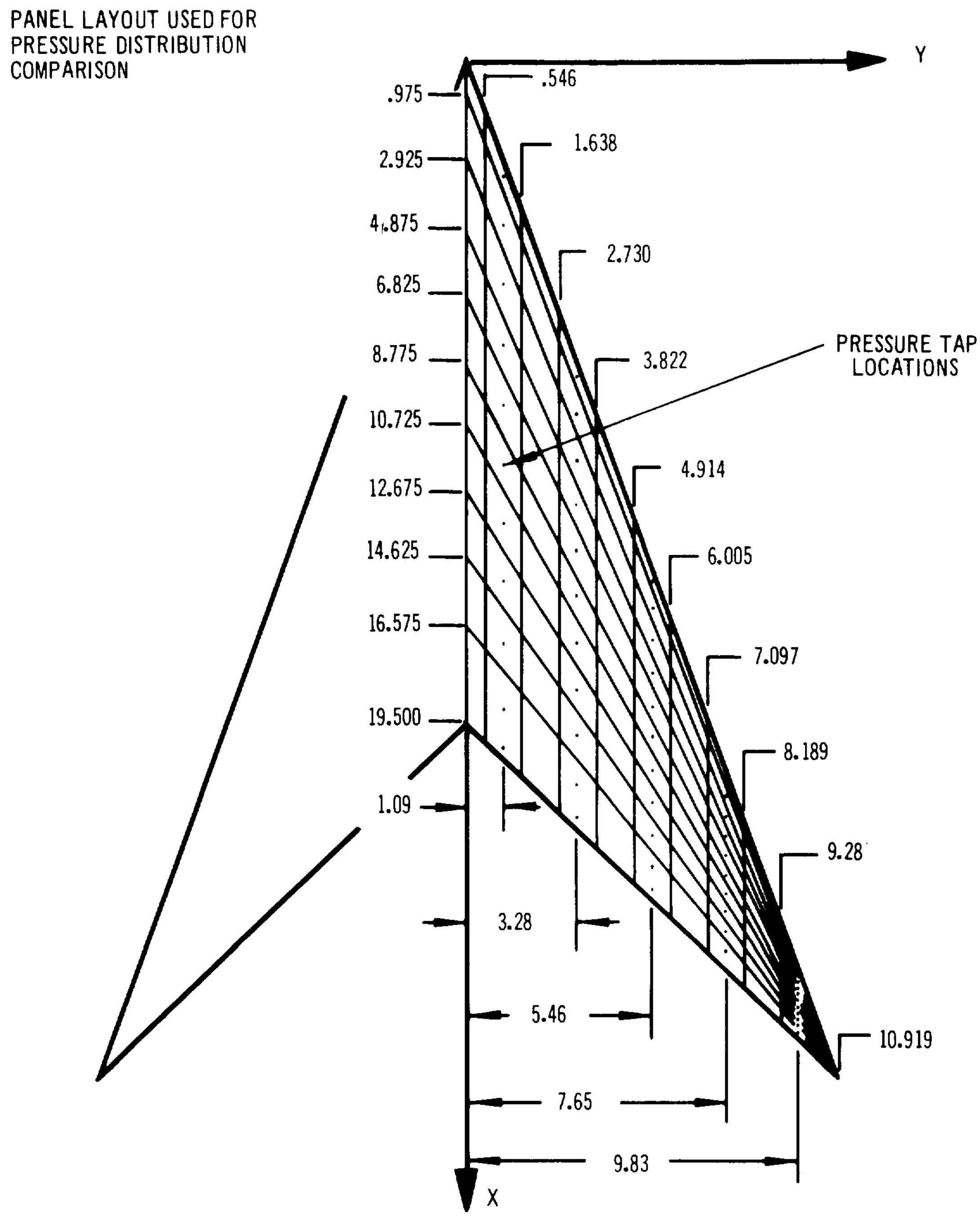

FIGURE 26 ARROW WING PLANFORM AND PANELING DESCRIPTION

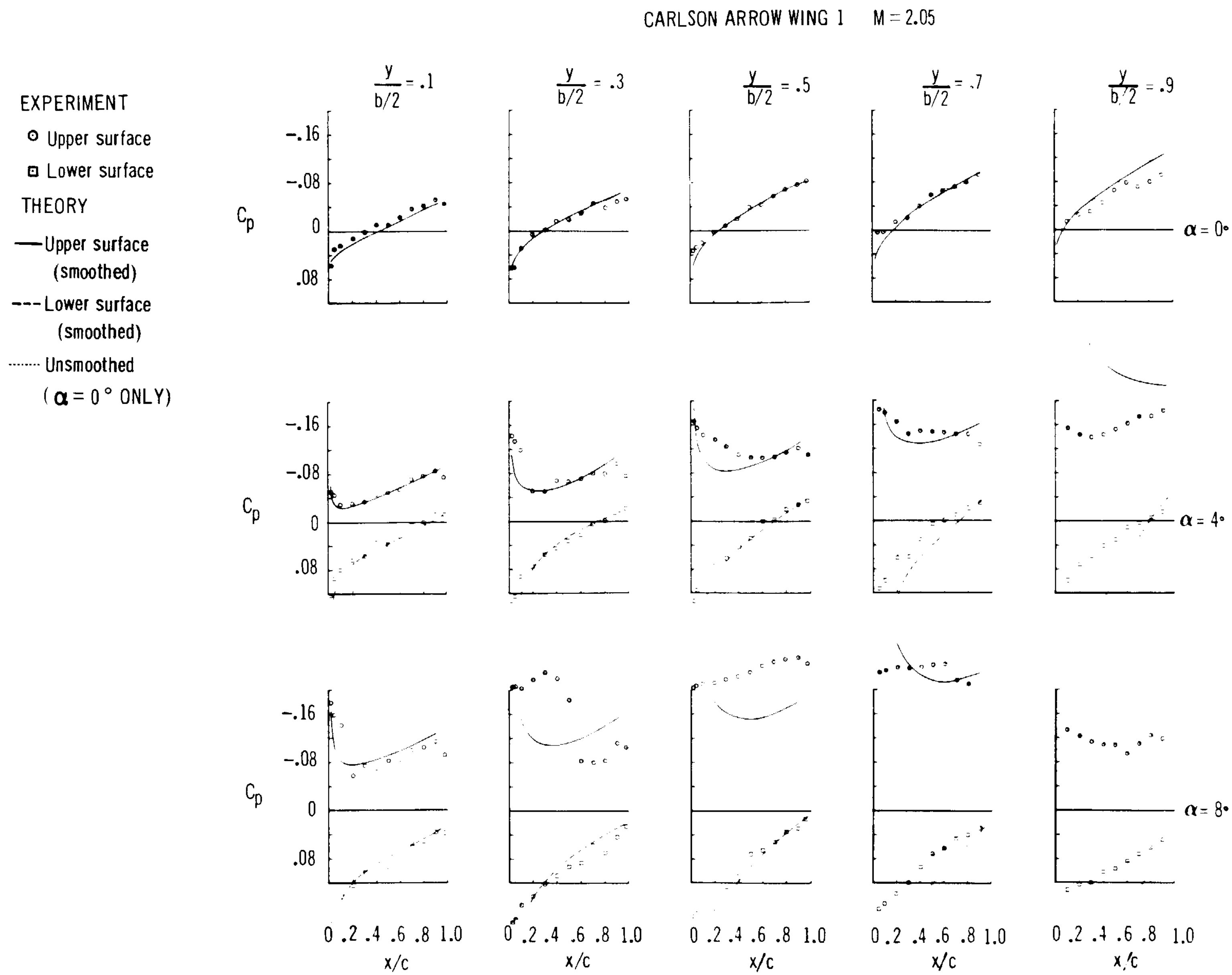

FIGURE 27 THEORETICAL AND EXPERIMENTAL PRESSURE DISTRIBUTIONS FOR AN UNCAMBERED ARROW WING

CARLSON ARROW WING 2   M 2.05

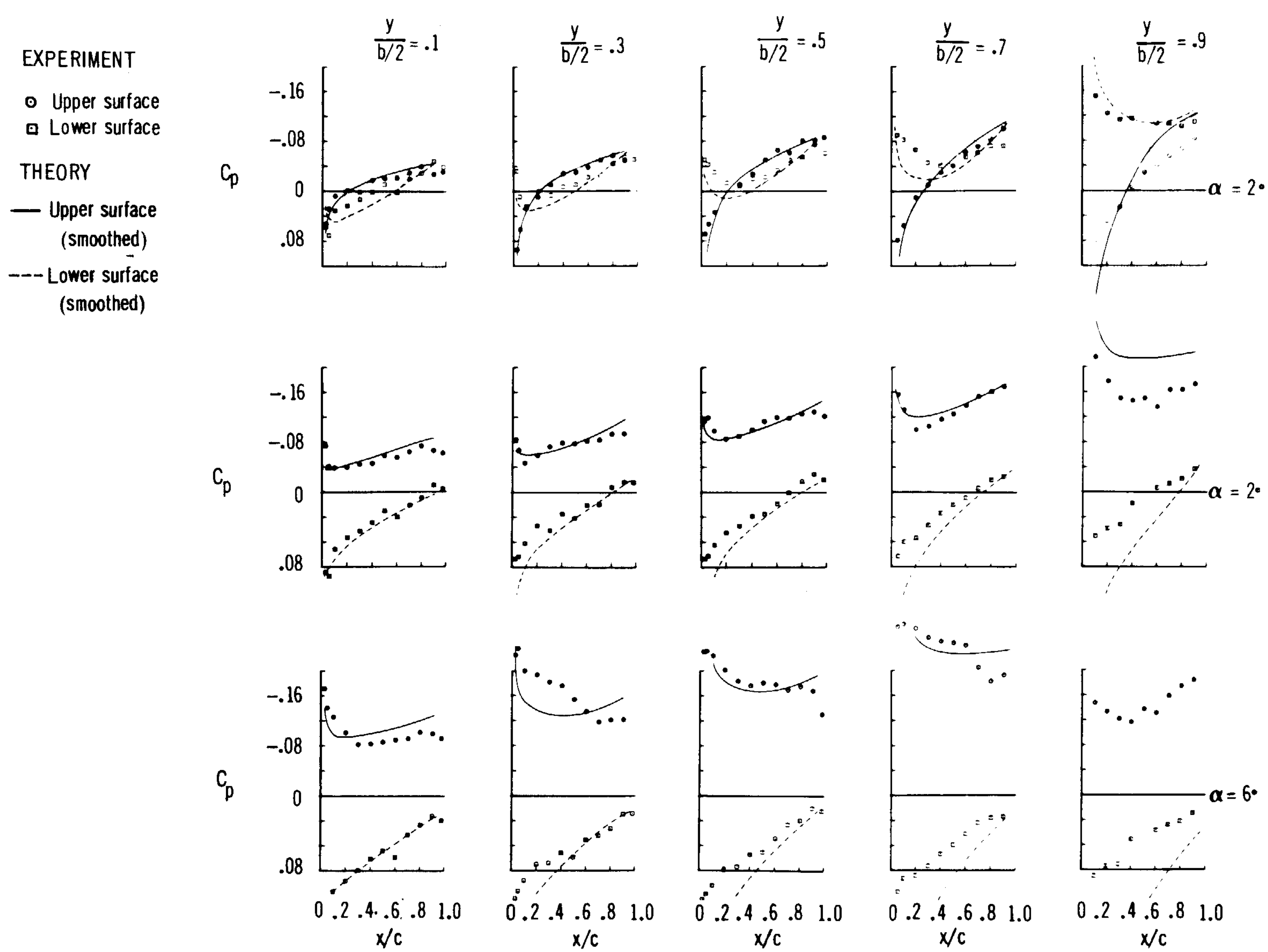

FIGURE 28 THEORETICAL AND EXPERIMENTAL PRESSURE DISTRIBUTIONS FOR A CAMBERED AND TWISTED ARROW WING

6.3 Nielsen Wing Body

A classical experiment in wing-body interference was reported by Nielsen in reference 15. The configuration tested was a circular body of revolution with an ogival nose and an unswept, constant-chord wing with a 10-percent thick wedge-shaped airfoil. Model dimensions and configuration paneling are shown in figure 29. The model was equipped with apparatus to permit changing the wing incidence relative to the body axis. Data comparisons are made for the wing at incidence to the body, and for the wing and body at the same angle of attack. Only the incremental pressure coefficients above the values obtained for the wing and body at zero incidence are shown.

For this analysis, the wing is assumed to have no thickness. The half-wing planform is divided into one hundred equal-area panels as shown in figure 29. The half-body region aft of the wing leading edge is represented by six equal longitudinal strips of fourteen panels each. The calculated pressure distributions at Mach 1.48 are presented in figures 30 through 33 at five spanwise wing stations and for three body meridians. In figure 30, the calculated pressure distributions are compared with Nielsen's theoretical predictions and the experimental data for $\alpha_{wing} = 1.92$ degrees; the body incidence is zero for this example. Both theoretical results for wing pressures agree well, except in the region enclosed by the Mach cone from the tip, $y/r = 3.92$, where the present theory tends to smooth out the pressure discontinuity. However, the program data does show acceptable agreement with the experimental data. The present theory for body pressures does not agree closely with Nielsen's predictions but does show excellent agreement with the wind-tunnel data.

Figures 32 and 33 show pressure data comparisons for the wing and body at the same angle of attack. The Mach number is 1.48 and the experimental data is for $\alpha_{wing} = \alpha_{body} = 2$ degrees. Both theories again show agreement, except on the body, where the pressures calculated by the program show closer correlation to the experimental data.

The wind-tunnel test Reynolds number for both cases above is 1.5 million.

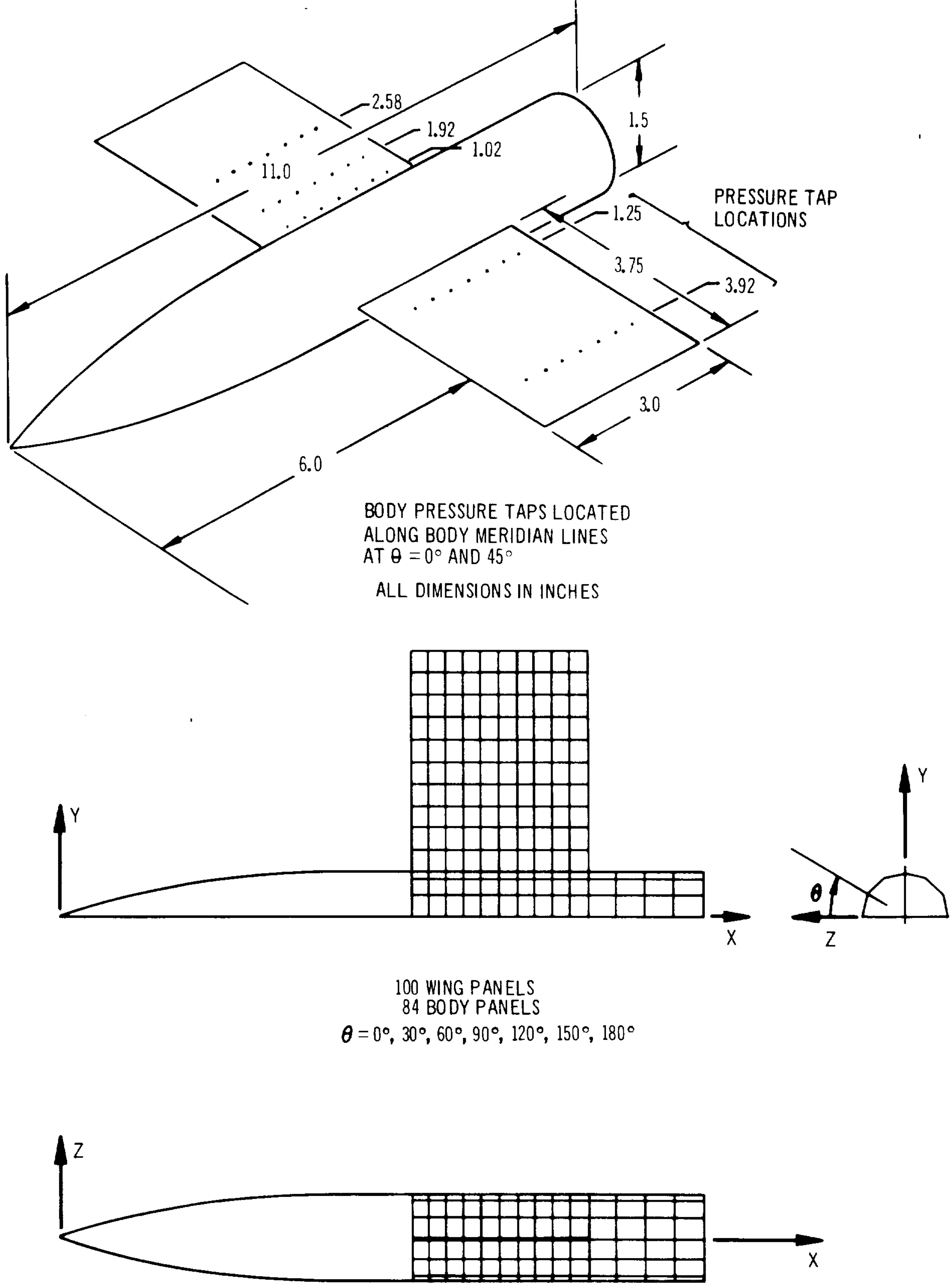

FIGURE 29 NIELSEN'S WING BODY CONFIGURATION AND PANELING SCHEME

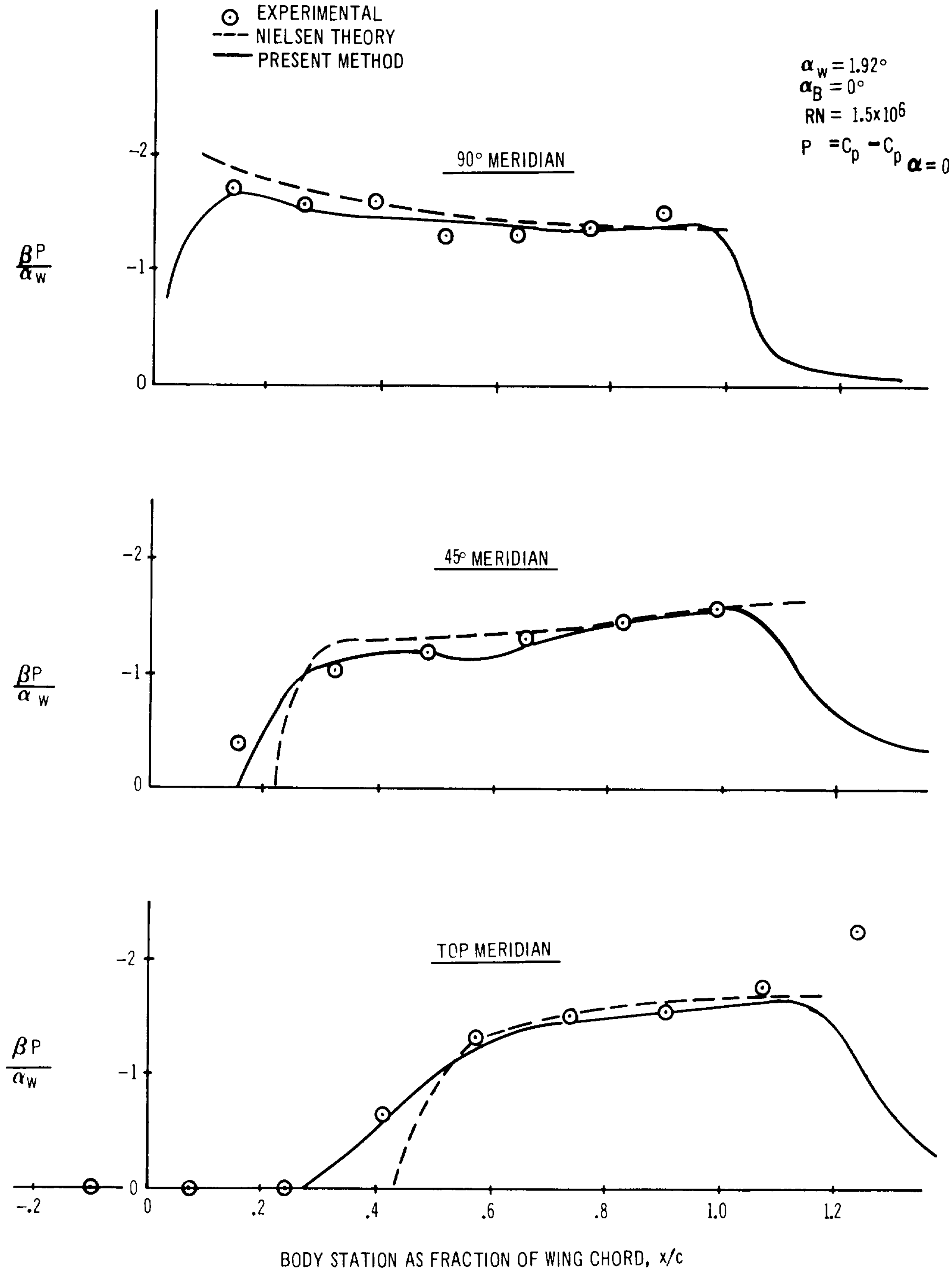

FIGURE 30 BODY PRESSURE DISTRIBUTION FOR NIELSEN WING-BODY COMBINATION WITH WING AT INCIDENCE

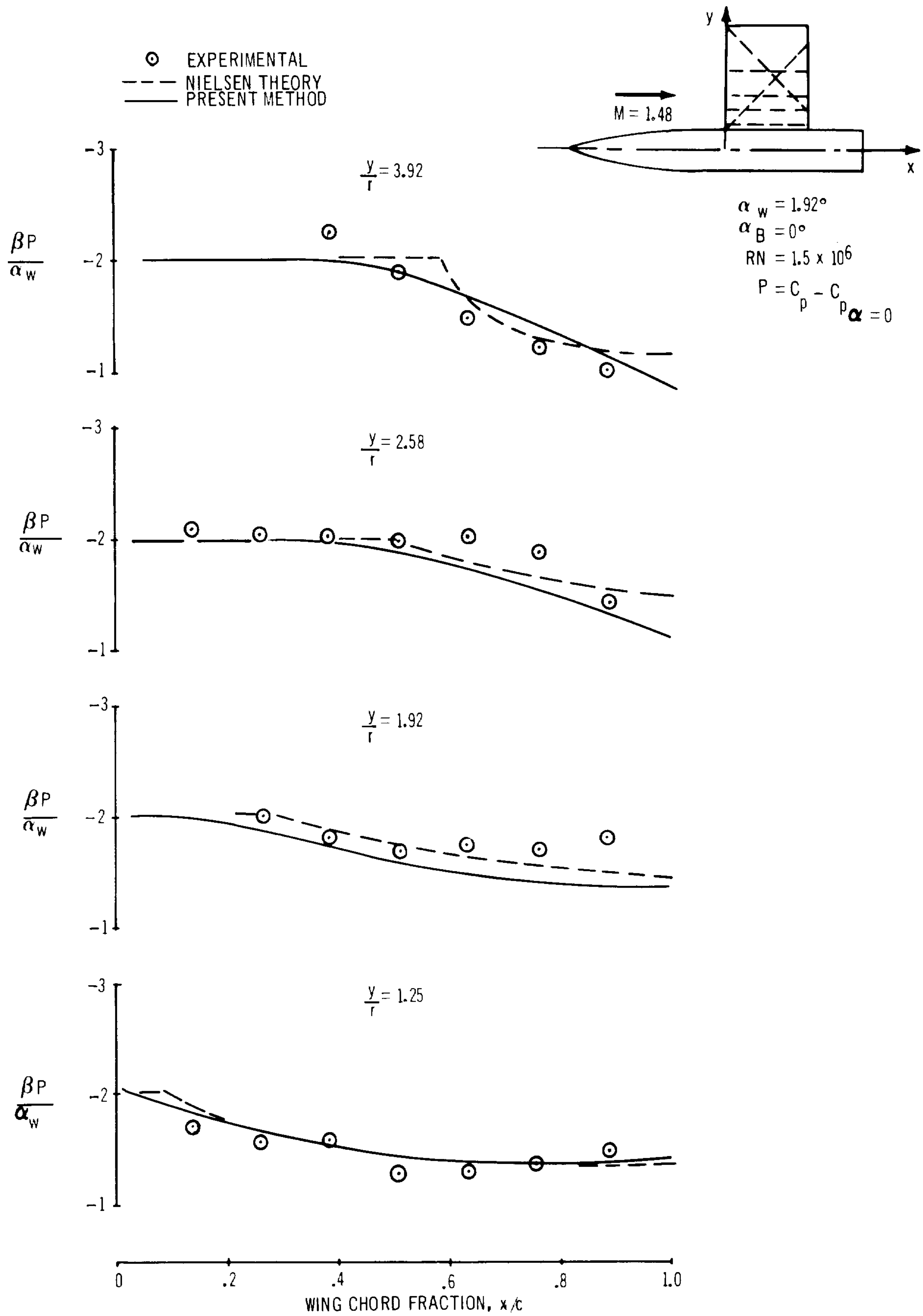

FIGURE 31 WING PRESSURE DISTRIBUTION FOR NIELSEN WING–BODY COMBINATION WITH WING AT INCIDENCE

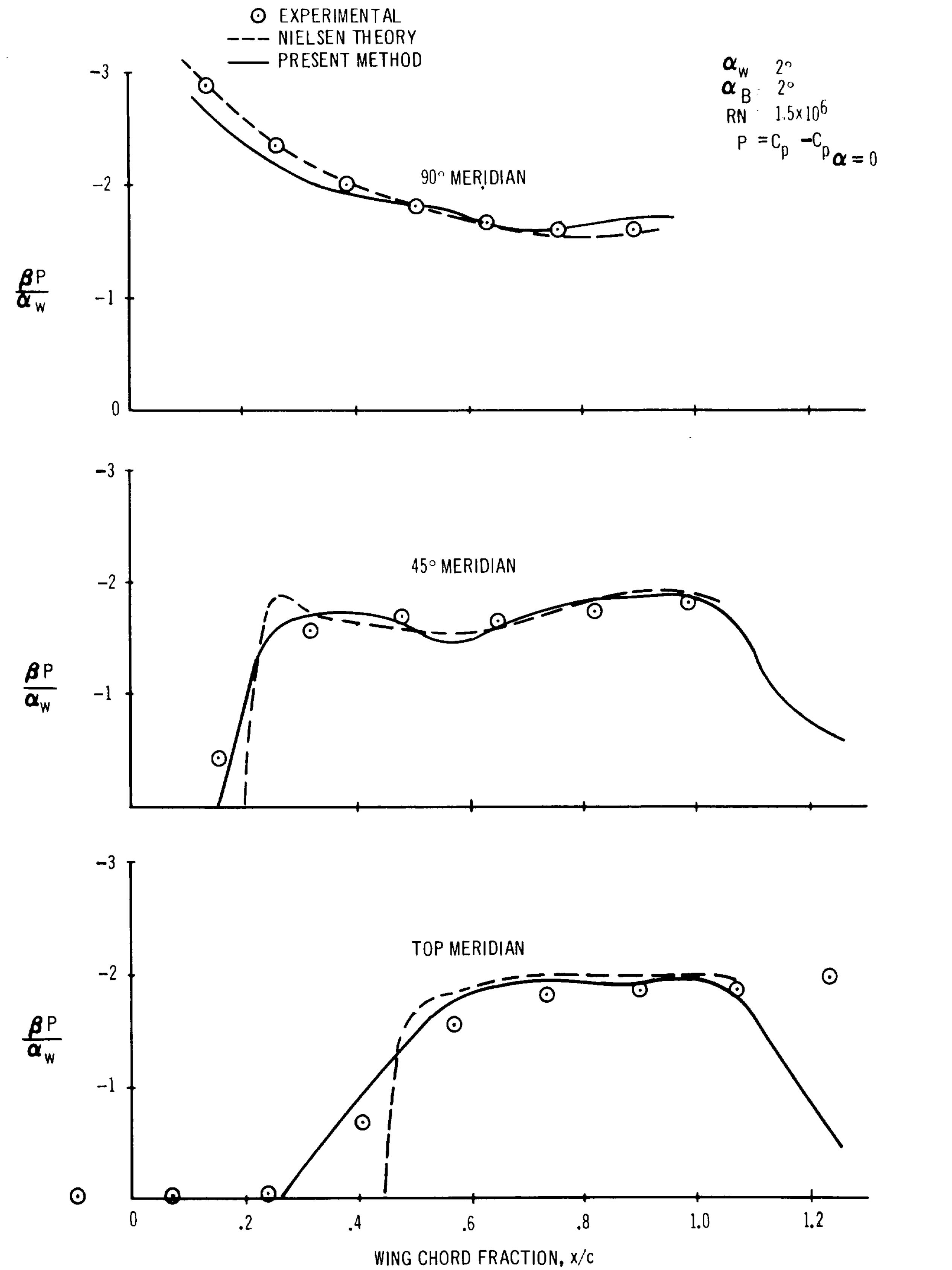

FIGURE 32 BODY PRESSURE DISTRIBUTION FOR NIELSEN WING-BODY COMBINATION WITH WING AND BODY AT INCIDENCE

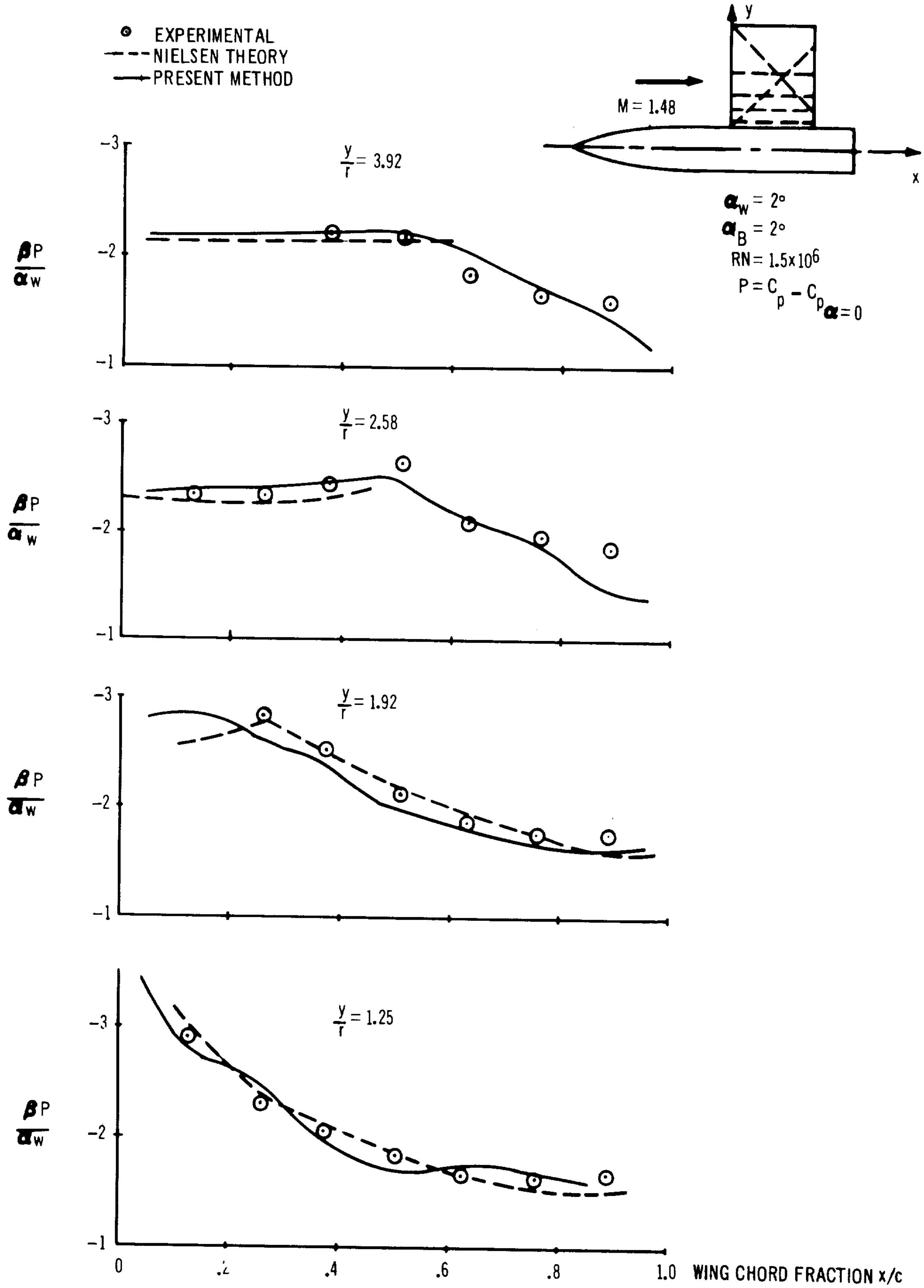

FIGURE 33 WING PRESSURE DISTRIBUTION FOR NIELSEN WING BODY COMBINATION WITH WING AND BODY AT INCIDENCE

6.4 Boeing Wing-Body

The wind-tunnel test model is a constant-chord, swept-wing configuration with a cambered cylindrical body. Model dimensions and pressure tap locations are given in figure 34. The body has a drooped nose and a small amount of boat tailing. Four streamwise rows of pressure taps are located on the upper and lower wing surfaces. The wing chord plane intersects the body side 0.25 inch below the body axis and has no incidence relative to the body. Five longitudinal rows of pressure taps are located on the body. The wing, with a 12-percent-thick airfoil oriented normal to the leading edge, is pretwisted to give a flat shape when aerodynamically loaded to a design C_L of 0.15 at Mach 1.8. Photographs in figure 36 show that the wing did achieve an untwisted shape at a 4-degree angle of attack. It is this untwisted wing with camber that is analyzed by the program.

The wing half-planform is represented by 100 panels spaced as shown in figure 37 on page 170 to obtain pressure coefficients at spanwise stations corresponding to wing pressure tap locations. The body aft of the wing leading edge is represented by 98 panels, 14 in each of 7 longitudinal strips.

Comparisons of wind tunnel and calculated wing and body pressure data are shown in figures 37 and 38. The Mach number is 1.8 and the comparison is for α = 4 degrees. Wing pressure predictions are good for the inboard stations. The experimental pressure distributions indicate the formation of a shock wave on the upper wing surface near the root trailing edge, which extends outboard and rearward across the span. Photographs of oil flow patterns taken during the wind-tunnel test verify the formation and location of the shock wave. The rapid recompression aft of the shock and subsequent flow separation are not well represented by the linear theory calculations.

Pressures calculated on the surface of the body, shown in figure 38, exhibit good agreement with wind-tunnel data. The body pressures due to thickness are calculated by the nonlinear pressure coefficient formula, equation (102). The wing pressures and pressures on the body due to the wing are predicted by the linear pressure coefficient formula, equation (105). The total body pressure distribution shown includes body thickness and wing interference effects. The interference pressures due to the wing are added to the isolated body thickness pressures in the region influenced by the wing.

The program input format for this wing-body configuration, paneled as shown in figure 37, for nonlinear pressure calculations on wing and body, is presented on pages 145 through 149 of section 5.4. This same wing-body configuration, but with a different wing paneling scheme, was optimized for minimum drag at a wing C_L of 0.159. Discussion of the optimization follows in section 7.0. The program input format for this latter case is contained in Appendix C.

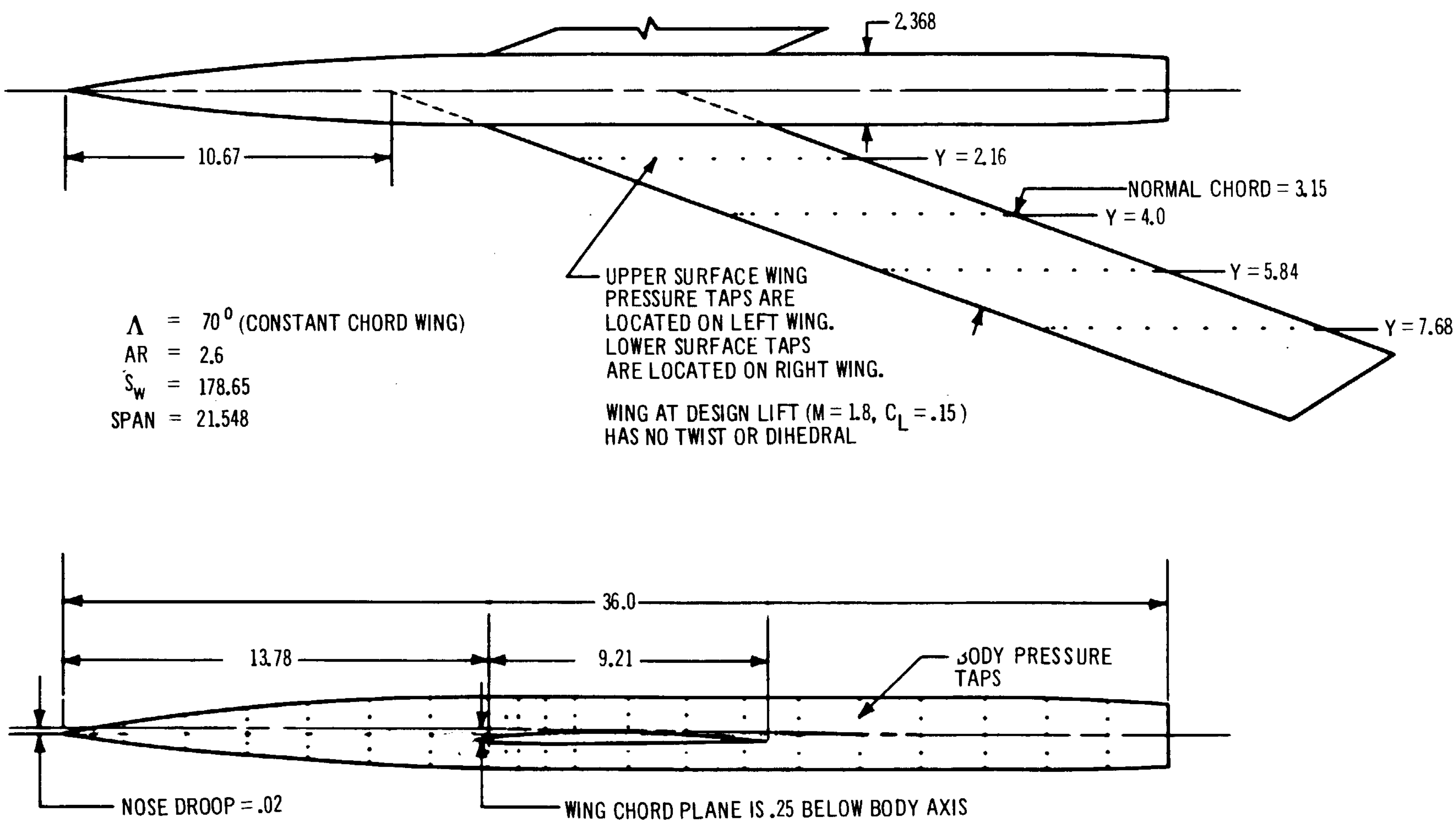

FIGURE 34 BOEING WING-BODY WIND-TUNNEL MODEL DESCRIPTION (ALL DIMENSIONS IN INCHES)

VIEW OF SUPERSONIC PRESSURE MODEL SHOWING PRESSURE LEADS FROM BODY

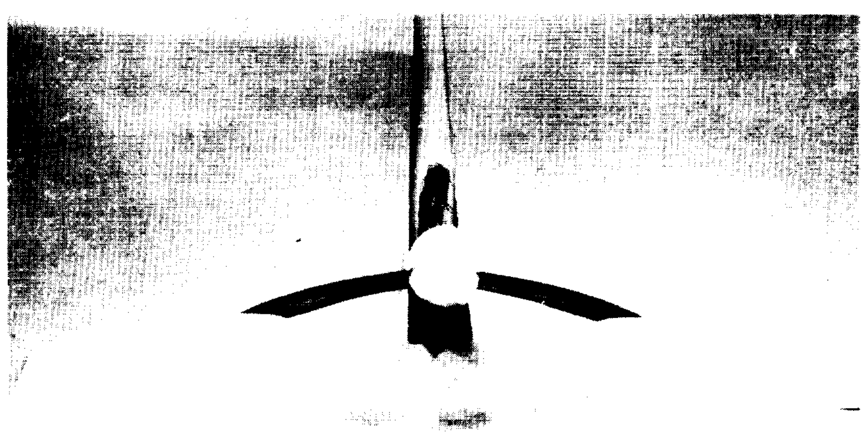

FRONT VIEW OF PRESHAPED WING

FIGURE 35 PHOTOS OF BOEING MODEL USED TO OBTAIN EXPERIMENTAL DATA

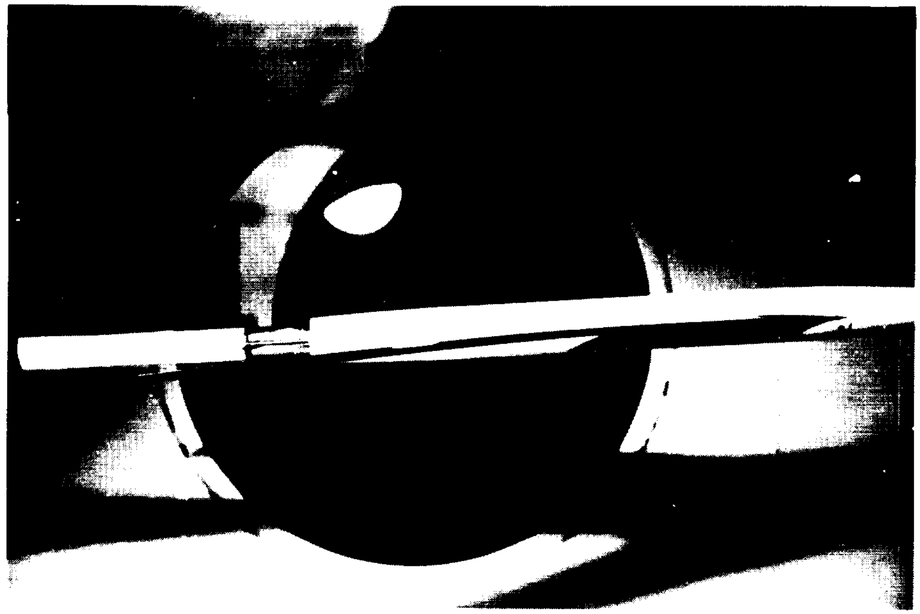

WIND-OFF CONDITION WITH THE TEST SECTION STING PITCHED TO 4° ANGLE OF ATTACK. THE BUILT-IN DOWNWARD DEFLECTION OF THE WING IS READILY APPARENT.

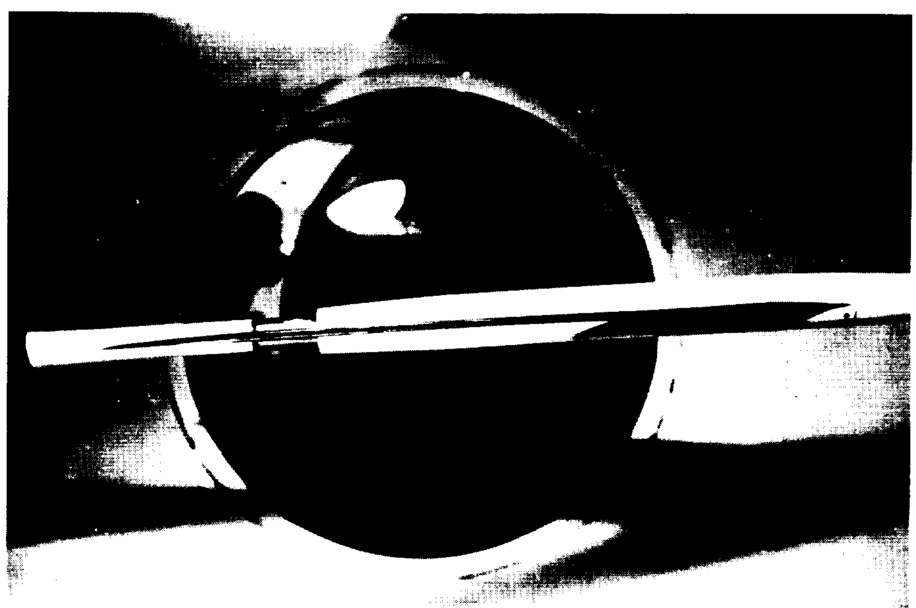

WIND-ON CONDITION FOR $\alpha = 4°$ and M = 1.8. THE WING IS AT DESIGN C_L AND HAS DEFLECTED INTO A FLAT SHAPE UNDER THE AERODYNAMIC LOAD.

FIGURE 36 COMPARISON OF WING SHAPE WITH AND WITHOUT AIRLOAD

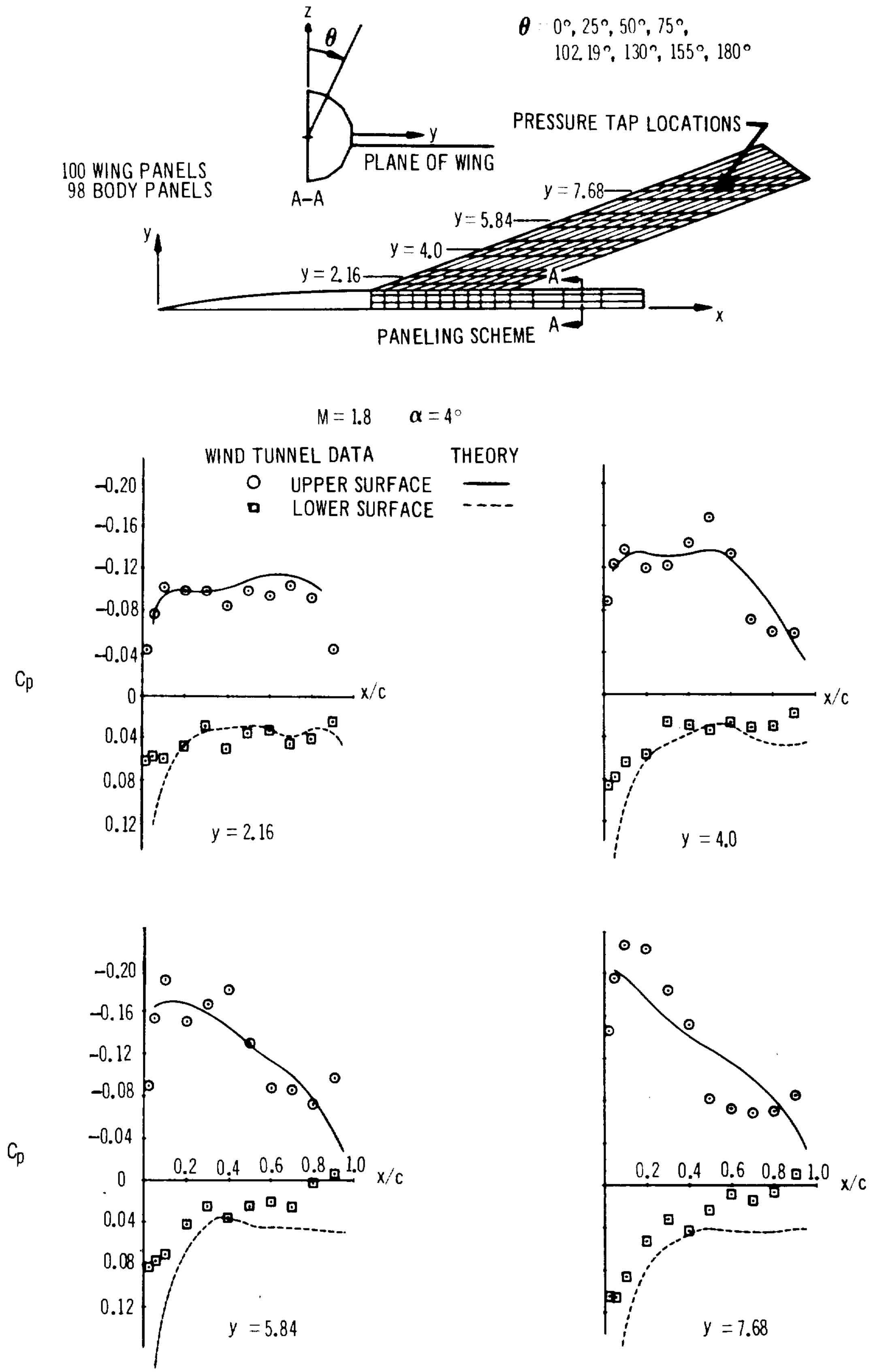

FIGURE 37 WING PRESSURE DISTRIBUTION FOR BOEING WING BODY MODEL

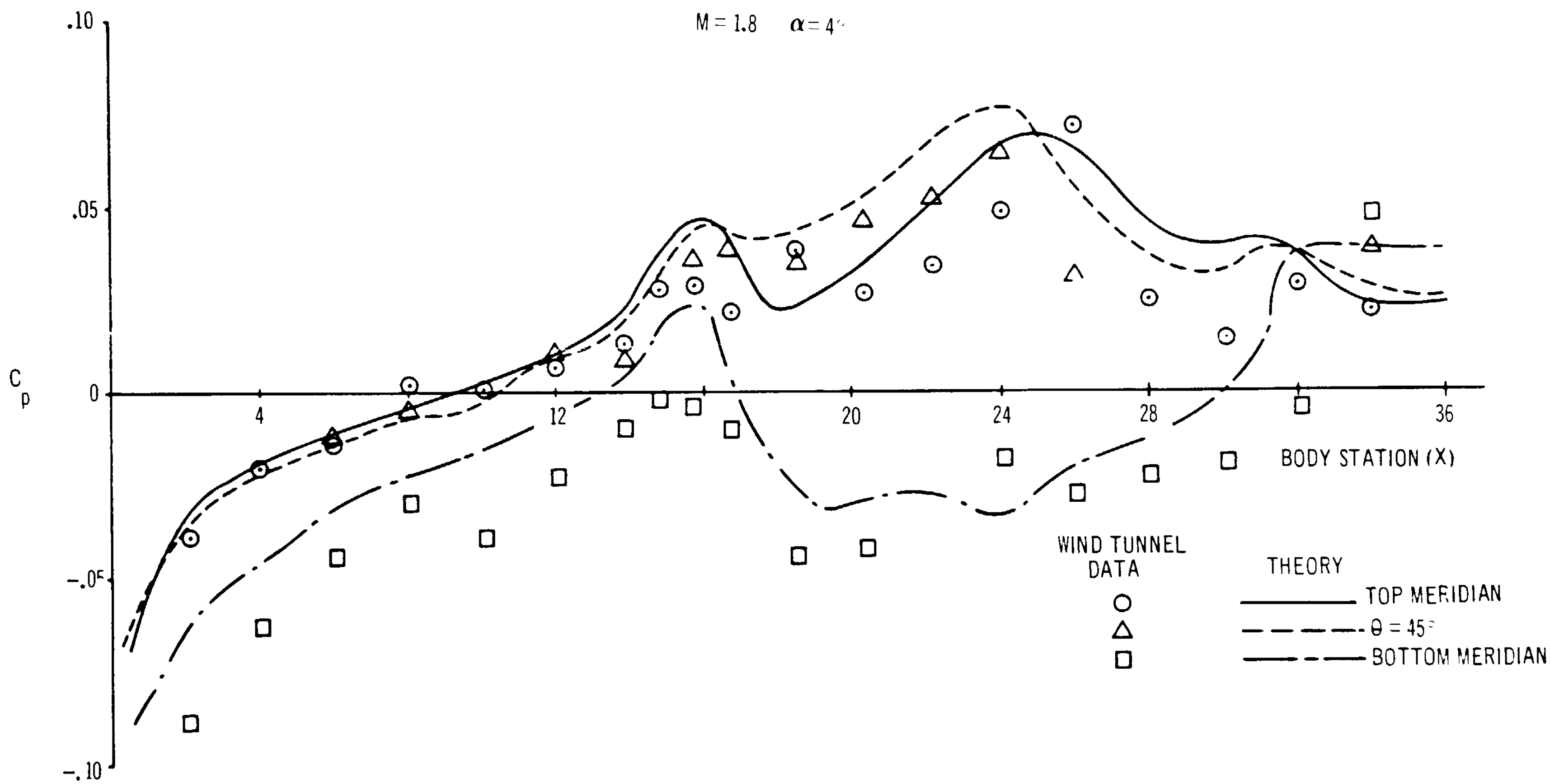

FIGURE 38 BODY PRESSURE DISTRIBUTION FOR BOEING WING-BODY MODEL

7. THEORETICAL OPTIMIZATION

The wing camber surface of the Boeing wing-body configuration, as described in the previous section, was optimized for minimum drag with constrained lift. Some graphical comparisons with the untwisted case are shown in figure 39, and a complete input-output tabulation is presented in Appendix C. The paneling chosen for this case was uniformly spaced both spanwise and chordwise on the wing. This paneling scheme differed slightly from that used in the example presented in section 6.4; in which the panels were chosen to coincide with the pressure tap locations. Both paneling schemes are illustrated on figure 40, page 189. Uniform panel spacing tends to minimize any undesirable oscillations in the wing geometry or pressure distributions, in wing optimization calculations.

At the wind-tunnel model design angle of attack of 4 degrees and Mach 1.8, the wing lift coefficient (based on the exposed wing) was 0.159. The optimized wing lift coefficient was constrained to the same value, and the body was kept at the same angle of attack. No constraint was placed on the center of pressure. The optimized wing camber surface reduced the wing drag by 19 percent (from 0.00936 to 0.00761) and the total configuration drag by 23 percent (from 0.01101 to 0.00849). A greater load was carried by the wing root, improving the spanwise lift distribution. The additional body load increased the total lift and reduced the negative pitching moment.

The additional load on the body due to the wing is shown by the top and bottom meridian pressure distributions in figure 39. Changes in the body interference pressures are larger toward the wing-body junction leading edge, where the major change occurred in the wing root pressure distribution. The chordwise pressure distributions on the wing show the effect of the optimized camber surface. Wing thickness effects are unchanged. In general the maximum camber location was moved more toward the trailing edge. Viscous limitations on the pressure gradients at the trailing edge would probably make some of the camber revision impractical.

Although the details of the optimized wing geometry are not shown in figure 39, the tabular panel slope data are given in Appendix C. The optimization shows an increase in wing incidence at the root and a decrease in the incidence of the next-to-last spanwise station near the highly loaded wing tip. Additional fine paneling in each of these areas could give more detail of the optimum geometry.

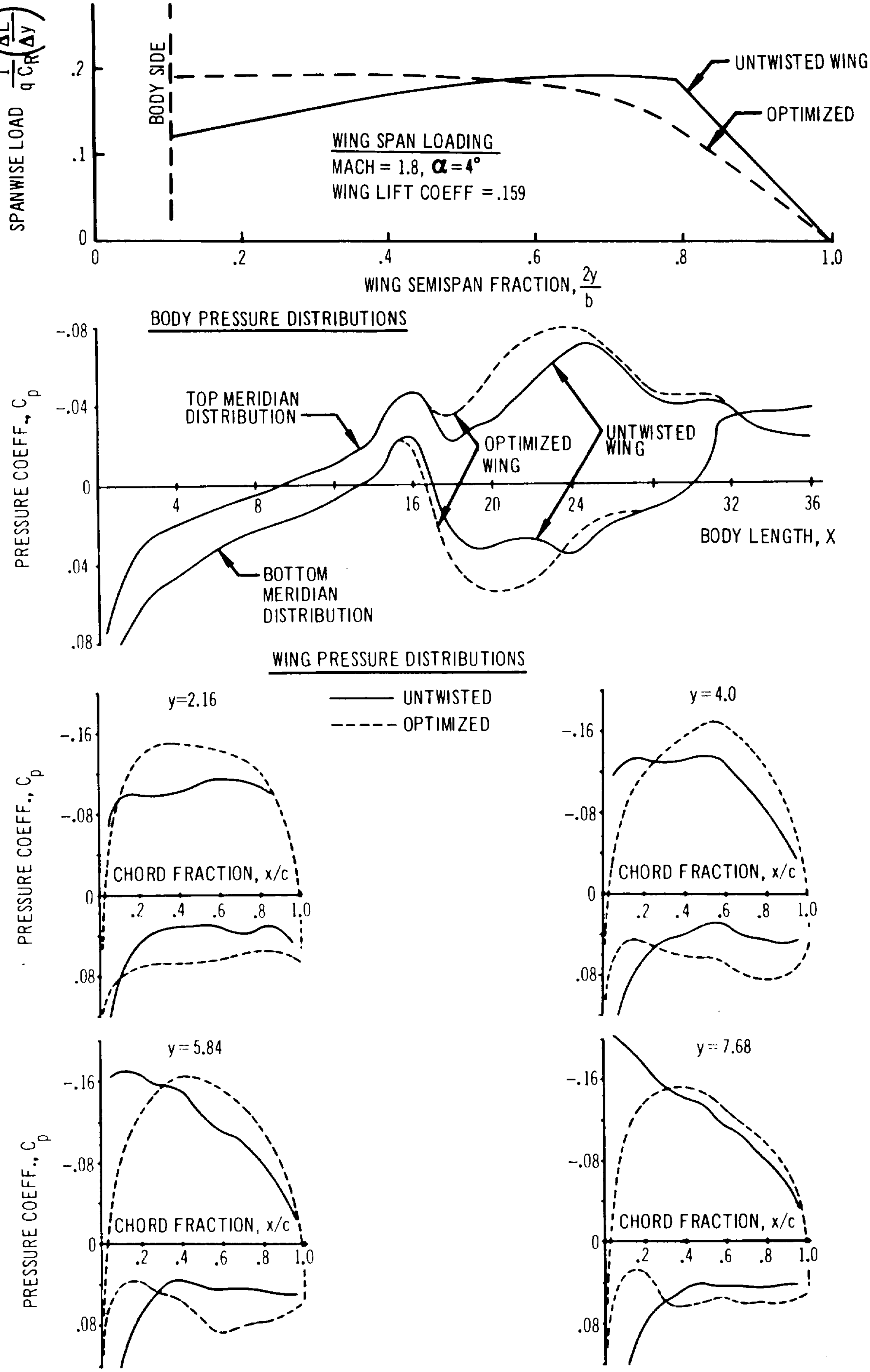

FIGURE 39 COMPARISON OF UNTWISTED AND OPTIMIZED DISTRIBUTIONS

8. CONCLUSIONS

A digital computer program for calculating wing-body interference problems in supersonic flow has been developed. The program is based on the method of aerodynamic influence coefficients. A special effort has been made to reduce the number of geometric description inputs, and has significantly increased the practical value of the program.

A wide variety of aerodynamic problems involving wings, bodies, or wing-body combinations can be solved. The program may be used to determine the pressures, forces, and moments on given configurations; or to determine the wing camber surface corresponding to a given aerodynamic loading. In particular, the wing camber surface required to minimize the drag under given constraints of lift, or lift and pitching moment, may be calculated. The results of the program have been compared with other theories and experiments, and show good agreement in all cases.

9.1 Appendix A - Preliminary Results of Integration

In the solution of certain problems concerning the linearized theory of supersonic aerodynamics, several integrals of standard form occur repeatedly; their evaluation can be carried out by elementary methods. Here is given a brief outline of the integration procedure and a summary of the results.

$$J_1 = \int \frac{d\,v}{(v^2 + e^2)\sqrt{a^2 v^2 + 2b\,v + c}} \;,$$

$$J_2 = \int \frac{v\,d\,v}{(v^2 + e^2)\sqrt{a^2 v^2 + 2b\,v + c}} \;.$$

Let the following substitution be made:

$$v = \sqrt{\frac{b^2 - a\,c}{a^2}}\,\frac{u^2 + 1}{u^2 - 1} - \frac{b}{a} \;.$$

then

$$J_1 = -\frac{2a^2}{\sqrt{a}} \int \frac{(u^2 - 1)\,d\,u}{(b^2 - a\,c)(u^2 + 1)^2 - 2b\sqrt{b^2 - a\,c}\,(u^4 - 1) + b^2(u^2 - 1)^2 + e^2\,a^2(u^2 - 1)^2}$$

$$= \frac{\sqrt{a}}{e\,i}\,\frac{1}{\sqrt{a^2 e^2 + 2ab\,e\,i - a\,c}}\,\tan^{-1}\sqrt{\frac{\sqrt{b^2 - a\,c} - b + a\,e\,i}{\sqrt{b^2 - a\,c} + b - a\,e\,i}}\;u$$

$$- \frac{\sqrt{a}}{e\,i}\,\frac{1}{\sqrt{a^2 e^2 - 2ab\,e\,i - a\,c}}\,\tan^{-1}\sqrt{\frac{\sqrt{b^2 - a\,c} - b - a\,e\,i}{\sqrt{b^2 - a\,c} + b + a\,e\,i}}\;u \;.$$

The above results can be simplified by the following consideration:

let $$\tan^{-1}\sqrt{\frac{\sqrt{b^2 - a\,c} - b + a\,e\,i}{\sqrt{b^2 - a\,c} + b - a\,e\,i}}\;u = \alpha + i\,\beta \;,$$

and $$\sqrt{a\,e^2 + 2b\;ei - c} = \gamma + i\,\delta$$

then $\gamma^2 - \delta^2 = a\,e^2 - c$ and $\gamma\,\delta = b\,e$, and γ satisfies the equation:

$$\gamma^4 - (a\,e^2 - c)\,\gamma^2 - b^2\,e^2 = 0 .$$

Furthermore,

$$J_1 = \frac{\sqrt{a}}{ei}\,\frac{\alpha + i\beta}{\sqrt{a}\,(\gamma + i\,\delta)} - \frac{\sqrt{a}}{ei}\,\frac{\alpha - i\beta}{\sqrt{a}\,(\gamma - i\,\delta)}$$

$$= -\frac{b\,\gamma}{\gamma^4 + b^2\,e^2}\,2\alpha + \frac{1}{e}\,\frac{\gamma^3}{\gamma^2 + b^2\,e^2}\,2\beta .$$

On the other hand, since $\tan(\alpha + i\,\beta) = \sqrt{\dfrac{\sqrt{b^2 - a\,c} - b + a\,ei}{\sqrt{b^2 - a\,c} + b - a\,ei}}$, there follows

$$\frac{\tan 2\alpha + i\,\tanh 2\beta}{1 - i\,\tan 2\alpha\,\tanh 2\beta} = \frac{\sqrt{a\,v^2 + 2b\,v + c}\,(\gamma + i\,\delta)}{b\,v + c - i\,(b + a\,v)\,e} .$$

Equating the real and the imaginary parts of the above equation, we get

$$(b\,v + c)\tan 2\alpha + (b + a\,v)\,e\tanh 2\beta = \sqrt{a\,v^2 + 2b\,v + c}\,(\gamma + \delta\tan 2\alpha\,\tanh 2\beta)$$

$$(b\,v + c)\tanh 2\beta - (b + a\,v)\,e\tan 2\alpha = \sqrt{a\,v^2 + 2b\,v + c}\,(\delta - \gamma\tan 2\alpha\,\tanh 2\beta)$$

which gives the following solution for α and β:

$$\alpha = \frac{1}{2}\tan^{-1}\frac{\gamma^2 - b\,v}{\gamma\sqrt{a\,v^2 + 2b\,v + c}}\,; \qquad \alpha = \frac{1}{2}\tan^{-1}\frac{\gamma\sqrt{a\,v^2 + 2b\,v + c}}{b\,v - \gamma^2}$$

$$\beta = \frac{1}{2}\tanh^{-1}\frac{v\,\gamma + e\,\delta}{e\sqrt{a\,v^2 + 2b\,v + c}}\,; \qquad \beta = \frac{1}{2}\tanh^{-1}\frac{e\sqrt{a\,v^2 + 2b\,v + c}}{v\,\gamma + e\,\delta}$$

The above results for α and β can now be substituted for the expression for J_1, and, omitting the integration constant, we have

$$\int\frac{d\,v}{(v^2 + e^2)\sqrt{a\,v^2 + 2b\,v + c}} = \frac{b\,\gamma}{\gamma^4 + b^2\,e^2}\tan^{-1}\frac{b\,v - \gamma^2}{\gamma\sqrt{a\,v^2 + 2b\,v + c}}$$

$$+ \frac{1}{e} \frac{\gamma^3}{\gamma^4 + b^2 e^2} \tanh^{-1} \frac{e\sqrt{a\, v^2 + 2b\, v + c}}{v\,\gamma + e\,\delta}$$

$$\text{or} \quad = \frac{b\,\gamma}{\gamma^4 + b^2 e^2} \tan^{-1} \frac{\gamma \sqrt{a\, v^2 + 2b\, v + c}}{\gamma^2 - b\, v}$$

$$+ \frac{1}{e} \frac{\gamma^3}{\gamma^4 + b^2 e^2} \tanh^{-1} \frac{v\,\gamma + e\,\delta}{e\sqrt{a\, v^2 + 2b\, v + c}}$$

where γ is a non-zero root of the equation: $\gamma^4 - (a\, e^2 - c)\, \gamma^2 - b^2 e^2 = 0$ and $\gamma\, \delta = b\, e$. For $e = 0$ then taking $\gamma = \sqrt{-c}$ we obtain

$$\int \frac{d\, v}{v^2 \sqrt{a\, v^2 + 2b\, v + c}} = - \frac{b}{c\sqrt{-c}} \tan^{-1} \frac{b\, v + c}{\sqrt{-c}\,\sqrt{a\, v^2 + 2b\, v + c}} - \frac{\sqrt{a\, v^2 + 2b\, v + c}}{c\, v}$$

$$\text{or} \quad = - \frac{b}{c\sqrt{-c}} \tan^{-1} \frac{\sqrt{-c}\,\sqrt{a\, v^2 + 2b\, v + c}}{-(b\, v + c)} - \frac{\sqrt{a\, v^2 + 2b\, v + c}}{c\, v}$$

In a like manner, the integral for J_2 can be evaluated:

$$\int \frac{v\, d\, v}{(v^2 + e^2)\sqrt{a\, v^2 + 2b\, v + c}} = \frac{\gamma^3}{\gamma^4 + b^2 e^2} \tan^{-1} \frac{b\, v - \gamma^2}{\gamma \sqrt{a\, v^2 + 2b\, v + c}}$$

$$- \frac{b\, e\, \gamma}{\gamma^4 + b^2 e^2} \tanh^{-1} \frac{e\sqrt{a\, v^2 + 2b\, v + c}}{v\, \gamma + e\, \delta}$$

$$\text{or} \quad = \frac{\gamma^3}{\gamma^4 + b^2 e^2} \tan^{-1} \frac{\gamma \sqrt{a\, v^2 + 2b\, v + c}}{\gamma^2 - b\, v}$$

$$- \frac{b\, e\, \gamma}{\gamma^4 + b^2 e^2} \tanh^{-1} \frac{v\, \gamma + e\, \delta}{e\sqrt{a\, v^2 + 2b\, v + c}}$$

where γ and δ are defined as before.

Equations (58) and (59) in the text give expressions for the three velocity components, u', v', w', at a point (x', y', z'), induced by a surface distribution of singularities located in the plane $z' = ax'$, and bounded by the x', y' plane and the plane $y' = mx'$. The primed coordinate system has its origin at the apex of this triangular region, with the x' axis parallel to the free stream.

Three velocity functions, P, S, and D, are defined by equation (59) in terms of the variables a', b', ξ', y', and z', where

$$a' = \beta\, a = \beta \tan\alpha$$

$$b' = \frac{1}{\beta\, m} = \frac{\tan\Lambda}{\beta}$$

$$\xi' = x'/\beta$$

and x', y', and z' are given in equation (57).

At points for which $\xi' > \sqrt{y'^2 + z'^2}$, the functions P, S, and D may in turn be expressed most simply in terms of seven auxiliary functions, F1 through F7, as given in equation (37). These functions are rewritten below in terms of the primed variables.

$$F1 = \frac{z' - a'\xi'}{|z' - a'\xi'|}\cos^{-1}\frac{y'(b'y' - \xi') - a'(a'b'y' - z') + b'(z' - a'\xi')^2}{\sqrt{\left[(z' - a'\xi')^2 + (1 - a'^2)y'^2\right]\left[(b'y' - \xi')^2 + b'^2(z' - a'\xi')^2 - (a'b'y' - z')^2\right]}} \tag{1}$$

For $z' = a'\xi'$

$$F1 = \pi \quad \text{for} \quad 0 < y' < \xi'/b'$$

$$= \pi/2 \quad \text{for} \quad y' = 0,\ \xi'/b'$$

$$= 0 \quad \text{for} \quad y' < 0,\ y' > \xi'/b'$$

$$F2 = \frac{1}{\sqrt{b'^2(1 - a'^2) - 1}}\cosh^{-1}\frac{b'\xi' - y' - a'b'z'}{\sqrt{(b'y' - \xi')^2 + b'^2(z' - a'\xi')^2 - (a'b'y' - z')^2}} \tag{2}$$

$$\text{for} \quad b' > 1/\sqrt{1 - a'^2}$$

$$= \frac{\sqrt{\xi'^2 - y'^2 - z'^2}}{\xi' - y} \qquad \text{for} \quad b' = 1/\sqrt{1 - a'^2}$$

$$= \frac{1}{\sqrt{1 - b'^2(1 - a'^2)}} \cos^{-1} \frac{b'\xi' - y' - a'b'z'}{\sqrt{(b'y' - \xi')^2 + b'^2(z' - a'\xi')^2 - (a'b'y' - z')^2}}$$

$$\text{for} \quad b' < 1/\sqrt{1 - a'^2} \, .$$

$$F3 = \frac{z' - a'b'y'}{|z' - a'b'y'|} \cos^{-1} \frac{-\xi'(y' + a'b'z') + b'(y'^2 + z'^2)}{\sqrt{(y'^2 + z'^2)\,(b'y' - \xi')^2 + b'^2(z' - a'\xi')^2 - (a'b'y' - z')^2}} \tag{3}$$

For $z' = a'b'y'$

$$\begin{aligned} F3 &= \pi && \text{for} \quad 0 < y' < \xi'/b' \\ &= \pi/2 && \text{for} \quad y' = 0, \quad y' = \xi'/b' \\ &= 0 && \text{for} \quad y' < 0, \quad y' > \xi'/b' \end{aligned}$$

For $z' = y' = 0$

$$F3 = F1 = -\cos^{-1} \frac{a'b'}{\sqrt{1 + a'^2 b'^2}}$$

$$\begin{aligned} F4 &= F3 - (1 + a'^2 b'^2)\, F1 && \text{for} \quad y' < 0 \\ &= -a'^2 b'^2\, F3 && \text{for} \quad y' = 0 \\ &= F3 - (1 + a'^2 b'^2)\,(F1 + 2\pi) && \text{for} \quad y' > 0, \\ & && \text{and} \quad a'b'y' < z' < a'\xi' \\ &= -(1 + a'^2 b'^2)\,(F1 + \pi) && \text{for} \quad y' > 0, \\ & && \text{and} \quad a'b'y' = z' < a'\xi' \end{aligned} \tag{4}$$

$$F5 = \cosh^{-1} \frac{\xi'}{\sqrt{y'^2 + z'^2}} \tag{5}$$

$$F6 = \sqrt{1 - a'^2} \quad \cosh^{-1} \frac{\xi' - a'z'}{\sqrt{(z' - a'\xi')^2 + (1 - a'^2)\, y'^2}} \tag{6}$$

$$F7 = F5 - (1 + a'^2 b'^2)\, F6 \tag{7}$$

For surface distributions of vorticity (constant pressure surfaces), the velocity functions may now be expressed in terms of these seven auxiliary functions, as follows, provided $\xi' > \sqrt{y'^2 + z'^2}$ and $a' > 0$:

$$P = -\frac{F1}{\pi}$$

$$S = \frac{a'b'\left[b'^2(1 - a'^2) - 1\right] F2 + b' \, F3 + F7/a'}{\pi(1 + a'^2 b'^2)}$$

$$D = -\frac{\left[b'^2(1 - a'^2) - 1\right] F2 - b' \, F5 + F4/a'}{\pi(1 + a'^2 b'^2)}$$

If $a' = 0$, the same expressions apply, except

$$F4/a' \longrightarrow \frac{y'}{y'^2 + z'^2} \sqrt{\xi'^2 - (y'^2 + z'^2)}$$

$$F7/a' \longrightarrow \frac{z'}{y'^2 + z'^2} \sqrt{\xi'^2 - (y'^2 + z'^2)}$$

If $a' < 0$, the velocity functions are the same as for $a' > 0$, except that a' is replaced by $-a'$, z' is replaced by $-z'$, and D by $-D$. In addition, $P = -P$ if $z = a'\xi'$, for $a' < 0$.

For $\xi' \leq \sqrt{y'^2 + z'^2}$, the functions P, S, and D are zero except within the envelope of the Mach cones from the leading edge for the supersonic leading-edge case (that is, $b' < 1/\sqrt{1 - a'^2}$).

In this case, for $\xi' = \dfrac{b'(y' + a'b'z') + |z' - a'b'y'| \sqrt{1 - b'^2(1 - a'^2)}}{1 + a'^2 b'^2}$

$$P = \pm \beta/2$$

$$\left.\begin{aligned} S &= \pm \frac{\beta' b'}{2(1 + a'^2 b'^2)} \left(1 \mp a'\sqrt{1 - b'^2(1 - a'^2)}\right) \\ D &= \frac{\beta}{2(1 + a'^2 b'^2)} \left(\pm a'b' + \sqrt{1 - b'^2(1 - a'^2)}\right) \end{aligned}\right\} \begin{aligned} &\text{for} \\ &y' \geq \frac{b'\xi'}{1 + a'^2 b'^2}\left(1 \mp a'\sqrt{1 - b'^2(1 - a'^2)}\right) \\ &\text{or} \\ &y' \leq \xi'/b' \end{aligned}$$

$$P = S = D = 0 \quad \text{for} \quad y' < \frac{b'\xi'}{1 + a'^2 b'^2} \; 1 \mp a'\sqrt{1 - b'^2(1 - a'^2)}$$

$$\text{or} \quad y' > \xi'/b'$$

$$\text{For} \quad \xi' = \frac{b'(y' + a'b'z') + z' - a'b'y' \sqrt{1 - b'^2(1 - a'^2)}}{1 + a'^2 b'^2}$$

$$\text{and} \quad \xi'/b' = y' = \frac{b' \xi'}{1 + a'^2 b'^2} \left(1 \mp a' \sqrt{1 - b'^2(1 - a'^2)}\right)$$

$$P = \beta \qquad \text{for } z' \geq a' \xi'$$

$$= -\beta \qquad \text{for } z' < a' \xi'$$

$$\left.\begin{aligned} S &= \frac{\beta b'}{1 + a'^2 b'^2}\left(1 - a'\sqrt{1 - b'^2(1 - a'^2)}\right) \\ D &= \frac{\beta}{1 + a'^2 b'^2}\left(a'b' + \sqrt{1 - b'^2(1 - a'^2)}\right) \end{aligned}\right\} \quad \text{for} \quad z' > a'b'y'$$

$$\left.\begin{aligned} S &= \frac{-\beta b'}{1 + a'^2 b'^2}\left(1 + a'\sqrt{1 - b'^2(1 - a'^2)}\right) \\ D &= \frac{\beta}{1 + a'^2 b'^2}\left(-a'b' + \sqrt{1 - b'^2(1 - a'^2)}\right) \end{aligned}\right\} \quad \text{for} \quad z' < a'b'y'$$

$$\left.\begin{aligned} S &= \frac{-\beta a'b'}{1 + a'^2 b'^2}\sqrt{1 - b'^2(1 - a'^2)} \\ D &= \frac{\beta}{1 + a'^2 b'^2}\sqrt{1 - b'^2(1 - a'^2)} \end{aligned}\right\} \quad \text{for} \quad z' = a'b'y'$$

The geometry of this case is illustrated in the sketch in the following page

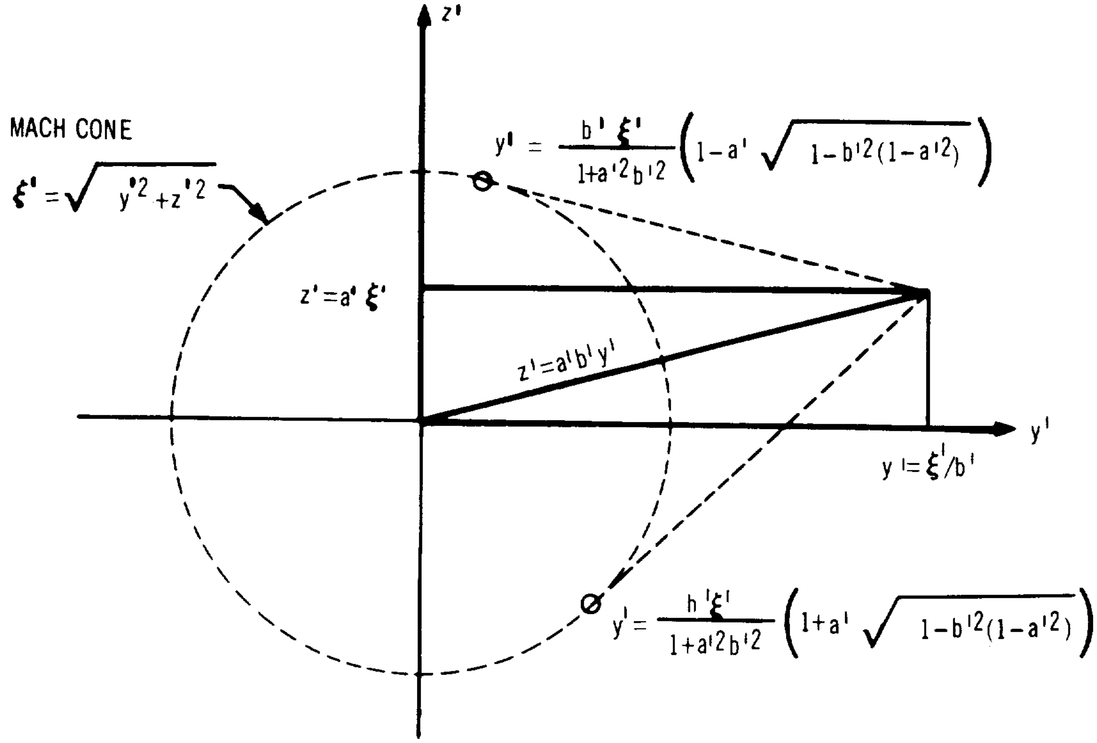

ENVELOPE OF MACH CONES FROM LEADING EDGE:

$$\xi' = \frac{b'(y'+a'b'z') + |z' - a'b'y'| \sqrt{1-b'^2(1-a'^2)}}{1+a'^2b'^2}$$

For surface distributions of sources, the velocity components are required only for the case $a' = 0$. Then, for $\xi' > \sqrt{y'^2 + z'^2}$

$$P = -\frac{F2}{\beta\,\pi}$$

$$S = \frac{1}{\beta\,\pi}\,(b'\ F2 - F5)$$

$$D = \frac{F1}{\beta\,\pi}$$

For $\xi' \leq \sqrt{y'^2 + z'^2}$, the functions are all zero except within the envelope of the Mach cones from the leading edge of the supersonic leading-edge case, $b' < 1$.

In this case, for $\xi' = b'y' + |z'| \sqrt{1 - b'^2}$

$$\left.\begin{aligned} P &= \frac{1}{2\sqrt{1 - b'^2}} \\ S &= \frac{b'}{2\sqrt{1 - b'^2}} \\ D &= \pm \frac{1}{2} \end{aligned}\right\} \quad \begin{aligned} y' &\geq b'\xi' \\ y' &\leq \xi'/b' \end{aligned}$$

$$P = S = D = 0 \quad \text{for} \quad y' < b'\xi', \quad \text{or} \quad y' > \xi'/b'$$

For $\xi' > b'y' + z' \sqrt{1 - b'^2}$

and $\xi'/b' > y' b' \xi'$

$$P = \frac{1}{\sqrt{1 - b'^2}}$$

$$S = \frac{b'}{2\sqrt{1 - b'^2}}$$

$$D = \pm 1$$

where the upper sign corresponds to $z \geq 0$.

9.3 Appendix C - Sample Wing-Body Case Printout

A sample printout is given here for the wing optimization of the Boeing wind-tunnel model described in section 6.4 A comparison between the planar and optimized wing cases is presented in section 7.0.

The uniform panel layout used for this example is shown in the upper sketch on figure 40.

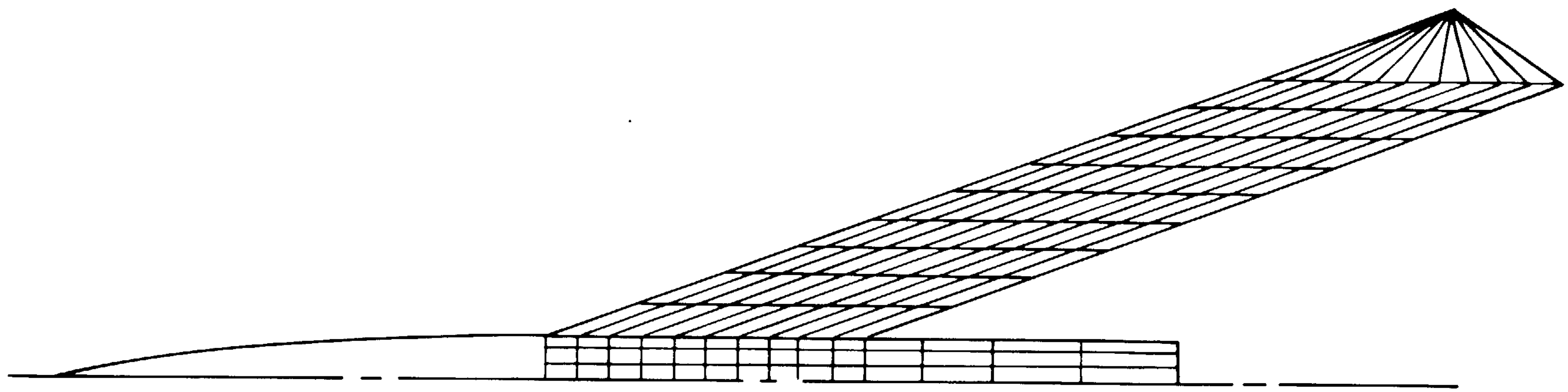

REVISED PANELING WITH CONSTANT WIDTH PANELS;
OPTIMIZATION SATISFACTORY EXCEPT AT TIP.

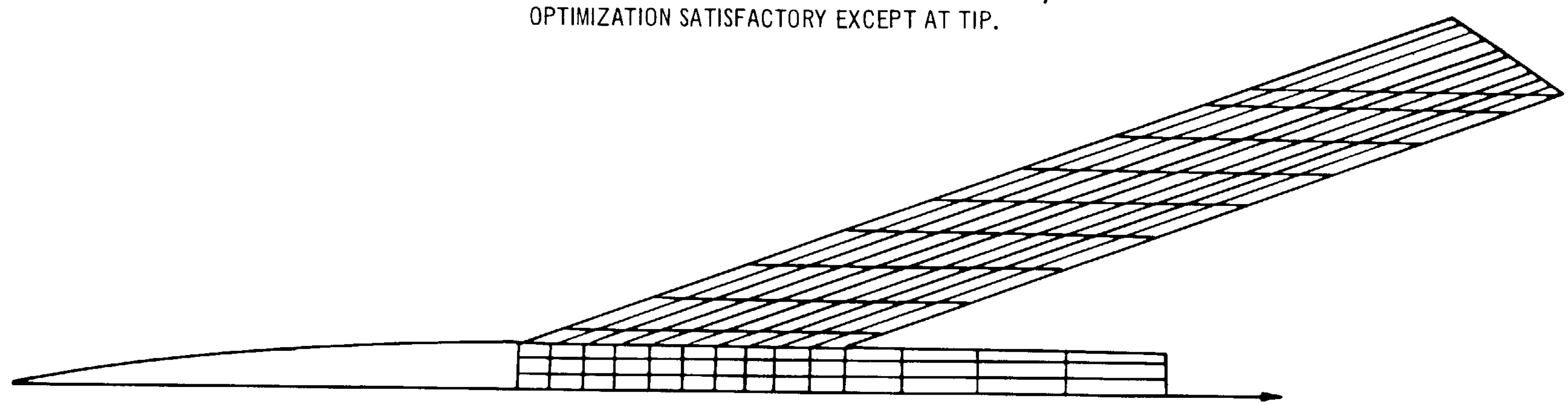

ORIGINAL PANEL WITH UNEVEN WIDTH PANELS; UNSATISFACTORY OPTIMIZATION
(PANEL WIDTHS CHOSEN TO MATCH MODEL PRESSURE TAP LOCATIONS)

FIGURE 40 COMPARISON OF PANELING SCHEMES TESTED FOR WING OPTIMIZATION

```
DATA CARDS ARE LISTED BELOW

DEFINE                                                                    1D
BODY                                                                      2D
TR-805 EQUIVALENT BODY                                                    3D
24.       8.                                                              4D
0.        25.       50.       75.       102.19    130.                    5D
155.      180.                                                            5D
0.                            2.        0.                                6D
1.5                           2.        .270                              6D
3.                            2.        .4464                             6D
4.5                           2.        .5943                             6D
6.                            2.        .7234                             6D
7.5                           2.        .837                              6D
9.                            2.        .9364                             6D
10.5                          2.        1.0223                            6D
12.                           2.        1.0936                            6D
13.5                          2.        1.1479                            6D
15.                           2.        1.184                             6D
15.1                          0.                                          6D
17.5                          0.                                          6D
20.                           0.                                          6D
22.5                          0.                                          6D
25.                           0.                                          6D
27.5                          0.                                          6D
29.9                          0.                                          6D
31.                           2.        1.174                             6D
32.                           2.        1.154                             6D
33.                           2.        1.124                             6D
34.                           2.        1.084                             6D
35.                           2.        1.034                             6D
36.                           2.        1.                                6D
WING                                                                      10D
TR-805 WING (WCP=-.25)                                                    11D
2.        3.        4.        11.       1.                                12D
1.        1.                                                              13D
10.67     0.        40.27     10.774                                      14D
19.88     0.        43.518    8.603     40.27     10.774                  15D
3.                  0.        0.        2.                                16D
0.        -.25      9.21      -.25                                        17D
1.        0.        5.                                                    16D
3.                  8.603     8.603     2.                                16D
0.        -.25      9.21      -.25                                        17D
3.                  10.774    10.774    2.                                16D
0.        -.25      0.        -.25                                        17D
0.        10.       20.       30.       40.       50.                     18D
60.       70.       80.       90.       100.                              18D
WBX                                                                       19D
2.        .0001                                                           20D
DEFEND                                                                    22D
PANEL                                                                     1P
50.       0.        1.        1.        .001                              2P
.95       0.                                                              3P
BODY PANEL                                                                4P
4.        11.       .02                                                   5P
```

```
25.        27.        29.5       32.415                                      6P
1.         2.         3.         4.         5.         6.                    7P
7.         8.         9.         10.        11.                              7P
WING PANEL                                                                   8P
10.        1.         1.         .05                                         9P
1.9846     2.8119     3.6392     4.4665     5.2938     6.1211                10P
6.9484     7.7757     8.603                                                  10P
0.         40.27      10.774     40.27      10.774                           11P
15.                                                                          12P
0.         0.         .025       .0108      .05        .01556                12P
.1         .02155     .15        .02548     .2         .02832                12P
.3         .03215     .4         .0342      .5         .03385                12P
.6         .03112     .7         .02599     .8         .01915                12P
.9         .01084     .95        .00616     1.         0.                    12P
15.                                                                          13P
0.         0.         .025       -.00257    .05        -.00325               13P
.1         -.00428    .15        -.0051     .2         -.00581               13P
.3         -.00701    .4         -.00735    .5         -.0065                13P
.6         -.00469    .7         -.00239    .8         -.00068               13P
.9         0.         .95        0.         1.         0.                    13P
PANEND                                                                       14P
AERODYNAMIC                                                                  1A
1.8        1.                                                                2A
TR-805 MIN DRAG CLBAR=.159                                                   3A
3.         0.         0.         1.         1.                               4A
89.375     0.         0.                                                     5A
TR-805     BODY CAMBER                                                       6A
0.         .025       .043       .056       .068       .079       .089       6A
.099       .108       .1165      .125       .134       .142       .148       6A
.156       .162       .167       .172       .175       .178       .180       6A
.179       .1779      .1768      .1757      .1746      .1735      .1724      6A
.1713      .1702      .1691      .168       .1679      .1668      .1657      6A
.1646      .1635      .1624      .1613      .1602      .1591      .158       6A
.1569      .1558      .1547      .1536      .1525      .1514      .1503      6A
.1492                                                                        6A
0.         .159                                                              9A
                                                                             11A
                                                                             11A
```

AUG 23, 1965

BODY RADIUS AND Z-COORDINATE OF BODY CENTROID VERSUS X-PRIME

NO.	X-PRIME	RADIUS	Z-PRIME
1	0.	0.	0.
2	0.7243	0.1304	0.
3	1.4485	0.2607	0.
4	2.1728	0.3491	0.
5	2.8970	0.4343	0.
6	3.6213	0.5077	0.
7	4.3456	0.5791	0.
8	5.0698	0.6433	0.
9	5.7941	0.7057	0.
10	6.5184	0.7627	0.
11	7.2426	0.8175	0.
12	7.9669	0.8679	0.
13	8.6911	0.9159	0.
14	9.4154	0.9602	0.
15	10.1397	1.0017	0.
16	10.8639	1.0396	0.
17	11.5882	1.0740	0.
18	12.3124	1.1049	0.
19	13.0367	1.1311	0.
20	13.7610	1.1542	0.
21	14.5023	1.1720	0.
22	15.2436	1.1840	0.
23	15.9849	1.1840	0.
24	16.7262	1.1840	0.
25	17.4675	1.1840	0.
26	18.2088	1.1840	0.
27	18.9501	1.1840	0.
28	19.6914	1.1840	0.
29	20.4327	1.1840	0.
30	21.1740	1.1840	0.
31	21.9153	1.1840	0.
32	22.6566	1.1840	0.
33	23.3979	1.1840	0.
34	24.1392	1.1840	0.
35	24.8805	1.1840	0.
36	25.6218	1.1840	0.
37	26.3631	1.1840	0.
38	27.1044	1.1840	0.
39	27.8457	1.1840	0.
40	28.5870	1.1840	0.
41	29.3283	1.1840	0.
42	30.0696	1.1825	0.
43	30.8109	1.1757	0.
44	31.5522	1.1630	0.
45	32.2935	1.1452	0.
46	33.0348	1.1226	0.
47	33.7761	1.0930	0.
48	34.5174	1.0581	0.
49	35.2587	1.0252	0.
50	36.0000	1.0000	0.

BODY PANEL

BODY PANEL CORNER POINT COORDINATES
1 AND 2 INDICATE BODY PANEL LEADING-EDGE POINTS, 3 AND 4 INDICATE TRAILING-EDGE POINTS

PANEL NO	PARTS	X_1	Y_1	Z_1	X_2	Y_2	Z_2	X_3	Y_3	Z_3	X_4	Y_4	Z_4
1	1	13.76097	0.	1.15418	13.76097	0.48778	1.04604	14.75289	0.00504	1.17693	14.75289	0.49282	1.06880
2	1	14.75289	0.	1.17805	14.75289	0.49787	1.06768	15.69159	0.00126	1.18372	15.69159	0.49912	1.07335
3	1	15.69159	0.	1.18400	15.69159	0.50038	1.07307	16.61262	0.	1.18400	16.61262	0.50038	1.07307
4	1	16.61262	0.	1.18400	16.61262	0.50038	1.07307	17.53366	0.	1.18400	17.53366	0.50038	1.07307
5	1	17.53366	0.	1.18400	17.53366	0.50038	1.07307	18.45469	0.	1.18400	18.45469	0.50038	1.07307
6	1	18.45469	0.	1.18400	18.45469	0.50038	1.07307	19.37572	0.	1.18400	19.37572	0.50038	1.07307
7	1	19.37572	0.	1.18400	19.37572	0.50038	1.07307	20.29676	0.	1.18400	20.29676	0.50038	1.07307
8	1	20.29676	0.	1.18400	20.29676	0.50038	1.07307	21.21779	0.	1.18400	21.21779	0.50038	1.07307
9	1	21.21779	0.	1.18400	21.21779	0.50038	1.07307	22.13882	0.	1.18400	22.13882	0.50038	1.07307
10	1	22.13882	0.	1.18400	22.13882	0.50038	1.07307	23.05986	0.	1.18400	23.05986	0.50038	1.07307
11	1	23.05986	0.	1.18400	23.05986	0.50038	1.07307	25.00000	0.	1.18400	25.00000	0.50038	1.07307
12	1	25.00000	0.	1.18400	25.00000	0.50038	1.07307	27.00000	0.	1.18400	27.00000	0.50038	1.07307
13	1	27.00000	0.	1.18400	27.00000	0.50038	1.07307	29.50000	0.	1.18400	29.50000	0.50038	1.07307
14	1	29.50000	0.00897	1.18201	29.50000	0.49141	1.07506	32.41500	0.	1.14155	32.41500	0.48244	1.03460
15	1	13.76097	0.48778	1.04604	13.76097	0.88415	0.74189	14.75289	0.50197	1.06453	14.75289	0.89834	0.76038
16	1	14.75289	0.49787	1.06768	14.75289	0.90244	0.75724	15.69159	0.50140	1.07228	15.69159	0.90598	0.76184
17	1	15.69159	0.50038	1.07307	15.69159	0.90700	0.76106	16.61262	0.50038	1.07307	16.61262	0.90700	0.76106
18	1	16.61262	0.50038	1.07307	16.61262	0.90700	0.76106	17.53366	0.50038	1.07307	17.53366	0.90700	0.76106
19	1	17.53366	0.50038	1.07307	17.53366	0.90700	0.76106	18.45469	0.50038	1.07307	18.45469	0.90700	0.76106
20	1	18.45469	0.50038	1.07307	18.45469	0.90700	0.76106	19.37572	0.50038	1.07307	19.37572	0.90700	0.76106
21	1	19.37572	0.50038	1.07307	19.37572	0.90700	0.76106	20.29676	0.50038	1.07307	20.29676	0.90700	0.76106
22	1	20.29676	0.50038	1.07307	20.29676	0.90700	0.76106	21.21779	0.50038	1.07307	21.21779	0.90700	0.76106
23	1	21.21779	0.50038	1.07307	21.21779	0.90700	0.76106	22.13882	0.50038	1.07307	22.13882	0.90700	0.76106
24	1	22.13882	0.50038	1.07307	22.13882	0.90700	0.76106	23.05986	0.50038	1.07307	23.05986	0.90700	0.76106
25	1	23.05986	0.50038	1.07307	23.05986	0.90700	0.76106	25.00000	0.50038	1.07307	25.00000	0.90700	0.76106
26	1	25.00000	0.50038	1.07307	25.00000	0.90700	0.76106	27.00000	0.50038	1.07307	27.00000	0.90700	0.76106
27	1	27.00000	0.50038	1.07307	27.00000	0.90700	0.76106	29.50000	0.50038	1.07307	29.50000	0.90700	0.76106
28	1	29.50000	0.50767	1.06748	29.50000	0.89971	0.76665	32.41500	0.48244	1.03460	32.41500	0.87448	0.73377
29	1	13.76097	0.88415	0.74189	13.76097	1.11485	0.29872	14.75289	0.90483	0.75265	14.75289	1.13553	0.30949
30	1	14.75289	0.90244	0.75724	14.75289	1.13791	0.30490	15.69159	0.90759	0.75992	15.69159	1.14306	0.30758
31	1	15.69159	0.90700	0.76106	15.69159	1.14366	0.30644	16.61262	0.90700	0.76106	16.61262	1.14366	0.30644
32	1	16.61262	0.90700	0.76106	16.61262	1.14366	0.30644	17.53366	0.90700	0.76106	17.53366	1.14366	0.30644
33	1	17.53366	0.90700	0.76106	17.53366	1.14366	0.30644	18.45469	0.90700	0.76106	18.45469	1.14366	0.30644
34	1	18.45469	0.90700	0.76106	18.45469	1.14366	0.30644	19.37572	0.90700	0.76106	19.37572	1.14366	0.30644
35	1	19.37572	0.90700	0.76106	19.37572	1.14366	0.30644	20.29676	0.90700	0.76106	20.29676	1.14366	0.30644
36	1	20.29676	0.90700	0.76106	20.29676	1.14366	0.30644	21.21779	0.90700	0.76106	21.21779	1.14366	0.30644
37	1	21.21779	0.90700	0.76106	21.21779	1.14366	0.30644	22.13882	0.90700	0.76106	22.13882	1.14366	0.30644
38	1	22.13882	0.90700	0.76106	22.13882	1.14366	0.30644	23.05986	0.90700	0.76106	23.05986	1.14366	0.30644
39	1	23.05986	0.90700	0.76106	23.05986	1.14366	0.30644	25.00000	0.90700	0.76106	25.00000	1.14366	0.30644
40	1	25.00000	0.90700	0.76106	25.00000	1.14366	0.30644	27.00000	0.90700	0.76106	27.00000	1.14366	0.30644
41	1	27.00000	0.90700	0.76106	27.00000	1.14366	0.30644	29.50000	0.90700	0.76106	29.50000	1.14366	0.30644
42	1	29.50000	0.91124	0.75291	29.50000	1.13941	0.31459	32.41500	0.87448	0.73377	32.41500	1.10265	0.29545
43	1	13.76097	1.11485	0.29872	13.76097	1.12816	-0.24371	14.75289	1.13805	0.29929	14.75289	1.15135	-0.24314
44	1	14.75289	1.13791	0.30490	14.75289	1.15149	-0.24875	15.69159	1.14369	0.30504	15.69159	1.15727	-0.24861
45	1	15.69159	1.14366	0.30644	15.69159	1.15730	-0.25001	16.61262	1.14366	0.30644	16.61262	1.15730	-0.25001
46	1	16.61262	1.14366	0.30644	16.61262	1.15730	-0.25001	17.53366	1.14366	0.30644	17.53366	1.15730	-0.25001
47	1	17.53366	1.14366	0.30644	17.53366	1.15730	-0.25001	18.45469	1.14366	0.30644	18.45469	1.15730	-0.25001
48	1	18.45469	1.14366	0.30644	18.45469	1.15730	-0.25001	19.37572	1.14366	0.30644	19.37572	1.15730	-0.25001
49	1	19.37572	1.14366	0.30644	19.37572	1.15730	-0.25001	20.29676	1.14366	0.30644	20.29676	1.15730	-0.25001
50	1	20.29676	1.14366	0.30644	20.29676	1.15730	-0.25001	21.21779	1.14366	0.30644	21.21779	1.15730	-0.25001
51	1	21.21779	1.14366	0.30644	21.21779	1.15730	-0.25001	22.13882	1.14366	0.30644	22.13882	1.15730	-0.25001
52	1	22.13882	1.14366	0.30644	22.13882	1.15730	-0.25001	23.05986	1.14366	0.30644	23.05986	1.15730	-0.25001

53	1	23.05986	1.14366	0.30644	23.05986	1.15730	-0.25001	25.00000	1.14366	0.30644	25.00000	1.15730	-0.25001
54	1	25.00000	1.14366	0.30644	25.00000	1.15730	-0.25001	27.00000	1.14366	0.30644	27.00000	1.15730	-0.25001
55	1	27.00000	1.14366	0.30644	27.00000	1.15730	-0.25001	29.50000	1.14366	0.30644	29.50000	1.15730	-0.25001
56	1	29.50000	1.14390	0.29647	29.50000	1.15706	-0.24003	32.41500	1.10265	0.29545	32.41500	1.11581	-0.24104
57	1	13.76097	1.12816	-0.24371	13.76097	0.88415	-0.74189	14.75289	1.14897	-0.25390	14.75289	0.90496	-0.75209
58	1	14.75289	1.15149	-0.24875	14.75289	0.90244	-0.75724	15.69159	1.15668	-0.25129	15.69159	0.90763	-0.75978
59	1	15.69159	1.15730	-0.25001	15.69159	0.90700	-0.76106	16.61262	1.15730	-0.25001	16.61262	0.90700	-0.76106
60	1	16.61262	1.15730	-0.25001	16.61262	0.90700	-0.76106	17.53366	1.15730	-0.25001	17.53366	0.90700	-0.76106
61	1	17.53366	1.15730	-0.25001	17.53366	0.90700	-0.76106	18.45469	1.15730	-0.25001	18.45469	0.90700	-0.76106
62	1	18.45469	1.15730	-0.25001	18.45469	0.90700	-0.76106	19.37572	1.15730	-0.25001	19.37572	0.90700	-0.76106
63	1	19.37572	1.15730	-0.25001	19.37572	0.90700	-0.76106	20.29676	1.15730	-0.25001	20.29676	0.90700	-0.76106
64	1	20.29676	1.15730	-0.25001	20.29676	0.90700	-0.76106	21.21779	1.15730	-0.25001	21.21779	0.90700	-0.76106
65	1	21.21779	1.15730	-0.25001	21.21779	0.90700	-0.76106	22.13882	1.15730	-0.25001	22.13882	0.90700	-0.76106
66	1	22.13882	1.15730	-0.25001	22.13882	0.90700	-0.76106	23.05986	1.15730	-0.25001	23.05986	0.90700	-0.76106
67	1	23.05986	1.15730	-0.25001	23.05986	0.90700	-0.76106	25.00000	1.15730	-0.25001	25.00000	0.90700	-0.76106
68	1	25.00000	1.15730	-0.25001	25.00000	0.90700	-0.76106	27.00000	1.15730	-0.25001	27.00000	0.90700	-0.76106
69	1	27.00000	1.15730	-0.25001	27.00000	0.90700	-0.76106	29.50000	1.15730	-0.25001	29.50000	0.90700	-0.76106
70	1	29.50000	1.15282	-0.25917	29.50000	0.91148	-0.75190	32.41500	1.11581	-0.24104	32.41500	0.87448	-0.73377
71	1	13.76097	0.88415	-0.74189	13.76097	0.48778	-1.04604	14.75289	0.89834	-0.76038	14.75289	0.50197	-1.06453
72	1	14.75289	0.90244	-0.75724	14.75289	0.49787	-1.06768	15.69159	0.90598	-0.76184	15.69159	0.50140	-1.07228
73	1	15.69159	0.90700	-0.76106	15.69159	0.50038	-1.07307	16.61262	0.90700	-0.76106	16.61262	0.50038	-1.07307
74	1	16.61262	0.90700	-0.76106	16.61262	0.50038	-1.07307	17.53366	0.90700	-0.76106	17.53366	0.50038	-1.07307
75	1	17.53366	0.90700	-0.76106	17.53366	0.50038	-1.07307	18.45469	0.90700	-0.76106	18.45469	0.50038	-1.07307
76	1	18.45469	0.90700	-0.76106	18.45469	0.50038	-1.07307	19.37572	0.90700	-0.76106	19.37572	0.50038	-1.07307
77	1	19.37572	0.90700	-0.76106	19.37572	0.50038	-1.07307	20.29676	0.90700	-0.76106	20.29676	0.50038	-1.07307
78	1	20.29676	0.90700	-0.76106	20.29676	0.50038	-1.07307	21.21779	0.90700	-0.76106	21.21779	0.50038	-1.07307
79	1	21.21779	0.90700	-0.76106	21.21779	0.50038	-1.07307	22.13882	0.90700	-0.76106	22.13882	0.50038	-1.07307
80	1	22.13882	0.90700	-0.76106	22.13882	0.50038	-1.07307	23.05986	0.90700	-0.76106	23.05986	0.50038	-1.07307
81	1	23.05986	0.90700	-0.76106	23.05986	0.50038	-1.07307	25.00000	0.90700	-0.76106	25.00000	0.50038	-1.07307
82	1	25.00000	0.90700	-0.76106	25.00000	0.50038	-1.07307	27.00000	0.90700	-0.76106	27.00000	0.50038	-1.07307
83	1	27.00000	0.90700	-0.76106	27.00000	0.50038	-1.07307	29.50000	0.90700	-0.76106	29.50000	0.50038	-1.07307
84	1	29.50000	0.89971	-0.76665	29.50000	0.50767	-1.06748	32.41500	0.87448	-0.73377	32.41500	0.48244	-1.03460
85	1	13.76097	0.48778	-1.04604	13.76097	0.	-1.15418	14.75289	0.49282	-1.06880	14.75289	0.00504	-1.17693
86	1	14.75289	0.49787	-1.06768	14.75289	0.	-1.17805	15.69159	0.49912	-1.07335	15.69159	0.00126	-1.18372
87	1	15.69159	0.50038	-1.07307	15.69159	0.	-1.18400	16.61262	0.50038	-1.07307	16.61262	0.	-1.18400
88	1	16.61262	0.50038	-1.07307	16.61262	0.	-1.18400	17.53366	0.50038	-1.07307	17.53366	0.	-1.18400
89	1	17.53366	0.50038	-1.07307	17.53366	0.	-1.18400	18.45469	0.50038	-1.07307	18.45469	0.	-1.18400
90	1	18.45469	0.50038	-1.07307	18.45469	0.	-1.18400	19.37572	0.50038	-1.07307	19.37572	0.	-1.18400
91	1	19.37572	0.50038	-1.07307	19.37572	0.	-1.18400	20.29676	0.50038	-1.07307	20.29676	0.	-1.18400
92	1	20.29676	0.50038	-1.07307	20.29676	0.	-1.18400	21.21779	0.50038	-1.07307	21.21779	0.	-1.18400
93	1	21.21779	0.50038	-1.07307	21.21779	0.	-1.18400	22.13882	0.50038	-1.07307	22.13882	0.	-1.18400
94	1	22.13882	0.50038	-1.07307	22.13882	0.	-1.18400	23.05986	0.50038	-1.07307	23.05986	0.	-1.18400
95	1	23.05986	0.50038	-1.07307	23.05986	0.	-1.18400	25.00000	0.50038	-1.07307	25.00000	0.	-1.18400
96	1	25.00000	0.50038	-1.07307	25.00000	0.	-1.18400	27.00000	0.50038	-1.07307	27.00000	0.	-1.18400
97	1	27.00000	0.50038	-1.07307	27.00000	0.	-1.18400	29.50000	0.50038	-1.07307	29.50000	0.	-1.18400
98	1	29.50000	0.49141	-1.07506	29.50000	0.00897	-1.18201	32.41500	0.48244	-1.03460	32.41500	0.	-1.14155

BODY PANEL CENTROID AND CONTROL POINT COORDINATES

PANEL	X_C	Y_C	Z_C	X_{CP}	Y_{CP}	Z_{CP}	AREA	THETA-INCLIN	ALPHA-INCID
1	14.25863	0.24642	1.11153	14.70330	0.24868	1.12173	0.50085	-0.21817	0.02349
2	15.22264	0.24956	1.12570	15.64465	0.25013	1.12825	0.47991	-0.21817	0.00619
3	16.15210	0.25019	1.12853	16.56657	0.25019	1.12853	0.47206	-0.21817	0.
4	17.07314	0.25019	1.12853	17.48760	0.25019	1.12853	0.47206	-0.21817	0.
5	17.99417	0.25019	1.12853	18.40864	0.25019	1.12853	0.47206	-0.21817	0.
6	18.91521	0.25019	1.12853	19.32967	0.25019	1.12853	0.47206	-0.21817	0.
7	19.83624	0.25019	1.12853	20.25070	0.25019	1.12853	0.47206	-0.21817	0.
8	20.75727	0.25019	1.12853	21.17174	0.25019	1.12853	0.47206	-0.21817	0.
9	21.67831	0.25019	1.12853	22.09277	0.25019	1.12853	0.47206	-0.21817	0.
10	22.59934	0.25019	1.12853	23.01381	0.25019	1.12853	0.47206	-0.21817	0.
11	24.02993	0.25019	1.12853	24.90299	0.25019	1.12853	0.99438	-0.21817	0.
12	26.00000	0.25019	1.12853	26.90000	0.25019	1.12853	1.02506	-0.21817	0.
13	28.25000	0.25019	1.12853	29.37500	0.25019	1.12853	1.28132	-0.21817	0.
14	30.94863	0.24573	1.10843	32.26925	0.24167	1.09010	1.46739	-0.21817	-0.01422
15	14.25863	0.69308	0.90324	14.70330	0.69944	0.91153	0.50085	-0.65450	0.02349
16	15.22264	0.70192	0.91476	15.64465	0.70351	0.91683	0.47991	-0.65450	0.00619
17	16.15210	0.70369	0.91706	16.56657	0.70369	0.91706	0.47206	-0.65450	0.
18	17.07314	0.70369	0.91706	17.48760	0.70369	0.91706	0.47206	-0.65450	0.
19	17.99417	0.70369	0.91706	18.40864	0.70369	0.91706	0.47206	-0.65450	0.
20	18.91521	0.70369	0.91706	19.32967	0.70369	0.91706	0.47206	-0.65450	0.
21	19.83624	0.70369	0.91706	20.25070	0.70369	0.91706	0.47206	-0.65450	0.
22	20.75727	0.70369	0.91706	21.17174	0.70369	0.91706	0.47206	-0.65450	0.
23	21.67831	0.70369	0.91706	22.09277	0.70369	0.91706	0.47206	-0.65450	0.
24	22.59934	0.70369	0.91706	23.01381	0.70369	0.91706	0.47206	-0.65450	0.
25	24.02993	0.70369	0.91706	24.90299	0.70369	0.91706	0.99438	-0.65450	0.
26	26.00000	0.70369	0.91706	26.90000	0.70369	0.91706	1.02506	-0.65450	0.
27	28.25000	0.70369	0.91706	29.37500	0.70369	0.91706	1.28132	-0.65450	0.
28	30.94863	0.69115	0.90072	32.26925	0.67972	0.88583	1.46739	-0.65450	-0.01422
29	14.25863	1.00988	0.52571	14.70330	1.01914	0.53053	0.50085	-1.09083	0.02349
30	15.22264	1.02275	0.53241	15.64465	1.02507	0.53362	0.47991	-1.09083	0.00619
31	16.15210	1.02533	0.53375	16.56657	1.02533	0.53375	0.47206	-1.09083	0.
32	17.07314	1.02533	0.53375	17.48760	1.02533	0.53375	0.47206	-1.09083	0.
33	17.99417	1.02533	0.53375	18.40864	1.02533	0.53375	0.47206	-1.09083	0.
34	18.91521	1.02533	0.53375	19.32967	1.02533	0.53375	0.47206	-1.09083	0.
35	19.83624	1.02533	0.53375	20.25070	1.02533	0.53375	0.47206	-1.09083	0.
36	20.75727	1.02533	0.53375	21.17174	1.02533	0.53375	0.47206	-1.09083	0.
37	21.67831	1.02533	0.53375	22.09277	1.02533	0.53375	0.47206	-1.09083	0.
38	22.59934	1.02533	0.53375	23.01381	1.02533	0.53375	0.47206	-1.09083	0.
39	24.02993	1.02533	0.53375	24.90299	1.02533	0.53375	0.99438	-1.09083	0.
40	26.00000	1.02533	0.53375	26.90000	1.02533	0.53375	1.02506	-1.09083	0.
41	28.25000	1.02533	0.53375	29.37500	1.02533	0.53375	1.28132	-1.09083	0.
42	30.94863	1.00706	0.52424	32.26925	0.99040	0.51557	1.46739	-1.09083	-0.01422
43	14.25863	1.13314	0.02779	14.70330	1.14354	0.02805	0.54393	-1.54627	0.02339
44	15.22264	1.14759	0.02815	15.64465	1.15019	0.02821	0.52119	-1.54627	0.00616
45	16.15210	1.15048	0.02822	16.56657	1.15048	0.02822	0.51266	-1.54627	0.
46	17.07314	1.15048	0.02822	17.48760	1.15048	0.02822	0.51266	-1.54627	0.
47	17.99417	1.15048	0.02822	18.40864	1.15048	0.02822	0.51266	-1.54627	0.
48	18.91521	1.15048	0.02822	19.32967	1.15048	0.02822	0.51266	-1.54627	0.
49	19.83624	1.15048	0.02822	20.25070	1.15048	0.02822	0.51266	-1.54627	0.
50	20.75727	1.15048	0.02822	21.17174	1.15048	0.02822	0.51266	-1.54627	0.
51	21.67831	1.15048	0.02822	22.09277	1.15048	0.02822	0.51266	-1.54627	0.
52	22.59934	1.15048	0.02822	23.01381	1.15048	0.02822	0.51266	-1.54627	0.

53	24.02993	1.15048	0.02822	24.90299	1.15048	0.02822	1.07991	-1.54627	0.
54	26.00000	1.15048	0.02822	26.90000	1.15048	0.02822	1.11323	-1.54627	0.
55	28.25000	1.15048	0.02822	29.37500	1.15048	0.02822	1.39154	-1.54627	0.
56	30.94863	1.12998	0.02771	32.26925	1.11129	0.02726	1.59361	-1.54627	-0.01415
57	14.25863	1.01660	-0.49792	14.70330	1.02593	-0.50248	0.55609	-2.02624	0.02336
58	15.22264	1.02956	-0.50426	15.64465	1.03189	-0.50541	0.53284	-2.02624	0.00615
59	16.15210	1.03215	-0.50553	16.56657	1.03215	-0.50553	0.52412	-2.02624	0.
60	17.07314	1.03215	-0.50553	17.48760	1.03215	-0.50553	0.52412	-2.02624	0.
61	17.99417	1.03215	-0.50553	18.40864	1.03215	-0.50553	0.52412	-2.02624	0.
62	18.91521	1.03215	-0.50553	19.32967	1.03215	-0.50553	0.52412	-2.02624	0.
63	19.83624	1.03215	-0.50553	20.25070	1.03215	-0.50553	0.52412	-2.02624	0.
64	20.75727	1.03215	-0.50553	21.17174	1.03215	-0.50553	0.52412	-2.02624	0.
65	21.67831	1.03215	-0.50553	22.09277	1.03215	-0.50553	0.52412	-2.02624	0.
66	22.59934	1.03215	-0.50553	23.01381	1.03215	-0.50553	0.52412	-2.02624	0.
67	24.02993	1.03215	-0.50553	24.90299	1.03215	-0.50553	1.10406	-2.02624	0.
68	26.00000	1.03215	-0.50553	26.90000	1.03215	-0.50553	1.13812	-2.02624	0.
69	28.25000	1.03215	-0.50553	29.37500	1.03215	-0.50553	1.42265	-2.02624	0.
70	30.94863	1.01376	-0.49653	32.26925	0.99699	-0.48831	1.62924	-2.02624	-0.01413
71	14.25863	0.69308	-0.90324	14.70330	0.69944	-0.91153	0.50085	-2.48709	0.02349
72	15.22264	0.70192	-0.91476	15.64465	0.70351	-0.91683	0.47991	-2.48709	0.00619
73	16.15210	0.70369	-0.91706	16.56657	0.70369	-0.91706	0.47206	-2.48709	0.
74	17.07314	0.70369	-0.91706	17.48760	0.70369	-0.91706	0.47206	-2.48709	0.
75	17.99417	0.70369	-0.91706	18.40864	0.70369	-0.91706	0.47206	-2.48709	0.
76	18.91521	0.70369	-0.91706	19.32967	0.70369	-0.91706	0.47206	-2.48709	0.
77	19.83624	0.70369	-0.91706	20.25070	0.70369	-0.91706	0.47206	-2.48709	0.
78	20.75727	0.70369	-0.91706	21.17174	0.70369	-0.91706	0.47206	-2.48709	0.
79	21.67831	0.70369	-0.91706	22.09277	0.70369	-0.91706	0.47206	-2.48709	0.
80	22.59934	0.70369	-0.91706	23.01381	0.70369	-0.91706	0.47206	-2.48709	0.
81	24.02993	0.70369	-0.91706	24.90299	0.70369	-0.91706	0.99438	-2.48709	0.
82	26.00000	0.70369	-0.91706	26.90000	0.70369	-0.91706	1.02506	-2.48709	0.
83	28.25000	0.70369	-0.91706	29.37500	0.70369	-0.91706	1.28132	-2.48709	0.
84	30.94863	0.69115	-0.90072	32.26925	0.67972	-0.88583	1.46739	-2.48709	-0.01422
85	14.25863	0.24642	-1.11153	14.70330	0.24868	-1.12173	0.50085	-2.92343	0.02349
86	15.22264	0.24956	-1.12570	15.64465	0.25013	-1.12825	0.47991	-2.92343	0.00619
87	16.15210	0.25019	-1.12853	16.56657	0.25019	-1.12853	0.47206	-2.92343	0.
88	17.07314	0.25019	-1.12853	17.48760	0.25019	-1.12853	0.47206	-2.92343	0.
89	17.99417	0.25019	-1.12853	18.40864	0.25019	-1.12853	0.47206	-2.92343	0.
90	18.91521	0.25019	-1.12853	19.32967	0.25019	-1.12853	0.47206	-2.92343	0.
91	19.83624	0.25019	-1.12853	20.25070	0.25019	-1.12853	0.47206	-2.92343	0.
92	20.75727	0.25019	-1.12853	21.17174	0.25019	-1.12853	0.47206	-2.92343	0.
93	21.67831	0.25019	-1.12853	22.09277	0.25019	-1.12853	0.47206	-2.92343	0.
94	22.59934	0.25019	-1.12853	23.01381	0.25019	-1.12853	0.47206	-2.92343	0.
95	24.02993	0.25019	-1.12853	24.90299	0.25019	-1.12853	0.99438	-2.92343	0.
96	26.00000	0.25019	-1.12853	26.90000	0.25019	-1.12853	1.02506	-2.92343	0.
97	28.25000	0.25019	-1.12853	29.37500	0.25019	-1.12853	1.28132	-2.92343	0.
98	30.94863	0.24573	-1.10843	32.26925	0.24167	-1.09010	1.46739	-2.92343	-0.01422

WING PANEL

WING PANEL CORNER POINT COORDINATES
1 AND 2 INDICATE WING PANEL LEADING-EDGE POINTS, 3 AND 4 INDICATE TRAILING-EDGE POINTS

PANEL NO	PARTS	X_1	Y_1	Z_1	X_2	Y_2	Z_2	X_3	Y_3	Z_3	X_4	Y_4	Z_4
1	1	13.83186	1.15087	-0.25001	16.12240	1.98460	-0.25001	14.75289	1.15087	-0.25001	17.04346	1.98460	-0.25001
2	1	14.77055	1.15730	-0.25001	17.04346	1.98460	-0.25001	15.69159	1.15730	-0.25001	17.96452	1.98460	-0.25001
3	1	15.69159	1.15730	-0.25001	17.96452	1.98460	-0.25001	16.61262	1.15730	-0.25001	18.88557	1.98460	-0.25001
4	1	16.61262	1.15730	-0.25001	18.88557	1.98460	-0.25001	17.53366	1.15730	-0.25001	19.80663	1.98460	-0.25001
5	1	17.53366	1.15730	-0.25001	19.80663	1.98460	-0.25001	18.45469	1.15730	-0.25001	20.72769	1.98460	-0.25001
6	1	18.45469	1.15730	-0.25001	20.72769	1.98460	-0.25001	19.37572	1.15730	-0.25001	21.64875	1.98460	-0.25001
7	1	19.37572	1.15730	-0.25001	21.64875	1.98460	-0.25001	20.29676	1.15730	-0.25001	22.56980	1.98460	-0.25001
8	1	20.29676	1.15730	-0.25001	22.56980	1.98460	-0.25001	21.21779	1.15730	-0.25001	23.49086	1.98460	-0.25001
9	1	21.21779	1.15730	-0.25001	23.49086	1.98460	-0.25001	22.13882	1.15730	-0.25001	24.41192	1.98460	-0.25001
10	1	22.13882	1.15730	-0.25001	24.41192	1.98460	-0.25001	23.05986	1.15730	-0.25001	25.33298	1.98460	-0.25001
11	1	16.12240	1.98460	-0.25001	18.39529	2.81190	-0.25001	17.04346	1.98460	-0.25001	19.31637	2.81190	-0.25001
12	1	17.04346	1.98460	-0.25001	19.31637	2.81190	-0.25001	17.96452	1.98460	-0.25001	20.23745	2.81190	-0.25001
13	1	17.96452	1.98460	-0.25001	20.23745	2.81190	-0.25001	18.88557	1.98460	-0.25001	21.15853	2.81190	-0.25001
14	1	18.88557	1.98460	-0.25001	21.15853	2.81190	-0.25001	19.80663	1.98460	-0.25001	22.07961	2.81190	-0.25001
15	1	19.80663	1.98460	-0.25001	22.07961	2.81190	-0.25001	20.72769	1.98460	-0.25001	23.00070	2.81190	-0.25001
16	1	20.72769	1.98460	-0.25001	23.00070	2.81190	-0.25001	21.64875	1.98460	-0.25001	23.92178	2.81190	-0.25001
17	1	21.64875	1.98460	-0.25001	23.92178	2.81190	-0.25001	22.56980	1.98460	-0.25001	24.84286	2.81190	-0.25001
18	1	22.56980	1.98460	-0.25001	24.84286	2.81190	-0.25001	23.49086	1.98460	-0.25001	25.76394	2.81190	-0.25001
19	1	23.49086	1.98460	-0.25001	25.76394	2.81190	-0.25001	24.41192	1.98460	-0.25001	26.68502	2.81190	-0.25001
20	1	24.41192	1.98460	-0.25001	26.68502	2.81190	-0.25001	25.33298	1.98460	-0.25001	27.60611	2.81190	-0.25001
21	1	18.39529	2.81190	-0.25001	20.66817	3.63920	-0.25001	19.31637	2.81190	-0.25001	21.58928	3.63920	-0.25001
22	1	19.31637	2.81190	-0.25001	21.58928	3.63920	-0.25001	20.23745	2.81190	-0.25001	22.51038	3.63920	-0.25001
23	1	20.23745	2.81190	-0.25001	22.51038	3.63920	-0.25001	21.15853	2.81190	-0.25001	23.43149	3.63920	-0.25001
24	1	21.15853	2.81190	-0.25001	23.43149	3.63920	-0.25001	22.07961	2.81190	-0.25001	24.35260	3.63920	-0.25001
25	1	22.07961	2.81190	-0.25001	24.35260	3.63920	-0.25001	23.00070	2.81190	-0.25001	25.27370	3.63920	-0.25001
26	1	23.00070	2.81190	-0.25001	25.27370	3.63920	-0.25001	23.92178	2.81190	-0.25001	26.19481	3.63920	-0.25001
27	1	23.92178	2.81190	-0.25001	26.19481	3.63920	-0.25001	24.84286	2.81190	-0.25001	27.11591	3.63920	-0.25001
28	1	24.84286	2.81190	-0.25001	27.11591	3.63920	-0.25001	25.76394	2.81190	-0.25001	28.03702	3.63920	-0.25001
29	1	25.76394	2.81190	-0.25001	28.03702	3.63920	-0.25001	26.68502	2.81190	-0.25001	28.95813	3.63920	-0.25001
30	1	26.68502	2.81190	-0.25001	28.95813	3.63920	-0.25001	27.60611	2.81190	-0.25001	29.87923	3.63920	-0.25001
31	1	20.66817	3.63920	-0.25001	22.94106	4.46650	-0.25001	21.58928	3.63920	-0.25001	23.86219	4.46650	-0.25001
32	1	21.58928	3.63920	-0.25001	23.86219	4.46650	-0.25001	22.51038	3.63920	-0.25001	24.78332	4.46650	-0.25001
33	1	22.51038	3.63920	-0.25001	24.78332	4.46650	-0.25001	23.43149	3.63920	-0.25001	25.70445	4.46650	-0.25001
34	1	23.43149	3.63920	-0.25001	25.70445	4.46650	-0.25001	24.35260	3.63920	-0.25001	26.62558	4.46650	-0.25001
35	1	24.35260	3.63920	-0.25001	26.62558	4.46650	-0.25001	25.27370	3.63920	-0.25001	27.54671	4.46650	-0.25001
36	1	25.27370	3.63920	-0.25001	27.54671	4.46650	-0.25001	26.19481	3.63920	-0.25001	28.46784	4.46650	-0.25001
37	1	26.19481	3.63920	-0.25001	28.46784	4.46650	-0.25001	27.11591	3.63920	-0.25001	29.38897	4.46650	-0.25001
38	1	27.11591	3.63920	-0.25001	29.38897	4.46650	-0.25001	28.03702	3.63920	-0.25001	30.31010	4.46650	-0.25001
39	1	28.03702	3.63920	-0.25001	30.31010	4.46650	-0.25001	28.95813	3.63920	-0.25001	31.23123	4.46650	-0.25001
40	1	28.95813	3.63920	-0.25001	31.23123	4.46650	-0.25001	29.87923	3.63920	-0.25001	32.15236	4.46650	-0.25001
41	1	22.94106	4.46650	-0.25001	25.21395	5.29380	-0.25001	23.86219	4.46650	-0.25001	26.13510	5.29380	-0.25001
42	1	23.86219	4.46650	-0.25001	26.13510	5.29380	-0.25001	24.78332	4.46650	-0.25001	27.05625	5.29380	-0.25001
43	1	24.78332	4.46650	-0.25001	27.05625	5.29380	-0.25001	25.70445	4.46650	-0.25001	27.97741	5.29380	-0.25001
44	1	25.70445	4.46650	-0.25001	27.97741	5.29380	-0.25001	26.62558	4.46650	-0.25001	28.89856	5.29380	-0.25001
45	1	26.62558	4.46650	-0.25001	28.89856	5.29380	-0.25001	27.54671	4.46650	-0.25001	29.81972	5.29380	-0.25001
46	1	27.54671	4.46650	-0.25001	29.81972	5.29380	-0.25001	28.46784	4.46650	-0.25001	30.74087	5.29380	-0.25001
47	1	28.46784	4.46650	-0.25001	30.74087	5.29380	-0.25001	29.38897	4.46650	-0.25001	31.66203	5.29380	-0.25001
48	1	29.38897	4.46650	-0.25001	31.66203	5.29380	-0.25001	30.31010	4.46650	-0.25001	32.58318	5.29380	-0.25001
49	1	30.31010	4.46650	-0.25001	32.58318	5.29380	-0.25001	31.23123	4.46650	-0.25001	33.50433	5.29380	-0.25001
50	1	31.23123	4.46650	-0.25001	33.50433	5.29380	-0.25001	32.15236	4.46650	-0.25001	34.42549	5.29380	-0.25001
51	1	25.21395	5.29380	-0.25001	27.48683	6.12110	-0.25001	26.13510	5.29380	-0.25001	28.40801	6.12110	-0.25001
52	1	26.13510	5.29380	-0.25001	28.40801	6.12110	-0.25001	27.05625	5.29380	-0.25001	29.32919	6.12110	-0.25001

53	1	27.05625	5.29380	-0.25001	29.32919	6.12110	-0.25001	27.97741	5.29380	-0.25001	30.25037	6.12110	-0.25001
54	1	27.97741	5.29380	-0.25001	30.25037	6.12110	-0.25001	28.89856	5.29380	-0.25001	31.17155	6.12110	-0.25001
55	1	28.89856	5.29380	-0.25001	31.17155	6.12110	-0.25001	29.81972	5.29380	-0.25001	32.09272	6.12110	-0.25001
56	1	29.81972	5.29380	-0.25001	32.09272	6.12110	-0.25001	30.74087	5.29380	-0.25001	33.01390	6.12110	-0.25001
57	1	30.74087	5.29380	-0.25001	33.01390	6.12110	-0.25001	31.66203	5.29380	-0.25001	33.93508	6.12110	-0.25001
58	1	31.66203	5.29380	-0.25001	33.93508	6.12110	-0.25001	32.58318	5.29380	-0.25001	34.85626	6.12110	-0.25001
59	1	32.58318	5.29380	-0.25001	34.85626	6.12110	-0.25001	33.50433	5.29380	-0.25001	35.77744	6.12110	-0.25001
60	1	33.50433	5.29380	-0.25001	35.77744	6.12110	-0.25001	34.42549	5.29380	-0.25001	36.69862	6.12110	-0.25001
61	1	27.48683	6.12110	-0.25001	29.75972	6.94840	-0.25001	28.40801	6.12110	-0.25001	30.68092	6.94840	-0.25001
62	1	28.40801	6.12110	-0.25001	30.68092	6.94840	-0.25001	29.32919	6.12110	-0.25001	31.60212	6.94840	-0.25001
63	1	29.32919	6.12110	-0.25001	31.60212	6.94840	-0.25001	30.25037	6.12110	-0.25001	32.52333	6.94840	-0.25001
64	1	30.25037	6.12110	-0.25001	32.52333	6.94840	-0.25001	31.17155	6.12110	-0.25001	33.44453	6.94840	-0.25001
65	1	31.17155	6.12110	-0.25001	33.44453	6.94840	-0.25001	32.09272	6.12110	-0.25001	34.36573	6.94840	-0.25001
66	1	32.09272	6.12110	-0.25001	34.36573	6.94840	-0.25001	33.01390	6.12110	-0.25001	35.28693	6.94840	-0.25001
67	1	33.01390	6.12110	-0.25001	35.28693	6.94840	-0.25001	33.93508	6.12110	-0.25001	36.20814	6.94840	-0.25001
68	1	33.93508	6.12110	-0.25001	36.20814	6.94840	-0.25001	34.85626	6.12110	-0.25001	37.12934	6.94840	-0.25001
69	1	34.85626	6.12110	-0.25001	37.12934	6.94840	-0.25001	35.77744	6.12110	-0.25001	38.05054	6.94840	-0.25001
70	1	35.77744	6.12110	-0.25001	38.05054	6.94840	-0.25001	36.69862	6.12110	-0.25001	38.97174	6.94840	-0.25001
71	1	29.75972	6.94840	-0.25001	32.03261	7.77570	-0.25001	30.68092	6.94840	-0.25001	32.95383	7.77570	-0.25001
72	1	30.68092	6.94840	-0.25001	32.95383	7.77570	-0.25001	31.60212	6.94840	-0.25001	33.87506	7.77570	-0.25001
73	1	31.60212	6.94840	-0.25001	33.87506	7.77570	-0.25001	32.52333	6.94840	-0.25001	34.79628	7.77570	-0.25001
74	1	32.52333	6.94840	-0.25001	34.79628	7.77570	-0.25001	33.44453	6.94840	-0.25001	35.71751	7.77570	-0.25001
75	1	33.44453	6.94840	-0.25001	35.71751	7.77570	-0.25001	34.36573	6.94840	-0.25001	36.63874	7.77570	-0.25001
76	1	34.36573	6.94840	-0.25001	36.63874	7.77570	-0.25001	35.28693	6.94840	-0.25001	37.55996	7.77570	-0.25001
77	1	35.28693	6.94840	-0.25001	37.55996	7.77570	-0.25001	36.20814	6.94840	-0.25001	38.48119	7.77570	-0.25001
78	1	36.20814	6.94840	-0.25001	38.48119	7.77570	-0.25001	37.12934	6.94840	-0.25001	39.40242	7.77570	-0.25001
79	1	37.12934	6.94840	-0.25001	39.40242	7.77570	-0.25001	38.05054	6.94840	-0.25001	40.32364	7.77570	-0.25001
80	1	38.05054	6.94840	-0.25001	40.32364	7.77570	-0.25001	38.97174	6.94840	-0.25001	41.24487	7.77570	-0.25001
81	1	32.03261	7.77570	-0.25001	34.30549	8.60300	-0.25001	32.95383	7.77570	-0.25001	35.22674	8.60300	-0.25001
82	1	32.95383	7.77570	-0.25001	35.22674	8.60300	-0.25001	33.87506	7.77570	-0.25001	36.14799	8.60300	-0.25001
83	1	33.87506	7.77570	-0.25001	36.14799	8.60300	-0.25001	34.79628	7.77570	-0.25001	37.06924	8.60300	-0.25001
84	1	34.79628	7.77570	-0.25001	37.06924	8.60300	-0.25001	35.71751	7.77570	-0.25001	37.99049	8.60300	-0.25001
85	1	35.71751	7.77570	-0.25001	37.99049	8.60300	-0.25001	36.63874	7.77570	-0.25001	38.91175	8.60300	-0.25001
86	1	36.63874	7.77570	-0.25001	38.91175	8.60300	-0.25001	37.55996	7.77570	-0.25001	39.83300	8.60300	-0.25001
87	1	37.55996	7.77570	-0.25001	39.83300	8.60300	-0.25001	38.48119	7.77570	-0.25001	40.75425	8.60300	-0.25001
88	1	38.48119	7.77570	-0.25001	40.75425	8.60300	-0.25001	39.40242	7.77570	-0.25001	41.67550	8.60300	-0.25001
89	1	39.40242	7.77570	-0.25001	41.67550	8.60300	-0.25001	40.32364	7.77570	-0.25001	42.59675	8.60300	-0.25001
90	1	40.32364	7.77570	-0.25001	42.59675	8.60300	-0.25001	41.24487	7.77570	-0.25001	43.51800	8.60300	-0.25001
91	1	34.30549	8.60300	-0.25001	40.27000	10.77400	-0.25001	35.22674	8.60300	-0.25001	40.27000	10.77400	-0.25001
92	1	35.22674	8.60300	-0.25001	40.27000	10.77400	-0.25001	36.14799	8.60300	-0.25001	40.27000	10.77400	-0.25001
93	1	36.14799	8.60300	-0.25001	40.27000	10.77400	-0.25001	37.06924	8.60300	-0.25001	40.27000	10.77400	-0.25001
94	1	37.06924	8.60300	-0.25001	40.27000	10.77400	-0.25001	37.99049	8.60300	-0.25001	40.27000	10.77400	-0.25001
95	1	37.99049	8.60300	-0.25001	40.27000	10.77400	-0.25001	38.91175	8.60300	-0.25001	40.27000	10.77400	-0.25001
96	1	38.91175	8.60300	-0.25001	40.27000	10.77400	-0.25001	39.83300	8.60300	-0.25001	40.27000	10.77400	-0.25001
97	1	39.83300	8.60300	-0.25001	40.27000	10.77400	-0.25001	40.75425	8.60300	-0.25001	40.27000	10.77400	-0.25001
98	1	40.75425	8.60300	-0.25001	40.27000	10.77400	-0.25001	41.67550	8.60300	-0.25001	40.27000	10.77400	-0.25001
99	1	41.67550	8.60300	-0.25001	40.27000	10.77400	-0.25001	42.59675	8.60300	-0.25001	40.27000	10.77400	-0.25001
100	1	42.59675	8.60300	-0.25001	40.27000	10.77400	-0.25001	43.51800	8.60300	-0.25001	40.27000	10.77400	-0.25001

WING PANEL CENTROID AND CONTROL POINT COORDINATES

PANEL	X C	Y C	Z C	X CP	Y CP	Z CP	AREA	Z THICK	ALPHA- THICK	Z CAMBER	ALPHA- CAMBER
1	15.41751	1.56126	-0.25001	15.83432	1.56126	-0.25001	0.77978	-0.16346	0.10816	-0.17193	0.04612
2	16.36252	1.56934	-0.25001	16.77758	1.56934	-0.25001	0.76494	-0.10920	0.05006	-0.14713	0.01658
3	17.28858	1.57095	-0.25001	17.70305	1.57095	-0.25001	0.76198	-0.07970	0.02486	-0.13461	0.01066
4	18.20963	1.57095	-0.25001	18.62410	1.57095	-0.25001	0.76198	-0.06237	0.00687	-0.12665	0.00482
5	19.13067	1.57095	-0.25001	19.54514	1.57095	-0.25001	0.76198	-0.05943	-0.00766	-0.12404	-0.00127
6	20.05172	1.57095	-0.25001	20.46619	1.57095	-0.25001	0.76198	-0.07285	-0.02199	-0.12792	-0.00782
7	20.97276	1.57095	-0.25001	21.38723	1.57095	-0.25001	0.76198	-0.10105	-0.03357	-0.14046	-0.01879
8	21.89381	1.57095	-0.25001	22.30828	1.57095	-0.25001	0.76198	-0.13855	-0.04035	-0.16352	-0.02997
9	22.81485	1.57095	-0.25001	23.22932	1.57095	-0.25001	0.76198	-0.17912	-0.04621	-0.19806	-0.04404
10	23.73590	1.57095	-0.25001	24.15037	1.57095	-0.25001	0.76198	-0.22164	-0.05182	-0.24687	-0.06404
11	17.71938	2.39825	-0.25001	18.13386	2.39825	-0.25001	0.76200	-0.16338	0.10816	-0.17192	0.04612
12	18.64045	2.39825	-0.25001	19.05493	2.39825	-0.25001	0.76200	-0.10918	0.05006	-0.14713	0.01658
13	19.56152	2.39825	-0.25001	19.97600	2.39825	-0.25001	0.76200	-0.07969	0.02486	-0.13461	0.01066
14	20.48259	2.39825	-0.25001	20.89707	2.39825	-0.25001	0.76200	-0.06237	0.00687	-0.12665	0.00482
15	21.40366	2.39825	-0.25001	21.81814	2.39825	-0.25001	0.76200	-0.05943	-0.00766	-0.12403	-0.00127
16	22.32473	2.39825	-0.25001	22.73921	2.39825	-0.25001	0.76200	-0.07284	-0.02199	-0.12792	-0.00782
17	23.24580	2.39825	-0.25001	23.66028	2.39825	-0.25001	0.76200	-0.10105	-0.03357	-0.14046	-0.01879
18	24.16687	2.39825	-0.25001	24.58135	2.39825	-0.25001	0.76200	-0.13855	-0.04035	-0.16351	-0.02997
19	25.08794	2.39825	-0.25001	25.50242	2.39825	-0.25001	0.76200	-0.17912	-0.04621	-0.19806	-0.04404
20	26.00901	2.39825	-0.25001	26.42349	2.39825	-0.25001	0.76200	-0.22164	-0.05182	-0.24687	-0.06404
21	19.99228	3.22555	-0.25001	20.40677	3.22555	-0.25001	0.76202	-0.16338	0.10816	-0.17192	0.04612
22	20.91337	3.22555	-0.25001	21.32787	3.22555	-0.25001	0.76202	-0.10917	0.05006	-0.14713	0.01658
23	21.83447	3.22555	-0.25001	22.24896	3.22555	-0.25001	0.76202	-0.07969	0.02486	-0.13460	0.01066
24	22.75556	3.22555	-0.25001	23.17006	3.22555	-0.25001	0.76202	-0.06236	0.00687	-0.12664	0.00482
25	23.67666	3.22555	-0.25001	24.09115	3.22555	-0.25001	0.76202	-0.05942	-0.00766	-0.12403	-0.00127
26	24.59775	3.22555	-0.25001	25.01224	3.22555	-0.25001	0.76202	-0.07284	-0.02199	-0.12792	-0.00782
27	25.51885	3.22555	-0.25001	25.93334	3.22555	-0.25001	0.76202	-0.10104	-0.03357	-0.14046	-0.01879
28	26.43994	3.22555	-0.25001	26.85443	3.22555	-0.25001	0.76202	-0.13855	-0.04035	-0.16351	-0.02997
29	27.36103	3.22555	-0.25001	27.77553	3.22555	-0.25001	0.76202	-0.17912	-0.04621	-0.19806	-0.04404
30	28.28213	3.22555	-0.25001	28.69662	3.22555	-0.25001	0.76202	-0.22164	-0.05182	-0.24687	-0.06404
31	22.26518	4.05285	-0.25001	22.67968	4.05285	-0.25001	0.76204	-0.16338	0.10816	-0.17192	0.04612
32	23.18630	4.05285	-0.25001	23.60080	4.05285	-0.25001	0.76204	-0.10917	0.05006	-0.14712	0.01658
33	24.10742	4.05285	-0.25001	24.52192	4.05285	-0.25001	0.76204	-0.07968	0.02486	-0.13460	0.01066
34	25.02853	4.05285	-0.25001	25.44304	4.05285	-0.25001	0.76204	-0.06236	0.00687	-0.12664	0.00482
35	25.94965	4.05285	-0.25001	26.36416	4.05285	-0.25001	0.76204	-0.05942	-0.00766	-0.12403	-0.00127
36	26.87077	4.05285	-0.25001	27.28527	4.05285	-0.25001	0.76204	-0.07283	-0.02199	-0.12791	-0.00782
37	27.79189	4.05285	-0.25001	28.20639	4.05285	-0.25001	0.76204	-0.10104	-0.03357	-0.14045	-0.01879
38	28.71301	4.05285	-0.25001	29.12751	4.05285	-0.25001	0.76204	-0.13854	-0.04035	-0.16351	-0.02997
39	29.63412	4.05285	-0.25001	30.04863	4.05285	-0.25001	0.76204	-0.17911	-0.04621	-0.19805	-0.04404
40	30.55524	4.05285	-0.25001	30.96975	4.05285	-0.25001	0.76204	-0.22164	-0.05182	-0.24687	-0.06404
41	24.53808	4.88015	-0.25001	24.95259	4.88015	-0.25001	0.76206	-0.16338	0.10816	-0.17192	0.04612
42	25.45922	4.88015	-0.25001	25.87373	4.88015	-0.25001	0.76206	-0.10917	0.05006	-0.14712	0.01658
43	26.38036	4.88015	-0.25001	26.79488	4.88015	-0.25001	0.76206	-0.07968	0.02486	-0.13460	0.01066
44	27.30151	4.88015	-0.25001	27.71602	4.88015	-0.25001	0.76206	-0.06235	0.00687	-0.12664	0.00482
45	28.22265	4.88015	-0.25001	28.63716	4.88015	-0.25001	0.76206	-0.05941	-0.00766	-0.12402	-0.00127
46	29.14379	4.88015	-0.25001	29.55830	4.88015	-0.25001	0.76206	-0.07283	-0.02199	-0.12791	-0.00782
47	30.06493	4.88015	-0.25001	30.47945	4.88015	-0.25001	0.76206	-0.10103	-0.03357	-0.14045	-0.01879
48	30.98607	4.88015	-0.25001	31.40059	4.88015	-0.25001	0.76206	-0.13854	-0.04035	-0.16351	-0.02997
49	31.90722	4.88015	-0.25001	32.32173	4.88015	-0.25001	0.76206	-0.17911	-0.04621	-0.19805	-0.04404
50	32.82836	4.88015	-0.25001	33.24287	4.88015	-0.25001	0.76206	-0.22164	-0.05182	-0.24687	-0.06404
51	26.81098	5.70745	-0.25001	27.22550	5.70745	-0.25001	0.76208	-0.16337	0.10816	-0.17192	0.04612
52	27.73214	5.70745	-0.25001	28.14667	5.70745	-0.25001	0.76208	-0.10916	0.05006	-0.14712	0.01658
53	28.65331	5.70745	-0.25001	29.06783	5.70745	-0.25001	0.76208	-0.07967	0.02486	-0.13459	0.01066

54	29.57448	5.70745	-0.25001	29.98900	5.70745	-0.25001	0.76208	-0.06235	0.00687	-0.12663	0.00482
55	30.49564	5.70745	-0.25001	30.91017	5.70745	-0.25001	0.76208	-0.05941	-0.00766	-0.12402	-0.00127
56	31.41681	5.70745	-0.25001	31.83133	5.70745	-0.25001	0.76208	-0.07283	-0.02199	-0.12791	-0.00782
57	32.33797	5.70745	-0.25001	32.75250	5.70745	-0.25001	0.76208	-0.10103	-0.03357	-0.14045	-0.01879
58	33.25914	5.70745	-0.25001	33.67367	5.70745	-0.25001	0.76208	-0.13854	-0.04035	-0.16351	-0.02997
59	34.18031	5.70745	-0.25001	34.59483	5.70745	-0.25001	0.76208	-0.17911	-0.04621	-0.19805	-0.04404
60	35.10147	5.70745	-0.25001	35.51600	5.70745	-0.25001	0.76208	-0.221[illegible]	[illegible].05182	-0.24687	-0.06404
61	29.08388	6.53475	-0.25001	29.49841	6.53475	-0.25001	0.76210	-0.16337	0.10816	-0.17191	0.04612
62	30.00507	6.53475	-0.25001	30.41960	6.53475	-0.25001	0.76210	-0.10916	0.05006	-0.14712	0.01658
63	30.92626	6.53475	-0.25001	31.34079	6.53475	-0.25001	0.76210	-0.07967	0.02486	-0.13459	0.01066
64	31.84745	6.53475	-0.25001	32.26198	6.53475	-0.25001	0.76210	-0.06234	0.00687	-0.12663	0.00482
65	32.76864	6.53475	-0.25001	33.18317	6.53475	-0.25001	0.76210	-0.05940	-0.00766	-0.12402	-0.00127
66	33.68983	6.53475	-0.25001	34.10436	6.53475	-0.25001	0.76210	-0.07282	-0.02199	-0.12790	-0.00782
67	34.61102	6.53475	-0.25001	35.02555	6.53475	-0.25001	0.76210	-0.10103	-0.03357	-0.14045	-0.01879
68	35.53221	6.53475	-0.25001	35.94674	6.53475	-0.25001	0.76210	-0.13853	-0.04035	-0.16350	-0.02997
69	36.45340	6.53475	-0.25001	36.86793	6.53475	-0.25001	0.76210	-0.17911	-0.04621	-0.19805	-0.04404
70	37.37459	6.53475	-0.25001	37.78912	6.53475	-0.25001	0.76210	-0.22164	-0.05182	-0.24685	-0.06404
71	31.35677	7.36205	-0.25001	31.77132	7.36205	-0.25001	0.76212	-0.16337	0.10816	-0.17191	0.04612
72	32.27799	7.36205	-0.25001	32.69253	7.36205	-0.25001	0.76212	-0.10916	0.05006	-0.14711	0.01658
73	33.19920	7.36205	-0.25001	33.61375	7.36205	-0.25001	0.76212	-0.07966	0.02486	-0.13459	0.01066
74	34.12042	7.36205	-0.25001	34.53496	7.36205	-0.25001	0.76212	-0.06234	0.00687	-0.12663	0.00482
75	35.04163	7.36205	-0.25001	35.45618	7.36205	-0.25001	0.76212	-0.05940	-0.00766	-0.12401	-0.00127
76	35.96285	7.36205	-0.25001	36.37739	7.36205	-0.25001	0.76212	-0.07282	-0.02199	-0.12790	-0.00782
77	36.88406	7.36205	-0.25001	37.29861	7.36205	-0.25001	0.76212	-0.10102	-0.03357	-0.14044	-0.01879
78	37.80527	7.36205	-0.25001	38.21982	7.36205	-0.25001	0.76212	-0.13853	-0.04035	-0.16350	-0.02997
79	38.72649	7.36205	-0.25001	39.14104	7.36205	-0.25001	0.76212	-0.17911	-0.04621	-0.19805	-0.04404
80	39.64770	7.36205	-0.25001	40.06225	7.36205	-0.25001	0.76212	-0.22164	-0.05182	-0.24686	-0.06404
81	33.62967	8.18935	-0.25001	34.04423	8.18935	-0.25001	0.76214	-0.16337	0.10816	-0.17191	0.04612
82	34.55091	8.18935	-0.25001	34.96547	8.18935	-0.25001	0.76214	-0.10915	0.05006	-0.14711	0.01658
83	35.47215	8.18935	-0.25001	35.88671	8.18935	-0.25001	0.76214	-0.07966	0.02486	-0.13458	0.01066
84	36.39339	8.18935	-0.25001	36.80795	8.18935	-0.25001	0.76214	-0.06233	0.00687	-0.12662	0.00482
85	37.31463	8.18935	-0.25001	37.72918	8.18935	-0.25001	0.76214	-0.05939	-0.00766	-0.12401	-0.00127
86	38.23587	8.18935	-0.25001	38.65042	8.18935	-0.25001	0.76214	-0.07281	-0.02199	-0.12790	-0.00782
87	39.15710	8.18935	-0.25001	39.57166	8.18935	-0.25001	0.76214	-0.10102	-0.03357	-0.14044	-0.01879
88	40.07834	8.18935	-0.25001	40.49290	8.18935	-0.25001	0.76214	-0.13853	-0.04035	-0.16350	-0.02997
89	40.99958	8.18935	-0.25001	41.41414	8.18935	-0.25001	0.76214	-0.17910	-0.04621	-0.19805	-0.04404
90	41.92082	8.18935	-0.25001	42.33538	8.18935	-0.25001	0.76214	-0.22163	-0.05182	-0.24686	-0.06404
91	36.60074	9.32667	-0.25001	36.87712	9.32667	-0.25001	1.00002	-0.19225	0.10816	-0.19794	0.04612
92	37.21491	9.32667	-0.25001	37.49129	9.32667	-0.25001	1.00002	-0.15610	0.05006	-0.18141	0.01658
93	37.82908	9.32667	-0.25001	38.10545	9.32667	-0.25001	1.00002	-0.13644	0.02486	-0.17306	0.01066
94	38.44325	9.32667	-0.25001	38.71962	9.32667	-0.25001	1.00002	-0.12489	0.00687	-0.16775	0.00482
95	39.05741	9.32667	-0.25001	39.33379	9.32667	-0.25001	1.00002	-0.12293	-0.00766	-0.16601	-0.00127
96	39.67158	9.32667	-0.25001	39.94795	9.32667	-0.25001	1.00002	-0.13188	-0.02199	-0.16860	-0.00782
97	40.28575	9.32667	-0.25001	40.56212	9.32667	-0.25001	1.00002	-0.15068	-0.03357	-0.17696	-0.01879
98	40.89991	9.32667	-0.25001	41.17629	9.32667	-0.25001	1.00002	-0.17569	-0.04035	-0.19233	-0.02997
99	41.51408	9.32667	-0.25001	41.79046	9.32667	-0.25001	1.00002	-0.20274	-0.04621	-0.21537	-0.04404
100	42.12825	9.32667	-0.25001	42.40462	9.32667	-0.25001	1.00002	-0.23109	-0.05182	-0.24791	-0.06404

PANEND

TR-805 MIN DRAG CLBAR=.159

DESCRIPTION OF CASE REQUESTED

SYMMETRICAL CONFIGURATION - PANELS LOCATED ON BOTH SIDES OF X-Z PLANE(SYM = 1.)

CASE = 3.   OPTIMIZE WING SHAPE

CPCALC = 0.   LINEAR CP

POLAR = 0.   POLARS NOT REQUESTED

THICK = 1.   WING THICKNESS PRESSURES TO BE ADDED

VOUT = 1.   VELOCITY COMPONENTS TO BE PRINTED

WING REFERENCE AREA =   89.3750

POINT ABOUT WHICH THE MOMENTS ARE TO BE COMPUTED
 X-COORDINATE =   0.
 Z-COORDINATE =   0.

MACH NUMBER =   1.8000

TR-805   BODY CAMBER   6A

INCLINATION OF BODY AXIS WITH RESPECT TO DEFINING AXIS =   0.   DEG.

ANGLE OF ATTACK WITH RESPECT TO BODY AXIS =   -0.   DEG.

HEIGHT OF WING PLANE ABOVE BODY AXIS =   -0.2500

WING OPTIMIZED FOR CL BAR =   0.1590

VELOCITY COMPONENTS ON BODY DUE TO BODY LINE SOURCES AND DOUBLETS

AXIAL(U)

THETA(DEG.) X	12.5000	37.5000	62.5000	88.5950	116.0950	142.5000	167.5000
0.	-0.07262	-0.07075	-0.06736	-0.06288	-0.05813	-0.05452	-0.05264
0.7243	-0.07262	-0.07075	-0.06736	-0.06288	-0.05813	-0.05452	-0.05264
1.4485	-0.06880	-0.06764	-0.06554	-0.06278	-0.05985	-0.05761	-0.05646
2.1728	-0.03327	-0.03279	-0.03192	-0.03078	-0.02957	-0.02865	-0.02817
2.8970	-0.03301	-0.03253	-0.03166	-0.03051	-0.02929	-0.02836	-0.02788
3.6213	-0.02469	-0.02429	-0.02355	-0.02259	-0.02156	-0.02078	-0.02038
4.3456	-0.02421	-0.02388	-0.02329	-0.02250	-0.02167	-0.02103	-0.02071
5.0698	-0.01980	-0.01943	-0.01876	-0.01788	-0.01694	-0.01622	-0.01585
5.7941	-0.01879	-0.01853	-0.01806	-0.01745	-0.01680	-0.01631	-0.01605
6.5184	-0.01520	-0.01498	-0.01459	-0.01406	-0.01351	-0.01308	-0.01286
7.2426	-0.01467	-0.01441	-0.01396	-0.01336	-0.01272	-0.01223	-0.01198
7.9669	-0.01241	-0.01208	-0.01147	-0.01067	-0.00983	-0.00918	-0.00885

8.6911	-0.01059	-0.01041	-0.01008	-0.00964	-0.00917	-0.00882	-0.00864
9.4154	-0.00702	-0.00711	-0.00726	-0.00746	-0.00768	-0.00784	-0.00793
10.1397	-0.00757	-0.00731	-0.00683	-0.00621	-0.00554	-0.00503	-0.00477
10.8639	-0.00407	-0.00410	-0.00415	-0.00422	-0.00430	-0.00436	-0.00438
11.5882	-0.00168	-0.00181	-0.00205	-0.00236	-0.00269	-0.00295	-0.00308
12.3124	-0.00017	-0.00024	-0.00037	-0.00055	-0.00073	-0.00087	-0.00094
13.0367	0.00381	0.00350	0.00292	0.00217	0.00136	0.00075	0.00043
13.7610	0.00461	0.00438	0.00397	0.00343	0.00285	0.00241	0.00219
14.5023	0.00828	0.00798	0.00743	0.00670	0.00592	0.00533	0.00503
15.2436	0.01318	0.01254	0.01136	0.00982	0.00818	0.00693	0.00628
15.9849	0.02021	0.01971	0.01879	0.01758	0.01629	0.01531	0.01481
16.7262	0.01648	0.01612	0.01547	0.01461	0.01369	0.01300	0.01264
17.4675	0.01345	0.01322	0.01279	0.01222	0.01162	0.01116	0.01092
18.2088	0.01105	0.01091	0.01056	0.01032	0.00996	0.00969	0.00954
18.9501	0.00916	0.00909	0.00896	0.00879	0.00861	0.00848	0.00841
19.6914	0.00767	0.00764	0.00761	0.00756	0.00751	0.00746	0.00744
20.4327	0.00649	0.00650	0.00652	0.00655	0.00658	0.00660	0.00661
21.1740	0.00556	0.00559	0.00565	0.00572	0.00580	0.00586	0.00589
21.9153	0.00482	0.00486	0.00494	0.00503	0.00513	0.00521	0.00525
22.6566	0.00423	0.00428	0.00435	0.00446	0.00456	0.00465	0.00469
23.3979	0.00299	0.00318	0.00351	0.00395	0.00442	0.00477	0.00496
24.1392	0.00353	0.00354	0.00355	0.00356	0.00357	0.00358	0.00359
24.8805	0.00320	0.00320	0.00320	0.00321	0.00321	0.00321	0.00322
25.6218	0.00290	0.00290	0.00290	0.00290	0.00290	0.00290	0.00290
26.3631	0.00264	0.00264	0.00264	0.00264	0.00264	0.00264	0.00263
27.1044	0.00241	0.00241	0.00241	0.00241	0.00241	0.00241	0.00240
27.8457	0.00221	0.00221	0.00221	0.00221	0.00221	0.00220	0.00220
28.5870	0.00203	0.00203	0.00203	0.00203	0.00203	0.00203	0.00203
29.3283	0.00187	0.00187	0.00187	0.00187	0.00187	0.00187	0.00187
30.0696	0.00295	0.00295	0.00295	0.00296	0.00296	0.00296	0.00297
30.8109	0.00677	0.00677	0.00678	0.00678	0.00679	0.00680	0.00680
31.5522	0.01062	0.01062	0.01063	0.01065	0.01067	0.01068	0.01069
32.2935	0.01297	0.01298	0.01300	0.01303	0.01305	0.01307	0.01308
33.0348	0.01474	0.01475	0.01478	0.01481	0.01485	0.01488	0.01489
33.7761	0.01788	0.01790	0.01794	0.01798	0.01804	0.01808	0.01810
34.5174	0.01874	0.01877	0.01881	0.01887	0.01894	0.01899	0.01902
35.2587	0.01365	0.01368	0.01374	0.01380	0.01388	0.01393	0.01396
36.0000	0.00509	0.00512	0.00517	0.00523	0.00530	0.00536	0.00539

RADIAL(VR)

THETA(DEG.)	12.5000	37.5000	62.5000	88.5950	116.0950	142.5000	167.5000
X							
0.	0.20063	0.19465	0.18381	0.16953	0.15435	0.14280	0.13682
0.7243	0.20063	0.19465	0.18381	0.16953	0.15435	0.14280	0.13682
1.4485	0.19187	0.18753	0.17967	0.16930	0.15828	0.14990	0.14556
2.1728	0.13550	0.13227	0.12643	0.11872	0.11053	0.10430	0.10107
2.8970	0.12989	0.12692	0.12152	0.11442	0.10686	0.10112	0.09814
3.6213	0.11363	0.11089	0.10593	0.09939	0.09244	0.08715	0.08441
4.3456	0.10969	0.10720	0.10268	0.09672	0.09039	0.08557	0.08309
5.0698	0.10046	0.09797	0.09345	0.08749	0.08116	0.07635	0.07385
5.7941	0.09658	0.09433	0.09025	0.08487	0.07915	0.07480	0.07255
6.5184	0.08893	0.08680	0.08294	0.07785	0.07245	0.06833	0.06620
7.2426	0.08608	0.08395	0.08009	0.07501	0.06961	0.06549	0.06337
7.9669	0.C8090	0.07865	0.07457	0.06919	0.06348	0.05913	0.05688
8.6911	0.07635	0.07434	0.07070	0.06590	0.06080	0.05692	0.05491
9.4154	0.06876	0.06724	0.06449	0.06085	0.05699	0.05405	0.05253
10.1397	0.06762	0.06561	0.06197	0.05718	0.05209	0.04822	0.04621

10.8639	0.06025	0.05873	0.05598	0.05236	0.04851	0.04557	0.04406
11.5882	0.05419	0.05292	0.05062	0.04759	0.04437	0.04192	0.04065
12.3124	0.04937	0.04811	0.04581	0.04279	0.03958	0.03713	0.03586
13.0367	0.04038	0.03961	0.03822	0.03638	0.03443	0.03294	0.03217
13.7610	0.03602	0.03525	0.03387	0.03204	0.03010	0.02862	0.02785
14.5023	0.02690	0.02640	0.02549	0.02429	0.02302	0.02205	0.02155
15.2436	0.01505	0.01529	0.01572	0.01628	0.01688	0.01734	0.01757
15.9849	-0.00144	-0.00117	-0.00068	-0.00003	0.00066	0.00118	0.00145
16.7262	-0.00145	-0.00118	-0.00068	-0.00003	0.00065	0.00118	0.00145
17.4675	-0.00145	-0.00118	-0.00068	-0.00004	0.00065	0.00118	0.00145
18.2088	-0.00145	-0.00118	-0.00068	-0.00004	0.00065	0.00118	0.00145
18.9501	-0.00145	-0.00118	-0.00068	-0.00004	0.00065	0.00118	0.00145
19.6914	-0.00145	-0.00118	-0.00068	-0.00004	0.00065	0.00118	0.00145
20.4327	-0.00145	-0.00118	-0.00069	-0.00004	0.00065	0.00118	0.00145
21.1740	-0.00145	-0.00118	-0.00069	-0.00004	0.00065	0.00118	0.00145
21.9153	-0.00145	-0.00118	-0.00069	-0.00004	0.00065	0.00118	0.00145
22.6566	-0.00145	-0.00118	-0.00068	-0.00004	0.00065	0.00118	0.00145
23.3979	-0.00013	-0.00011	-0.00006	-0.00000	0.00006	0.00011	0.00013
24.1392	-0.00145	-0.00118	-0.00069	-0.00004	0.00065	0.00118	0.00145
24.8805	-0.00145	-0.00118	-0.00069	-0.00004	0.00065	0.00118	0.00145
25.6218	-0.00145	-0.00118	-0.00069	-0.00004	0.00065	0.00118	0.00145
26.3631	-0.00145	-0.00118	-0.00069	-0.00004	0.00065	0.00118	0.00145
27.1044	-0.00145	-0.00118	-0.00069	-0.00004	0.00065	0.00118	0.00145
27.8457	-0.00145	-0.00118	-0.00069	-0.00004	0.00065	0.00118	0.00145
28.5870	-0.00145	-0.00118	-0.00069	-0.00004	0.00065	0.00118	0.00145
29.3283	-0.00145	-0.00118	-0.00069	-0.00004	0.00065	0.00118	0.00145
30.0696	-0.00354	-0.00326	-0.00277	-0.00212	-0.00143	-0.00091	-0.00064
30.8109	-0.01060	-0.01033	-0.00984	-0.00919	-0.00850	-0.00798	-0.00770
31.5522	-0.01885	-0.01858	-0.01809	-0.01744	-0.01675	-0.01622	-0.01595
32.2935	-0.02572	-0.02545	-0.02496	-0.02431	-0.02362	-0.02310	-0.02282
33.0348	-0.03237	-0.03210	-0.03161	-0.03096	-0.03027	-0.02975	-0.02947
33.7761	-0.04216	-0.04189	-0.04140	-0.04075	-0.04007	-0.03954	-0.03927
34.5174	-0.04930	-0.04903	-0.04854	-0.04790	-0.04721	-0.04669	-0.04642
35.2587	-0.04646	-0.04619	-0.04570	-0.04506	-0.04437	-0.04385	-0.04358
36.0000	-0.03562	-0.03535	-0.03486	-0.03421	-0.03353	-0.03300	-0.03273

TANGENTIAL(VT)

THETA(DEG.) X	12.5000	37.5000	62.5000	88.5950	116.0950	142.5000	167.5000
0.	0.00523	0.01471	0.02144	0.02416	0.02170	0.01471	0.00523
0.7243	0.00523	0.01471	0.02144	0.02416	0.02170	0.01471	0.00523
1.4485	0.00418	0.01177	0.01715	0.01932	0.01736	0.01177	0.00418
2.1728	0.00377	0.01061	0.01546	0.01743	0.01565	0.01061	0.00377
2.8970	0.00331	0.00931	0.01357	0.01529	0.01373	0.00931	0.00331
3.6213	0.00308	0.00867	0.01263	0.01424	0.01279	0.00867	0.00308
4.3456	0.00286	0.00803	0.01171	0.01319	0.01185	0.00803	0.00286
5.0698	0.00276	0.00775	0.01129	0.01273	0.01143	0.00775	0.00276
5.7941	0.00263	0.00739	0.01076	0.01213	0.01090	0.00739	0.00263
6.5184	0.00250	0.00704	0.01026	0.01157	0.01039	0.00704	0.00250
7.2426	0.00242	0.00681	0.00993	0.01119	0.01005	0.00681	0.00242
7.9669	0.00243	0.00684	0.00996	0.01123	0.01009	0.00684	0.00243
8.6911	0.00239	0.00672	0.00980	0.01104	0.00992	0.00672	0.00239
9.4154	0.00220	0.00619	0.00902	0.01017	0.00914	0.00619	0.00220
10.1397	0.00216	0.00606	0.00884	0.00996	0.00895	0.00606	0.00216
10.8639	0.00205	0.00578	0.00842	0.00949	0.00852	0.00578	0.00205
11.5882	0.00187	0.00526	0.00766	0.00864	0.00776	0.00526	0.00187
12.3124	0.00171	0.00481	0.00702	0.00791	0.00710	0.00481	0.00171

13.0367	0.00147	0.00414	0.00603	0.00680	0.00611	0.00414	0.00147
13.7610	0.00124	0.00350	0.00510	0.00575	0.00516	0.00350	0.00124
14.5023	0.00101	0.00284	0.00413	0.00466	0.00418	0.00284	0.00101
15.2436	0.00061	0.00173	0.00251	0.00283	0.00254	0.00173	0.00061
15.9849	0.00022	0.00062	0.00091	0.00102	0.00092	0.00062	0.00022
16.7262	-0.00008	-0.00023	-0.00033	-0.00038	-0.00034	-0.00023	-0.00008
17.4675	-0.00029	-0.00083	-0.00121	-0.00136	-0.00122	-0.00083	-0.00029
18.2088	-0.00043	-0.00122	-0.00177	-0.00200	-0.00180	-0.00122	-0.00043
18.9501	-0.00051	-0.00144	-0.00210	-0.00236	-0.00212	-0.00144	-0.00051
19.6914	-0.00055	-0.00154	-0.00224	-0.00253	-0.00227	-0.00154	-0.00055
20.4327	-0.00055	-0.00156	-0.00227	-0.00256	-0.00230	-0.00156	-0.00055
21.1740	-0.00054	-0.00152	-0.00222	-0.00250	-0.00224	-0.00152	-0.00054
21.9153	-0.00052	-0.00145	-0.00212	-0.00239	-0.00214	-0.00145	-0.00052
22.6566	-0.00049	-0.00137	-0.00200	-0.00226	-0.00203	-0.00137	-0.00049
23.3979	-0.00039	-0.00110	-0.00160	-0.00181	-0.00162	-0.00110	-0.00039
24.1392	-0.00035	-0.00098	-0.00143	-0.00161	-0.00144	-0.00098	-0.00035
24.8805	-0.00034	-0.00096	-0.00139	-0.00157	-0.00141	-0.00096	-0.00034
25.6218	-0.00034	-0.00095	-0.00139	-0.00156	-0.00140	-0.00095	-0.00034
26.3631	-0.00034	-0.00095	-0.00138	-0.00156	-0.00140	-0.00095	-0.00034
27.1044	-0.00034	-0.00095	-0.00138	-0.00156	-0.00140	-0.00095	-0.00034
27.8457	-0.00034	-0.00095	-0.00138	-0.00156	-0.00140	-0.00095	-0.00034
28.5870	-0.00034	-0.00095	-0.00138	-0.00156	-0.00140	-0.00095	-0.00034
29.3283	-0.00034	-0.00095	-0.00138	-0.00155	-0.00140	-0.00095	-0.00034
30.0696	-0.00034	-0.00095	-0.00138	-0.00155	-0.00140	-0.00095	-0.00034
30.8109	-0.00034	-0.00095	-0.00139	-0.00156	-0.00140	-0.00095	-0.00034
31.5522	-0.00034	-0.00096	-0.00140	-0.00158	-0.00142	-0.00096	-0.00034
32.2935	-0.00035	-0.00097	-0.00141	-0.00159	-0.00143	-0.00097	-0.00035
33.0348	-0.00035	-0.00098	-0.00143	-0.00161	-0.00145	-0.00098	-0.00035
33.7761	-0.00035	-0.00099	-0.00144	-0.00163	-0.00146	-0.00099	-0.00035
34.5174	-0.00036	-0.00100	-0.00146	-0.00164	-0.00147	-0.00100	-0.00036
35.2587	-0.00035	-0.00100	-0.00145	-0.00164	-0.00147	-0.00100	-0.00035
36.0000	-0.00035	-0.00098	-0.00142	-0.00160	-0.00144	-0.00098	-0.00035

VELOCITY COMPONENTS ON WING PANELS DUE TO BODY PANEL PRESSURE SINGULARITIES

AXIAL(U)

SPANWISE STATION / CHORDWISE STATION	1	2	3	4	5	6	7	8	9	10
1	-0.00423	-0.00091	0.00043	0.00352	0.00106	0.00131	-0.00014	-0.00070	-0.00111	-0.00105
2	-0.00050	-0.00018	0.00406	0.00163	0.00106	-0.00049	-0.00082	-0.00078	-0.00107	-0.00297
3	0.00290	0.00680	0.00508	0.00089	-0.00107	-0.00119	-0.00111	-0.00102	-0.00311	-0.00161
4	0.00875	0.00635	0.00248	-0.00040	-0.00176	-0.00194	-0.00108	-0.00331	-0.00181	-0.00162
5	0.00907	0.00391	0.00028	-0.00043	-0.00314	-0.00102	-0.00389	-0.00179	-0.00087	-0.00073
6	0.00669	0.00164	-0.00035	-0.00016	-0.00110	-0.00573	-0.00196	-0.00081	-0.00087	-0.00088
7	0.00497	0.00042	-0.00103	-0.00133	-0.00092	-0.00216	-0.00088	-0.00094	0.00054	0.00024
8	0.00222	-0.00085	-0.00201	-0.00090	-0.00244	-0.00090	-0.00104	0.00053	0.00071	0.00056
9	-0.00020	-0.00203	0.00127	-0.00272	-0.00086	-0.00118	0.00080	0.00072	0.00045	0.00057
10	-0.00211	-0.00237	-0.00024	-0.00055	-0.00144	0.00117	0.00070	0.00052	0.00025	0.00060

TRANSVERSE(V)

SPANWISE STATION / CHORDWISE STATION	1	2	3	4	5	6	7	8	9	10
1	0.00684	0.00195	-0.00047	-0.00561	-0.00225	-0.00266	-0.00040	0.00058	0.00134	0.00140

2	0.00304	0.00050	-0.00656	-0.00335	-0.00252	-0.00008	0.00062	0.00075	0.00135	0.00434
3	-0.00293	-0.01096	-0.00898	-0.00266	0.00046	0.00095	0.00110	0.00118	0.00452	0.00239
4	-0.01393	-0.01203	-0.00585	-0.00109	0.00144	0.00213	0.00115	0.00473	0.00270	0.00246
5	-0.01919	-0.00991	-0.00325	-0.00118	0.00354	0.00086	0.00547	0.00262	0.00135	0.00115
6	-0.02005	-0.00810	-0.00264	-0.00159	0.00063	0.00800	0.00280	0.00125	0.00142	0.00141
7	-0.02208	-0.00722	-0.00172	0.00033	0.00050	0.00298	0.00131	0.00152	-0.00071	-0.00024
8	-0.02172	-0.00581	-0.00010	-0.00015	0.00315	0.00126	0.00164	-0.00070	-0.00099	-0.00075
9	-0.02064	-0.00403	-0.00474	0.00308	0.00105	0.00180	-0.00112	-0.00102	-0.00065	-0.00078
10	-0.01901	-0.00318	-0.00182	0.00023	0.00207	-0.00169	-0.00098	-0.00076	-0.00036	-0.00084

VERTICAL(W)

SPANWISE STATION CHORDWISE STATION	1	2	3	4	5	6	7	8	9	10
1	0.01305	0.00774	0.00604	0.00496	0.00478	0.00461	0.00448	0.00427	0.00399	0.00364
2	0.03289	0.01242	0.00809	0.00665	0.00607	0.00557	0.00518	0.00471	0.00443	0.00371
3	0.05600	0.01717	0.01095	0.00858	0.00734	0.00647	0.00575	0.00523	0.00465	0.00392
4	0.08077	0.02275	0.01383	0.01032	0.00861	0.00720	0.00633	0.00551	0.00503	0.00409
5	0.10643	0.02836	0.01653	0.01217	0.00975	0.00796	0.00670	0.00592	0.00511	0.00413
6	0.13315	0.03453	0.01936	0.01384	0.01046	0.00847	0.00723	0.00617	0.00508	0.00409
7	0.15818	0.04012	0.02188	0.01479	0.01149	0.00912	0.00760	0.00611	0.00525	0.00419
8	0.18088	0.04495	0.02349	0.01624	0.01203	0.00961	0.00753	0.00627	0.00532	0.00420
9	0.20005	0.04819	0.02584	0.01698	0.01274	0.00959	0.00774	0.00641	0.00521	0.00423
10	0.21223	0.05210	0.02697	0.01812	0.01274	0.00989	0.00790	0.00630	0.00517	0.00427

VELOCITY COMPONENTS ON WING PANELS DUE TO WING PANEL PRESSURE SINGULARITIES

AXIAL(U)

SPANWISE STATION CHORDWISE STATION	1	2	3	4	5	6	7	8	9	10
1	0.04090	0.03525	0.02746	0.02433	0.02382	0.02389	0.02418	0.02442	0.01050	0.05445
2	0.05752	0.04852	0.03988	0.03722	0.03709	0.03743	0.03792	0.03801	0.02207	0.08822
3	0.06280	0.05325	0.04700	0.04571	0.04619	0.04676	0.04729	0.04787	0.03257	0.09560
4	0.06157	0.05422	0.05157	0.05172	0.05275	0.05335	0.05420	0.05360	0.03707	0.04967
5	0.05797	0.05353	0.05435	0.05593	0.05718	0.05778	0.05828	0.05277	0.04178	0.04671
6	0.05291	0.05207	0.05583	0.05825	0.05940	0.05968	0.05739	0.04850	0.04688	0.04241
7	0.04688	0.05005	0.05562	0.05823	0.05907	0.05717	0.05256	0.04515	0.05028	0.03700
8	0.03928	0.04679	0.05286	0.05523	0.05421	0.05064	0.04609	0.04166	0.05173	0.03149
9	0.03038	0.04019	0.04618	0.04691	0.04432	0.04121	0.03725	0.03644	0.04841	0.02444
10	0.01843	0.02790	0.03164	0.03094	0.02877	0.02705	0.02407	0.02531	0.03746	0.02840

TRANSVERSE(V)

SPANWISE STATION CHORDWISE STATION	1	2	3	4	5	6	7	8	9	10
1	-0.11236	-0.09685	-0.07544	-0.06683	-0.06543	-0.06564	-0.06643	-0.06708	-0.02886	-0.14959
2	-0.15802	-0.13331	-0.10956	-0.10226	-0.10191	-0.10283	-0.10417	-0.10443	-0.06063	-0.22805
3	-0.17253	-0.14630	-0.12912	-0.12558	-0.12690	-0.12846	-0.12993	-0.13153	-0.08948	-0.24206
4	-0.16915	-0.14895	-0.14167	-0.14211	-0.14492	-0.14658	-0.14891	-0.14726	-0.10185	-0.17434
5	-0.15927	-0.14706	-0.14932	-0.15367	-0.15708	-0.15875	-0.16012	-0.14498	-0.11479	-0.17123
6	-0.14535	-0.14305	-0.15340	-0.16004	-0.16321	-0.16396	-0.15766	-0.13325	-0.12880	-0.16854
7	-0.12880	-0.13749	-0.15282	-0.15998	-0.16228	-0.15707	-0.14439	-0.12405	-0.13814	-0.16745
8	-0.10790	-0.12855	-0.14524	-0.15173	-0.14893	-0.13914	-0.12663	-0.11445	-0.14211	-0.16868
9	-0.08345	-0.11042	-0.12688	-0.12888	-0.12177	-0.11321	-0.10233	-0.10011	-0.13299	-0.17324
10	-0.05063	-0.07665	-0.08693	-0.08499	-0.07905	-0.07431	-0.06612	-0.06953	-0.10292	-0.16901

VERTICAL(W)

SPANWISE STATION / CHORDWISE STATION	1	2	3	4	5	6	7	8	9	10
1	-0.04817	0.02529	0.05405	0.06242	0.06712	0.07290	0.07890	0.08445	0.11032	0.09366
2	-0.14230	-0.02108	0.02529	0.03786	0.04410	0.05097	0.05731	0.06424	0.11521	-0.00224
3	-0.22520	-0.06012	-0.00286	0.01274	0.02027	0.02805	0.03498	0.03526	0.11429	-0.05920
4	-0.29242	-0.09340	-0.03130	-0.01294	-0.00440	0.00429	0.00944	-0.00130	0.13016	-0.05142
5	-0.34804	-0.12240	-C.05927	-0.03953	-0.03015	-0.02177	-0.02092	-0.03146	0.14422	-0.05901
6	-0.39264	-0.14856	-0.08764	-0.06717	-0.05765	-0.05190	-0.04918	-0.05269	0.13255	-0.06353
7	-0.42823	-0.17416	-0.11660	-0.09634	-0.08907	-0.08106	-0.07396	-0.07268	0.10628	-0.06496
8	-0.45202	-0.20064	-0.14689	-0.12933	-0.12062	-0.10749	-0.10043	-0.09184	0.06585	-0.06517
9	-0.46546	-0.22609	-0.18088	-0.16360	-0.15036	-0.13490	-0.12830	-0.11417	0.01498	-0.06349
10	-0.46656	-0.25360	-0.21630	-0.19665	-0.18033	-0.16474	-0.15625	-0.13972	-0.05733	-0.07517

VELOCITY COMPONENTS ON WING PANELS DUE TO BODY LINE SOURCES AND DOUBLETS

AXIAL(U)

SPANWISE STATION / CHORDWISE STATION	1	2	3	4	5	6	7	8	9	10
1	0.00782	0.01024	0.00759	0.00550	0.00421	0.00331	0.00264	0.00216	0.00179	0.00147
2	0.01280	0.00888	0.00634	0.00469	0.00365	0.00287	0.00233	0.00193	0.00161	0.00137
3	0.01094	0.00756	0.00535	0.00406	0.00316	0.00252	0.00208	0.00172	0.00145	0.00129
4	0.00922	0.00627	0.00459	0.00353	0.00277	0.00225	0.00184	0.00155	0.00132	0.00121
5	0.00780	0.00534	0.00398	0.00307	0.00246	0.00200	0.00166	0.00140	0.00120	0.00114
6	0.00646	0.00460	0.00347	0.00272	0.00218	0.00179	0.00150	0.00128	0.00110	0.00107
7	0.00551	0.00400	0.00305	0.00240	0.00195	0.00162	0.00137	0.00117	0.00101	0.00102
8	0.00475	0.00349	0.00268	0.00214	0.00175	0.00147	0.00125	0.00108	0.00139	0.00096
9	0.00413	0.00306	0.00238	0.00192	0.00159	0.00134	0.00115	0.00143	0.00334	0.00118
10	0.00362	0.00269	0.00213	0.00174	0.00145	0.00123	0.00147	0.00305	0.00486	0.00191

TRANSVERSE(V)

SPANWISE STATION / CHORDWISE STATION	1	2	3	4	5	6	7	8	9	10
1	0.01038	-0.00343	-0.00408	-0.00333	-0.00278	-0.00231	-0.00189	-0.00159	-0.00134	-0.00112
2	-0.00061	-0.00324	-0.00320	-0.00272	-0.00232	-0.00191	-0.00161	-0.00137	-0.00115	-0.00103
3	-0.00104	-0.00275	-0.00252	-0.00225	-0.00190	-0.00161	-0.00140	-0.00117	-0.00101	-0.00094
4	-0.00099	-0.00204	-0.00206	-0.00188	-0.00159	-0.00139	-0.00117	-0.00101	-0.00089	-0.00086
5	-0.00085	-0.00162	-0.00171	-0.00153	-0.00137	-0.00118	-0.00101	-0.00089	-0.00078	-0.00080
6	-0.00045	-0.00133	-0.00141	-0.00131	-0.00115	-0.00100	-0.00088	-0.00078	-0.00069	-0.00074
7	-0.00032	-0.00110	-0.00118	-0.00109	-0.00098	-0.00087	-0.00078	-0.00069	-0.00062	-0.00068
8	-0.00024	-0.00091	-0.00098	-0.00093	-0.00084	-0.00076	-0.00068	-0.00061	-0.00125	-0.00063
9	-0.00018	-0.00076	-0.00082	-0.00079	-0.00073	-0.00067	-0.00060	-0.00121	-0.00428	-0.00100
10	-0.00020	-0.00060	-0.00070	-0.00068	-0.00064	-0.00059	-0.00117	-0.00377	-0.00678	-0.00213

VERTICAL(W)

SPANWISE STATION / CHORDWISE STATION	1	2	3	4	5	6	7	8	9	10
1	-0.00306	0.00064	0.00082	0.00065	0.00048	0.00034	0.00024	0.00017	0.00010	0.00007
2	0.00005	0.00100	0.00084	0.00061	0.00043	0.00029	0.00021	0.00013	0.00009	0.00007
3	0.00100	0.00113	0.00080	0.00055	0.00037	0.00025	0.00016	0.00010	0.00008	0.00007
4	0.00150	0.00112	0.00073	0.00048	0.00031	0.00020	0.00012	0.00010	0.00008	0.00006

5	0.00171	0.00105	0.00065	0.00041	0.00025	0.00015	0.00011	0.00009	0.00007	0.00006
6	0.00170	0.00095	0.00056	0.00034	0.00019	0.00014	0.00011	0.00008	0.00007	0.00006
7	0.00162	0.00085	0.00048	0.00024	0.00017	0.00013	0.00010	0.00008	0.00007	0.00006
8	0.00150	0.00074	0.00034	0.00022	0.00016	0.00012	0.00010	0.00008	0.00008	0.00005
9	0.00137	0.00053	0.00031	0.00021	0.00015	0.00012	0.00009	0.00010	0.00017	0.00006
10	0.00102	0.00048	0.00029	0.00020	0.00015	0.00011	0.00011	0.00018	0.00025	0.00009

VELOCITY COMPONENTS ON WING PANELS DUE TO WING SOURCES

AXIAL(U)

SPANWISE STATION CHORDWISE STATION	1	2	3	4	5	6	7	8	9	10
1	-0.02771	-0.02188	-0.01784	-0.01734	-0.01334	-0.00915	-0.00542	-0.00208	-0.00020	-0.00398
2	-0.00452	0.00231	0.00379	0.00813	0.01275	0.01673	0.02032	0.02365	0.02023	0.01740
3	0.00066	0.00476	0.00976	0.01504	0.01948	0.02329	0.02687	0.02367	0.02316	0.02429
4	0.00078	0.00778	0.01417	0.01929	0.02351	0.02730	0.02435	0.02368	0.02411	0.02925
5	0.00230	0.01133	0.01754	0.02234	0.02650	0.02378	0.02288	0.02275	0.02313	0.03678
6	0.00533	0.01397	0.01968	0.02435	0.02198	0.02072	0.02050	0.01990	0.02081	0.03492
7	0.00757	0.01513	0.02060	0.01871	0.01694	0.01656	0.01623	0.01496	0.01726	0.03436
8	0.00902	0.01607	0.01491	0.01230	0.01173	0.01165	0.01004	0.00985	0.01322	0.03457
9	0.01076	0.01104	0.00674	0.00590	0.00572	0.00406	0.00342	0.00391	0.00842	0.03106
10	0.00620	-0.00322	-0.00456	-0.00490	-0.00661	-0.00737	-0.00780	-0.00658	-0.00121	0.03087

TRANSVERSE(V)

SPANWISE STATION CHORDWISE STATION	1	2	3	4	5	6	7	8	9	10
1	0.02892	0.03581	0.03390	0.03488	0.02966	0.02350	0.01764	0.01216	0.00876	0.02395
2	-0.02620	-0.02545	-0.02480	-0.03019	-0.03697	-0.04328	-0.04924	-0.05493	-0.05029	-0.03204
3	-0.03062	-0.03003	-0.03583	-0.04358	-0.05071	-0.05717	-0.06339	-0.05923	-0.05881	-0.04321
4	-0.02456	-0.03197	-0.04149	-0.04992	-0.05726	-0.06404	-0.06046	-0.05990	-0.05915	-0.04733
5	-0.01900	-0.03369	-0.04451	-0.05325	-0.06098	-0.05806	-0.05728	-0.05746	-0.05431	-0.05247
6	-0.01516	-0.03321	-0.04459	-0.05384	-0.05194	-0.05080	-0.05094	-0.05039	-0.04504	-0.04026
7	-0.00980	-0.02935	-0.04151	-0.04126	-0.03966	-0.03969	-0.03962	-0.03796	-0.03104	-0.02930
8	-0.00391	-0.02524	-0.02819	-0.02587	-0.02584	-0.02625	-0.02414	-0.02284	-0.01372	-0.02119
9	0.00041	-0.01272	-0.00912	-0.00903	-0.00943	-0.00735	-0.00660	-0.00462	0.00716	-0.00546
10	0.01378	0.02067	0.02081	0.02039	0.02243	0.02329	0.02376	0.02686	0.04095	0.01009

VERTICAL(W)

SPANWISE STATION CHORDWISE STATION	1	2	3	4	5	6	7	8	9	10
1	0.10816	0.10816	0.10816	0.10816	0.10816	0.10816	0.10816	0.10816	0.10816	0.10816
2	0.05006	0.05006	0.05006	0.05006	0.05006	0.05006	0.05006	0.05006	0.05006	0.05006
3	0.02486	0.02486	0.02486	0.02486	0.02486	0.02486	0.02486	0.02486	0.02486	0.02486
4	0.00687	0.00687	0.00687	0.00687	0.00687	0.00687	0.00687	0.00687	0.00687	0.00687
5	-0.00766	-0.00766	-0.00766	-0.00766	-0.00766	-0.00766	-0.00766	-0.00766	-0.00766	-0.00766
6	-0.02199	-0.02199	-0.02199	-0.02199	-0.02199	-0.02199	-0.02199	-0.02199	-0.02199	-0.02199
7	-0.03357	-0.03357	-0.03357	-0.03357	-0.03357	-0.03357	-0.03357	-0.03357	-0.03357	-0.03357
8	-0.04035	-0.04035	-0.04035	-0.04035	-0.04035	-0.04035	-0.04035	-0.04035	-0.04035	-0.04035
9	-0.04621	-0.04621	-0.04621	-0.04621	-0.04621	-0.04621	-0.04621	-0.04621	-0.04621	-0.04621
10	-0.05182	-0.05182	-0.05182	-0.05182	-0.05182	-0.05182	-0.05182	-0.05182	-0.05182	-0.05182

VELOCITY COMPONENTS ON BODY PANELS DUE TO BODY PANEL PRESSURE SINGULARITIES

AXIAL(U)

THETA(DEG.)	12.5000	37.5000	62.5000	88.5950	116.0950	142.5000	167.5000
ROW NO.							
1	0.00002	0.00007	0.00027	0.00305	-0.00292	-0.00025	-0.00008
2	-0.00006	0.00040	0.00176	0.00648	-0.01349	-0.00118	-0.00043
3	-0.00064	0.00177	0.00387	0.01723	-0.02475	-0.00836	0.00131
4	0.00528	0.00101	0.00806	0.02459	-0.02544	-0.00952	-0.00147
5	0.00319	0.00951	0.01637	0.03227	-0.01912	-0.01229	-0.01031
6	0.00407	0.01013	0.01941	0.03197	-0.02082	-0.01562	-0.01604
7	0.00679	0.01162	0.01928	0.02976	-0.02083	-0.01925	-0.01931
8	0.01013	0.01293	0.01833	0.02605	-0.02102	-0.02079	-0.02079
9	0.01226	0.01374	0.01720	0.02150	-0.02005	-0.02132	-0.02138
10	0.01265	0.01393	0.01596	0.01689	-0.01777	-0.02102	-0.02182
11	0.01374	0.01341	0.01097	0.00515	-0.01286	-0.01720	-0.01948
12	0.01200	0.01055	0.00602	-0.00281	-0.00974	-0.01172	-0.01301
13	0.00938	0.00770	0.00487	0.00071	-0.00368	-0.00671	-0.00902
14	0.00559	0.00483	0.00309	0.00048	-0.00222	-0.00406	-0.00496

TRANSVERSE(V)

THETA(DEG.)	12.5000	37.5000	62.5000	88.5950	116.0950	142.5000	167.5000
ROW NO.							
1	-0.00002	-0.00010	-0.00025	-0.00767	0.00618	0.00041	0.00009
2	-0.00040	-0.00040	-0.00133	-0.02454	0.04328	0.00103	0.00025
3	0.00067	-0.00174	-0.00238	-0.07242	0.08607	0.00465	0.00273
4	0.00244	0.00018	-0.00722	-0.13397	0.13191	0.00411	-0.00256
5	-0.00060	-0.00519	-0.02212	-0.20615	0.16798	0.00905	-0.00128
6	-0.00016	-0.00625	-0.03320	-0.26907	0.21200	0.01957	-0.00035
7	-0.00042	-0.00595	-0.04371	-0.32791	0.25345	0.03006	0.00276
8	0.00038	-0.00719	-0.05594	-0.38097	0.29082	0.04141	0.00567
9	-0.00076	-0.01075	-0.06812	-0.42618	0.32276	0.05037	0.00765
10	-0.00123	-0.01384	-0.07976	-0.46191	0.34868	0.05992	0.01081
11	-0.00336	-0.02210	-0.10191	-0.48386	0.37808	0.07745	0.01573
12	-0.00480	-0.03105	-0.11454	-0.48322	0.39746	0.08787	0.01974
13	-0.01076	-0.04413	-0.12684	-0.48492	0.40422	0.09253	0.02181
14	-0.01469	-0.05460	-0.13769	-0.47428	0.37695	0.10051	0.02546

VERTICAL(W)

THETA(DEG.)	12.5000	37.5000	62.5000	88.5950	116.0950	142.5000	167.5000
ROW NO.							
1	0.00000	0.00007	0.00049	-0.00090	-0.00386	0.00031	0.00002
2	0.00009	0.00031	-0.00053	-0.00552	-0.02326	0.00401	0.00006
3	0.00204	-0.00149	-0.00187	-0.00993	-0.05031	0.00075	0.00780
4	-0.00611	0.00035	-0.00206	-0.01696	-0.07809	-0.00597	0.01369
5	-0.00340	-0.00474	-0.00940	-0.02279	-0.10600	-0.01537	0.00852
6	-0.00061	-0.00390	-0.01332	-0.03259	-0.13365	-0.02602	-0.00029
7	0.00066	-0.00647	-0.02057	-0.03702	-0.15838	-0.03845	-0.01078
8	0.00044	-0.00942	-0.02609	-0.04308	-0.18132	-0.05078	-0.02244
9	0.00005	-0.01166	-0.03159	-0.04813	-0.20229	-0.06450	-0.03486
10	-0.00116	-0.01482	-0.03689	-0.05229	-0.21937	-0.07658	-0.04691
11	-0.00781	-0.02324	-0.04550	-0.05488	-0.23617	-0.09637	-0.06896

12	-0.01915	-0.03558	-0.05508	-0.05733	-0.24613	-0.11000	-0.08242
13	-0.03610	-0.04658	-0.05905	-0.05707	-0.25054	-0.11808	-0.09272
14	-0.05073	-0.05730	-0.06565	-0.11847	-0.30335	-0.13155	-0.10715

VELOCITY COMPONENTS ON BODY PANELS DUE TO WING PANEL PRESSURE SINGULARITIES

AXIAL(U)

THETA(DEG.)	12.5000	37.5000	62.5000	88.5950	116.0950	142.5000	167.5000
ROW NO.							
1	-0.	-0.	-0.	0.01004	-0.00693	-0.	-0.
2	-0.	-0.	0.00652	0.01885	-0.01297	-0.00439	-0.
3	0.00213	0.00520	0.01222	0.02385	-0.01654	-0.00814	-0.00443
4	0.00751	0.01043	0.01676	0.02588	-0.01824	-0.01188	-0.00853
5	0.01208	0.01467	0.01952	0.02607	-0.01855	-0.01415	-0.01165
6	0.01530	0.01715	0.02083	0.02513	-0.01801	-0.01523	-0.01343
7	0.01687	0.01838	0.02109	0.02346	-0.01692	-0.01548	-0.01412
8	0.01739	0.01863	0.02059	0.02098	-0.01525	-0.01511	-0.01415
9	0.01731	0.01823	0.01916	0.01781	-0.01304	-0.01414	-0.01380
10	0.01669	0.01717	0.01726	0.01362	-0.01013	-0.01278	-0.01295
11	0.01375	0.01363	0.01045	0.00460	-0.00381	-0.00796	-0.00990
12	0.00881	0.00837	0.00680	0.00263	-0.00231	-0.00513	-0.00592
13	0.00644	0.00579	0.00426	0.00160	-0.00143	-0.00345	-0.00417
14	0.00435	0.00379	0.00267	0.00099	-0.00084	-0.00215	-0.00277

TRANSVERSE(V)

THETA(DEG.)	12.5000	37.5000	62.5000	88.5950	116.0950	142.5000	167.5000
ROW NO.							
1	0.	0.	0.	0.00823	-0.01255	0.	0.
2	0.	0.	0.00425	0.04441	-0.04938	-0.00622	0.
3	0.00200	0.00512	0.01470	0.09788	-0.09874	-0.01738	-0.00372
4	0.00324	0.01093	0.02902	0.15839	-0.15249	-0.02982	-0.00708
5	0.00499	0.01739	0.04456	0.21903	-0.20553	-0.04301	-0.01059
6	0.00684	0.02377	0.06034	0.27692	-0.25569	-0.05586	-0.01391
7	0.00855	0.03011	0.07587	0.33043	-0.30165	-0.06810	-0.01715
8	0.01033	0.03651	0.09084	0.37824	-0.34232	-0.07964	-0.02023
9	0.01210	0.04264	0.10434	0.41885	-0.37626	-0.08982	-0.02311
10	0.01358	0.04800	0.11633	0.45063	-0.40190	-0.09836	-0.02537
11	0.01619	0.05697	0.13348	0.47697	-0.42005	-0.10830	-0.02887
12	0.01807	0.06198	0.14212	0.48235	-0.42406	-0.11289	-0.02995
13	0.01919	0.06513	0.14601	0.48427	-0.42548	-0.11490	-0.03080
14	0.02000	0.06723	0.14863	0.47393	-0.38986	-0.11376	-0.03081

VERTICAL(W)

THETA(DEG.)	12.5000	37.5000	62.5000	88.5950	116.0950	142.5000	167.5000
ROW NO.							
1	0.	0.	0.	-0.02006	-0.00920	0.	0.
2	0.	0.	-0.01092	-0.04949	-0.01419	-0.00504	0.
3	-0.00263	-0.00763	-0.02268	-0.07326	-0.00987	-0.00795	-0.00327
4	-0.00820	-0.01459	-0.03294	-0.08940	0.00208	-0.00793	-0.00359
5	-0.01179	-0.01918	-0.03933	-0.09854	0.01954	-0.00385	-0.00066

6	-0.01284	-0.02058	-0.04229	-0.10226	0.04016	0.00320	0.00520
7	-0.01137	-0.01965	-0.04247	-0.10162	0.06241	0.01216	0.01292
8	-0.00833	-0.01700	-0.04045	-0.09689	0.08545	0.02224	0.02163
9	-0.00432	-0.01315	-0.03639	-0.08851	0.10827	0.03305	0.03078
10	0.00046	-0.00826	-0.03072	-0.07560	0.13067	0.04405	0.04020
11	0.01199	0.00437	-0.01120	-0.03714	0.16986	0.06745	0.05891
12	0.02588	0.02016	0.00662	-0.01250	0.19283	0.08499	0.07520
13	0.03749	0.03311	0.02217	0.00513	0.20979	0.09979	0.08863
14	0.05118	0.04873	0.04408	0.08738	0.27865	0.12098	0.10494

VELOCITY COMPONENTS ON BODY PANELS DUE TO WING SOURCES

AXIAL(U)

THETA(DEG.)	12.5000	37.5000	62.5000	88.5950	116.0950	142.5000	167.5000
ROW NO.							
1	-0.	-0.	-0.	-0.00275	-0.00157	-0.	-0.
2	-0.	-0.	-0.00644	-0.01260	-0.01133	-0.00520	-0.
3	-0.	-0.00685	-0.00900	-0.00732	-0.00729	-0.00784	-0.00584
4	-0.01111	-0.00697	-0.00644	-0.00367	-0.00405	-0.00954	-0.01250
5	-0.01121	-0.01124	-0.00893	-0.00580	-0.00705	-0.00875	-0.01017
6	-0.00888	-0.00824	-0.00610	-0.00291	-0.00373	-0.00599	-0.00735
7	-0.00611	-0.00529	-0.00299	0.00023	-0.00053	-0.00295	-0.00439
8	-0.00326	-0.00222	0.00014	0.00301	0.00235	0.00010	-0.00136
9	-0.00024	0.00077	0.00291	0.00530	0.00474	0.00291	0.00168
10	0.00268	0.00352	0.00541	0.00754	0.00706	0.00543	0.00439
11	0.00633	0.00718	0.00881	0.00309	0.00388	0.00862	0.00774
12	0.00741	0.00597	0.00467	0.00365	0.00411	0.00549	0.00453
13	0.00208	0.00192	0.00159	0.00128	0.00131	0.00155	0.00169
14	0.00092	0.00084	0.00070	0.00059	0.00061	0.00071	0.00078

TRANSVERSE(V)

THETA(DEG.)	12.5000	37.5000	62.5000	88.5950	116.0950	142.5000	167.5000
ROW NO.							
1	0.	0.	0.	-0.00015	-0.00106	0.	0.
2	0.	0.	-0.00215	-0.01925	-0.02229	-0.00479	0.
3	0.	-0.00460	-0.00836	-0.02393	-0.02408	-0.01139	-0.00698
4	-0.00260	-0.00749	-0.01098	-0.02212	-0.02122	-0.00713	-0.00055
5	-0.00051	0.00002	-0.00374	-0.01007	-0.00746	-0.00336	-0.00046
6	-0.00028	-0.00024	-0.00254	-0.00455	-0.00252	-0.00167	-0.00015
7	-0.00016	-0.00000	-0.00118	0.00102	0.00297	0.00000	0.00020
8	-0.00004	0.00046	0.00044	0.00643	0.00819	0.00182	0.00071
9	0.00015	0.00109	0.00216	0.01105	0.01252	0.00342	0.00112
10	0.00032	0.00154	0.00361	0.01488	0.01608	0.00469	0.00135
11	0.00066	0.00205	0.00561	0.01434	0.01247	0.00666	0.00165
12	-0.00173	-0.00105	0.00067	0.00265	0.00153	-0.00122	-0.00010
13	0.00013	0.00055	0.00128	0.00195	0.00170	0.00091	0.00027
14	0.00015	0.00048	0.00087	0.00112	0.00099	0.00060	0.00019

VERTICAL(W)

THETA(DEG.)	12.5000	37.5000	62.5000	88.5950	116.0950	142.5000	167.5000
ROW NO.							

1	0.	0.	0.	0.00415	-0.00211	0.	0.
2	0.	0.	0.00996	0.03004	-0.02053	-0.00663	0.
3	0.	0.01006	0.01694	0.02112	-0.01486	-0.01131	-0.00630
4	0.01364	0.01147	0.01421	0.01292	-0.00933	-0.01130	-0.01236
5	0.01432	0.01454	0.01281	0.00675	-0.00545	-0.00942	-0.01060
6	0.01203	0.01122	0.00836	0.00030	-0.00085	-0.00631	-0.00811
7	0.00894	0.00758	0.00354	-0.00596	0.00361	-0.00289	-0.00529
8	0.00552	0.00357	-0.00135	-0.01126	0.00745	0.00060	-0.00226
9	0.00172	-0.00051	-0.00574	-0.01521	0.01035	0.00381	0.00089
10	-0.00211	-0.00431	-0.00958	-0.01862	0.01288	0.00663	0.00378
11	-0.00718	-0.00947	-0.01472	-0.00827	0.00607	0.01035	0.00751
12	-0.00929	-0.00751	-0.00581	-0.00246	0.00212	0.00487	0.00493
13	-0.00329	-0.00306	-0.00240	-0.00094	0.00081	0.00182	0.00216
14	-0.00166	-0.00150	-0.00112	-0.00043	0.00036	0.00086	0.00107

PRESSURES, FORCES, AND MOMENTS ON ISOLATED BODY

CD = 0.00086 CL = 0.00009 CM = -0.00407

BODY PRESSURE COEFFICIENTS(CP)

THETA(DEG.) X	12.5000	37.5000	62.5000	88.5950	116.0950	142.5000	167.5000
0.	0.14524	0.14150	0.13471	0.12577	0.11627	0.10903	0.10529
0.7243	0.14524	0.14150	0.13471	0.12577	0.11627	0.10903	0.10529
1.4485	0.13759	0.13528	0.13109	0.12556	0.11970	0.11523	0.11292
2.1728	0.06653	0.06558	0.06385	0.06157	0.05914	0.05730	0.05634
2.8970	0.06603	0.06507	0.06332	0.06103	0.05858	0.05673	0.05576
3.6213	0.04938	0.04858	0.04711	0.04518	0.04313	0.04156	0.04076
4.3456	0.04843	0.04777	0.04658	0.04501	0.04334	0.04207	0.04141
5.0698	0.03960	0.03886	0.03752	0.03575	0.03388	0.03245	0.03171
5.7941	0.03757	0.03706	0.03613	0.03490	0.03360	0.03261	0.03210
6.5184	0.03040	0.02997	0.02917	0.02812	0.02701	0.02616	0.02573
7.2426	0.02933	0.02883	0.02792	0.02671	0.02544	0.02447	0.02396
7.9669	0.02482	0.02415	0.02294	0.02135	0.01965	0.01836	0.01769
8.6911	0.02119	0.02082	0.02016	0.01928	0.01835	0.01764	0.01727
9.4154	0.01404	0.01421	0.01452	0.01493	0.01536	0.01568	0.01585
10.1397	0.01514	0.01461	0.01366	0.01241	0.01108	0.01007	0.00954
10.8639	0.00814	0.00820	0.00831	0.00845	0.00860	0.00871	0.00877
11.5882	0.00335	0.00361	0.00409	0.00472	0.00539	0.00590	0.00616
12.3124	0.00034	0.00049	0.00075	0.00110	0.00146	0.00174	0.00189
13.0367	-0.00762	-0.00699	-0.00584	-0.00433	-0.00272	-0.00150	-0.00087
13.7610	-0.00922	-0.00877	-0.00794	-0.00686	-0.00570	-0.00483	-0.00437
14.5023	-0.01657	-0.01596	-0.01485	-0.01339	-0.01184	-0.01066	-0.01005
15.2436	-0.02636	-0.02507	-0.02273	-0.01964	-0.01635	-0.01386	-0.01256
15.9849	-0.04043	-0.03942	-0.03758	-0.03516	-0.03258	-0.03062	-0.02961
16.7262	-0.03295	-0.03223	-0.03093	-0.02921	-0.02739	-0.02600	-0.02528
17.4675	-0.02691	-0.02643	-0.02557	-0.02444	-0.02324	-0.02232	-0.02185
18.2088	-0.02211	-0.02182	-0.02131	-0.02064	-0.01992	-0.01937	-0.01909
18.9501	-0.01832	-0.01818	-0.01792	-0.01758	-0.01723	-0.01695	-0.01681
19.6914	-0.01533	-0.01529	-0.01521	-0.01512	-0.01501	-0.01493	-0.01489
20.4327	-0.01298	-0.C1300	-0.01305	-0.01310	-0.01316	-0.01320	-0.01323
21.1740	-0.01112	-0.01118	-0.01130	-0.01144	-0.01160	-0.01172	-0.01178
21.9153	-0.00965	-0.00973	-0.00987	-0.01006	-0.01027	-0.01042	-0.01050

22.6566	-0.00847	-0.00855	-0.00871	-0.00891	-0.00913	-0.00929	-0.00938
23.3979	-0.00598	-0.00635	-0.00702	-0.00790	-0.00884	-0.00955	-0.00992
24.1392	-0.00707	-0.00708	-0.00710	-0.00712	-0.00715	-0.00717	-0.00718
24.8805	-0.00640	-0.00640	-0.00641	-0.00641	-0.00642	-0.00643	-0.00643
25.6218	-0.00581	-0.00581	-0.00581	-0.00580	-0.00580	-0.00580	-0.00580
26.3631	-0.00528	-0.00528	-0.00528	-0.00528	-0.00527	-0.00527	-0.00527
27.1044	-0.00482	-0.00482	-0.00482	-0.00481	-0.00481	-0.00481	-0.00481
27.8457	-0.00441	-0.00441	-0.00441	-0.00441	-0.00441	-0.00441	-0.00441
28.5870	-0.00405	-0.00405	-0.00405	-0.00406	-0.00406	-0.00406	-0.00406
29.3283	-0.00374	-0.00374	-0.00374	-0.00374	-0.00375	-0.00375	-0.00375
30.0696	-0.00590	-0.00590	-0.00591	-0.00592	-0.00592	-0.00593	-0.00593
30.8109	-0.01353	-0.01354	-0.01355	-0.01357	-0.01358	-0.01360	-0.01360
31.5522	-0.02123	-0.02124	-0.02127	-0.02130	-0.02133	-0.02136	-0.02137
32.2935	-0.02594	-0.02597	-0.02600	-0.02605	-0.02611	-0.02615	-0.02617
33.0348	-0.02947	-0.02950	-0.02955	-0.02963	-0.02970	-0.02976	-0.02979
33.7761	-0.03576	-0.03580	-0.03587	-0.03597	-0.03607	-0.03615	-0.03619
34.5174	-0.03748	-0.03753	-0.03763	-0.03775	-0.03788	-0.03798	-0.03803
35.2587	-0.02731	-0.02737	-0.02747	-0.02761	-0.02775	-0.02787	-0.02792
36.0000	-0.01018	-0.01024	-0.01034	-0.01047	-0.01061	-0.01072	-0.01077

INCREMENTAL PRESSURES, FORCES, AND MOMENTS ON BODY PANELS DUE TO WING

CD = 0.00001 CL = 0.01760 CM = -0.39521

BODY PANEL PRESSURE COEFFICIENT(CP)

THETA(DEG.)	12.5000	37.5000	62.5000	88.5950	116.0950	142.5000	167.5000
ROW NO.							
1	-0.00004	-0.00013	-0.00054	-0.02069	0.02284	0.00051	0.00015
2	0.00011	-0.00079	-0.00368	-0.02546	0.08559	0.02152	0.00086
3	-0.00298	-0.00025	-0.01418	-0.06752	0.09717	0.04867	0.01791
4	-0.00335	-0.00894	-0.03674	-0.09359	0.09546	0.06187	0.04500
5	-0.00810	-0.02589	-0.05392	-0.10508	0.08943	0.07037	0.06425
6	-0.02098	-0.03810	-0.06829	-0.10840	0.08513	0.07368	0.07362
7	-0.03509	-0.04940	-0.07476	-0.10688	0.07655	0.07538	0.07563
8	-0.04853	-0.05868	-0.07813	-0.10009	0.06784	0.07161	0.07262
9	-0.05865	-0.06547	-0.07854	-0.08923	0.05671	0.06509	0.06700
10	-0.06403	-0.06925	-0.07727	-0.07610	0.04169	0.05674	0.06076
11	-0.06764	-0.06844	-0.06046	-0.02567	0.02556	0.03307	0.04329
12	-0.05644	-0.04979	-0.03499	-0.00694	0.01588	0.02271	0.02880
13	-0.03579	-0.03082	-0.02144	-0.00716	0.00760	0.01722	0.02301
14	-0.02173	-0.01892	-0.01292	-0.00413	0.00490	0.01101	0.01391

BODY PANEL SLOPE

THETA(DEG.)	12.5000	37.5000	62.5000	88.5950	116.0950	142.5000	167.5000
ROW NO.							
1	0.02349	0.02349	0.02349	0.02339	0.02336	0.02349	0.02349
2	0.00619	0.00619	0.00619	0.00616	0.00615	0.00619	0.00619
3	0.	0.	0.	0.	-0.	-0.	-0.
4	0.	0.	0.	0.	-0.	-0.	-0.

5	0.	0.	0.	0.	-0.	-0.	-0.
6	0.	0.	0.	0.	-0.	-0.	-0.
7	0.	0.	0.	0.	-0.	-0.	-0.
8	0.	0.	0.	0.	-0.	-0.	-0.
9	0.	0.	0.	0.	-0.	-0.	-0.
10	0.	0.	0.	0.	-0.	-0.	-0.
11	0.	0.	0.	0.	-0.	-0.	-0.
12	0.	0.	0.	0.	-0.	-0.	-0.
13	0.	0.	0.	0.	-0.	-0.	-0.
14	-0.01422	-0.01422	-0.01422	-0.01415	-0.01413	-0.01422	-0.01422

PRESSURES, FORCES, AND MOMENTS ON WING PANELS IN PRESENCE OF BODY

CD = 0.00761 CL = 0.15900 CM = -4.74761

SPANWISE CD DISTRIBUTION

SPANWISE STATION	1	2	3	4	5	6	7	8	9	10
	0.00329	0.00146	0.00095	0.00077	0.00063	0.00044	0.00030	0.00026	-0.00120	0.00072

SPANWISE CL DISTRIBUTION

SPANWISE STATION	1	2	3	4	5	6	7	8	9	10
	0.01602	0.01575	0.01577	0.01584	0.01578	0.01552	0.01498	0.01411	0.01292	0.02231

UPPER SURFACE WING PANEL PRESSURE COEFFICIENTS(CP)

SPANWISE STATION CHORDWISE STATION	1	2	3	4	5	6	7	8	9	10
1	-0.03353	-0.04540	-0.03528	-0.03201	-0.03150	-0.03871	-0.04251	-0.04761	-0.02197	-0.10176
2	-0.13060	-0.11906	-0.10815	-0.10335	-0.10909	-0.11307	-0.11949	-0.12563	-0.08567	-0.20805
3	-0.15460	-0.14473	-0.13437	-0.13139	-0.13552	-0.14278	-0.15028	-0.14450	-0.10813	-0.23912
4	-0.16066	-0.14924	-0.14563	-0.14829	-0.15454	-0.16193	-0.15862	-0.15103	-0.12138	-0.15703
5	-0.15427	-0.14820	-0.15230	-0.16182	-0.16598	-0.16507	-0.15786	-0.15026	-0.13049	-0.16778
6	-0.14278	-0.14456	-0.15726	-0.17033	-0.16493	-0.15292	-0.15485	-0.13774	-0.13585	-0.15506
7	-0.12988	-0.13919	-0.15650	-0.15601	-0.15406	-0.14636	-0.13855	-0.12068	-0.13818	-0.14524
8	-0.11054	-0.13101	-0.13691	-0.13754	-0.13051	-0.12573	-0.11269	-0.10622	-0.13410	-0.13516
9	-0.09014	-0.10452	-0.11315	-0.10401	-0.10153	-0.09087	-0.08523	-0.08500	-0.12122	-0.11452
10	-0.05227	-0.05002	-0.05796	-0.05445	-0.04434	-0.04415	-0.03687	-0.04461	-0.08270	-0.12355

LOWER SURFACE WING PANEL PRESSURE COEFFICIENTS(CP)

SPANWISE STATION CHORDWISE STATION	1	2	3	4	5	6	7	8	9	10
1	0.13005	0.09560	0.07456	0.06530	0.06377	0.05685	0.05421	0.05006	0.02004	0.11603
2	0.09947	0.07502	0.05136	0.04553	0.03928	0.03664	0.03218	0.02642	0.00260	0.14484
3	0.09659	0.06827	0.05362	0.05146	0.04924	0.04426	0.03889	0.04700	0.02215	0.14329
4	0.08562	0.06762	0.06063	0.05861	0.05646	0.05148	0.05817	0.06337	0.02691	0.04165
5	0.07762	0.06591	0.06510	0.06192	0.06272	0.06606	0.07526	0.06082	0.03663	0.01905
6	0.06884	0.06371	0.06608	0.06267	0.07269	0.08579	0.07469	0.05625	0.05167	0.01459
7	0.05765	0.06100	0.06600	0.07691	0.08221	0.08233	0.07168	0.05993	0.06294	0.00278

8	0.04656	0.05615	0.07455	0.08337	0.08632	0.07684	0.07168	0.06041	0.07280	-0.00921
9	0.03137	0.05624	0.07157	0.08363	0.07576	0.07396	0.06377	0.06075	0.07240	-0.01675
10	0.02145	0.06158	0.06861	0.06930	0.07076	0.06404	0.05940	0.05664	0.06714	-0.00996

WING PANEL PRESSURE DIFFERENCE(CL)

SPANWISE STATION / CHORDWISE STATION	1	2	3	4	5	6	7	8	9	10
1	0.16359	0.14101	0.10984	0.09730	0.09527	0.09556	0.09671	0.09767	0.04202	0.21779
2	0.23007	0.19409	0.15951	0.14888	0.14837	0.14971	0.15167	0.15205	0.08827	0.35289
3	0.25119	0.21301	0.18799	0.18284	0.18476	0.18703	0.18916	0.19150	0.13027	0.38241
4	0.24628	0.21686	0.20626	0.20690	0.21100	0.21341	0.21680	0.21439	0.14829	0.19868
5	0.23189	0.21411	0.21740	0.22374	0.22870	0.23113	0.23312	0.21108	0.16712	0.18683
6	0.21163	0.20827	0.22334	0.23300	0.23762	0.23871	0.22954	0.19400	0.18752	0.16965
7	0.18753	0.20018	0.22250	0.23292	0.23627	0.22869	0.21023	0.18061	0.20112	0.14802
8	0.15710	0.18716	0.21146	0.22091	0.21683	0.20257	0.18437	0.16663	0.20690	0.12595
9	0.12151	0.16076	0.18472	0.18764	0.17729	0.16483	0.14899	0.14575	0.19362	0.09777
10	0.07372	0.11160	0.12657	0.12375	0.11510	0.10819	0.09627	0.10125	0.14984	0.11359

UPPER SURFACE WING PANEL SLOPE

SPANWISE STATION / CHORDWISE STATION	1	2	3	4	5	6	7	8	9	10
1	0.07305	0.14120	0.16825	0.17554	0.18006	0.18568	0.19154	0.19688	0.22247	0.20546
2	-0.05935	0.04139	0.08344	0.09457	0.10022	0.10660	0.11254	0.11901	0.16970	0.05152
3	-0.14433	-0.01809	0.03294	0.04618	0.05247	0.05938	0.06559	0.06534	0.14380	-0.03042
4	-0.20478	-0.06378	-0.01060	0.00424	0.01108	0.01836	0.02264	0.01107	0.14206	-0.04046
5	-0.24928	-0.10110	-0.05041	-0.03502	-0.02806	-0.02148	-0.02189	-0.03321	0.14167	-0.06255
6	-0.28148	-0.13602	-0.09027	-0.07532	-0.06918	-0.06542	-0.06394	-0.06851	0.11564	-0.08153
7	-0.30361	-0.16761	-0.12828	-0.11512	-0.11115	-0.10550	-0.09993	-0.10013	0.07797	-0.09423
8	-0.31149	-0.19603	-0.16375	-0.15344	-0.14894	-0.13823	-0.13324	-0.12592	0.03082	-0.10132
9	-0.31162	-0.22410	-0.20125	-0.19283	-0.18383	-0.17151	-0.16677	-0.15396	-0.02602	-0.10547
10	-0.30614	-0.25332	-0.24115	-0.23035	-0.21941	-0.20667	-0.20016	-0.18524	-0.10398	-0.12272

LOWER SURFACE WING PANEL SLOPE

SPANWISE STATION / CHORDWISE STATION	1	2	3	4	5	6	7	8	9	10
1	-0.14328	-0.07513	-0.04808	-0.04078	-0.03627	-0.03065	-0.02479	-0.01944	0.00614	-0.01086
2	-0.15947	-0.05872	-0.01668	-0.00554	0.00011	0.00648	0.01243	0.01889	0.06958	-0.04859
3	-0.19405	-0.06781	-0.01677	-0.00354	0.00275	0.00966	0.01588	0.01563	0.09408	-0.08014
4	-0.21851	-0.07751	-0.02434	-0.00949	-0.00266	0.00462	0.00891	-0.00266	0.12832	-0.05420
5	-0.23396	-0.08578	-0.03509	-0.01969	-0.01274	-0.00616	-0.00656	-0.01788	0.15699	-0.04722
6	-0.23750	-0.09204	-0.04629	-0.03134	-0.02520	-0.02144	-0.01996	-0.02454	0.15962	-0.03755
7	-0.23648	-0.10047	-0.06115	-0.04798	-0.04402	-0.03837	-0.03279	-0.03300	0.14510	-0.02710
8	-0.23079	-0.11534	-0.08306	-0.07275	-0.06824	-0.05753	-0.05255	-0.04523	0.11151	-0.02063
9	-0.21920	-0.13169	-0.10883	-0.10042	-0.09142	-0.07910	-0.07435	-0.06155	0.06640	-0.01305
10	-0.20251	-0.14968	-0.13752	-0.12671	-0.11577	-0.10303	-0.09653	-0.08161	-0.00034	-0.01908

FORCES AND MOMENTS ON WING-BODY COMBINATION

CD = 0.00849 CL = 0.17669 CM = -5.14690

10. REFERENCES

1. Woodward, F. A.: A Method of Aerodynamic Influence Coefficients with Application to the Analysis and Design of Supersonic Wings. Boeing Document D6-8178, April 1962.
2. Middleton, Wilbur D.; and Carlson, Harry W.: Numerical Method of Estimating and Optimizing the Supersonic Aerodynamic Characteristics of Arbitrary Planform Wings. AIAA Journal of Aircraft, vol. 2, no. 4, July-August 1965.
3. Yoshihara, H.; Kainer, J.; and Strand, T.: On Optimum Thin Lifting Surfaces at Supersonic Speeds. Journal of the Aero/Space Sciences, vol. 25, no. 8, August 1958, pp. 473-479.
4. Grant, F. C.: The Proper Combination of Lift Loadings for Least Drag on a Supersonic Wing. NACA TR 1275, 1956.
5. Carlson, H. W.; and Middleton, W. D.: A Numerical Method for the Design of Camber Surfaces of Supersonic Wings with Arbitrary Planforms. NASA TN D-2341, June 1964.
6. Kawaguchi, A. S.; Brown, John; and La Rowe, Eugene: A Method of Optimizing Camber Surfaces of Wing-Body Combinations at Supersonic Speeds-Digital Computer Program. Boeing Document D6-10741, Part II, September 1965.
7. Aerodynamic Research Staff: Summary Description of a Method of Optimizing Camber Surfaces for Wing-Body Combinations at Supersonic Speeds. Boeing Document D6-10740, September 1965.
8. Heaslet, M. A.; Lomax, L.; and Jones, A. L.: Volterra's Solution of the Wave Equation as Applied to Three-Dimensional Supersonic Airfoil Problems. NACA Report 889, April 1947.
9. Liepmann, H. W.; and Roshko, A.: Elements of Gas Dynamics, John Wiley and Sons, 1957.
10. von Karman, T.; and Moore, N. B.: The Resistance of Slender Bodies Moving with Supersonic Velocities with Special Reference to Projectiles. Trans. ASME, vol. 54, pp. 303-310, 1932.
11. Tucker, W. A.: A Method for the Design of Sweptback Wings Warped to Produce Specified Flight Characteristics at Supersonic Speeds. NACA TR 1226, 1955.

12. Cohen, Doris; and Friedman, M. D.: Theoretical Investigation of the Supersonic Lift and Drag of Thin, Sweptback Wings with Increased Sweep Near the Root. NACA TN 2959, 1953.

13. Snow, R. N.: Aerodynamics of Thin Quadrilateral Wings at Supersonic Speeds. Quart. Appl. Math., vol. 5, 1948.

14. Ting, Lu: Diffraction of Disturbances Around a Convex Right Corner with Applications in Acoustics and Wing-Body Interference. Journal of the Aeronautical Sciences, vol. 24, no. 11, November 1957.

15. Nielsen, Jack, N.: Quasi-Cylindrical Theory of Wing-Body Interference at Supersonic Speeds and Comparison with Experiment. NACA Rept. 1252, 1952.

16. Donovan, A. F.; and Lawrence, H. R., ed.: Aerodynamic Components of Aircraft at High Speeds. Vol. VII, High Speed Aerodynamics and Jet Propulsion. Princeton University Press, Princeton, New Jersey, 1954.

17. Van Dyke, Milton D.: First- and Second-Order Theory of Supersonic Flow Past Bodies of Revolution. Journal of the Aeronautical Sciences, vol. 18, no. 3, 1951.

18. Carlson, Harry W.: Pressure Distributions at Mach Number 2.05 on a Series of Highly-Swept Arrow Wings Employing Various Degrees of Twist and Camber. NASA TN D-1264, 1962.